THE UNIVERSITY *of* EDINBURGH

THE UNIVERSITY
of EDINBURGH

The Dynamics of Wnt/β-catenin Signalling during Cerebellum Development

Hayden John Selvadurai

Thesis submitted for the degree of

Doctor of Philosophy

The University of Edinburgh

2011

For my mum, who fought cancer and won.
Your perseverance and positive attitude through life's
challenges will never cease to inspire me.

I (Hayden Selvadurai) composed this thesis and performed all of the experiments presented herein unless otherwise indicated in the text. No part of this work has been, or is being submitted for any other degree or professional qualification.

Signed……

Date……

Abstract

Medulloblastomas are tumours of cerebellar origin and are thought to arise from the malignant transformation of progenitor cells in the developing cerebellum. A number of developmental signalling pathways are required for the precise cell specification, proliferation, migration and differentiation involved in forming the mature cerebellum and it is the dysregulation of these processes that can lead to the eventual formation of a tumour. Genes encoding components of the canonical Wnt/β-catenin signaling pathway are mutated in around 15% of medulloblastomas and germline mutations that activate this pathway are known to predispose to medulloblastoma. Despite this, the contribution of Wnt/β-catenin signaling to normal cerebellum development is not yet well understood and the developmental origins of medulloblastoma arising from activation of this pathway are only beginning to be revealed. Therefore, the aims of this thesis were to characterise the spatio-temporal nature of Wnt/β-catenin signalling during cerebellum development and to investigate its function, with the broad goal of informing our understanding of how medulloblastoma arises from oncogenic activation of Wnt/β-catenin signalling.

To address the first aim I utilised a *LacZ* expressing Wnt/β-catenin signalling reporter mouse to characterize the spatio-temporal pattern of Wnt/β-catenin pathway activation during cerebellum development. Analysis of *LacZ* reporter expression revealed a pattern of transient Wnt/β-catenin activity in discrete cell populations throughout cerebellum development. I found that Wnt/β-catenin activity is present during the early specification of granule cells at the cerebellar rhombic lip but not during the expansion of this cell population at later stages. During perinatal development Wnt/β-catenin activity shifts to the cerebellar ventricular zone, a known germinal centre for GABAergic interneurons and glia, and was observed in cells radiating out from this region. By early postnatal development the expression of the Wnt/β-catenin reporter became progressively restricted to the developing Bergmann glia population.

To investigate the function of Wnt/β-catenin in these cell lineages and how its dysregulation could contribute to medulloblastoma, I used a combination of *ex vivo* organotypic culture, *in utero* electroporation and tissue-specific gene targeting to manipulate components of the pathway. Culturing slices of E18.5 cerebellum in the presence of small molecule activators of the Wnt/β-catenin pathway revealed a reduction in the expression of glial markers Sox9 and GFAP. In addition, interneuron lineage marker Pax2 was also reduced, supporting the conclusion that dysregulation of Wnt/β-catenin signalling affects the generation of cell lineages from the ventricular zone. To investigate this hypothesis further, I constitutively activated the Wnt/β-catenin signalling pathway in the developing cerebellum using Cre-*Lox* gene targeting to knock out *Apc*, a negative regulator of the pathway, in ventricular zone derived lineages. Cre-induced recombination of *Apc* resulted in nuclear accumulation of β-catenin, a sign that the pathway had become ectopically activated. Furthermore, a reduction in the expression of Sox9 and Pax2 was also observed in these mutant cells. From these data, I conclude a potential role for Wnt/β-catenin signaling in the regulation of glial/interneuron progenitors.

Combined, these data support a model where Wnt/β-catenin signalling could perform multiple functions in specification of the granule lineage, regulation of glial/interneuron progenitors and in glial differentiation/maturation. Importantly, dysregulation of progenitor self-renewal and differentiation is widely acknowledged to promote tumourigenesis. Thus, the data in this thesis support a potential mechanism for the development of medulloblastoma from the dysregulation of ventricular zone progenitors.

Acknowledgements

I am indebted to my supervisor John Mason for the guidance, insight, mentorship and never-ending patience he has shown throughout the duration of this project. I also thank Dave Price, Iain Whittle and Tom Pratt for useful discussions.

I could not have completed the work presented in this thesis without the technical assistance of numerous DBUG members. Particular thanks are owed to Vasiliki Fotaki for her expert training in various metholodogies and to Mike Molinek for his indispensable knowledge of everything in the lab. Thanks are also owed to Tom Nowakowski for assistance with *in utero* electroporation techniques and Dario Magnani for *ex vivo* culturing techniques.

I thank the rest of DBUG and the CIP for making this such a vibrant, stimulating and enjoyable workplace.

I thank Trudi Gillespie from the IMPACT Imaging facility for expert assistance with confocal microscopy and image analysis. I also thank Alan, Neil, Anne and the rest of the BRR technicians for their assistance with animal care.

Thank you to Louise Bicknell for taking on the horrendously boring task of proofreading my thesis.

Thank you to my fellow Wellcome Trust classmates Elise, Lynne, Robert and Tom for all the good times over the last four years. Thanks also to all the other friends I've had the good fortune to meet here in Edinburgh.

To my family, thank you for your unfaltering support and encouragement.

To Máire, thank you for always being there with a hug, a sympathetic ear or a cup of tea when I needed it. I could not have achieved this without you by my side.

Table of contents

Table legends

Figure legends

Abbreviations

β-gal	β-galactosidase
BAT-gal	β-catenin activated transgene driving β-galactosidase
BIO	6-bromoindirubin-3'-oxime
BLBP	Brain lipid binding protein
BrdU	5-Bromo-2'-deoxyuridine
Casp3	Caspase 3
CHIR	CHIR99021
CP	Choroid plexus
CNS	Central nervous system
CV	Cresyl violet
DAB	Diaminobenzidine
DCN	Deep cerebellar nuclei
E	Embryonic day
EGL	External granule layer
GABA	γ-Aminobutyric acid
GC	Granule cell
GFAP	Glial fibrillary acidic protein
GFP	Green fluorescent protein
GLAST	Glutamate aspartate transporter
GPC	Granule progenitor cells
HB	Hindbrain
IGL	Internal granule layer
IPC	Intermediate progenitor cell
IsO	Isthmic organiser
IWP2	Inhibitor of Wnt production 2
LI	Labelling index
LOH	Loss of hetrozygosity
LRL	Lower rhombic lip
MB	Midbrain

MHB	Midbrain-hindbrain
MHJ	Midbrain-hindbrain junction
ML	Molecular layer
NSC	Neural stem cell
NTZ	Nuclear transitory zone
P	Postnatal day
PBS	Phosphate buffered saline
PC	Purkinje cells
PCL	Purkinje cell layer
PCP	Planar cell polarity
PCNA	Proliferating cell nuclear antigen
PFA	Paraformaldehyde
r	Rhombomere
RL	Rhombic lip
SC	Subcutaneous
SPS	Sub-pial stream
UBC	Unipolar brush cells
URL	Upper rhombic lip
VM	Velum Medullaris
VZ	Ventricular zone
WM	White matter
WT	Wild type
YFP	Yellow fluorescent protein
XAV	XAV939

1 Introduction

Developmental signalling pathways regulate the myriad interacting processes required for the generation and maintenance of complex body structures from a small number of progenitor cells. The processes of cell specification, proliferation, migration, differentiation and apoptosis are all required throughout development and are controlled by a number of different developmental signalling pathways. Dysregulation of these processes can endow a cell lineage with a survival advantage such that it can, over time, accumulate the additional mutations required for a tumour to develop. The Wnt/β-catenin signalling pathway is a well-established regulator of various developmental processes and its oncogenic activation has been identified in a number of different cancers. Medulloblastoma, an aggressive tumour that forms in the cerebellum, is one such cancer that has been associated with activated Wnt/β-catenin signalling. This suggests that these tumours could arise as a result of Wnt/β-catenin signalling becoming dysregulated during development. However, the function of this pathway in cerebellum development is not yet fully understood.

1.1 Anatomy of the cerebellum

The cerebellum is a brain region primarily responsible for fine coordination of motor control. To achieve this, the cerebellum acts as a site for integration and modulation of electrical impulses from a variety of different central and peripheral nervous system regions. This task is carried out through the internal circuitry of a surprisingly small number of interconnected inhibitory and excitatory neuronal cell types. The identity of these cells and their anatomical location has been well described over the course of the last century (Altman and Bayer, 1997).

1.1.1 Gross anatomy of the cerebellum

Formed from tissue of the metencephalon (the most anterior region of the hindbrain – HB), the cerebellum sits above the fourth ventricle and HB immediately posterior to the midbrain (MB) (Fig. 1.1A-B). In mammals, the cerebellum can be partitioned

along the medial-lateral axis into two symmetrical lateral hemispheres and a distinct medial portion called the vermis. These regions can be readily distinguished by the anterior-posterior foliation pattern. This was described by the comparative anatomist Olof Larsell, who identified that the vermis of all mammals studied can be divided into 10 key lobes (designated as roman numerals I-X, Fig 1.1C) with the more complex foliation observed in species like humans and other apes resulting from subdivisions of these 10 lobes (Larsell, 1970). This conservation of basic structure suggests the mechanisms responsible for development of the cerebellum are conserved between species.

1.1.2 Cellular composition of the cerebellum

Within each lobe the cerebellum displays a surprisingly homogenous laminated histology comprised of three neuronal layers, each of which can be characterised by their component neurons (Fig 1.1D). At the centre of the cerebellar cortex sits the white matter (WM), which consists of myelinated axonal tracts surrounding three symmetrical clusters of deep cerebellar nuclei (DCN). The DCN are composed of two key neuronal lineages: the inhibitory γ-Aminobutyric acid (GABA)ergic inhibitory neurons, and glutamatergic excitatory neurons. The internal granule layer (IGL) is the first neuronal layer and borders the white matter core of the cerebellum. This layer is densely populated by granule cells (GCs) – the most abundant type of neuron in the brain. In addition, a considerably smaller population of interneurons resides within the IGL – consisting of GABAergic Golgi and Lugaro interneuons, as well as the excitatory glutamatergic unipolar brush cells (UBCs) and velate protoplasmic astrocytes. Superior to the IGL sits the Purkinje cell (PC) layer (PCL), which contains the somata of PCs arranged in a monolayer across the surface of the IGL. Wedged between the sizable PCs sit a unique class of radial glial cell called the Bergmann glia. Both PCs and Bergmann glia extend their processes from the PCL into the outermost layer of the cerebellum – the molecular layer (ML). The main components of this cell sparse layer are the characteristic arboreous PC dendrites and parallel GC axon fibres. In addition, the Bergmann glial radial processes span the entire width of the ML and terminate in end feet at the pial surface. Sparsely populated throughout the ML are two further populations of GABAergic inhibitory

interneurons, basket and stellate cells (Fig 1.1D). This arrangement of excitatory and inhibitory neurons and the microcircuitry between them allows for the modulation of signals entering the cerebellum.

1.1.3 Functional circuitry within the cerebellum

The cerebellum receives input signals from most regions of the brain as well as the spinal cord via two major afferents, mossy fibres and climbing fibres, which terminate within the IGL and ML respectively (Fig. 1.2). Within the IGL, mossy fibres provide input to the GCs through a structure called the glomerulus, which consists of mossy fibre axon terminals, Golgi interneuron axon terminals and GC dendritic boutons sheathed in velate astrocyte fibres (Chan-Palay and Palay, 1972; Itoh, 1984). The climbing fibres in contrast transcend the IGL and terminate at multiple points within a single PC dendritic tree. After GC activation by mossy fibres (modulated by the inhibitory Golgi cells), the signal is transferred through their axons, which extend from the GC into the ML and bifurcate into parallel fibres that run along the medial-lateral axis and synapse with PC dendrites across its path. Thus, a single mossy fibre input can influence hundreds of different PCs (Altman and Bayer, 1997). An additional level of signal complexity is offered by the extent of PC dendrite arborisation within the ML such that a single PC can contact as many as 200,000 GC axons (Tyrrell and Willshaw, 1992). This excitatory input to the PCs from the mossy fibres via GCs is modulated by the additional excitatory input from climbing fibres that synapse directly with the PC dendrite shaft and inhibitory inputs from the two ML interneuron populations. Stellate cell axons synapse onto PC dendrites, while basket cell axons synapse with the PC somata. Thus, all cerebellar inputs and microciruits converge on the PCs (Fig. 1.2), which integrate them into a single output that is carried via the PC axons to the DCN and onwards to the spine, brain stem and thalamus.

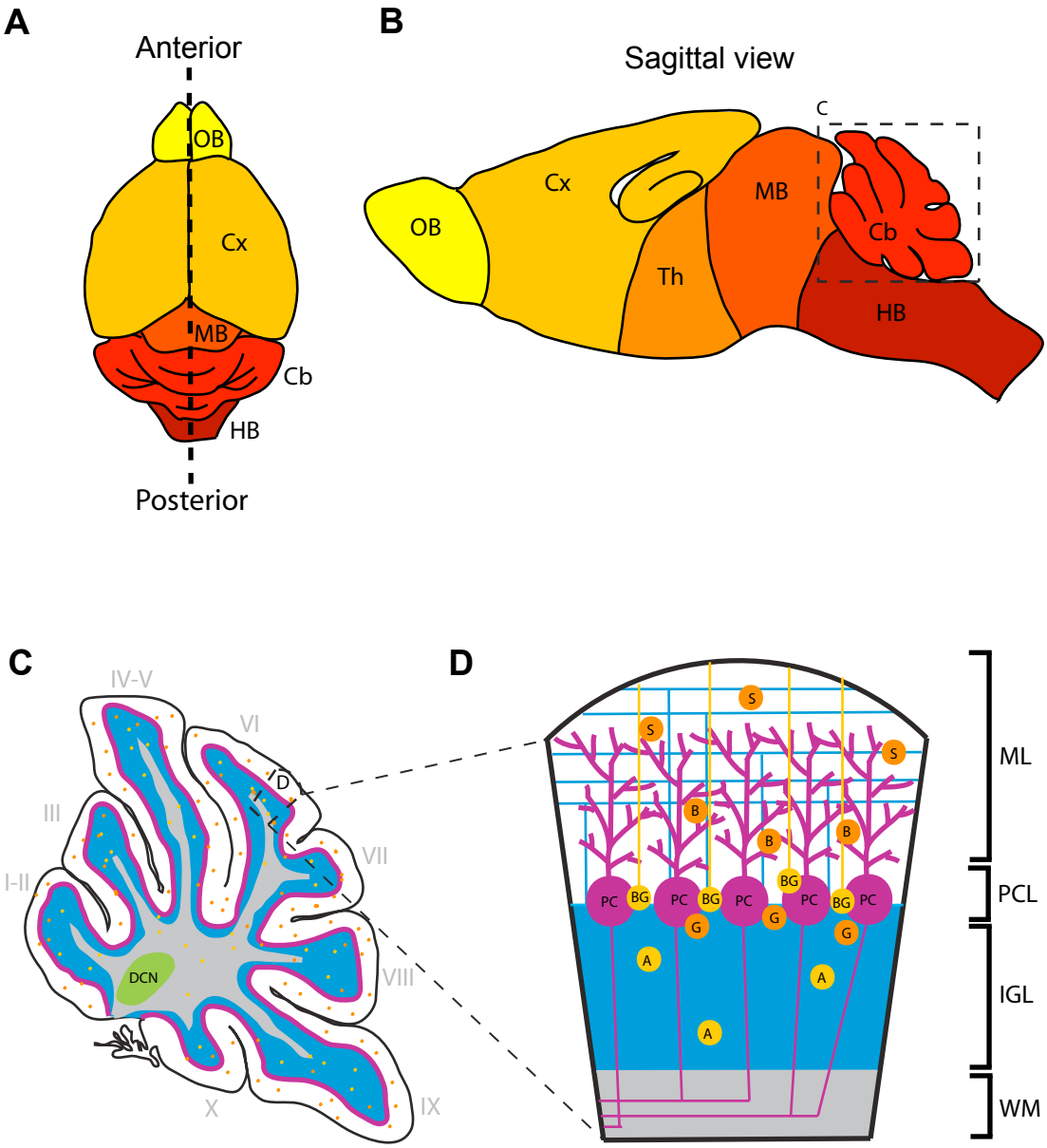

Figure 1.1 - Anatomy of the adult mouse cerebellum.
The adult mouse cerebellum is located betwen the MB and HB regions (A-B). The vermis of the cerebellum can be divided into 10 lobes (I-X), each with a similar laminated structure (C). The cellular composition of the cerebellum consists of a WM core, surrounded by the IGL, PCL and then ML (D). (**Brain regions**: OB = olfactory bulb, Cx = cortex, Th = thalamus, MB = midbrain, Cb = cerebellum, HB = hindbrain. **Cell types**: DCN = deep cerebellar nuclei, A = astrocyte, B = basket cell, BG = Bergmann glia, G = Golgi cell, PC = Purkinje cells, S = Stellate cells. **Cell layers**: ML = molecular layer, PCL = Purkinje cell layer, IGL = internal granule layer, WM = white matter.)

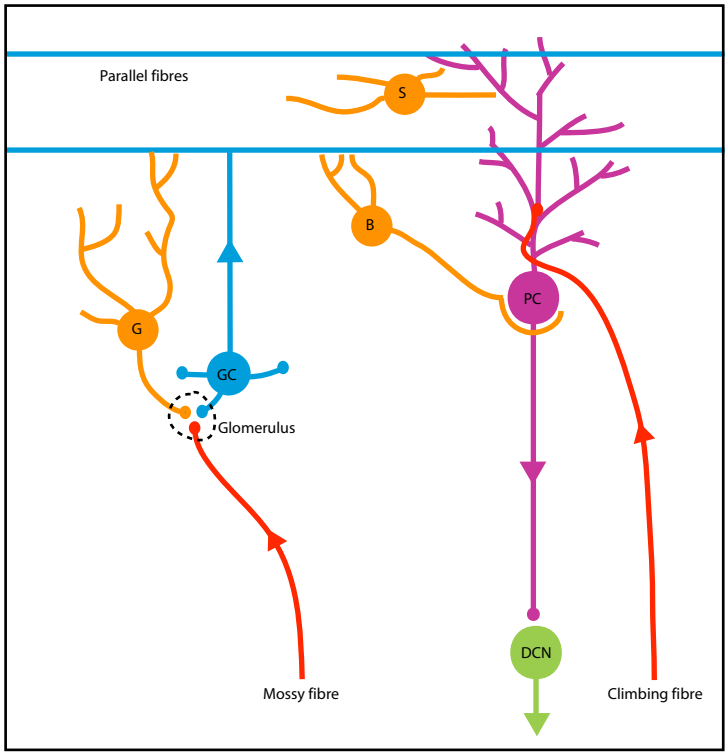

Figure 1.2 - Cerebellar circuitry.
Cerebellar input signals are brought via the mossy fibre or climbing fibre afferents. Mossy fibres terminate in the glomerulus, which contains the GC dendrite terminals and inhibitory Golgi cell axon terminals. This signal is transfered through the parallel axon fibres to many PC dendrites. PCs also receive input from the climbing fibre afferents. These two inputs converge on the PC and exit the cerebellum via the DCN. Inhibitory modulation is provided to the GCs by Golgi cells and to PCs by basket and stellate cells. Adapted from Wang and Zoghbi (2001).

1.2 Development of the cerebellum

The structural complexity and cellular heterogeneity of the adult cerebellum forms as the result of a tightly regulated programme of cell specification, proliferation, differentiation, migration and maturation beginning in embryogenesis and continuing until adulthood. These processes occur under the control of several interacting developmental signalling pathways, with myriad downstream transcription factors and cellular effectors. Below, the general cellular processes involved in cerebellum development is described and several of the key signalling molecules known to be involved are highlighted.

1.2.1 Tissue specification and early organisation

Unlike other brain regions, the cerebellar primordium is specified during the later stages of embryogenesis (approximately embryonic day (E) 9.5 in mouse). At this time point the main compartments of the central nervous system (CNS) can be morphologically distinguished from anterior to posterior: the telencephalon and diencephalon (forebrain), mesencephalon (midbrain), and the metencephalon and myelencephalon (hindbrain). Between the mesencephalon and metencephalon a morphological boundary develops, called the midbrain-hindbrain junction (MHJ), with the metencephalic tissue immediately posterior to this giving rise to the cerebellum (Zervas et al., 2004). The initial specification and patterning of the cerebellar anlage occurs under the control of signals from an organising centre at the MHJ called the isthmic organiser (IsO) (Brand et al., 1996; Martínez et al., 1995; Martinez et al., 1991).

This signalling centre forms by E7.5 at the expression boundary of two opposing homeobox transcription factors: *Otx2* (expressed in the mesencephalon) and *Gbx2* (expressed in the metencephalon and myelencephalon) (Simeone, 2000). A cascade of genetic interactions then follows, culminating in the combined expression of secreted signalling molecules FGF8 and Wnt1, and the transcription factor En1 that, by E9.5, demarcates the IsO gene expression signature: *Wnt1* and *Otx2* expressed to the anterior, *Fgf8* and *Gbx2* expressed to the posterior and *En1* expressed across the

boundary (Fig 1.3A) (Crossley and Martin, 1995; Davis and Joyner, 1988; Simeone, 2000). The importance of *Wnt1* expression as an organising molecule is demonstrated by knockout mouse models, which display severe MB-HB (MHB) developmental abnormalities (McMahon and Bradley, 1990; Thomas and Capecchi, 1990). The transcriptional link between *Wnt1* and *En1* was demonstrated by a study that showed firstly *Wnt1* expression is required for *En1* expression and secondly that the phenotype of the *Wnt1* knockout mouse can be rescued by addition of *En1* (Danielian and McMahon, 1996). Furthermore, it has also been shown that *En1* expression is required for the maintenance (but not initiation) of *Fgf8* expression (Liu and Joyner, 2001) and that the expression of *Wnt1* is in turn maintained by *Fgf8* expression (Adams et al., 2000).

Thus, a picture begins to emerge of a complex and interconnected gene network within the IsO whereby the active genes feedback on each other (Fig 1.3B). However, while all these genes (and their downstream partners) are required for IsO function, the key effector molecule for patterning of the surrounding regions is FGF8 (Crossley and Martin, 1995; Crossley et al., 1996; Martinez et al., 1999; Meyers et al., 1998; Reifers et al., 1998). These studies highlighted the IsO as a key *Fgf8* expression domain and demonstrated that loss of FGF8 results in a failure of the surrounding MB and cerebellar tissue to develop while ectopic expression of FGF8 in other brain regions causes the ectopic development of MB/cerebellar structures. From these early inductive cues provided by the IsO, the cerebellar primordium is established and the cell lineages are specified.

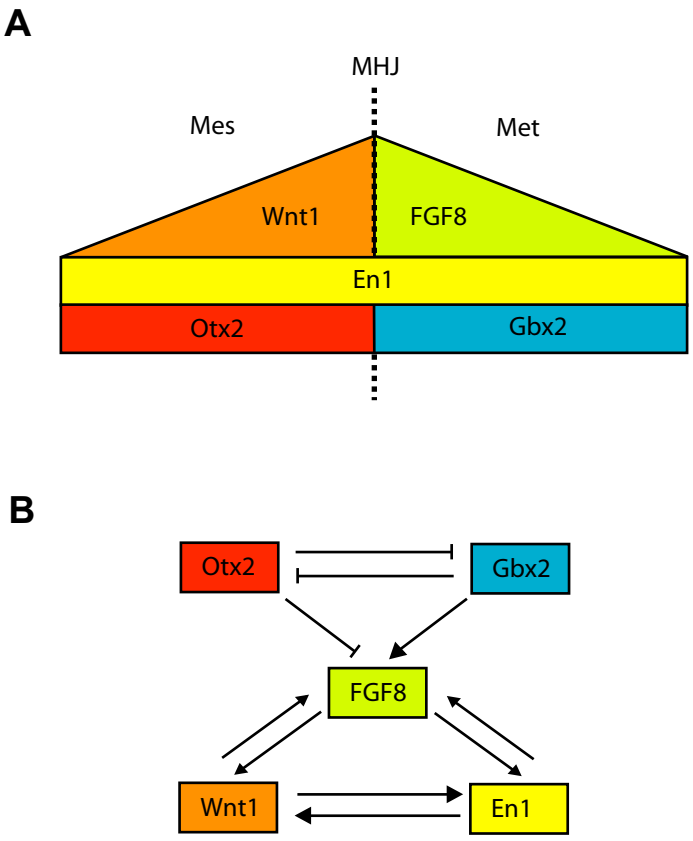

Figure 1.3 - Specification of the isthmic organiser.
The isthmic organiser is defined by a gene expression boundary at the midbrain hindbrain junction (MHJ) between *Otx2* in the mesencephalon (Mes) and *Gbx2* in the metencephalon (Met). This then initiates the expression of *Fgf8* to the posterior, *Wnt1* to the anterior and *En1* across the boundary (A). All five genes act in a self-regulating circuit (B). Adapted from Wang and Zoghbi (2001).

1.2.2 Cell specification within the ventricular zone and white matter

Cell birth in the cerebellar primordium begins at the ventricular zone (VZ), a layer of specialised radial glia lining the dorsal aspect of the fourth ventricle (Fig 1.4). Marked by the expression of known radial glial markers GLAST, Nestin, GFAP and BLBP (Casper and McCarthy, 2006; Dahlstrand et al., 1995; Hegedus et al., 2007), The VZ is one of the primary germinal zones for the cerebellum and produces the entire complement of cerebellar GABAergic and glial cell lineages. This begins at E10.5 with the birth of GABAergic DCN neurons (Hoshino et al., 2005; Sudarov et al., 2011), which migrate into a cell-sparse cluster called the nuclear transitory zone (NTZ) towards the anterior of the early cerebellum. PCs are then born in sequential waves from E10.5 until E13.5 (Altman and Bayer, 1997; Hashimoto and Mikoshiba, 2003; Miale and Sidman, 1961; Sudarov et al., 2011). Importantly, these two populations have been recently shown to develop from discrete and non-overlapping domains of the VZ neuroepithelium (Mizuhara et al., 2010), supporting the conclusion that the cells making up the VZ are developmentally heterogenous. After becoming post-mitotic, PCs initiate expression of the calcium binding protein Calbindin (Andressen et al., 1993) and migrate radially towards the pial surface of the cerebellum along the glial scaffold provided by the VZ radial glia (Edwards et al., 1990). Following the birth of the PC population, the VZ generates a population of Bergmann glia progenitors which have been birth dated to within 24 hours after PCs and have been shown to closely follow their radial migration path through the early cerebellum (Yamada et al., 2000; Yamada and Watanabe, 2002; Yuasa, 1996). Slightly overlapping with the tail end of PC and Bergmann glia cell birth, VZ radial glia then begin to produce the remainder of the inhibitory GABAergic lineage (stellate, basket, Golgi and Lugaro interneurons) (Hoshino et al., 2005) and the remaining glia. However, the precise temporal development of these different cell types has only recently been resolved.

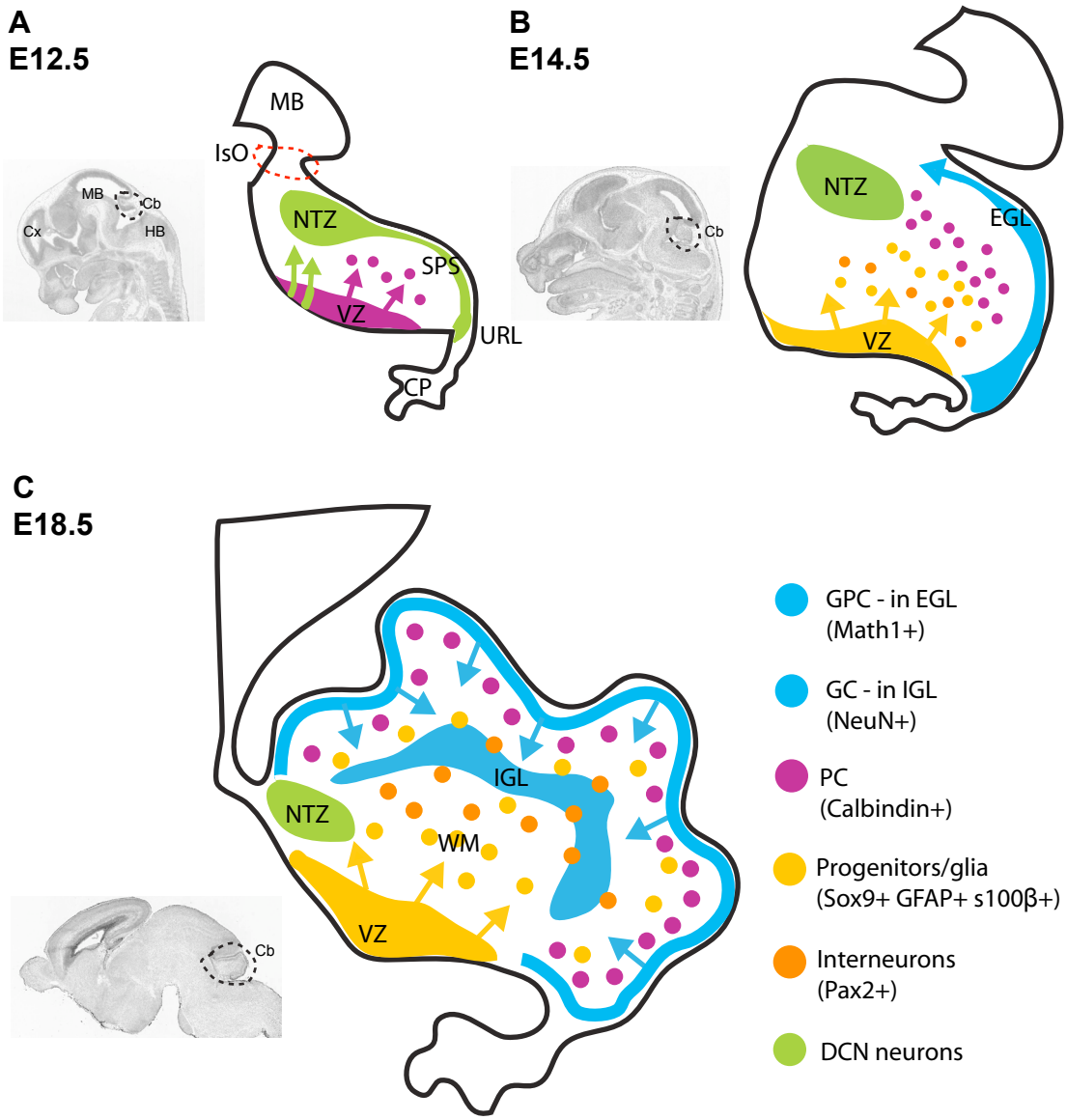

Figure 1.4 - Development of cell lineages within the cerebellum.
The germinal centres in the developing cerebellum can be defined by the cell lineages they produce: glutamatergic neurons at the URL and GABAergic neurons/glia at the VZ. By E12.5 (A) the cerebellum has begun to generate glutamatergic DCN neurons at the URL which migrate in the SPS to the NTZ. GABAergic DCN neurons and PCs are born at the VZ. By E14.5 (B) the URL has switched to the production of GPCs, which migrate over the pial surface to form the EGL. The VZ has produced the Bergmann glia progenitors and begins generating the progenitors that give rise to interneurons. By E18.5 (C) cerebellum lamination and foliation becomes apparent as the GPCs within the EGL begin to terminally differentiate and migrate into the IGL. PCs and Bergmann glia form a monolayer of cells during this process. The interneurons and remaining glia are then born from VZ-derived progenitors within the WM (NTZ = nuclear transitory zone, SPS = sub pial stream. URL = upper rhombic lip, VZ = ventricular zone). Histological images adapted from http://www.brain-map.org

BrdU birth-dating experiments have revealed that the Golgi, basket and stellate interneurons are born in an inside-out manner (Leto et al., 2009), with Golgi cells becoming post-mitotic first, followed by basket and then stellate cells – a process that is not complete until approximately postnatal day (P)15. The development of this cell lineage can be followed through the expression of Pax2, which is expressed during the final mitosis and persists until the cells become terminally differentiated (Maricich and Herrup, 1999; Weisheit et al., 2006). These studies identified expression of Pax2 in cells adjacent to, but not physically present in, the VZ from E12.5 (likely the developing DCN interneurons) and were able to trace the expression of Pax2 through to P15 from which point expression begins to diminish to undetectable levels by P30. This expression pattern followed that predicted by sequential interneuron development identified by birth dating studies (Leto et al., 2009) with expression spreading and then regressing from inside out.

Interestingly, additional evidence suggests that the generation of interneurons does not occur directly from the VZ but from progenitors that delaminate and continue to proliferate in the WM (Leto et al., 2006; Milosevic and Goldman, 2002; Milosevic and Goldman, 2004; Zhang and Goldman, 1996). More recent findings have shed new light onto the precise temporal nature of GABAergic interneuron development. Sudarov et al. (2011) used a tamoxifen inducible Cre-recombinase allele driven by the *Ascl1* promoter to carry out an elegant series of genetic fate mapping experiments tracing the generation of cell lineages from the VZ during development. Ascl1 has previously been demonstrated as essential for the generation of the full complement of cerebellar interneurons (Grimaldi et al., 2009). In this study, Sudarov et al. found that all VZ derived neurons and glia arise from *Ascl1* expressing progenitors and that the differentiation of all GABAergic interneurons occurs sequentially, first from *Ascl1* expressing VZ radial glia and then in an inside out pattern from *Ascl1* expressing WM progenitors. It was further revealed that the generation of astrocytes, after the early birth of the Bergmann glia population, also occurs from the *Ascl1* expressing progenitor population. This has recently been shown to occur in response to a secreted BMP signal (Zhang et al., 2011b).

However, the neuronal/glial potency of these WM progenitors remains unclear. The findings by Zhang and Goldman (1996) demonstrated that WM progenitors labelled in early postnatal rats gave rise to Golgi, basket and stellate interneurons as well as Bergmann glia and velate astrocytes but it was not clear whether these arose from a single or multiple progenitor populations. Consistent with the latter, Milosevic and Goldman (2002) revealed that the WM progenitor population can be separated into distinct and non-overlapping glial or neuronal lineages. However, a subsequent publication (Milosevic and Goldman, 2004) revealed that a limited number of isolated progenitors from the early postnatal WM were able to generate heterogenous neuronal and glial cell populations *in vitro*. Furthermore, they demonstrated that progenitors isolated from the VZ generated heterogenous populations at a greater frequency, supporting a model where progenitors delaminating from the VZ lose their potential early during migration through the WM and become progressively restricted to the glial or neuronal lineages. This conclusion is supported by recent evidence that GFAP expressing WM progenitors can give rise to both glia and interneurons over specific time windows during early postnatal development (Silbereis et al., 2009). Additionally, Sudarov et al. (2011) found that reduced Ascl1 expression leads to an increase in the production of astrocytes within the cerebellum, suggesting the gene could play a role in fate decisions from a multipotent progenitor pool. While further investigation is clearly required to conclusively determine the nature of WM progenitors during cerebellum development, the recent observation that the adult cerebellum contains a population of multipotent cells, based on the expression of neural stem cell marker CD133 (Lee et al., 2005), would support the hypothesis that multipotent progenitors persist from postnatal development through to adulthood.

1.2.3 Cell specification at the upper rhombic lip

In contrast to the glia and GABAergic neurons of the cerebellum, all glutamatergic neurons are derived from a separate germinal zone called the rhombic lip (RL). This relatively late-forming transient structure arises towards the caudal limit of the cerebellum at the interface between the developing neural tube and the roof plate of the fourth ventricle (Wingate, 2001). Sagittal sections through the early cerebellum

reveal the RL as a caudal extension of the VZ neuroepithelium, although importantly it is the physical interaction of the most caudal of these cells with the roof plate that endows cells with the inductive RL signals (Wingate, 2001; Wingate and Hatten, 1999). The RL is split into two domains, the upper RL (URL), which forms the edge of rhombomere (r)1 and the fourth ventricle, and the more extensive lower RL (LRL), which forms the boundary between r2-8 and the fourth ventricle. Between these two domains the choroid plexus (CP) invaginates into the fourth ventricle. Both of these RL domains can be molecularly defined by the expression of the transcription factor Math1 (Ben-Arie et al., 1997; Machold and Fishell, 2005; Wang et al., 2005), which has been shown to be essential for the development of GCs and neurons of the HB pre-cerebellar nuclei (Ben-Arie et al., 1997; Ben-Arie et al., 1996). Wnt1 and Wnt3A are also expressed in both the URL and LRL (Dymecki and Tomasiewicz, 1998; Landsberg et al., 2005; Louvi et al., 2007; Nichols and Bruce, 2006; Rodriguez and Dymecki, 2000).

It is from the URL that the glutamatergic neurons of the cerebellum arise (Fig. 1.4). The first of these are the projection neurons of the DCN, which are born from E10.5 to E12.5 (Fink et al., 2006). Initially expressing the transcription factor Pax6 followed by Tbr1 and Tbr2, these neurons are specified within the germinal region at the URL and migrate across the pial surface of the developing cerebellar anlage in a caudal to rostral direction forming a cell layer called the sub-pial stream (SPS). Upon reaching the rostral end of the SPS the cells bundle into the NTZ, which later gives rise to the DCN. From E12.5 onwards, development of the GC lineage commences with the birth of granule progenitor cells (GPCs) at the URL (Machold and Fishell, 2005; Wang et al., 2005). GPCs maintain the expression of Math1 and Pax6 as they proliferate within the URL before adopting a unipolar morphology and exiting the URL zone from E13.5. GPCs then migrate in a caudal to rostral direction over the pial surface of the cerebellum forming the external granule layer (EGL) (Alder et al., 1996; Wingate and Hatten, 1999). As the URL progenitors continue to proliferate and produce migratory GPCs, the EGL expands to surround the entire cerebellar anlage by E16.5. In addition to transcription factors Tbr2, Pax6 and Math1, the GPCs within the EGL are also known to express the zinc finger proteins Zic1, 2 and 3,

which are required for full development of the GC population (Aruga et al., 2002; Aruga et al., 1998; Gebbia et al., 1997; Nagai et al., 1997). The third cell population generated from URL progenitors are the UBCs. These glutamatergic neurons are born towards the end of URL GPC genesis, at around E18.5 (Englund et al., 2006). Similar to the preceding two populations of glutamatergic neurons generated at the URL, UBCs also express the transcription factors Math1, Pax6 and Tbr2, and exit the URL along two migratory paths. Initially, UBCs migrate in a rostral direction below the EGL to the developing WM, where they become widely dispersed before migrating into the postnatal IGL. In addition, a population of UBCs was found to migrate rostrally in a ventral stream along the VZ before exiting the cerebellum and ending in the hindbrain (Englund et al., 2006).

1.2.4 Cell specification at the lower rhombic lip

Like the URL, the LRL also exists as a transient progenitor domain. Given its close anatomical and developmental proximity to the URL, it generates a strikingly different complement of neurons – both in terms of anatomy and function. Quail-chick embryo grafting experiments revealed that the LRL gives rise to a ventrally migrating population of cells that populated the pre-cerebellar nuclei within the brain stem from E12.5 through to late embryogenesis (Tan and Le Douarin, 1991; Wingate and Hatten, 1999). Genetic fate mapping experiments following the progeny of *Wnt1* expressing LRL progenitors confirmed these findings and demonstrated that the LRL can be further separated into dorsal and ventral domains, with the dorsal progenitors giving rise to mossy fibre neurons that populate the multiple pre-cerebellar nuclei within the brain stem and ventral progenitors giving rise to climbing fibre neurons that exclusively populate the inferior olive nuclei (Landsberg et al., 2005; Rodriguez and Dymecki, 2000). *Math1* fate mapping experiments support this identification of individual progenitor domains within the LRL (Wang et al., 2005).

1.2.5 Lineage differentiation and lamination of the cerebellum

As the cells of the cerebellum are specified and begin their migration from the two germinal centres, a series of coordinated events leads to the cerebellum acquiring its laminated and foliated adult cellular structure. The most notable of these is the

considerable expansion of GPCs within the EGL followed by their subsequent migration and population of the IGL (Fig 1.4). The EGL is characterised by extensive proliferation from E18.5 during the first two weeks of postnatal development, as the abundant GC population is generated from the GPCs. Several lines of evidence suggest that this proliferation is dependent on paracrine interactions with neighbouring GCs and also on the Sonic hedgehog (Shh) morphogen secreted by the PCs which sit below the EGL (Dahmane and Ruiz i Altaba, 1999; Gao et al., 1991; Wechsler-Reya and Scott, 1999). Consistent with this, ectopic activation of the Shh signalling pathway in the cerebellum results in EGL hyperplasia (Goodrich et al., 1997; Kim et al., 2003; Oliver et al., 2005) and the Zic proteins, expressed in the GPCs, have been shown to transcriptionally regulate the Gli family of Shh signal transduction proteins (Koyabu et al., 2001). The Notch signalling pathway has also been implicated in GPC expansion (Lütolf et al., 2002). The Notch pathway functions through the binding of a Jagged ligand to a Notch receptor, which then induces the activity of a family of Hes transcription factors. Within the GPC population, the ligand Jagged-1 has been shown to promote proliferation of GPCs through the receptor Notch-2 and the downstream effector Hes-1 (Solecki et al., 2001). Interestingly this activity is thought to function downstream of the Shh pathway (Dakubo et al., 2006). In addition, FGF signalling has been shown to modulate the Shh response in GPCs (Yu et al., 2011), illustrating how different pathways converge to regulate a developmental process.

While proliferation of the EGL occurs until approximately P15, populations of GCs become post mitotic and exit the cell cycle from the early postnatal period, raising the question of what forces particular GCs to exit the cell cycle while their neighbours remain in a proliferative state. Interestingly, two domains of the EGL have been identified – the inner and outer EGL – with the inner EGL expressing cell cycle inhibitors, such as P27/kip1 (Miyazawa et al., 2000) and REN (Argenti et al., 2005). REN has been shown to function as a Shh signal antagonist, providing an explanation for how cells previously cycling under the control of Shh can exit the cell cycle while Shh persists in the extracellular environment (Argenti et al., 2005). The external factors that signal this change to cell cycle dynamics are likely to be

complex, but one theory is that this is mediated by an FGF signal within the EGL. Consistent with this, an array of FGF ligands and receptors have been identified throughout the developing cerebellum (Yaguchi et al., 2009). FGF2, in particular, was identified within the EGL during early postnatal stages (Yaguchi et al., 2009) and has been shown experimentally to reduce GPC proliferation and promote GC differentiation (Fogarty et al., 2007). Signalling by BMP secreted factors is also known to promote the differentiation of GPCs. The BMP2 ligand, expressed within the EGL, has been shown to antagonise the Shh signal through its downstream effector Smad5 (Rios et al., 2004).

During the proliferation of GPCs from late embryonic to early postnatal stages, the PCs, originally specified at the VZ, begin dispersing to form a monolayer of cells below the EGL. The dispersal of PCs from a multilayered cell cluster to a consistent monolayer occurs as the cerebellum expands with the proliferation of GPCs. This process is thought to be controlled by the expression of Reelin from the NTZ initially and then from the GPCs (Rice and Curran, 2001). Reelin is an extracellular matrix (ECM) protein and was identified as the gene product mutated in the *reeler* mouse model (D'Arcangelo et al., 1995) - a well-studied model of ataxia characterised by extensive cellular disorganisation within the cerebellum (Rice and Curran, 2001).

The Bergmann glia provide structural support for the continued development of the cerebellum and have been shown to closely follow PCs from their birth at the VZ. Analysis of glial proteins GLAST and Tenascin reveal extensive expression immediately below the developing PC population during late embryogenesis-early postnatal development (Yamada et al., 2000; Yamada and Watanabe, 2002; Yuasa, 1996). This layer then becomes progressively compacted around the PCL as the PCs establish their monolayer during the first postnatal week. However, ^{3}H-thymidine label retention analysis has revealed that glial cells continue to be generated from the VZ and to expand within the developing cerebellar WM at this late embryonic-early postnatal stage (Altman and Bayer, 1997). By P7 the Bergmann glia become distinguishable from other astrocytes, characterised primarily by their unipolar shape and the early extension of glial fibres through the PCL into the expanding ML and

proliferating EGL (Yamada and Watanabe, 2002). Expression of members of the Sprouty family of FGF feeback antagonsists in the developing Bergmann glia population suggests tight regulation of this pathway is important for their development (Yu et al., 2011). Notch signalling is also known to be required for the correct positioning of Bergmann glia within the PCL (Komine et al., 2007; Lütolf et al., 2002).

During this early postnatal time frame, the GCs begin to exit the inner EGL and migrate radially into the cerebellum via specific interactions with the developing Bergmann glial fibres (called interstitial junctions) that extend into the ML - a region that forms from the space left behind by migrating GCs. During this exit from the EGL, GCs begin to express a number of mature neuronal markers such as class 3 β-tubulin and NeuN (Tomoda et al., 1999; Weyer and Schilling, 2003). The GCs then migrate through the PCL to their final location within the IGL, a process that is complete by P21 (Altman and Bayer, 1997; Sillitoe and Joyner, 2007; Wang and Zoghbi, 2001). During their migration, GCs leave behind the characteristic bifurcated axon fibre in the ML, which will eventually synapse with the developing PC and Golgi cell dendrites. As the terminally differentiated GCs begin to enter the IGL, the cerebellar anlage starts to expand resulting in the formation of the folia. Initially, the pial surface of the cerebellum appears smooth. However, by E17.5 several shallow fissures become evident that produce the five primary lobes (anterobasal, anterodorsal, central, posterior and inferior). During postnatal growth these primary lobes undergo extensive growth and begin to subdivide into the subsequent 10 mature lobes that make up the gross appearance of the adult cerebellum (I-X) (Altman and Bayer, 1997; Larsell, 1970). The generation of the fissures that lead to the primary and then the final folia are the result of anchoring centres forming at the base of each fissure (Sudarov and Joyner, 2007). This begins with an inward thickening of the EGL at each presumptive fissure, which then causes a slight invagination of the PCs and a fanning out of the glial fibres from the pial edge of the fissure. After this, expansion of the folia becomes largely mechanical as the influx of GCs causes the overall structure to grow between each fixed anchoring centre.

During this time, the populations of Golgi, basket and stellate interneurons become terminally differentiated from the WM progenitor population and migrate to their final locations within the IGL and ML, a process that is complete around the time GC population of the IGL ends (P21). The genetic fate mapping study undertaken by Sudarov et al. (2011), the most high resolution summary of temporal interneuron generation to date, revealed that the IGL-resident Golgi interneurons are born first (between E14.5-E18.5). Basket and then stellate interneurons are then born from WM progenitors up until P7 before migrating to their final location in the inner and outer ML respectively.

As a result of these processes (Fig. 1.5), the full lamination of the cerebellum is evident by P21, with the DCN forming the cerebellar core surrounded by the WM, which carries the key afferents in and out of the cerebellum, in turn surrounded by the densely packed IGL, the PCL monolayer and finally the extended ML. The last stage of cerebellum development, which continues well into early adulthood, is the growth of axons and dendrites as the microcircuitry within the cerebellum becomes established and refined.

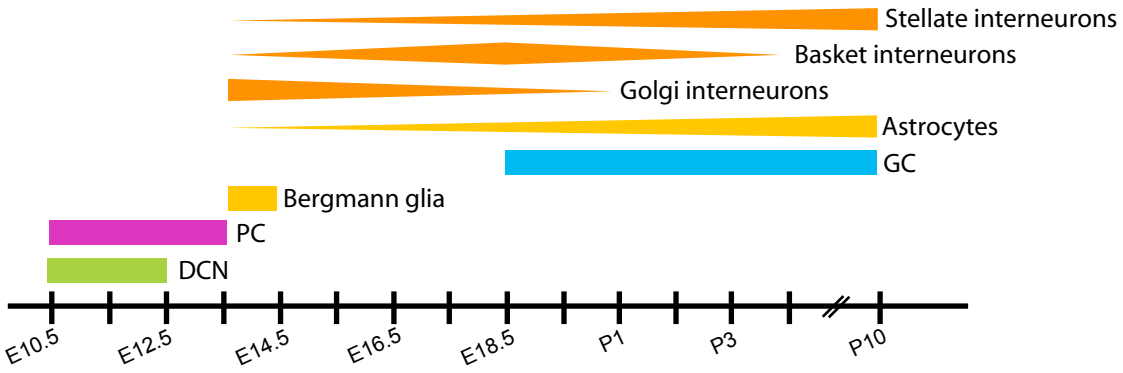

Figure 1.5 - Timing of cell birth during cerebellum development.
Initial differentiation of the various cerebellar cell lineages has been established from numerous studies using birth dating and genetic fate mapping approaches. Adapted from Sudarov et al. (2011).

1.2.6 Development of cerebellar circuitry

The generation of the connections required for cerebellum function begins with the arrival of the two key cerebellar inputs – mossy and climbing fibres. Retrograde tracing experiments carried out a number of years ago revealed that mossy fibre afferents from the various pre-cerebellar nuclei into the developing IGL occurs sequentially from mid-embryonic to early postnatal periods (Ashwell and Zhang, 1992). These early axons then branch off and send small projections towards the developing PCL, which make contact with PCs and early migrating GCs. The establishment of GC-mossy fibre synapses then follows and it is the early activity between these GC-mossy fibre connections that is thought to initiate the full maturation of GCs (Hatten and Heintz, 1995).

The arrival of climbing fibre inputs and the establishment of connections with PCs coincides with the dispersal of PCs into the monolayer at around E17.5 (Ashwell and Zhang, 1992; Hatten and Mason, 1990). As the key output generators for the cerebellum, PCs undergo a number of changes during their maturation once they have established the monolayer between the IGL and ML. The most notable of these is the growth and elaboration of their extensive dendritic arbours through the entire width of the ML. Beginning within the second postnatal week, this process is known to be dependent on the interaction between PCs with neighbouring PCs and, most importantly, GC axons (Baptista et al., 1994). These initial contacts between PC dendrites and the GC axons eventually lead to mature synapse formation. Concordantly, the axons from the PCs exit the cerebellum through the WM to form contacts with the DCN neurons. After the establishment of cerebellar input and output connections and the key connections between PCs and GC, the inhibitory interneuron connections with each of these cell populations are formed. Little is currently understood about this, but the connections formed are important for modulation of the excitatory signals generated by GCs.

1.3 The Wnt/β-catenin signalling pathway

The process of generating a fully functional adult cerebellum relies on the coordinated action of a number of different developmental signalling molecules and their downstream transduction pathways. As discussed above, the signalling molecules Shh, Notch, BMP and FGF are all known to function at various points during cerebellum development. Signalling by the Wnt family of secreted glycolipoproteins represents another key mechanism for regulation of cell proliferation, polarity, migration, apoptosis and fate determination during tissue development and homeostasis (Logan and Nusse, 2004). Wnt signalling is known to be actively involved in neural development and, not surprisingly, its dysregulation is linked to developmental defects and cancer. Below follows a description of Wnt signalling, with particular attention paid to signalling through the Wnt/β-catenin pathway.

1.3.1 A brief history of Wnt signalling

The name Wnt comes from a combination of *wingless* and *Int1* – two gene homologues identified in *Drosophila* and mouse respectively in the 1980s (Rijsewijk et al., 1987). The *Int1* gene was initially identified as an oncogene that, upon activation by the mouse mammary tumour virus (MMTV), contributed to the development of mammary carcinoma (Nusse and Varmus, 1982). This gene was then shown to be homologous to the *Drosophila* development gene *wingless* (Rijsewijk et al., 1987), which is required for embryo segmentation and leads to severe cuticle abnormalities when mutated. The observation in *Drosophila* that mutations in *porcupine, dishevelled* and *armadillo* genes led to a similar phenotype, followed by genetic epistasis experiments analysing the relationship between them, allowed the initial construction of a Wnt signal transduction pathway with *porcupine* lying upstream of *wingless* and then *dishevelled, shaggy/zeste-white 3* and *armadillo* lying downstream (Noordermeer et al., 1994). Concurrently, it was noted that injection of mouse *Wnt1* mRNA into early stage *Xenopus* embryos resulted in body axis duplication (McMahon and Moon, 1989), allowing development of a robust assay to test the extent of Wnt pathway conservation. Indeed, injection of Dsh (vertebrate

homologue of *dishevelled*), β-catenin (vertebrate homologue of *armadillo*) and a dominant-negative GSK3 (vertebrate homologue of *shaggy/zeste-white 3*) into *Xenopus* embryos revealed an identical phenotype to *Wnt1* mRNA injection (Guger and Gumbiner, 1995; He et al., 1995), consistent with the components and activity of the newly identified Wnt pathway being conserved between invertebrates and vertebrates.

Combined, these early *Drosophila* and *Xenopus* studies revealed the nature of a highly conserved signalling pathway activated by a secreted Wnt ligand. Since then, comparative genomics has identified 19 different secreted mammalian Wnt ligands, which can be further divided into 12 subfamilies that are conserved across the animal kingdom, from *Nematostella* and *Drosophila* to *Xenopus*, mouse and human (van Amerongen and Nusse, 2009). In addition, three families of Wnt receptor molecules (termed Fz in mammals) have been identified across the same animal groups, with a total of 10 Fz molecules (Fz1-10) in mice and humans (van Amerongen and Nusse, 2009). This illustrates the potential for a remarkable degree of Wnt signalling complexity (particularly in mammals) based on the different permutations of receptor/ligand combinations.

Initially, Wnt pathway functions were divided into either 'canonical' or 'non-canonical' groups based on the correlation of the former with an increase in the cellular levels of β-catenin and an increase in β-catenin mediated transcription (Shimizu et al., 1997). The non-canonical pathways have traditionally been defined as the planar cell polarity (PCP) pathway and the Wnt/Ca^{2+} pathway. The first of these was based on findings in *Drosophila* that *wingless* is required for cell polarity independently of *armadillo* (the *Drosophila* β-catenin homologue) (Vinson and Adler, 1987), while the second stemmed from observations in *Xenopus* that certain Wnt ligands can stimulate intracellular Ca^{2+} release, again through a β-catenin independent mechanism (Slusarski et al., 1997). However, as will be discussed below, recent findings suggest this classification is an oversimplification (van Amerongen and Nusse, 2009). Thus, for the remainder of this thesis Wnt-induced β-

catenin mediated activation of downstream target genes is referred to as the 'Wnt/β-catenin signalling pathway' as opposed to the 'canonical' pathway.

1.3.2 Wnt/β-catenin signal transduction and components of the pathway

The 19 mammalian Wnt ligands are cysteine rich proteins of between 350-400 amino acids with an N-terminal secretion peptide (MacDonald et al., 2009). After translation, Wnt proteins undergo several modifications that are essential for their function, including glycosylation and palmitoylation of a conserved cysteine residue by the acyltransferase Porcupine (Porcn) (Takada et al., 2006; Willert et al., 2003). An additional gene termed *Wntless* (*WIs* - also known as *evenness interrupted, evi*) was identified in *Drosophila* as responsible for trafficking the Wnt ligand from the Golgi to the plasma membrane for secretion (Bänziger et al., 2006). After secretion by the Wnt-producing cells, the ligand binds the seven-pass transmembrane Fz receptor at the surface of the target cell (Bhanot et al., 1996). For Wnt/β-catenin signalling the binding of a Wnt ligand to the Fz receptor also involves the cooperation of a single-pass transmembrane protein called LRP5/6 in mammals (Pinson et al., 2000). Interestingly, multiple Wnts have been observed to bind single Fz receptors and vice versa (Bhanot et al., 1996), indicating a degree of promiscuity between the ligand/receptor interaction.

At the level of receptor binding, Wnt signalling (through β-catenin dependent or independent pathways) is subject to modulation by a series of agonists and antagonists. The secreted Fz related proteins (sFRPs) and Wnt inhibitory protein (WIF) act antagonistically by binding to Wnt and, in the case of SFRPs, also to Fz (Bovolenta et al., 2008). Adding to the complexity of this modulation, SFRPs have also been shown to act as agonists of the pathway in certain contexts (Esteve et al., 2011). An additional antagonist of Wnt signalling is the protein Dickkopf (Dkk), which is technically an antagonist of the LRP5/6 co-receptor (Semënov et al., 2001) and thus only affects Wnt/β-catenin signalling. Agonists of Wnt/β-catenin signalling include two proteins called Norrin and R-spondin, both of which have been shown to bind Fz causing activation of the Wnt/β-catenin pathway (Kazanskaya et al., 2004;

Xu et al., 2004). Although R-spondin was recently shown to complement Wnt/β-catenin activity by signalling through an independent pathway mediated by the Lgr5 receptor (de Lau et al., 2011).

Binding of a Wnt ligand to the Fz/LRP5/6 receptor complex initiates signalling through the key effector molecule β-catenin. Under conditions when the Fz/LRP5/6 receptor complex is not engaged by a ligand, the cytoplasmic levels of β-catenin are regulated by a protein complex called the β-catenin destruction complex (Fig 1.6). This complex consists of a number of proteins, including tumour suppressors Axin and APC, and the kinases CK1 and GSK3 (which is present in both α and β isoforms). Due to the ability of Axin to bind each of these constituent proteins it is thought to act as a general scaffold for the complex (Kimelman and Xu, 2006; Lee et al., 2003). Once recruited to the complex, CK1 and GSK3 sequentially phosphorylate β-catenin at a series of residues near its N-terminus, signalling the phospho-β-catenin for destruction by a ubiquitin ligase complex (Aberle et al., 1997). The role of APC in the destruction complex is surprisingly less well understood – despite the well-documented genetic evidence of its importance in β-catenin regulation (Kinzler and Vogelstein, 1996; Morin et al., 1997; Sansom et al., 2004). However, several conserved Axin and β-catenin binding motifs have been identified in the APC protein (Näthke, 2004). In addition, it has been shown to interact directly with GSK3β (Rubinfeld et al., 1996), strongly suggesting a role in mediating phosphorylation of β-catenin.

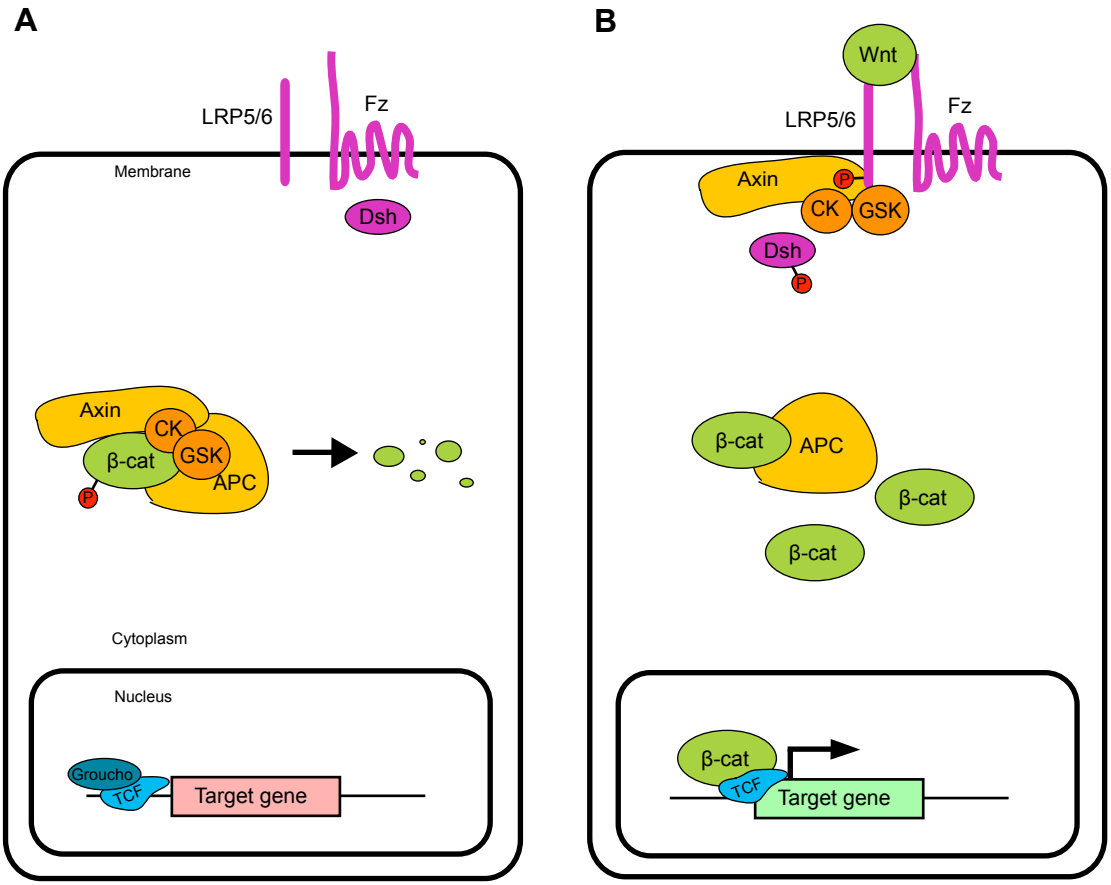

Figure 1.6 - Core components of the Wnt/β-catenin signalling pathway.
(A) In the absence of a bound Wnt ligand, a protein complex consisting of Axin, APC, CK1 and GSK3 mediates the phosphorylation of β-catenin, marking it for ubiquitination and subsequent degradation. (B) When a Wnt ligand binds the Fz/LRP5/6 co-receptor complex, a cascade of events is inititated involving phosphorylation of Dsh and LRP5/6 and removal of the protein complex from β -catenin. This allows non-phosphorylated β-catenin to accumulate and translocate into the nucleus where it disrupts the Groucho/TCF repressor complex and initiates transcription of downstream Wnt target genes. Adapted from Clevers (2006).

The destruction complex also appears to demonstrate a number of self-regulatory mechanisms. In addition to phosphorylating β-catenin, CK1 and GSK3β have been shown to also phosphorylate Axin and APC, which leads to increased affinity for β-catenin and subsequently enhanced β-catenin degradation (Kimelman and Xu, 2006). The opposite effect has been shown to result from the action of two external phosphatases, PP1 and PP2A, which dephosphorylate Axin and APC (Luo et al., 2007) causing a reduction in the activity of the destruction complex. Furthermore, the overall kinetics of β-catenin destruction appears to be largely regulated by cellular Axin levels, which are considerably lower than the other destruction complex components (Lee et al., 2003). This provides a potential explanation for how Wnt/β-catenin signal transduction can be insulated by fluctuating levels in the other components, which are known to be involved in additional cellular processes. Current understanding of these events is limited, but together this suggests the destruction complex is a considerably more fluid entity than described by classical Wnt signalling dogma.

Upon engagement by their respective ligands, the Fz/LRP5/6 complex initiates a sequence of events that results in the inhibition of β-catenin destruction complex kinase activity (Fig 1.6). The key action of this intracellular signalling cascade is the Wnt ligand-induced phosphorylation of LRP5/6, which generates a docking site for Axin (Mao et al., 2001; Tamai et al., 2004). Interestingly this phosphorylation is understood to be carried out by Axin-bound GSK3 and CK1 (Zeng et al., 2008; Zeng et al., 2005). Recruitment of the Axin/GSK3/CK1 protein complex to the membrane is thought to be carried out by Dsh, which interacts with Fz and becomes phosphorylated upon binding of a Wnt ligand (Wallingford and Habas, 2005). Combined, this leads to the generally accepted theory that Wnt induced activation of Fz/LRP5/6 causes the Dsh-mediated recruitment of Axin-GSK3/CK1 to the membrane allowing for the phosphorylation of LRP5/6. However, the specific sequence of events that then results in the inhibition of β-catenin phosphorylation is currently uncertain. For example, it is not clear whether the whole destruction complex is recruited to the membrane or whether it is disrupted in the cytoplasm and only Axin/GSK3/CK1 are relocated to the membrane. The observation of

dephosphorylated β-catenin initially at the plasma membrane shortly after Fz/LRP5/6 activation would support the latter (Hendriksen et al., 2008). Regardless, the end result is the inhibition of destruction complex activity and the accumulation of dephosphorylated β-catenin in the cytoplasm.

After cytoplasmic stabilisation of β-catenin, it translocates to the nucleus through association with the transcription factor FoxM1 (Zhang et al., 2011a) to initiate the downstream transcriptional response. This occurs through an interaction with the TCF/LEF transcription factor complex. In the absence of Wnt/β-catenin signalling, TCF/LEF represses gene expression through interaction with the transcriptional repressor Groucho. β-catenin has been shown to displace Groucho, resulting in the formation of a transcriptionally active complex (Daniels and Weis, 2005). This transcriptional complex recognises a conserved DNA seqeuence containing a CCTTTGATC motif (Korinek et al., 1997) that is present in the regulatory region of Wnt/β-catenin target genes. The specificity of the β-catenin/TCF/LEF complex for the DNA motif has been demonstrated by transgenic reporter mice that expressa reporter protein, usually β-galactosidase (β-gal) or green fluorescent protein (GFP), under the control of several of these binding sites (DasGupta and Fuchs, 1999; Korinek et al., 1997; Maretto et al., 2003). A large number of taget genes have been identified that are activated by the β-catenin/TCF/LEF transcriptional complex (see http://www.wnt.stanford.edu for a comprehensive summary), resulting in the potential for Wnt/β-catenin signaling to activate a variety of transcriptional programmes. Consistent with this, a wide range of cellular processes are known to be regulated by Wnt/β-catenin activity, the majority of which appear to be specific to cell type and developmental stage (Logan and Nusse, 2004).

1.3.3 Complexities and recent insights into Wnt signal transduction

It is important to note that a number of the components of the Wnt/β-catenin pathway also hold alternative cellular functions that need to be taken into consideration when discussing experimental manipulation of Wnt signalling. β-catenin, for example, is a well characterised component of adherens junctions (Peifer et al., 1992) in addition to its role as a signalling molecule. Unlike the highly dynamic nature of β-catenin involved in Wnt signalling, the pool of β-catenin bound

to adherens junctions appears highly stable. APC has also been shown to have a number of structural functions in addition to its role as a signalling molecule, including microtubule assembly (Kroboth et al., 2007; Zumbrunn et al., 2001) and mitotic spindle orientation (Yamashita et al., 2003). The relationship between these alternative functions and Wnt/β-catenin signalling is not well understood.

The dynamics of Wnt signal transduction are also not as clear-cut as traditionally presented. It is widely known that, in addition to signalling via β-catenin, Wnt ligands can also induce the PCP or Ca^{2+} pathways through Fz binding (Slusarski et al., 1997; Vinson and Adler, 1987). However, it is becoming evident that there is a certain degree of interaction between these three pathways. For example, activation of the LRP5/6 co-receptor, known to induce signalling through β-catenin, has been shown to inhbit signalling through the PCP pathway by disrupting the ability of non-canonical Wnt ligands (e.g. Wnt5A) to bind Fz (Bryja et al., 2009; Tahinci et al., 2007). Similarly, the Wnt/β-catenin pathway antagonist Dkk has also been shown to affect PCP signalling through the LRP5/6 co-receptor (Caneparo et al., 2007). There is also evidence to suggest that signalling through β-catenin can feedback on itself, both positively and negatively. Activation of Wnt/β-catenin signalling can induce expression of Axin and Dkk, both negative regulators of the pathway (Chamorro et al., 2005; Jho et al., 2002). Conversely, Wnt/β-catenin signalling can also positively feed forward through the activation of R-spondin and TCF/LEF expression (Hovanes et al., 2001; Kazanskaya et al., 2004). These observations all suggest that Wnt signal transduction is better thought of as a network of interactions with multiple outcomes, cross-talk and regulatory inputs, rather than several distinct linearly progressing pathways (van Amerongen and Nusse, 2009).

1.4 Multiple roles for Wnt/β-catenin signalling in neural development

The large network of proteins involved in Wnt/β-catenin signalling and the numerous downstream target genes make the cellular response to a Wnt signal highly

context dependent. Such complexity is consistent with the wide range of developmental processes that Wnt/β-catenin signalling has been implicated in; including proliferation, fate determination, differentiation, migration and apoptosis (Clevers, 2006). All of these processes are required for the induction, patterning, growth and maturation of the central nervous system and, not surprisingly, Wnt/β-catenin signalling has been identified as a key developmental pathway coordinating a range of developmental processes at each of these stages.

1.4.1 Neural patterning

After induction of neural tissue in the early embryo, development of the central nervous system begins with the regionalisation and patterning of the area. This is achieved through the diffusion of multiple signalling molecules across the anterior-posterior, medial-lateral and dorsal-ventral axes endowing all cells with positional information. Wnt/β-catenin signalling has been proposed to act early on in neural development as an anterior-posterior patterning factor. Wnt ligands are expressed in a gradient from posterior-high to anterior-low in the developing neural tube and that this signal is necessary and sufficient for the anterior-posterior patterning of the early neural tube (Kiecker and Niehrs, 2001). Additionally, the development of anterior brain structures then relies on the inhibition of Wnt/β-catenin signalling in the anterior, partly through the expression of the Wnt antagonist Dkk by anterior cells (Glinka et al., 1998; Mukhopadhyay et al., 2001). Wnt/β-catenin signalling is also important for establishing the dorsal-ventral axis, with experiments in chick embryos showing that Wnt expression suppresses ventral cell fates and induces dorsal characteristics in the developing telencephalon (Gunhaga et al., 2003). Any given cell's positional identity is then defined based on the receipt of a combination of different secreted molecules and subsequently an appropriate transcriptional response is generated. The developing neural tissue is therefore compartmentalised into defined regions (e.g. telencephalon, diencephalon, mesencephalon) that allows the development of specific neural structures to proceed (e.g. cortex, thalamus, colliculus).

1.4.2 Regulation of neural stem cell function

Within specific brain regions, Wnt/β-catenin signalling is then involved as a key regulator of the progenitor populations responsible for generating the various lineages of differentiated cell types present within the adult brain. Establishment of full cerebral cortical lamination, for example, results from the regulation of progenitor and transit amplifying cell proliferation and differentiation. Cortical neurons are produced during embryogenesis from a population of radial glia that line the lateral ventricles. These multipotent neural stem cells (NSCs) divide asymmetrically to produce either terminally differentiated neurons, intermediate progenitor cells (IPCs) or an additional daughter radial glia. IPCs are essentially transit amplifying cells and act to amplify the neurogenic pool by dividing to produce two terminally differentiated neurons (Molyneaux et al., 2007). Considerable experimental evidence suggests this process is regulated, at least in part, by the Wnt/β-catenin signalling pathway (Fig 1.7).

A number of Wnt ligands have been identified expressed in a gradient from a signalling centre (the cortical hem), which resides near the dorsal midline of the cortex (Fotaki et al., 2010; Grove et al., 1998; Machon et al., 2007). From here, the Wnt signal is thought to play a role in regulation of the radial glia lining the lateral ventricle. Consistent with this, activation of Wnt/β-catenin signalling in chick cortical explants generated a concordant increase in the expression of dorsal cortical transcription factors such as Pax6 (Gunhaga et al., 2003). The role of Wnt/β-catenin signalling in regulation of the radial glia population was originally thought to be mitogenic (Megason and McMahon, 2002), a conclusion that has been supported by a combination of loss/gain-of-function studies. Loss of the LRP6 co-receptor or β-catenin causes a drastic reduction in cortical growth, likely due to the premature differentiation of radial glia (Woodhead et al., 2006; Zhou et al., 2006). Conversely, an increase in cortical Wnt/β-catenin activity promotes the self-renewal of radial glia and causes an expansion of the cortex (Chenn and Walsh, 2002; Ivaniutsin et al., 2009; Machon et al., 2007). These findings support a role for Wnt/β-catenin signalling in regulating self-renewal of the radial glial population.

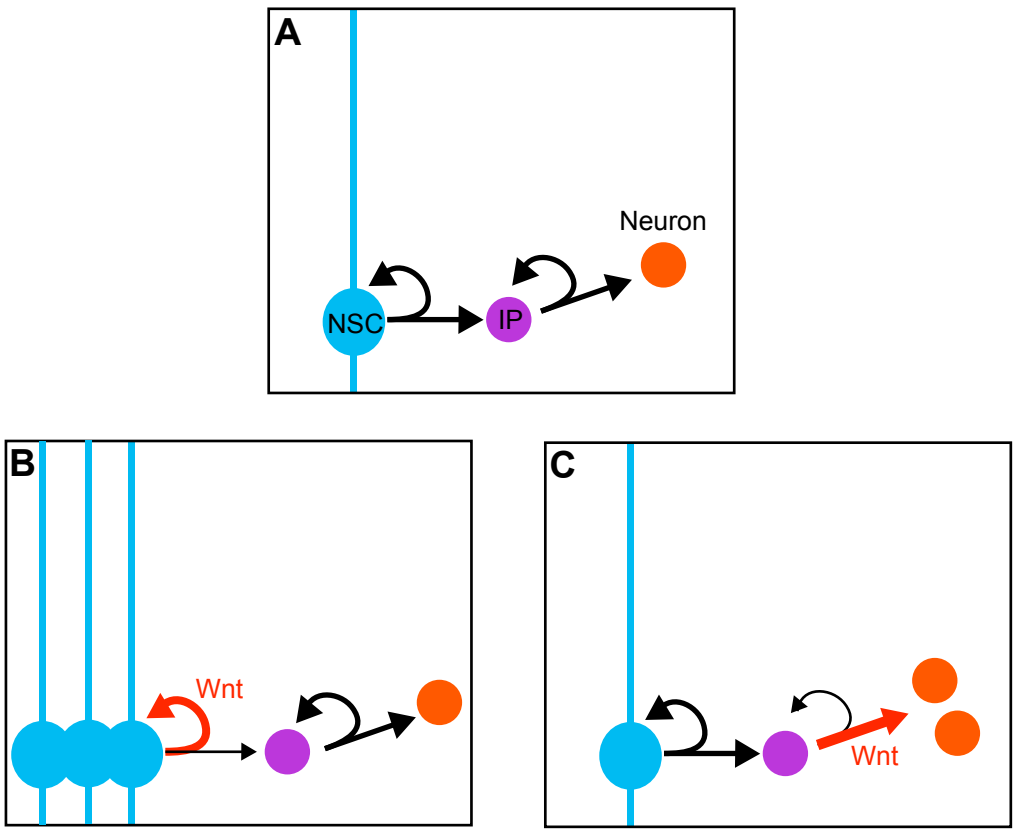

Figure 1.7 - Wnt/β-catenin signalling and NSC regulation.
Wnt/β-catenin signalling is known to regulate two processes in the generation of neurons from NSCs in the cortex. (A) Under normal conditions the NSC divides to produce an additional NSC and a transit amplifying IP cell. This then undergoes further asymmetric division to produce a daughter neuron and an additional IP cell - thus amplifying the total neuronal pool over time. Activated Wnt/β-catenin signalling has been shown experimentally to increase the self-renewal of NSCs (B), or force the differentiation of neurons from IP cells (C). The former results in a larger cortex due to a larger stem cell pool, while the latter results in a small cortex due to the depleted IP cell pool and a net loss in total neuron production.

A more spatio-temporal specific role in neurogenesis was determined by further work that controversially suggested that Wnt/β-catenin signalling can also act to promote neurogenesis (rather than self-renewal) (Hirabayashi et al., 2004). However, recent evidence has reconciled this inconsistency as the result of an additional role for Wnt/β-catenin signalling in driving neurogenesis from IPCs (Munji et al., 2011). This further reflects the context specificity for the responses generated by Wnt/β-catenin signal transduction – self renewal and proliferation in one cell type (NSCs) and differentiation in another (IPCs).

1.4.3 Development of cellular connections

While thought to function through cytoskeletal modifications rather than β-catenin mediated transcription, it is worth briefly mentioning the fact that a number of Wnt ligands are known to be required for the development of neuronal connections during brain development, particularly within the cerebellum. Wnt7a has been identified as a ligand expressed by GCs during development at the time when they first begin to form connections with mossy fibre axons (Lucas and Salinas, 1997) and induces axonal remodelling in the incoming mossy fibres through cytoskeletal changes mediated by GSK3β inhibition and Dsh activation (Ciani et al., 2004; Hall et al., 2000; Lucas and Salinas, 1997). On the other side of a synapse, Wnt ligands have been identified as regulators of dendritogenesis. In hippocampal neurons, Wnt7b is required for dendritic arborisation. The Wnt antagonist Sfrp1 (one of the secreted frizzled related proteins) inhibits dendritic branching of hippocampal neurons *in vitro*, while overexpression of Wnt7b causes over-elaboration (Rosso et al., 2005). Wnt3 expression has been identified in PCs during postnatal growth when their dendritic trees are developing (Salinas et al., 1994), although it has not yet been demonstrated to be an essential regulator of this process. Lastly, Wnt signalling has also been implicated in the process of synaptogenesis. During the development of GC/mossy fibre connections the expression of Wnt7a is maintained throughout synaptogenesis and increases expression of synapsin 1, a pre-synaptic protein involved in synapse formation and maturation (Hall et al., 2000; Lucas and Salinas, 1997). Combined, the processes of axon guidance, dendritic elaboration and synaptogenesis are all required for one neuron to make a connection to another and

cellular mechanisms initiated upon binding of a Wnt ligand are clearly an important component of these activities.

1.5 Medulloblastoma: Cerebellum development gone wrong

When developmental signalling pathways like the Wnt/β-catenin pathway become dysregulated, cancer is often the end result. At a fundamental level, cancer arises from a multistep process involving the accumulation of genetic aberrations that drives the progressive transformation of a normal cell lineage into a malignant derivative (Hanahan and Weinberg, 2000). The malignancy of cancer cells arises from a number of characteristics that are endowed upon them from these genetic or epigenetic changes, including resistance to cell death, sustained proliferation, replicative immortality and the ability to invade surrounding tissue (Hanahan and Weinberg, 2011; Hanahan and Weinberg, 2000). Given the link between the classic developmental signalling pathways (such as Shh, Wnt and BMP signalling) and these traits, it is not surprising that their dysregulation is implicated in a wide variety of tumour types, including the cerebellar neoplasm medulloblastoma.

1.5.1 Wnt/β-catenin signalling and cancer

The association between dysregulated Wnt/β-catenin signalling and cancer is long established. Indeed, discovery of the first mammalian Wnt ligand was born from a study into the transcriptional mechanisms of viral-mediated mammary tumourigenesis (Nusse and Varmus, 1982). Since then, the most well documented malignancy established primarily from dysregulated Wnt/β-catenin signalling is colorectal cancer, characterised by aberrant growth of the epithelial lining of the lower gastrointestinal tract. Individuals with a predisposition syndrome to this cancer (called familial adenomatous polyposis – FAP) were found to harbour a mutation in *APC* (Kinzler et al., 1991a; Kinzler et al., 1991b). Patients thus inherit one defective *APC* allele and as a result develop large numbers of epithelial outgrowths, termed polyps, in which the second *APC* allele is subsequently lost. Inevitably some of these polyps develop into a malignant growth termed adenocarcinoma. Loss of *APC* is also

observed in about 90% of sporadic colorectal cancer cases (Kinzler and Vogelstein, 1996).

Loss of APC function in intestinal epithelia leads to the stabilisation of β-catenin and the activation of Wnt/β-catenin signalling, resulting in a number of defects to intestinal self renewal (Sansom et al., 2004). Under normal conditions, intestinal epithelial cells are continuously produced by a stem cell compartment at the base of each villus called the intestinal crypt. Each crypt stem cell divides asymmetrically to produce a daughter transit amplifying cell, which then goes on to produce the mature epithelial cells that migrate along the surface of the villi before being shed – a process that takes approximately 3-5 days in humans. Wnt/β-catenin signalling has been shown to maintain the self-renewal of crypt stem cells (van de Wetering et al., 2002) and to control the EphB receptor / ephrin-B ligand gradient, which plays a role in maintaining the crypt niche environment. When Wnt/β-catenin is constitutively activated in crypt stem cells this process becomes disrupted and results in the accumulation of crypt stem cells that are unable to migrate or differentiate (Sansom et al., 2004). This is what constitutes a benign polyp, which eventually accumulates the additional mutations required for progression to an adenoma. This phenotype has also been observed in mice that harbour a somatic *Apc* mutation, similar to that observed in patients with FAP (Moser et al., 1990). Strikingly, these mice develop severe intestinal polyposis, mirroring the human condition. The mutation was subsequently identified in the *Apc* gene (Su et al., 1992) and given the name Apc^{min} (multiple intestinal neoplasia).

This observation that a disruption in Wnt/β-catenin mediated stem/progenitor cell self-renewal and differentiation leads to cancer has also been inferred from other systems. Within the hair follicle, for example, Wnt/β-catenin signalling has been established as a key factor regulating the transit amplifying cell population (DasGupta and Fuchs, 1999) and constitutive activation has been shown to lead to hair follicle tumours (Gat et al., 1998). Consistent with these observations, activating mutations in the Wnt/β-catenin signalling pathway have been identified in human cases of hair follicle tumours (pilomatricomas) (Chan et al., 1999). Combined with

observations from the intestine, these observations suggest that dysregulation of Wnt/β-catenin signalling is an important contributing factor to cancer originating from tissues where normal development relies on this pathway.

1.5.2 Clinical details and neuropathology of medulloblastoma

Medulloblastoma is the most common paediatric malignancy of the central nervous system and covers a family of related cerebellar tumours. Although mainly occurring in children, medulloblastoma has also been reported in adolescents and adults. Medulloblastomas are classified as primitive neuroectodermal tumours, which covers a wider range of brain tumours (not limited to the cerebellum) that exhibit a number of characteristics, including the fact they are usually high-grade, undifferentiated, neuroepithelial in origin and can consist of both neuronal and glial components (Rorke, 1983). Within the medulloblastoma family, tumours have been classified into three main categories, based primarily on histopathological features (Fig. 1.8 A-D), age of onset and prognosis: classical, nodular/desmoplastic and large cell/anaplastic (Louis et al., 2007). Classical medulloblastomas develop primarily within the vermis of the cerebellum, account for around 75% of medulloblastomas and are characterised by densely packed small, homogenous round cells. These tumours arise late in childhood and have the least severe prognosis of medulloblastoma. Desmoplastic medulloblastoma accounts for about 10% of cases and is characterised by a biphasic tissue pattern with regions of high cellular differentiation and low cell density (nodules) surrounded by areas of more undifferentiated cells. This variant predominates in a slightly older age group than classical medulloblastoma but has a worse prognosis. Lastly, the large cell/anaplastic variant accounts for the remainder of cases and is characterised by large cells with pleiomorphic nuclei, abundant cytoplasm and a high mitotic index. In addition, these tumours arise in the youngest age group (normally around 3 years of age), are much more invasive and have the worst prognosis (Behesti and Marino, 2008; Gilbertson and Ellison, 2008; Hatten and Roussel, 2011).

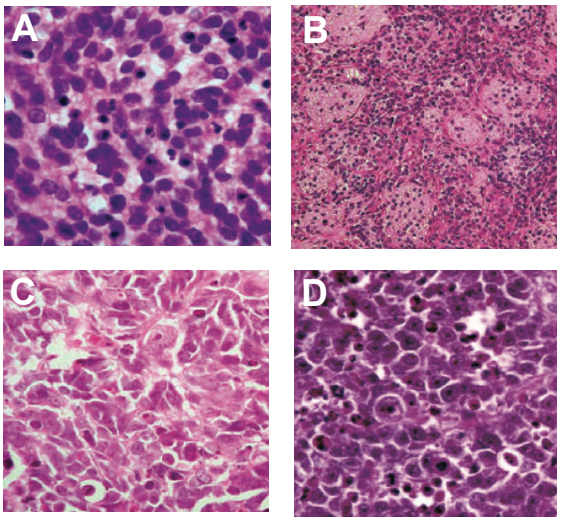

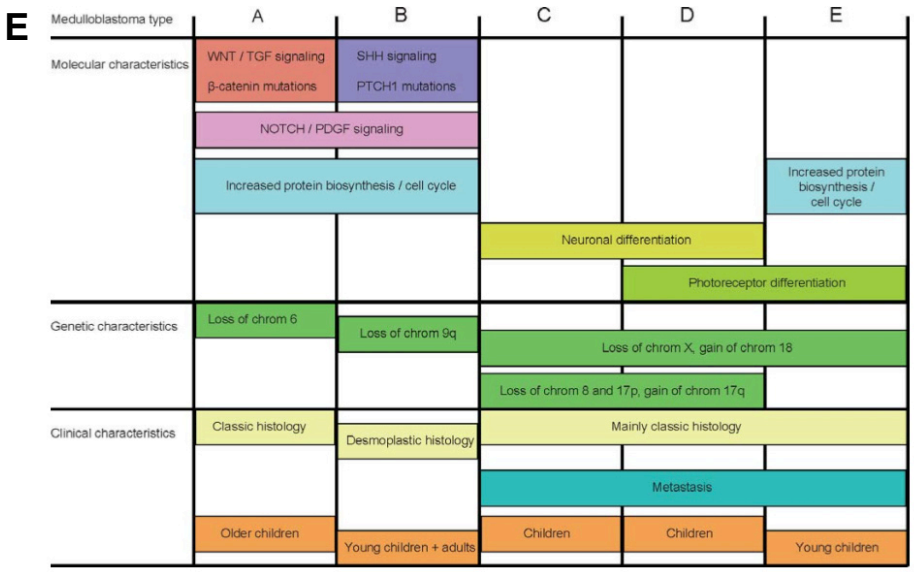

Figure 1.8 - Histopathological variants and molecular subtypes of medulloblastoma.
Medulloblastoma can be divided into four histopathological variants: Classic (A), nodular/desmoplastic (B), anaplastic (C) and large-cell (D). Classification of medulloblastoma by transcriptomic profile revealed five subtypes (E). Those with activated Wnt/β-catenin or Shh signalling were present in two defined groups with consistent histopathological and clinical profiles. The remaining three molecular subtypes are less well defined. A-D adapted from Gilbertson and Ellison (2008). E adapted from Kool et al. (2008).

1.5.3 Molecular characterisation of medulloblastoma

While the neuropathology of medulloblastoma variants has been established for some time, recent advances in the molecular characterisation of medulloblastoma are now beginning to offer important insights into the mechanisms that drive growth of the different variants of the disease. Much of our current understanding of the molecular basis of medulloblastoma has arisen from studies into two hereditary syndromes that predispose to the disease (Taylor et al., 2000). Gorlin syndrome is one such disease that predisposes to medulloblastoma, amongst other tumours including meningioma and basal carcinoma of the skin. This disorder was originally linked to chromosome nine in humans (Farndon et al., 1992) and then further mapped to a mutation in the *PTCH1* gene (Hahn et al., 1996), which encodes the Shh membrane receptor Patched. Further analysis revealed *PTCH1* mutations in a subset of sporadic medulloblastomas (Raffel et al., 1997), strongly implicating a role for Shh in the aetiology of a subset of medulloblastoma. A knockout mouse model for *Ptch* provided corroborating evidence for a role of Shh in medulloblastoma. Similar to Gorlin syndrome, 15% of mice heterozygous for a *Ptch1* mutation developed medulloblastoma at between three to six months of age (Goodrich et al., 1997). Furthermore, activating mutations in Shh pathway regulators Sufu and Smo have been identified in sporadic medulloblastoma (Reifenberger et al., 1998; Taylor et al., 2002). Combined with the identification of *Ptch1* mutations, medulloblastomas with activated Shh signalling are thought to account for around 25% of human cases (Zurawel et al., 1998).

Turcot syndrome is the second familial cancer predisposition syndrome with a high occurrence of medulloblastoma. This disease is characterised by the association of primary brain tumours with multiple colorectal adenomas (Hamilton et al., 1995). Consistent with the intestinal phenotype but providing a completely novel insight into medulloblastoma aetiology at the time, the genetic cause of this syndrome was mapped to a mutation in *APC* (Hamilton et al., 1995), implicating the Wnt/β-catenin signalling pathway in the manifestation of medulloblastoma for the first time. Furthermore, a number of patients with sporadic medulloblastoma have been

identified with mutations in *APC* (Huang et al., 2000) and other components of the pathway including β-catenin (*CTNNB1)* (Eberhart et al., 2000; Zurawel et al., 1998) and Axin (*AXIN)* (Baeza et al., 2003), accounting for around 10-15% of medulloblastomas (Hatten and Roussel, 2011). These early mutational analyses importantly revealed that two developmental signalling pathways were activated in a subset of medulloblastoma.

Building upon this finding, advances in DNA sequencing and gene expression analyses have led to the discovery that the activation of Shh or Wnt signalling occurs in mutually exclusive subsets of medulloblastoma and that different histological variants of medulloblastoma contain distinct transcriptional profiles (Kool et al., 2008; Northcott et al., 2010; Parsons et al., 2011; Pomeroy et al., 2002; Schwalbe et al., 2011; Thompson et al., 2006). One of the earliest transcriptional characterisations of medulloblastoma was carried out by Pomeroy et al. (2002), who identified a striking difference in the transcriptional profile between the classical and desmoplastic variants. Intriguingly, they also identified a clustering of Shh induced genes in the desmoplastic variant compared to the classical. This classification was notably extended by Thompson et al. (2006) who used more extensive gene expression analysis to identify five distinct molecular subtypes of medulloblastoma (Designated A-E). This was also the first study to demonstrate that Wnt and Shh signalling are activated in two mutually exclusive groups (A for Wnt, B for Shh). This clustering of medulloblastoma into five molecular subtypes was also achieved independently by Kool et al. (2008). Importantly, they also correlated their data with clinical details to identify that the Shh subtype presented as the desmoplastic or anaplastic variants in young children, compared to the Wnt subtype that presented almost exclusively as the classical variant in older children (Fig. 1.8 E). The clinical relevance of the previously established Wnt and Shh medulloblastoma subtypes was demonstrated recently by Schwalbe et al. (2011), who reported the development and validation of a rapid gene expression assay for diagnosis of Shh and Wnt subtype tumours.

While the difference between Wnt and Shh induced tumours is clear, the molecular classification of the latter three subtypes (C-E) has been less convincing. A recent study by Northcott et al. (2010) only grouped the non-Shh/Wnt subtypes into two additional subtypes, as opposed to three that had been identified previously. This inconsistency reflects the multiple genetic and transcriptomic aberrations identified in this group of medulloblastomas and the different clustering methods employed. Importantly, these latter molecular subtypes represent the majority of medulloblastomas (Gilbertson and Ellison, 2008). Furthermore, there is incomplete overlap between the histopathologic and molecular profiles. Aside from the observations that Wnt and Shh subtypes cluster within the classical and desmoplastic/anaplastic variants respectively, there is little consistency between the remaining molecular subtypes. Thus, further profiling is necessary in order to build a completely complementary picture of the histopathology and genetic profiles of medulloblastoma.

1.5.4 Developmental origins of Shh subtype medulloblastoma

The identification of clear molecular and histopathological variants of medulloblastoma suggests that different genetic aberrations in different cell types lead to the different classes of the disease. Combined with present knowledge of the molecular mechanisms controlling cerebellum development, this provides important insight into the developmental origins of medulloblastoma. The most convincing example of this is the identification that activating mutations in the Shh pathway lead to tumours arising from the GPC population within the EGL.

Observations that GPC proliferation is largely promoted by a Shh signal (Dahmane and Ruiz i Altaba, 1999; Gao et al., 1991) coupled with the consistent identification of a molecular subtype of medulloblastoma with activated Shh signalling led to the original hypothesis that this subtype of medulloblastoma arises from the transformation of GPCs. Initial support for this hypothesis has been generated from mice lacking the negative Shh regulator Patched, which show evidence for EGL hyperplasia and an increased risk of medulloblastoma (Goodrich et al., 1997; Kim et al., 2003; Oliver et al., 2005). However, the fact that the mutation is present in all

cerebellar cell types does not conclusively prove that the GPC is the cell of origin for the tumours observed. The advent of conditional genetic manipulation has since provided convincing evidence in support of this hypothesis from studies that have activated the Shh pathway solely in GPC cells and demonstrated the formation of medulloblastomas strikingly similar to the Shh molecular subtype previously identified.

Yang et al. (2008) utilised a Cre recombinase driven by *Math1*, a transcription factor expressed exclusively in rhombic lip derivatives (Ben-Arie et al., 1997; Machold and Fishell, 2005; Wang et al., 2005) to target a *Ptch1*^{lox} allele. This mutation promoted extensive proliferation within the EGL, causing obvious hyperplasia and eventually medulloblastoma by eight weeks of age. Importantly, the authors then targeted the mutation to non-lineage restricted progenitors using a *GFAP* driven Cre, which is expressed in multipotent progenitors at the VZ and RL prior to lineage commitment (Casper and McCarthy, 2006). While these mice showed evidence for an expanded NSC pool (including an expansion of the VZ) and advanced medulloblastoma by only four weeks of age, the tumours only arose from GPCs – as evident by the abundant EGL hyperplasia and the GPC markers present in the medulloblastomas. These findings were complemented by a study published concurrently using an additional RL-specific Cre transgene (*Olig2)* to constitutively activate Shh to the same result (Schüller et al., 2008). Thus, these studies were the first to demonstrate that activating mutations in the Shh pathway only generate medulloblastoma from the granule lineage – entirely consistent with the GPC cell-of-origin for the Shh subtype of medulloblastoma.

1.5.5 Developmental origins of Wnt/β-catenin subtype medulloblastoma

While the developmental origin of Shh subtype medulloblastoma is now well established, a potential link between development and the Wnt medulloblastoma subtype has only recently become apparent. As described above, dysregulated Wnt signalling occurs in approximately 10-15% of medulloblastoma cases based on the identification of pathway activating mutations in *APC, CTNNB1* and *AXIN*. This Wnt subtype of medulloblastoma tends to correlate predominantly with the classic

histopathological variant, affects older children and has a more favourable prognosis (Ellison et al., 2005). These observations support the suggestion that, like the Shh subtype, medulloblastomas arising from dysregulated Wnt/β-catenin signalling arises in a distinct cell population. However, unlike Shh signalling, our understanding of Wnt/β-catenin signalling in cerebellum development is surprisingly limited, making predictions on a Wnt subtype medulloblastoma cell-of-origin difficult.

While a role for Wnt/β-catenin signalling during the initial stages of MHB cell specification at the IsO is well established (Danielian and McMahon, 1996; McMahon and Bradley, 1990; Thomas and Capecchi, 1990), this is unlikely to be involved in the aetiology of medulloblastoma as dysregulation of a signalling centre such as this would generate a more severe developmental abnormality. Wnt/β-catenin signalling is also known to be active during development of cell lineages from the URL (Davis and Joyner, 1988; Dymecki and Tomasiewicz, 1998; Fischer et al., 2007; Nichols and Bruce, 2006; Wilkinson et al., 1987) and LRL (Landsberg et al., 2005; Rodriguez and Dymecki, 2000). However, attempts to constitutively activate Wnt/β-catenin signalling in the URL-derived granule lineage have not revealed any changes that would be consistent with tumourigenesis (Kratz et al., 2002; Lorenz et al., 2011). Lastly, the fact Wnt/β-catenin signalling is known to be an important regulator of neural stem cell self-renewal and differentiation (Munji et al., 2011) has led to the hypothesis that it could play a role in development of cell lineages arising at the VZ and that its dysregulation in this process is what leads to the Wnt subtype of medulloblastoma (Gilbertson and Ellison, 2008). While a demonstration of Wnt/β-catenin signalling within this cell population is yet to be undertaken, the effects of Wnt/β-catenin pathway activation in the VZ (alongside the URL and LRL) during cerebellum development was recently demonstrated (Gibson et al., 2010).

The study by Gibson et al. (2010) used a *BLBP* promoter, which is active in NSCs throughout the CNS during development (Hegedus et al., 2007). Importantly, the authors identified that the *BLBP-Cre* transgene was expressed in all key germinal centres in the developing cerebellum, including the VZ, URL and LRL. Using this

Cre transgene to activate a mutant β-catenin allele (Harada et al., 1999), the authors report that the only abnormality in the cerebellum of this mouse model was an accumulation of LRL-derived cells on the DHB surface by E16.5. The authors also demonstrate that this is not a result of increased proliferation, but instead is due to a migrational defect where the LRL-derived cells are unable to migrate to their respective HB nuclei. Following the loss of tumour suppressor gene *TP53*, medulloblastomas were then observed that displayed a classical histopathology and a transcriptomic signature identical to the Wnt subtype.

The conclusion that dysregulation of Wnt/β-catenin signalling at the LRL leads to a migrational defect and eventually medulloblastoma is supported by the evidence presented by Gibson et al. However, the data presented is not sufficient to conclude that all Wnt/β-catenin subtype medulloblastomas arise in this manner. Firstly, while the authors identify expression of a reporter allele and observe the accumulation of nuclear β-catenin in the VZ and URL, suggesting the transgene is active in these respective germinal centres, further analysis of the effects of the mutation in the cell lineages arising is lacking. The only analysis performed on cells at the VZ and EGL was the expression of proliferation and apoptosis markers at E16.5, which did not reveal an effect. The effects on progenitor cell self-renewal, differentiation and migration were not analysed. Furthermore, while the authors used an additional Cre-recombinase transgene to activate Wnt/β-catenin signalling solely in the Math1 positive(+) URL-derived cell lineage, in order to further test the effects of Wnt/β-catenin pathway activation in the granule lineage, their results are in stark contrast to those observed by Lorenz et al. (2011) who undertook a similar experiment using the same Cre-recombinase transgene (Matei et al., 2005) and same floxed β-catenin allele (Harada et al., 1999). Lorenz et al. observed extensive developmental abnormalities in GC development after Wnt/β-catenin activation, while Gibson et al. did not report any abnormalities. Finally, the removal of *TP53* (required for full tumour development) was only carried out in the *BLBP-Cre* line and thus it is hard to be certain the medulloblastomas observed arose solely from the LRL. This experiment now needs to be performed using Cre-reombinase transgenes exclusively expressed in the VZ or the URL to demonstrate that constitutive Wnt/β-catenin

activation in these germinal centres alone does not contribute to medulloblastoma. Thus, while a compelling case for the identification of the developmental origins of Wnt/β-catenin induced medulloblastoma has been presented (Gibson et al., 2010), the shortcomings within necessitate further experimentation. In addition, further investigation into the developmental role of Wnt/β-catenin signalling in the cerebellum is required in order to try and reconcile the observations made by Gibson et al. with a developmental process.

1.6 Aims of thesis

The identification of dysregulated Wnt/β-catenin signalling in a subtype of medulloblastoma and the correlation between this molecular profile and a consistent histopathology and clinical outcome suggests a degree of conservation in the development of medulloblastoma arising as a result of dysregulated Wnt/β-catenin signalling. Combined with the fact that Wnt/β-catenin signalling is a well established regulator of stem/progenitor cell populations in a number of tissues (including the CNS), this leads to the hypothesis that Wnt/β-catenin signalling plays a role in cerebellum development and that its dysregulation contributes to the aetiology of a subtype of medulloblastoma. To test this hypothesis a more thorough developmental profile of Wnt/β-catenin signalling in the cerebellum needs to be established and an investigation into the normal function of Wnt/β-catenin signalling is required. Thus, for this thesis I proposed to address the following three aims:

1. To characterise the extent of Wnt/β-catenin signalling throughout cerebellum development.
2. To investigate the function of Wnt/β-catenin signalling during cerebellum development.
3. To clarify how the dysregulation of this function contributes to the developmental origins of medulloblastoma.

In order to address these aims I first carried out a spatio-temporal analysis of Wnt/β-catenin signalling activity throughout cerebellum development using a β-galactosidase expressing Wnt/β-catenin transgenic reporter mouse model. Informed by the results from this analysis, I carried out a functional investigation into the role of Wnt/β-catenin signalling using a combination of small molecule-mediated modulation of the pathway *ex vivo* and genetic activation of the pathway *in vivo* during development.

2 Materials and methods

2.1 Animal procedures

2.1.1 Husbandry

Animal care was carried out in accordance with institutional guidelines and UK Home Office regulations. Mice were maintained in a 12 hour dark/light cycle with food and water provided *ad libitum*. For timed mating, the morning the vaginal plug was detected was designated as E0.5 and the day of birth as P0.

2.1.2 Mouse lines

Mice harbouring the BAT-gal reporter allele were maintained on a C57Bl/6J genetic background. Wild type mice on the same background were obtained by crossing mice hemizygous for the BAT-gal allele and used as negative controls. Mice carrying the *Nestin-CreER^{T2}* (*Nestin-Cre*) transgene were obtained on a mixed C57Bl/6J background, mice carrying the *Apc^{lox}*, *Rosa26eYFP* (*R26YFP)* or *Emx1-CreER^{T2} (Emx1-Cre)* transgenes were all obtained on a CBA/C57Bl/6J mixed background. Founder animals carrying individual *Nestin-Cre*, *Emx1Cre*, *Apc^{lox}* or *R26YFP* alleles were crossed in order to generate experimental mice with the following genotypes (as detailed in the relevant results sections):

Nestin-Cre$^{+/-}$; R26YFP^{+-} (Chapter 5)

Nestin-Cre$^{+/-}$; Apc$^{lox/lox}$ (Chapter 5)

Nestin-Cre$^{+/-}$; Apc$^{lox/lox}$; R26YFP$^{+/-}$ (Chapter 5)

Emx1Cre$^{+/-}$; R26YFP$^{+/+}$ (Chapter 5)

Apc$^{lox/lox}$ (Chapter 6)

Apc$^{lox/lox}$; R26YFP$^{+/-}$ (Chapter 6)

All transgenic mice were viable prior to intervention. For Cre-mediated *Apc* recombination, controls were either *Cre$^{-/-}$* or *Apc$^{lox/+}$* as detailed in the relevant figures.

2.1.3 Injection of S-phase tracer

For pulse labelling of S-phase cells at *in vivo* experimental end points, 200 μl of a 100 μg/ml Bromodeoxyuridine (BrdU, Sigma) solution in 0.9% NaCl was injected intra-peritoneally (IP) to pregnant females two hours prior to dissection.

2.1.4 Tamoxifen-induced gene recombination

To activate CreER^{T2} transgene activity, tamoxifen (Sigma) was dissolved in corn oil (Sigma) by sonication for one hour at 37°C at dose-dependent concentrations. Induction in embryos was performed using a single dose between 10-12 mg (as specified in the relevant results section) administered in 200 μl corn oil by gavage into the stomach of pregnant mothers bearing embryos aged between E13.5 and E16.5. Induction in early postnatal pups was performed using a single dose of 1.5 mg administered in 50 μl corn oil by subcutaneous (SC) injection to the neck fold. 4-hydroxy (4-OH) tamoxifen was prepared by sonication in 10% Cremaphor (Sigma) /H_2O and a final amount of 50 μg was also delivered by the same SC method.

2.1.5 *In utero* electroporation mediated gene recombination

E13.5 timed pregnant females were anaesthetised by inhalation with isoflurane and maintained in anaesthesia with O_2 delivered through a facemask. Uterine horns were surgically exposed and approximately 3 μl of purified *pCAG-Cre-IRES2-EGFP* plasmid DNA (Woodhead et al., 2006) (>1.5 μg/μl) in H_2O with 2 mg/ml Fast Green (Sigma) was injected into the fourth ventricle to each embryo using pulled glass capillaries inserted through the roof plate into the ventricle. A PV820 Picrospritzer (WPI) was used to deliver short bursts of plasmid solution until the Fast Green dye was visible filling the ventricle. Forceps-type electrodes (7 mm, Harvard Apparatus) were then positioned around the MHJ of embryos outside the uterine wall (anode oriented to the right) and a CUY21 electroporator (Nepa-gene) was used to deliver five pulses with the following parameters: intensity = 45V, pulse length = 50ms, pulse interval = 950ms. At the end of the procedure uterine horns were repositioned in the abdomen and the smooth muscle lining was closed with grade 5 sutures and the skin was closed with 5 mm wound staples. Brains were dissected at defined

stages during embryonic development and those with successful electroporations were identified by epifluorescence microscopy for GFP expression within the cerebellum.

2.2 Molecular biology based methods

2.2.1 Genomic DNA extraction

Genotypes of all mouse lines were determined using polymerase chain reaction (PCR) on genomic DNA extracted from collected embryo limb or adult mouse ear clip using the HotShot DNA extraction method (Truett et al., 2000). Tissue was lysed by heating to 96°C for 30 minutes in 50 μl lysis buffer (25 mM NaOH, 0.2 mM disodium EDTA, pH 12). Samples were then cooled to 4°C and neutralised by adding an equal volume of neutralisation buffer (40 mM Tris-HCL, pH5) prior to storage at -20°C.

2.2.2 Genotyping

Oligonucleotide primers used to genotype by polymerase chain reaction (PCR), their appropriate cycling conditions and expected product sizes differed between alleles being tested for (Table 2.1). Reactions were all prepared using 12.5 μl GoTaq Green master mix (Promega), 0.4 μM of each primer, 2 μl genomic DNA and H_2O to a total reaction volume of 25 μl. PCR products were separated using gel electrophoresis. 2% agarose gels were prepared by dissolving agarose (Seakem) with heat in 1x TBE before adding SyberSafe (Invitrogen) at a dilution of 1/10,000. Gels were set at room temperature for 30 minutes before PCR products were loaded and electrophoresed between 60-80 volts for varying amounts of time. Products were visualised using an InGenius transilluminator (Syngene) and GeneSnap imaging software (Syngene) and size was judged based on a known DNA ladder.

2.2.3 Reverse transcriptase PCR (RT-PCR)

RNA extraction for reverse transcriptase PCR (RT-PCR) was performed on <5 mg freshly dissected and snap frozen cerebellum tissue. Tissue was dissected after inhaled anaesthetisation with isoflurane followed by decapitation. RNA was extracted using an RNeasy Minikit (Qiagen) or, for snap frozen *ex vivo* cerebellum slices, using an RNeasy Microkit (Qiagen) following the manufacturers instructions. On-column DNA digestion was performed in all cases during extraction to eliminate genomic DNA contamination. cDNA was synthesised from 50ng RNA (measured by Nanodrop, Thermo Scientific) using a Sensiscript reverse transcription kit (Qiagen). The reactions were prepared with 50ng sample RNA added to 1X RT-Buffer, 10 μM random hexamer primers (Promega), 0.5 mM dNTPs (Invitrogen), 10 u RNAse inhibitor (Promega), 1 μl Sensiscript reverse transcriptase and made up to 20 μl with nuclease free water. Identical reactions were set up in tandem excluding reverse transcriptase (-RT) to serve as negative controls for possible genomic DNA carryover. Reactions were carried out at 37°C for 60 minutes and stored at -20°C. PCR reactions on the synthesised cDNA were carried out as described above using conditions specific to each primer pair (Table 2.2).

2.2.4 Quantitative gene expression analysis

Quantitative RT-PCR (qRT-PCR) was performed using a Precision qPCR SYBRgreen detection kit (PrimerDesign) and commercially synthesised primer pairs (PrimerDesign) with an Opticon DNA Engine (MJ Research) following the manufacturer's instructions. All primers used had annealing temperatures of ~58°C and an amplicon size of 90-120bp. Reactions were prepared in 20 μl with 1X Precision qPCR mastermix, 300nM custom primer pairs, 0.5 μl cDNA (synthesised as above) and made up to 20 μl with nuclease free H_2O. Reactions were set up in a 96 well white PCR plate (Bio-Rad) using a QIAgility automated pipetter (Qiagen). H_2O and –RT negative controls were included for each gene tested. Each reaction was begun with a 10 minute 95°C denaturation step followed by 40 cycles of: denaturation 15 seconds 95°C, data collection 60 seconds 60°C. Fluorescence was monitored at each cycle and then a melt curve analysis was performed.

For each gene analysed a set of six two-fold serial dilutions of control cDNA (a pooled collection of all sample cDNAs analysed) was tested in order to generate a standard curve of arbitrarily assigned transcript units. Relative amounts of gene-specific template present in the sample cDNA were then interpolated from this graph. Quantitation was carried out by comparing the relative amounts of gene-specific template cDNA to a housekeeping reference gene. The appropriate reference gene for analysis was identified using a GeNorm reference gene selection kit (PrimerDesign). This involved a test of six common reference genes by qPCR with a sample of the test cDNA followed by statistical analysis using qBase^{PLUS} (BioGazelle). This analysis determined *EIF4A2* and *18S* as the genes that varied least between samples. Direct comparison of these two genes across all samples revealed the least amount of variation in expression of *EIF4A2* therefore this was used for analysis (Appendix 1). Relative amounts of transcript for each gene analysed were normalised to *EIF4A2* in each case and expressed as a ratio. For every gene analysed, samples were run in triplicate using cDNA collected from three individual slices from each sample group.

2.2.5 Plasmid transformation, cloning and purification

TOP10 chemically competent *E. coli* cells (Invitrogen) were transformed with purified plasmid DNA by incubating on ice for 30 seconds followed by heat shock at 42°C for 90 seconds before returning to ice. Cells were recovered in 450 μl SOC medium (Invitrogen) at 37°C for one hour with shaking before being plated onto pre-warmed LB agar (1% tryptone, 0.5% yeast extract, 1% NaCl, 1.5% agar, pH 7, Sigma) ampicillin (50 μg/ml, Roche) plates and incubated overnight at 37°C. Colonies were picked, streaked onto a fresh plate and incubated at 37°C for 4-6 hours. Cloning was carried out by inoculating 150 ml LB medium (Sigma) with cells scraped from a single plate and growing overnight at 37°C with shaking. Midiprep or Miniprep (Qiagen) plasmid purification was then carried out according to the manufacturers instructions.

Table 2.1 - Primer sequences and conditions used for PCR genotyping

Allele	Primer sequence	Product size (bp)	Cycling conditions
Apc	**Fw** 5′ CACTCAAAACGCTTTTGAGGGTTGAAT 3′ **Rv** 5′ GTTCTGTATCATGGAAAGATAGGTGGT 3′ **Δ** 5′ GAGTACGGGGTCTCTGTCTCAGTGAA 3′	**Wt** 226 **LoxP** 314 **Δ** 258	94°C 30” 59°C 30” 72°C 40” **x35**
Cre	**Fw** 5′ CATTTGGGCCAGCTAAACAT 3′ **Rv** 5′ ATTCTCCCACCGTCAGTACG 3′	300	94°C 30” 59°C 30” 72°C 30” **x35**
R26YFP	**Fw** 5′ AAAGTCGCTCTGAGTTGTTAT 3′ **Rv** 5′ GGAGCGGGAGAAATGGATATG 3′ **YFP** 5′ GCGAAGAGTTTGTCCTCAACC 3′	**Wt** 250 **YFP** 550	94°C 30” 59°C 30” 72°C 30” **x35**
LacZ	**Fw** 5′ CGAAATCCCGAATCTCTATCGTGC 3′ **Rv** 5′ GATCATCGGTCAGACGATTCATTGG 3′	500	94°C 1’ 64°C 1’ 72°C 1’ **x35**
Mg	**Fw** 5′ CCCCCAAGTTGGTGTCAAAAGCC 3′ **Rv** 5′ ATGCTCTCTGCTTTAAGGAGTCAG 3′	120	94°C 1’ 64°C 1’ 72°C 1’ **x35**

Table 2.2 - Primer sequences and conditions used for RT-PCR

Gene	Sequence	Product size (bp)	Cycling conditions
Wnt1	**Fw:** 5′ TGCACCTGCGACTACCGGCG 3′ **Rv:** 5′ GTGCGCGGGGTGTTCGGGCT 3′	392	95°C 30” 62°C 30” 72°C 40” **x35**
Wnt2	**Fw:** 5′ CGGCCTTGTTTACGCCATC 3′ **Rv:** 5′ TGAATACAGTAGTCTGGAGAA 3′	496	95°C 30” 55°C 30” 72°C 45” **x35**
Wnt2b	**Fw:** 5′ GCCAAAGAGAAGAGGCTTAA 3′ **Rv:** 5′ TCAGTCCGGGTGGCGTGGCG 3′	290	95°C 30” 58°C 30” 72°C 45” **x35**
Wnt3	**Fw:** 5′ GCCGACTTCGGGGTGCTGGT 3′ **Rv:** 5′ CTTGAAGAGCGCGTACTTAG 3′	320	95°C 30” 62°C 30” 72°C 45” **x35**
Wnt3a	**Fw:** 5′ ATTGAATTTGGAGGAATGGT 3′ **Rv:** 5′ CTTGAAGTACGTGTAACGTG 3′	320	95°C 30” 55°C 30” 72°C 45” **x35**
Wnt4	**Fw:** 5′ GGCGTAGCCTTCTCACAGTC 3′ **Rv:** 5′ TGCATTCCGAGGCACCAGCG 3	300	95°C 30” 62°C 30” 72°C 45” **x35**
Wnt5a	**Fw:** 5′ TCCTATGAGAGCGCACGCAT 3′ **Rv:** 5′ CAGCTTGCCCCGGCTGTTGA 3′	230	95°C 30” 59°C 30” 72°C 45” **x35**
Wnt6	**Fw:** 5′ ATGGATGCGCAGCACAAGCG 3′ **Rv:** 5′ TTTGCCGTCGTTGGTGCCCA 3′	310	95°C 30” 62°C 30” 72°C 40” **x35**
Wnt7a	**Fw:** 5′ CAAGGCCAGTACCACTGGGA 3′ **Rv:** 5′ GGCTCCACGTGGACGGCCTC 3′	310	95°C 30” 55°C 30” 72°C 45” **x35**
Wnt7b	**Fw:** 5′ CAAGGCTACTACAACCAGGC 3′ **Rv:** 5′ CACCTCCACCTGCACCGCTG 3′	310	95°C 30” 62°C 30” 72°C 40” **x35**
Wnt9a	**Fw:** 5′ CAGCACTACCAATGAAGCCA 3′ **Rv:** 5′ CCTCGGCCACAACAAATACT 3′	220	95°C 30” 58°C 30” 72°C 45” **x35**

Wnt9b	**Fw:** 5′ CTACGCTATGACACGGCTGT 3′ **Rv:** 5′ GTACTTGCTGGGCCGGCAGA 3′	171	95°C 30” 62°C 30” 72°C 40” **x35**
Wnt10a	**Fw:** 5′ AAAGTCCCCTACGAGAGCCC 3′ **Rv:** 5′ CAGCTTCCGACGGAAAGCTT 3′	180	95°C 30” 55°C 30” 72°C 40” **x35**
Wnt10b	**Fw:** 5′ CGGCTGCCGCACCACAGCGC 3′ **Rv:** 5′ CAGCTTGGCTCTAAGCCGGT 3′	180	95°C 30” 62°C 30” 72°C 40” **x35**
Wnt11	**Fw:** 5′ GCCATGAAGGCCTGCCGTAG 3′ **Rv:** 5′ GATGGTGTGACTGATGGTGG 3′	160	95°C 30” 62°C 30” 72°C 40” **x35**
Wnt16	**Fw:** 5′ CCCTCTTTGGCTATGAGCTG 3′ **Rv:** 5′ CATGCCGTACTGGACATCAT 3′	209	95°C 30” 55°C 30” 72°C 45” **x35**
Axin2	**Fw:** 5′ GGCCCAGAGCAAGAGAGGTATC 3′ **Rv:** 5′ ACGCACGATTTCCCTCTCAGC 3′	492	95°C 30” 62°C 30” 72°C 45” **x35**
β-Actin	**Fw:** 5′ GAACAACAGCGTTGTCTCCA 3′ **Rv:** 5′ TGGGGAGGTAGCCACATAAG 3′	260	95°C 30” 58°C 30” 72°C 45” **x35**

2.3 Tissue preparation

2.3.1 Tissue collection and fixation

Embryos were collected between E12.5 and E18.5 and pups between P1 and P21. Heads from embryos up to E15.5 and brains dissected from E16.5-E18.5 embryos were immersion fixed in 4% paraformaldehyde in phosphate buffered saline (PBS) overnight at 4°C.

2.3.2 Transcardial perfusion

All postnatal mice were transcardially perfused prior to tissue fixation. Mice were terminally anaesthetised with sodium pentobarbital delivered via IP injection. The thoracic cavity was opened, exposing the heart, and perfusion was carried out through the left cardiac ventricle with 5-10 ml PBS followed by 5-10 ml 4% PFA/PBS. Tissue of interest was dissected and then immersion fixed overnight in 4% PFA.

2.3.3 Tissue preparation and sectioning

After fixation, embryonic and postnatal tissue for wax embedding was washed and dehydrated through increasing concentrations of ethanol prior to embedding in paraffin wax using an automated tissue processor (Tissue-Tek, Sakura). 10 μm serial sections were cut on a microtome and mounted on Superfrost plus slides (BDH). Tissue for *in situ* hybridisation and frozen immunohistochemistry was fixed as above before being cryoprotected in 30% sucrose/PBS overnight and then embedded in a 1:1 solution of 30% sucrose/OCT (Raymond A Lamb Ltd) and snap frozen on dry ice. Frozen sections were stored at -80°C and serially sectioned on a cryostat at 10-14 μm.

2.4 Histological analysis

2.4.1 DAB immunohistochemsitry

For immunohistochemistry with a diaminobenzidine (DAB) chromogenic end point, sections were dewaxed in xylene before being rehydrated through decreasing concentrations of ethanol to PBS. Antigen retrieval was achieved by microwaving sections at full power in 10 mM citrate buffer (pH6.0) for five minutes followed by 15 minutes at medium power. Slides were left to cool for 20 minutes and washed in 0.1% Triton-X (Sigma)/PBS (PBST) before blocking in 10% normal goat serum (NGS) in PBST. Primary antibody incubations were carried out overnight at 4°C with antibodies diluted in blocking solution and then washed in PBST (primary antibodies used and their concentrations are detailed in Table 2.3). Secondary antibody incubation was carried out using species-specific biotin-conjugated antibodies (goat anti-mouse IgG and goat anti-rabbit IgG, 1:200 Dako) for one hour at room temperature. After a further PBST wash, bound antibody was revealed after incubation for one hour with an ABC kit (Vector), followed by a DAB and hydrogen peroxide reaction using the DAB detection kit (Vector) for 1-3 minutes. Following DAB reaction certain slides were counterstained with Harris-haematoxylin for 30 seconds (Thermo Shandon). After staining, slides were washed and dehydrated through increasing concentrations of ethanol and xylene prior to mounting under coverslips in DPX mounting solution (BDH).

2.4.2 Fluorescent immunohistochemistry

For immunofluorescent staining, wax sections were rehydrated as above, while frozen sections were air-dried and washed in PBS. Antigen retrieval was carried out as above for wax sections, alternatively frozen sections (if antigen retrieval was carried out) were microwave heated on a medium setting for five minutes followed by gently simmering for 15 minutes. Blocking and primary antibody incubation was carried out in an identical manner to that for DAB immunohistochemsitry. For double immunofluorescence, primary antibodies raised in two different species were selected. Importantly, serum used for blocking was always from the same species as

the secondary antibody used. Primary antibodies were then detected using species specific secondary antibodies conjugated to Alexa fluor-488 or -568 dyes (goat anti-rabbit, goat anti-mouse, donkey anti-goat, donkey anti-rabbit, donkey anti-mouse, 1:200, Molecular Probes) for 1 hour at room temperature. Nuclei were counterstained with TOPRO3 (1:1000, Molecular Probes), washed in PBS and mounted under coverslips in Vetashield hardest (Vectorlabs) or ProLong Gold (Invitrogen). Appropriate controls were used in all cases by incubating sections with all but the primary antibodies. No staining was observed under these conditions.

2.4.3 RNA *in situ* hybridisation

In situ hybridisation on frozen section was performed as described previously (Wallace and Raff, 1999). *LacZ* and *Axin2* antisense riboprobes (Fotaki et al., 2011b) were obtained in plasmid DNA from V. Fotaki (University of Edinburgh). Plasmid cloning and purification was undertaken as described above. 10 μg Axin2 plasmid DNA was linearised by restriction digest with *Kpn1* (New England Biolabs) and β-gal was linearised with *Not1* (Promega) in a 200 μl reaction with 1X restriction digest buffer (New England Biolabs, Promega) and nuclease free H_2O at 37°C for three hours. Successful digestion was confirmed by gel electroporesis on a 1% agarose gel and the linear product was purified using a standard phenol-chloroform isoamyl alcohol (PCIA) DNA precipitation protocol (Appendix 2). DIG-UTP labelled RNA probes were then transcribed and labelled from 1 μg purified linear plasmid DNA using a T7 (LacZ) or T3 (Axin2) RNA polymerase (Roche) with a DIG-UTP RNA labelling kit (Roche) following the manufacturers instructions. Labelled probes were purified by digestion with DNaseI (Roche) at 37°C for 15 minutes followed by precipitation of the probe with LiCl in absolute ethanol at -20°C overnight. Precipitate was isolated by centrifugation and then resuspended in 50 μl nuclease free H_2O and stored at -20°C.

Frozen sections for *in situ* hybridisation were brought to room temperature in a sealed container (to minimise RNA degradation from condensation on slides) for 30 minutes. DIG-labelled RNA probes were diluted (Axin2 1/20, lacZ 1/50) in hybridisation buffer (Appendix 3) and denatured for 10 minutes at 70°C. Denatured

diluted probe was then diluted a further 1/100 in hybridisation buffer and applied to sections. Slides were covered with coverslips and incubated overnight at 65°C in a humidified box. Slides were washed three times in wash buffer (Appendix 3) at 65°C for 30 minutes followed by two washes in MABT (Appendix 3) at room temperature for 30 minutes. Sections were then blocked for 2-4 hours at room temperature in blocking solution (Appendix 3) before applying a 1:1500 dilution of sheep anti-DIG antibody (BM) in blocking solution and incubating overnight at 4°C. Following antibody incubation slides were washed in MABT five times for 20 minutes each and then equilibrated in pre-staining buffer (Appendix 3) for 10 minutes before being developed in NBT/BCIP staining buffer (Appendix 3) in the dark at room temperature until a stain was observed. Slides were then washed in PBS and mounted under coverslips with Aquamount (BDH). In all experiments, some sections were treated without any probe to control for background staining.

2.4.4 Microscopy and image analysis

A Leica brightfield microscope connected to a Leica DFC 480 digital camera was used to capture images of DAB labelled sections. A Leica brightfield microscope connected to a Leica DFC360Fx camera was used to capture images of fluorescently labelled sections. High resolution fluorescent microscopy was carried out using an inverted Zeiss LSM510 confocal system in the IMPACT facility, School of Biomedical Sciences. Images were processed for analysis and presentation using Photoshop CS4 (Adobe) or ImageJ (v10.2). Occasionally brightness and contrast of images were adjusted to improve clarity. In all images that were adjusted, changes were applied consistently across the entire image.

Table 2.3 - Primary antibody details and suppliers

Antigen	Species	Monoclonal/ polyclonal	Concentration (v/v)	Supplier
β-catenin	Mouse	Monoclonal	1:500	BD Biosciences
β-galactosidase	Rabbit	Polyclonal	1:1000 (wax) 1:500 (frozen)	Molecular Probes
β-galactosidase	Mouse	Monoclonal	1:100	DSHB*
BrdU	Mouse	Monoclonal	1:50	BD Biosciences
Calbindin	Mouse	Monoclonal	1:500	Swant
Caspase3	Mouse	Monoclonal	1:50	New England Biosciences
GFP	Goat	Polyclonal	1:400	Abcam
GFP	Rabbit	Polyclonal	1:1000	Abcam
Nestin	Mouse	Monoclonal	1:50	DSHB*
NeuN	Mouse	Monoclonal	1:500	Millipore
GFAP	Rabbit	Polyclonal	1:400	Sigma
Pax2	Rabbit	Polyclonal	1:200	Covance
PCNA	Mouse	Monoclonal	1:500	Abcam
s100β	Mouse	Monoclonal	1:500	Abcam
Sox9	Rabbit	Polyclonal	1:1000	Millipore

*DSHB developed under the auspices of the NICHD and maintained by the University of Iowa, Department of Biological Sciences, Iowa City, IA 52242.

2.5 Organotypic culture methods

2.5.1 Tissue preparation

Organotypic slice culture procedures generally followed those of Anderson et al. (Anderson et al., 1997). Embryos were dissected at E18.5 in 1X Kreb's buffer on ice. Brains were removed and placed into 1X Kreb's buffer with 10 mM HEPES buffer (Invitrogen), Gentamicin (Sigma) and Penicillin-Streptomycin (Invitrogen). The MHB regions were microdissected and embedded in molten 4% LMP agarose (Seakem)/PBS at 43°C with stirring and solidified on ice. Tissue was sectioned sagitally on a vibratome (Leica) at a thickness of 300μm. Slices were collected into 1X Kreb's buffer with HEPES and antibiotics and held on ice prior to culturing.

2.5.2 Culturing technique

Collected vibratome slices were transferred to 13 mm, 8 μm nucleopore polycarbonate membranes (Whatman) floating on 2 ml of 10% FCS (Gibco) and 0.5% glucose (Sigma) supplemented MEM (Gibco) with Penicillin-Streptomycin in a 7cm Petri dish. The time this was done was taken as T_0. Explants were allowed to recover at 37°C with 5% CO_2 for one hour before media was replaced with serum-free Neurobasal medium (Gibco) supplemented with 2% B-27 (Sigma), glucose, L-glutamine and Penicillin-Streptomycin ($T_0 + 1$).

2.5.3 Small molecule administration

Small molecules for activation or inhibition of the Wnt/β-catenin signalling pathway (Table 2.4) were dissolved to a stock concentration of 10 mM in DMSO (Sigma) and stored at -80°C for long term or -20°C for short term storage. Working solutions were prepared at varying concentrations in pre-warmed Neurobasal medium plus supplements so that DMSO never had a final concentration of >1%. After explant slices were equilibrated in Neurobasal medium plus supplements for three hours, the medium was replaced with that containing the particular small molecule ($T_0 + 3$). Cultures were left for 24 hours from this point.

2.5.4 Processing of slices for analysis

At T_0 + 25, BrdU was added to the culture medium (final concentration 10 mg/ml) before the end point at T_0 + 27. For histological analysis slices were lifted from the membranes and immersion fixed in 4% PFA/PBS overnight at 4°C. Slices were then washed in PBS before cryoprotecting in 30% Sucrose at 4°C for 2-4 hours and embedding in a 1:1 solution of 30% sucrose/OCT and snap freezing on dry ice. Slices were then further sectioned at 14μm on a cryostat. For RNA extraction and qRT-PCR, slices were lifted from the membranes and the agarose was removed in cold, sterile PBS before the slice was snap frozen on dry ice.

2.6 Statistical analysis

The extent of statistical analysis performed in this thesis was limited to direct comparison of two individual groups. Thus, the student's T-test was used, assuming unequal variance and normal distribution unless otherwise stated. Analyses were performed and charts prepared using Prism 4 (GraphPad). Specific quantitation methods used for each experiment are detailed in the methods sections of the relevant results chapters.

Table 2.4 - **Small molecule Wnt/β-catenin pathway modulators used**

Compound	Full name	Pathway effect	Source	Reference
BIO	6-bromoindirubin-3'-oxime	Activator	Sigma	(Sato et al., 2004)
CHIR	CHIR99021	Activator	Cambridge Biosciences	(Ying et al., 2008)
IWP2	Inhibitor of Wnt production – 2	Inhibitior	Sigma	(Chen et al., 2009)
XAV	XAV939	Inhibitor	Sigma	(Huang et al., 2009)
iCRT3	Inhibitor of β-catenin responsive transcription	Inhibitor	eMolecules	(Gonsalves et al., 2011)

3 *In vivo* analysis of Wnt/β-catenin signalling during cerebellum development

3.1 Introduction

A number of developmental signalling pathways have been identified that direct cerebellum development, however a role for the Wnt/β-catenin signalling pathway has only been partially resolved – despite a number of functions having been defined in development of the cortex (Kalani et al., 2008; Munji et al., 2011; Mutch et al., 2009; Wexler et al., 2009). In order to understand *how* the Wnt/β-catenin signalling pathway contributes to development of the cerebellum, I first sought to identify *where* and *when* its activity is present. However, the complexity of the Wnt/β-catenin signalling pathway presents a number of challenges in approaching a spatio-temporal analysis such as this.

The Wnt/β-catenin pathway is only a small part of a large signal transduction network. 19 known Wnt ligands bind in a myriad of different permutations with 10 different Fz receptors and LRP5/6 co-receptors and then go on to signal through three interacting pathways – of which the Wnt/βcatenin pathway is one (van Amerongen and Nusse, 2009). In addition, downstream gene expression directed by the Wnt/β-catenin pathway is entirely context dependent (i.e. different cell types at different developmental stages will respond to a Wnt/β-catenin signal with the expression of different downstream target genes). Combined, the complexity of this signalling network means there is no universal read-out for Wnt/β-catenin signalling in the form of an endogenous gene or protein that can be readily used to identify active signalling domains. A generally accepted exception to this is the protein *Axin2*, which is routinely used as a marker for Wnt/β-catenin signalling. *Axin2* encodes a negative feeback inhibitor of the Wnt/β-catenin signalling pathway and is a direct target of TCF/LEF-mediated transcription (Jho et al., 2002). Unlike other downstream Wnt/β-catenin target genes *Axin2* is peculiar in that it does not appear to be context dependent and its expression can be observed in most areas of Wnt/β-

catenin activity. However, it remains an endogenous Wnt/β-catenin target and is therefore subject to a certain degree of regulation that raises concern about its ability to report Wnt/β-catenin signalling in *all* contexts.

To address this, a number of different transgenic reporter mice have been generated that express an easily detectable protein (usually β-gal) in cells transducing a Wnt/β-catenin signal. The first of these was the TOPGAL line (DasGupta and Fuchs, 1999), which expresses β-gal under control of a minimal promoter (*c-fos)* and three TCF/LEF binding sites. Similar mice have been generated with the same construct theme, including the BAT-gal line (Maretto et al., 2003), the TCF/Lef-LacZ line (Mohamed et al., 2004) and the BAT*LacZ* line (Nakaya et al., 2005) – the key differences being the minimal promoters used and the number of TCF/LEF binding sites regulating expression of the reporter gene. While a number of limitations exist for the use of artificial reporter systems such as these (Barolo, 2006), as long as due caution is exercised in interpretation of results they can provide an efficient and convenient method for identifying sites of Wnt/β-catenin signalling activity.

3.2 Aims and experimental design

The aims for this chapter were to:

1. Identify the regional localisation of Wnt/β-catenin signalling activity in the developing cerebellum.
2. To determine the cell lineages responding to Wnt/β-catenin signalling during development.

To address these aims I utilised the BAT-gal reporter mouse line (Maretto et al., 2003) and performed a series of immunohistochemistry and *in situ* hybridisation experiments for the β-gal reporter protein, its encoding mRNA *LacZ* and an independent Wnt/β-catenin target *Axin2* at the following time points: E12.5, E14.5, E18.5, P1, P5, P10 and P21. These time points were chosen as they cover the key developmental events during cerebellum development. Further to the identification

of the key signalling domains, a series of double immunofluorescence experiments for the β-gal reporter protein and markers of the main cerebellar cell lineages were performed in order to determine the identity of cells expressing the β-gal reporter protein and thus responding to a Wnt/β-catenin signal. Lastly, a follow up experiment was performed using RT-PCR on RNA extracted from dissected cerebellum at E18.5 onwards to identify the Wnt ligands expressed.

3.3 Analysis of Wnt/β-catenin signalling in the embryonic cerebellum

3.3.1 β-gal protein expression at E12.5

Serial sagittal sections of E12.5 cerebellum tissue were analysed for expression of the β-gal reporter protein. DAB immunohistochemistry revealed diffuse expression centred around the IsO at the anterior end of the cerebellar anlage and the RL to the posterior (Fig. 3.1A-B). From these two key signalling centres β-gal expression spreads in an apparent gradient, with staining stronger towards the pial surface. This pattern was consistent for both medial (Fig. 3.1A) and lateral (Fig. 3.1B) sections, although the diffuse nature of the staining is more apparent medially while laterally the staining becomes more restricted to the anterior and posterior ends of the cerebellum revealing a void of β-gal expression within the VZ. In addition, β-gal expression is also observed in the dorsal monolayer of cells making up the surface of the CP (Fig. 3.1B), compared to the ventral surface of the CP which shows no evidence of β-gal expression. However, the ventral surface of the CP leads into the LRL and DHB, which display patchy expression of the β-gal reporter protein.

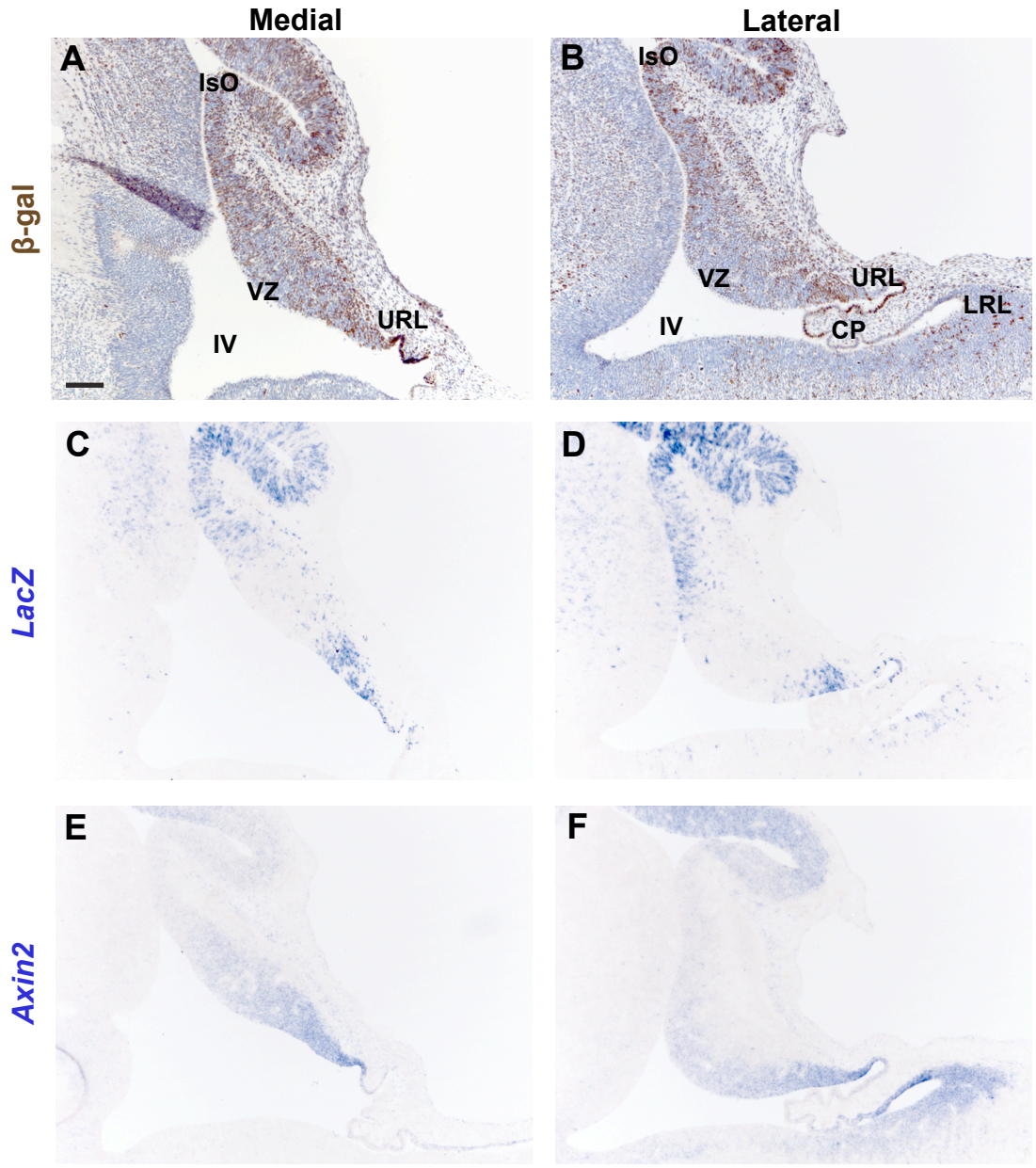

Figure 3.1 - Expression of the BAT-gal reporter and Wnt/β-catenin target gene *Axin2* in the E12.5 cerebellum.
DAB immunohistochemsitry for β-gal on medial (A) and lateral (B) sagittal sections of E12.5 cerebellum revealed expression at the isthmis organizer (IsO) and the upper rhombic lip (URL). β-gal protein was validated as a Wnt/β-catenin reporter by *in situ* hybridisation for its encoding *LacZ* mRNA (C-D) and independent Wnt/β-catenin downstream target *Axin2* (E-F) on matched sections. Both of these revealed similar, although not identical, expression patterns. Scale bar = 100 µm. (CP = choroid plexus, IV = fourth ventricle, LRL = lower rhombic lip, VZ = ventricular zone)

3.3.2 *LacZ* mRNA expression at E12.5

As the β-gal protein may persist in cells after transcription of the BAT-gal transgene has ceased, immunohistochemsitry for β-gal may stain cells that are no longer transducing a Wnt/β-catenin signal. Therefore, analysis of *LacZ* mRNA (the coding sequence for the β-gal protein) was carried out to test whether the β-gal expression pattern identified reliably reflects transcription of the BAT-gal transgene. *In situ* hybridisation analysis using riboprobes for *LacZ* mRNA was undertaken on sagittal sections of E12.5 cerebellum matched to those analysed with β-gal immunohistochemistry (Fig. 3.1C-D). Consistent with the observations made with β-gal immunohistochemistry, *LacZ* mRNA expression was observed at the Iso in the anterior and the RL in the posterior of the cerebellar anlage, with a notable void in staining observed along the ventricular zone and internally between the two domains. This pattern was consistent between both medial (Fig. 3.1C) and lateral (Fig. 3.1D) sections. However, it is clear that the *LacZ* mRNA represents a slightly more restricted pattern than the β-gal protein (compare Fig. 3.1A-B with Fig. 3.1C-D). Particularly in the medial region, the extent of β-gal protein expression appears considerably more widespread than *LacZ* mRNA. Another clear difference between β-gal protein and *LacZ* mRNA expression patterns is observed within the dorsal monolayer of cells lining the CP. While β-gal protein is expressed in this cell population from the RL to the midpoint of the CP, *LacZ* mRNA expression is markedly more restricted and does not extend quite so far around. Taken together, these results show a minor disparity between β-gal protein expression and *LacZ* mRNA expression indicative of perdurance of the protein in certain cells beyond the cessation of Wnt/β-catenin signal transduction.

3.3.3 *Axin2* mRNA expression at E12.5

As an independent verification that the BAT-gal reporter expression observed through β-gal immunohistochemistry and *LacZ in situ* hybridisation represents bona fide Wnt/β-catenin signalling activity, *in situ* hybridisation was performed with riboprobes to detect downstream Wnt/β-catenin target gene *Axin2*. Analysis of

sections matched to those used for BAT-gal reporter expression analysis revealed *Axin2* expression in the key domains identified as Wnt/β-catenin responsive areas (Fig. 3.1E-F). Namely, the RL and IsO – thus supporting the BAT-gal expression identified in these regions as genuine. However, several notable differences are obvious when the two expression profiles are compared (compare Fig. 3.1A-D with Fig. 3.1E-F).

Firstly, *Axin2* appears to be expressed in a much more diffuse gradient than β-gal or *LacZ*. For example, the RL displays strong expression of *Axin2,* which gradually decreases along the ventricular surface in an anterior direction, a pattern not mirrored by β-gal or *LacZ* expression. The expression of *Axin2* appears to spread further away from the RL than β-gal or *LacZ*, and also appears to spread along the ventral surface, while β-gal and *LacZ* are not expressed as strongly in the VZ. This is particularly evident in lateral sections (Fig. 3.1B,D,F). Secondly, the LRL and dorsal hindbrain also display strong expression of *Axin2* (Fig. 3.1F), which is not consistent with the pattern of β-gal or *LacZ* observed (Fig. 3.1 B,D). *Axin2* is expressed in a gradient from the ventral CP through the LRL and into the DHB, while β-gal and *LacZ* are expressed more sporadically throughout this region and in no clear gradient. Finally, there is also some disparity between the expression of *Axin2* and the BAT-gal reporter at the IsO. While β-gal and *LacZ* are both expressed at the IsO and in a large region of cerebellar tissue immediately posterior to the IsO, *Axin2* expression is markedly more restricted. The *Axin2* expression at the IsO is not as strong as that observed at the RL, and is not expressed as abundantly in the anterior cerebellum as β-gal or *LacZ*.

3.3.4 β-gal protein expression at E14.5

I next examined sections of E14.5 cerebellum for expression of the β-gal reporter protein. By E14.5 the cerebellum has grown in size, and the fate of cells being generated at the two germinal centres have changed. DAB immunohistochemistry on sagittal sections revealed an expression similar, but not identical, to that observed at E12.5. Consistent with E12.5, expression of β-gal was observed at the IsO and the

cerebellar tissue immediately posterior to it, and at the RL (Fig. 3.2A). However, a number of differences can be observed between the expression patterns at E14.5 and E12.5.

Firstly, expression of β-gal along the VZ appears more restricted at E14.5, except for the region immediately anterior to the RL and posterior to the IsO, indicating that the cell types being generated along most of the length of the VZ at this time point are not doing so in response to a Wnt/β-catenin signal. This is particularly evident in coronal sections of the E14.5 cerebellum, which shows the medial-lateral extent of the VZ in each of the cerebellar hemispheres with β-gal staining being restricted to the RL, which lies at the lateral edges in this plane of section (Fig. 3.2B). In addition, β-gal expression at the anterior and posterior limits of the cerebellum (the IsO and RL respectively) appears generally more restricted than at E12.5, with less diffuse staining within the cerebellar anlage. At the RL, while some diffuse expression was observed anterior to the URL at E12.5, the expression at E14.5 is restricted to the URL and spreads in a specific dorsal and anterior direction away from the URL – likely representing GPCs migrating away from the URL on the pial surface forming the early EGL.

Double immunofluorescence for β-gal and PCNA – a DNA binding protein involved in DNA replication and cell division (Hall, 1990) that marks cells in mitotically active germinal centres – confirms the expression of β-gal within the URL and in the EGL (Fig. 3.2C-D). Fluorescent immunohistochemsitry for PCNA clearly identifies the VZ, URL and EGL. β-gal expression is expectedly restricted to the IsO and RL. Closer magnification of the URL reveals the extent of colocalisation between β-gal and PCNA in this region (Fig. 3.2D).

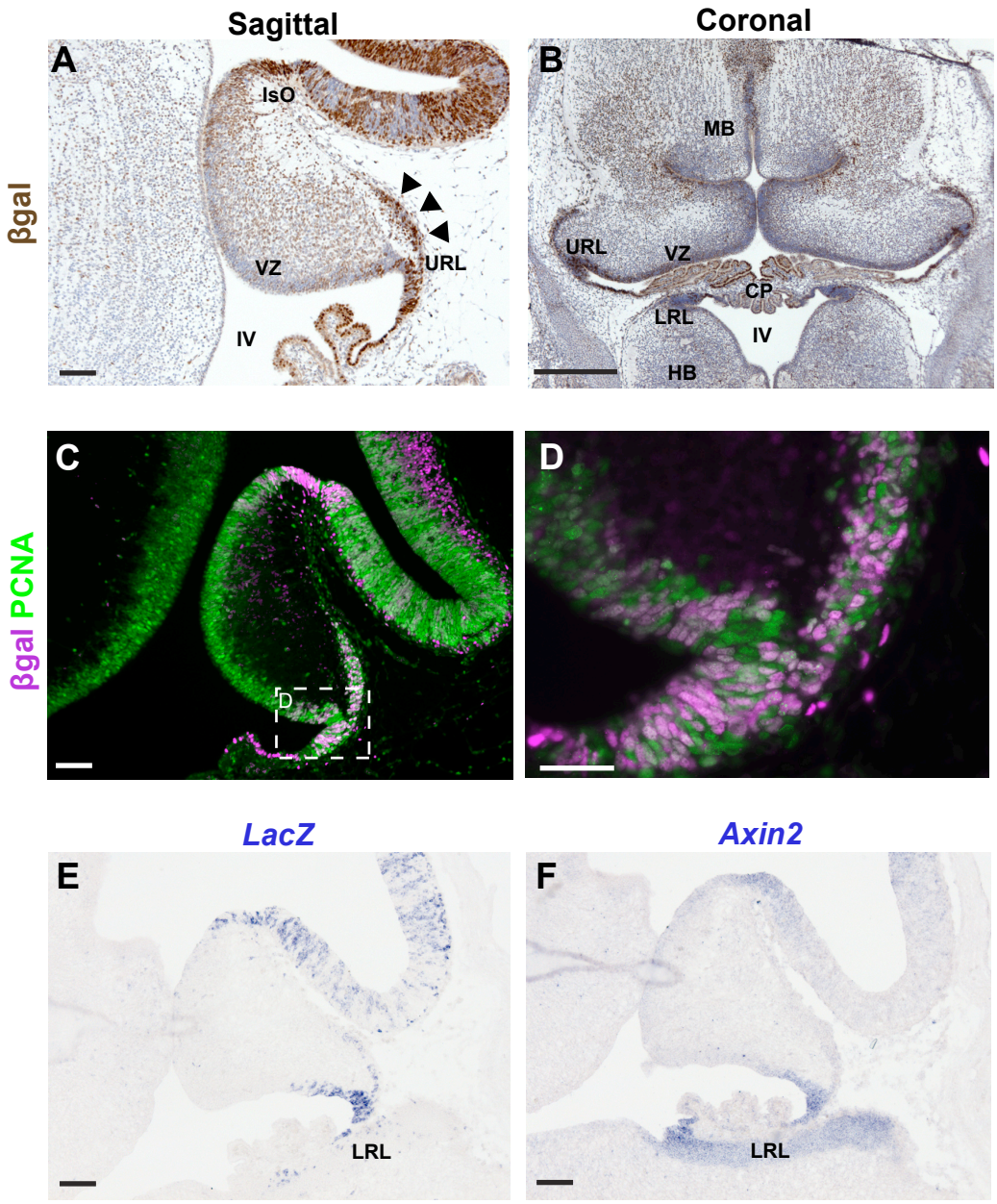

Figure 3.2 - Expression of the BAT-gal reporter and Wnt/β-catenin target gene *Axin2* in the E14.5 cerebellum.
At E14.5 immunohistochemsitry on sagittal sections (A) revealed β-gal expression at the IsO, RL and early EGL (arrowheads). Coronal sections (B) confirmed the lack of β-gal expression along the medial-lateral extent of the VZ. Double immunofluorescence for β-gal and PCNA (C) confirmed the expression pattern observed. Higher magnification confirmed the presence of β-gal+ cells in the URL and early EGL (D). *In situ* hybridisation for *LacZ* (E) and *Axin2* (F) showed a similar although not identical expression pattern. Scale bars: A,C,E-F = 100 µm, B = 500 µm, D = 50 µm. (EGL = external granule layer, MG = midbrain, HB = hindbrain)

3.3.5 *LacZ* mRNA expression at E14.5

Analysis of *LacZ* mRNA expression at E14.5 by *in situ* hybridisation revealed a pattern that was clearly more restricted than that observed for the β-gal protein (Fig. 3.2E), again likely reflecting the perdurance of the β-gal protein. Importantly though, the key domains identified through β-gal expression at E14.5 were readily identifiable as expressing *LacZ*, namely, the IsO, RL and early EGL. The URL in particular shows very clear staining that is restricted to that domain and does not extend into adjacent cerebellar tissue, with the exception of the bifurcated pattern with expression observed in the early EGL and most posterior region of the VZ. In addition, staining for *LacZ* mRNA ceases at the posterior end of the URL while the β-gal protein can be detected extending along the dorsal surface of the CP (Fig. 3.2A). Light DAB staining for β-gal is also observed within the cerebellar anlage, which is absent from the *LacZ* staining observed, again, likely reflecting perdurance of β-gal protein. In comparison to the *LacZ* expression pattern observed at E12.5, expression at E14.5 appears much more restricted to the anterior and posterior limits of the cerebellum, with less spreading of *LacZ* expression into the cerebellar anlage.

3.3.6 *Axin2* mRNA expression at E14.5

Axin2 mRNA expression at E14.5 was analysed by *in situ* hybridisation in order to test the validity of the β-gal and *LacZ* expression patterns observed (Fig. 3.2F). Importantly, *Axin2* mRNA expression is observed in the key domains identified through β-gal and *LacZ* expression – the IsO and RL – supporting the conclusion that these areas are sites of active Wnt/β-catenin signalling. However, there are several notable differences between the expression of *LacZ*/β-gal and *Axin2* at E14.5. Consistent with observations made at E12.5, the LRL at E14.5 displays sporadic expression of *LacZ* (Fig. 3.2E) whereas *Axin2* expression appears much more widespread from the ventral limit of the CP and across the extent of the LRL with an abrupt boundary at the DHB (Fig. 3.2F). In addition to this clear difference, *Axin2* does not appear to be expressed quite so markedly within the forming EGL compared to the obvious expression of β-gal and *LacZ* in this region. Instead *Axin2* expression at the URL appears tightly limited to the URL.

3.4 Analysis of Wnt/β-catenin signalling in the perinatal cerebellum

3.4.1 β-gal protein expression at E18.5

The cerebellum undergoes a number of obvious morphological changes between embryonic (E12.5-E14.5) and perinatal (E18.5-P1) stages. One notable difference is the extension of the EGL around the entire pial surface of the cerebellum and its expansion to a layer several cells thick, a result of the layer having begun extensive proliferation. The ballooning of the anlage and the initiation of the fissures that will eventually lead to the mature folia is also noticeable as terminally differentiated GCs begin to migrate internally from the EGL to the early IGL. Consistent with the significant changes to cerebellar morphology at E18.5, β-gal immunohistochemsitry revealed a strikingly different expression pattern than that observed at the earlier time points.

While the early forming EGL at E14.5 showed expression of β-gal (Fig. 3.2A), the more advanced EGL at E18.5 did not (Fig. 3.3A). Scattered β-gal+ cells can be observed at the posterior limit of the EGL (site of the former URL) but they become increasingly rare along the length of the EGL in an anterior direction. This is confirmed by double immunofluorescence for β-gal and PCNA on matched sections (Fig. 3.3B-C). PCNA labels the highly mitotic EGL and very few β-gal+ cells can be observed within the layer (Fig. 3.3B). Higher magnification of the anterior EGL reveals the lack of β-gal expression within the layer (Fig. 3.3C). Interestingly, β-gal expression is observed abundantly within the developing cerebellum at E18.5 (Fig. 3.3A-B), compared to embryonic stages where it appeared limited to the anterior and posterior limits of the cerebellum. Double immunofluorescence with PCNA reveals both β-gal+/PCNA- and β-gal+/PCNA+ cell populations (Fig. 3.3C), likely reflecting different states of mitotic activity within the β-gal+ cell population at this time point.

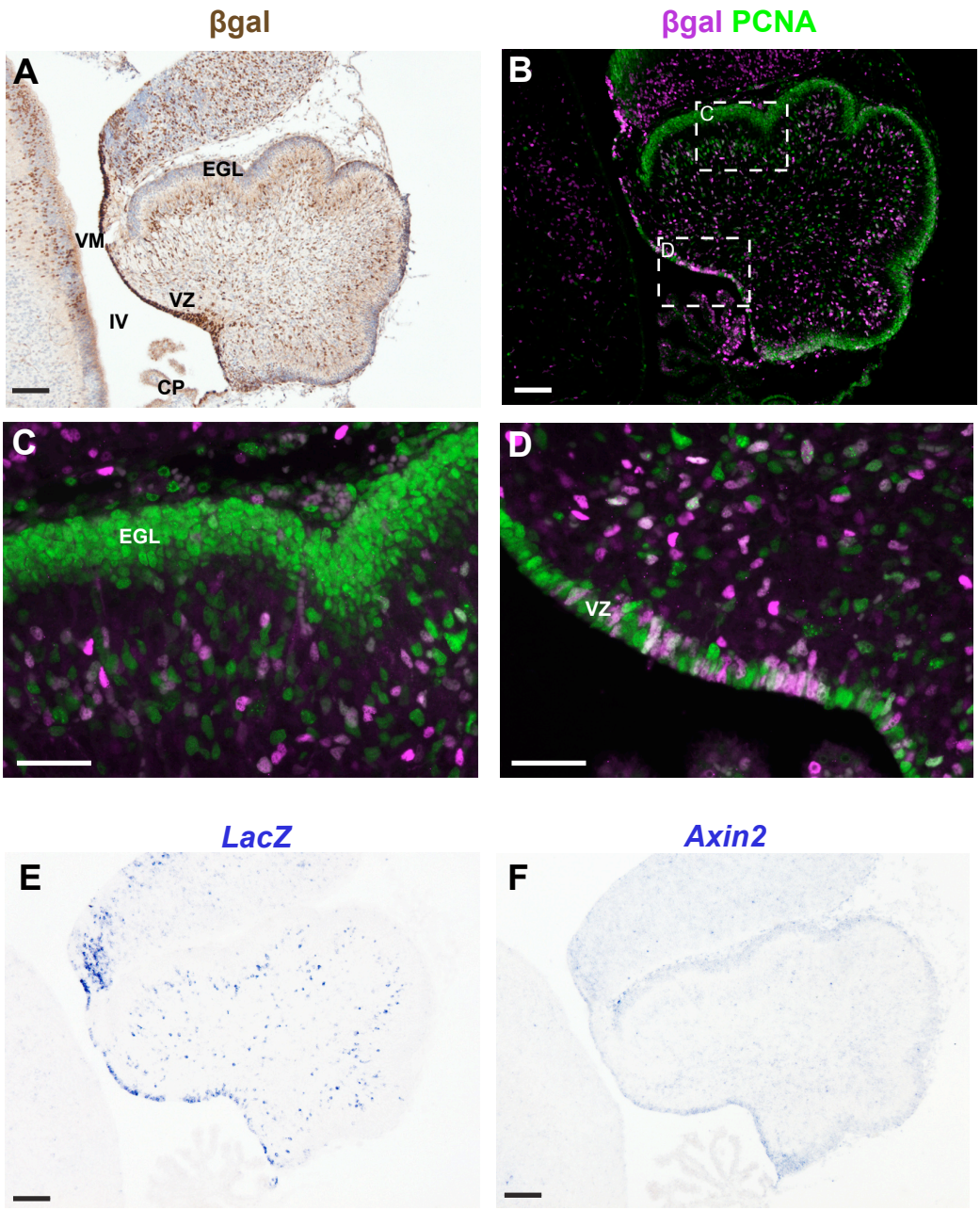

Figure 3.3 - Expression of the BAT-gal reporter and Wnt/β-catenin target gene *Axin2* in the E18.5 cerebellum.
DAB immunohistochemistry for β-gal on E18.5 sagittal sections (A) revealed widespread expression, including predominant staining in the VZ and velem medullaris. A similar pattern is observed with double immunofluorescence for β-gal and PCNA (B), which confirms the lack of β-gal in the EGL (C) and the presence at the VZ (D) under high magnification. *In situ* hybridisation for *LacZ* (E) revealed a similar expression pattern to β-gal, with notable expression at the VZ and within the developing cerebellum. This pattern was not seen with *in situ* hybridisation for *Axin2* (F) wich displayed a much fainter and more homogenous expression pattern. Scale bars: A-B,E-F = 100 µm, C-D = 50 µm.

The most striking observation at E18.5 was the expression of β-gal within the VZ (Fig. 3.3A), a region with less β-gal expression at earlier time points. Expression can be observed extending along the entire length of the VZ from the IsO, the velum medullaris (VM - the thin stretch of cells that joins the IsO to the VZ) to the posterior limit of the EGL. An active germinal centre, the VZ expresses PCNA along its length (Fig. 3.3B), although double immunofluorescence for β-gal and PCNA reveals a mosaic β-gal expression pattern along the length of the VZ, with a mixture of β-gal+ and β-gal- cell types in the cell layer and in the cells radiating away from the VZ.

3.4.2 *LacZ* expression at E18.5

Reflecting the pattern of β-gal protein expression observed at this time point, *in situ* hybridisation for *LacZ* on matched sections revealed a notable lack of staining within the EGL, abundant staining along the length of the VZ and scattered staining within the cerebellum itself (Fig. 3.3E). This confirms that the β-gal+ cells identified through immunohistochemistry at this time point are actively transducing a Wnt/β-catenin signal.

3.4.3 *Axin2* expression at E18.5

In situ hybridisation for *Axin2* revealed a fainter and more homogenous expression pattern (Fig. 3.3F). Consistent with the β-gal and *LacZ* expression patterns observed, *Axin2* was present along the VZ. However, staining was also observed at low levels within the EGL and very faintly throughout the cerebellum. Overall the expression of *Axin2* is not entirely consistent with the marked β-gal or *LacZ* expression observed at E18.5.

3.4.4 β-gal expression at P1

The rapid growth of the perinatal cerebellum is evident in the dramatic increase in size between E18.5 and P1, particularly with regards to the more developed extent of foliation. β-gal immunohistochemistry on sagittal sections at this time point revealed a similar pattern of β-gal expression to that observed at E18.5. The most obvious features being the lack of β-gal+ cells within the EGL, the predominant β-gal

expression along the length of the VZ and the widespread expression of β-gal+ cells within the cerebellum (Fig. 3.4A). Double immunofluorescence with β-gal and PCNA confirmed the lack of β-gal+ cells within the EGL (Fig. 3.4B-C), and also demonstrated the mitotic heterogeneity of β-gal+ cells inferior to the EGL (i.e. there was a mixed population of β-gal+/PCNA- and β-gal+/PCNA+ cell types). The VZ also shows a similar pattern of β-gal expression to E18.5 with clear expression observed along the length of the VZ cell layer – reflecting the potential of a continued role for Wnt/β-catenin signalling in development of this area from E18.5. Double immunofluorescence with PCNA to help identify the VZ showed a reduction in expression at the VZ, consistent with a reduction in proliferation of this region. There was also a more heterogenous cell population compared to E18.5 – with a greater mix of PCNA+, β-gal+, and PCNA+/β-GAL+ cells both at the VZ and radiating away from the the VZ.

3.4.5 *LacZ* expression at P1

In situ hybridisation for *LacZ* mRNA at P1 (Fig. 3.4E) confirmed the β-gal expression pattern observed (Fig. 3.4A-D). No *LacZ* expression was observed within the EGL, whereas expression was observed within the VZ and internally within the cerebellum. However, while the β-gal immunohistochemistry revealed quite a widespread pattern of expression within the cerebellum, *LacZ* appeared more restricted to the PCL, which can be seen clearly as a layer that internally outlines the developing folia. Thus, while *LacZ* and β-gal appear similar, there are minor discrepancies between the two expression patterns at this age.

3.4.6 *Axin2* expression at P1

In situ hybridisation for *Axin2* at P1 (Fig. 3.4F) revealed a pattern similar to that observed at E18.5. Namely, the general expression pattern appeared faint and widespread to the point that identifying clear *Axin2* expressing domains was difficult. Thus, at this time point there is a clear discrepancy between the expression of *Axin2* and β-gal/*LacZ*.

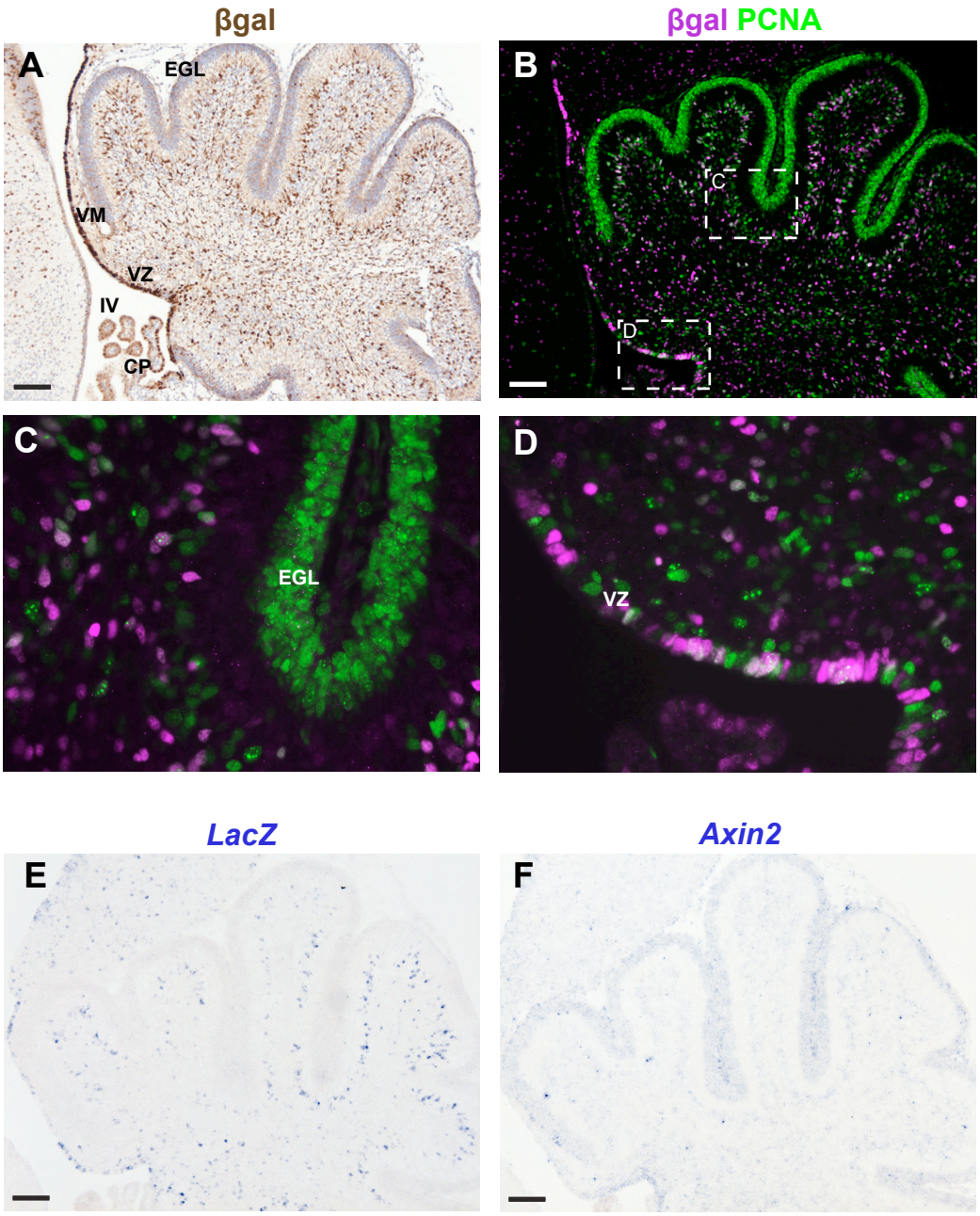

Figure 3.4 - Expression of the BAT-gal reporter and Wnt/β-catenin target gene *Axin2* in the P1 cerebellum.
DAB immunohistochemistry for β-gal on P1 sagittal sections (A) revealed widespread expression, including predominant staining in the VZ and VM. A similar pattern is observed with double immunofluorescence for β-gal and PCNA (B), which confirms the lack of β-gal in the EGL (C) and the presence at the VZ (D) under high magnification. *In situ* hybridisation for *LacZ* (E) revealed a similar albeit more restricted expression pattern to β-gal, with notable expression at the VZ and within the developing cerebellum. This pattern was not seen with *in situ* hybridisation for *Axin2* (F), which displayed a much fainter and more homogenous expression pattern. Scale bars: A-B,E-F = 100 µm, C-D = 50 µm.

3.4.7 Analysis of β-gal and VZ derived lineage markers at E18.5-P1

In order to determine the lineage of cells expressing the β-gal reporter protein during this perinatal period I tested sections from both E18.5 and P1 cerebellum for expression of the interneuron marker Pax2 and glial marker Sox9. The transcription factor Pax2 is expressed in committed cerebellar interneuron progenitors after their exit from the ventricular zone and prior to their terminal differentiation (Maricich and Herrup, 1999), while Sox9 is expressed in VZ progenitors (Kordes et al., 2005; Pompolo and Harley, 2001) and subsequently in cells that have become restricted to the glial lineage (Kordes et al., 2005; Sottile et al., 2006). Combined, these two markers cover the binary nature of cells generated at the VZ at this time point (i.e. neuronal or glial). Double immunofluorescence for β-gal and Pax2 at E18.5 (Fig. 3.5A) and P1 (Fig. 3.5B) revealed that, despite the extensive expression of both markers, in no event was there evidence for β-gal expression within the Pax2+ cell population. In contrast, double immunofluorescence for β-gal and Sox9 at E18.5 (Fig. 3.5C) and P1 (Fig. 3.5D) revealed that all β-gal+ cells express Sox9. These data suggest that of the cell lineages generated at the VZ perinatally, the β-gal reporter protein is expressed within multipotent progenitors and/or those restricted to the glial lineage.

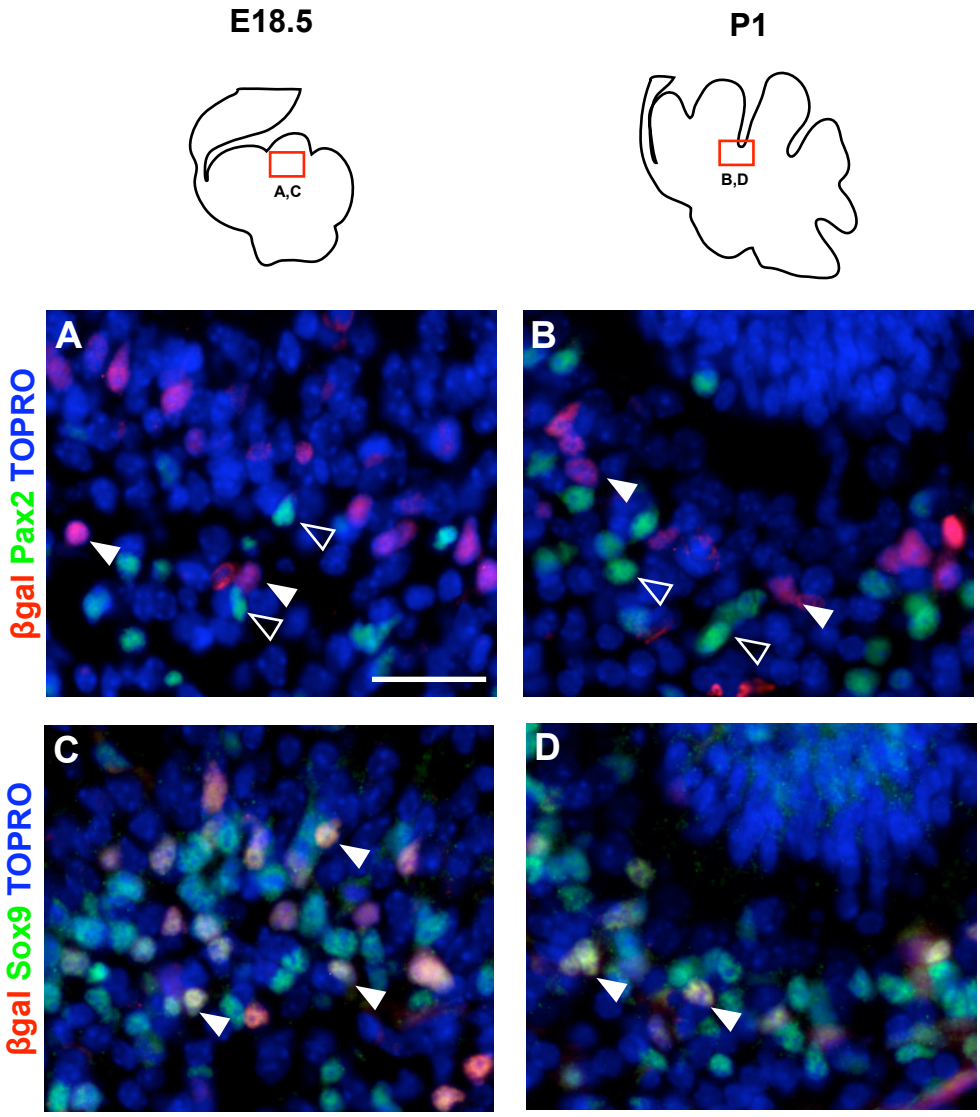

Figure 3.5 - Analysis of β-gal and VZ derived lineage markers at E18.5-P1. Double immunofluorescence for β-gal and interneuron marker Pax2 (A-B) revealed intermingled expression of β-gal (filled arrowheads) and Pax2 (empty arrowheads), but no colocalisation of the two was observed in any cell at E18.5 (A) or P1 (B). Analysis of β-gal and glial marker Sox9 (C-D) revealed extensive expression of Sox9 at both E18.5 (C) and P1 (D), and that all β-gal+ cells also expressed Sox9 (white arrows), suggesting the β-gal+ cell population consists of glia or glial progenitors. Images counterstained with TOPRO3. Scale bar = 50 µm.

3.5 Analysis of Wnt/β-catenin signalling during postnatal development

3.5.1 β-gal expression at P5

By P5 the cerebellum continues to produce vast quantities of granule neurons from the EGL resulting in the expansion of the cerebellum to the extent that all 10 folia are identifiable. The laminar structure is also more evident at this stage as the mature cell types of the cerebellum become differentiated and assume their terminal positions in the WM, IGL, PCL and ML. The VZ becomes greatly reduced in size as the anterior and posterior limits of the cerebellum come together and the WM generates the remaining populations of VZ-derived cell lineages. Sagittal sections of P5 BAT-gal cerebellum were analysed with DAB immunohistochemistry for the expression of β-gal. In both medial (Fig. 3.6A) and lateral (Fig. 3.6B) regions of the cerebellum, β-gal expression was most clearly observed in the PCL outlining the internal aspects of the folia and within the WM. Higher magnification confirmed the presence of β-gal+ cells within the PCL and WM (Fig. 3.6C), but β-gal+ cells could also be seen in other cell layers. The IGL contained β-gal+ cells (although not to the same extent as the PCL and WM), as did the ML. The EGL, consistent with earlier ages analysed, was void of β-gal expression.

3.5.2 *LacZ*/*Axin2* expression at P5

In situ hybridisation for *LacZ* on matched sections at P5 (Fig. 3.6D) revealed a similar expression pattern to β-gal immunohistochemistry, with a lack of staining in the EGL and expression observed in all other cell layers. However, the staining appeared more diffuse and not as clearly restricted to the PCL and WM as β-gal. This was also seen with *in situ* hybridisation for *Axin2* (Fig. 3.6E), which was expressed in a pattern similar to that seen at P1 with considerable widespread faint staining observed throughout the cerebellum making it difficult to discern *Axin2* expressing regions clearly.

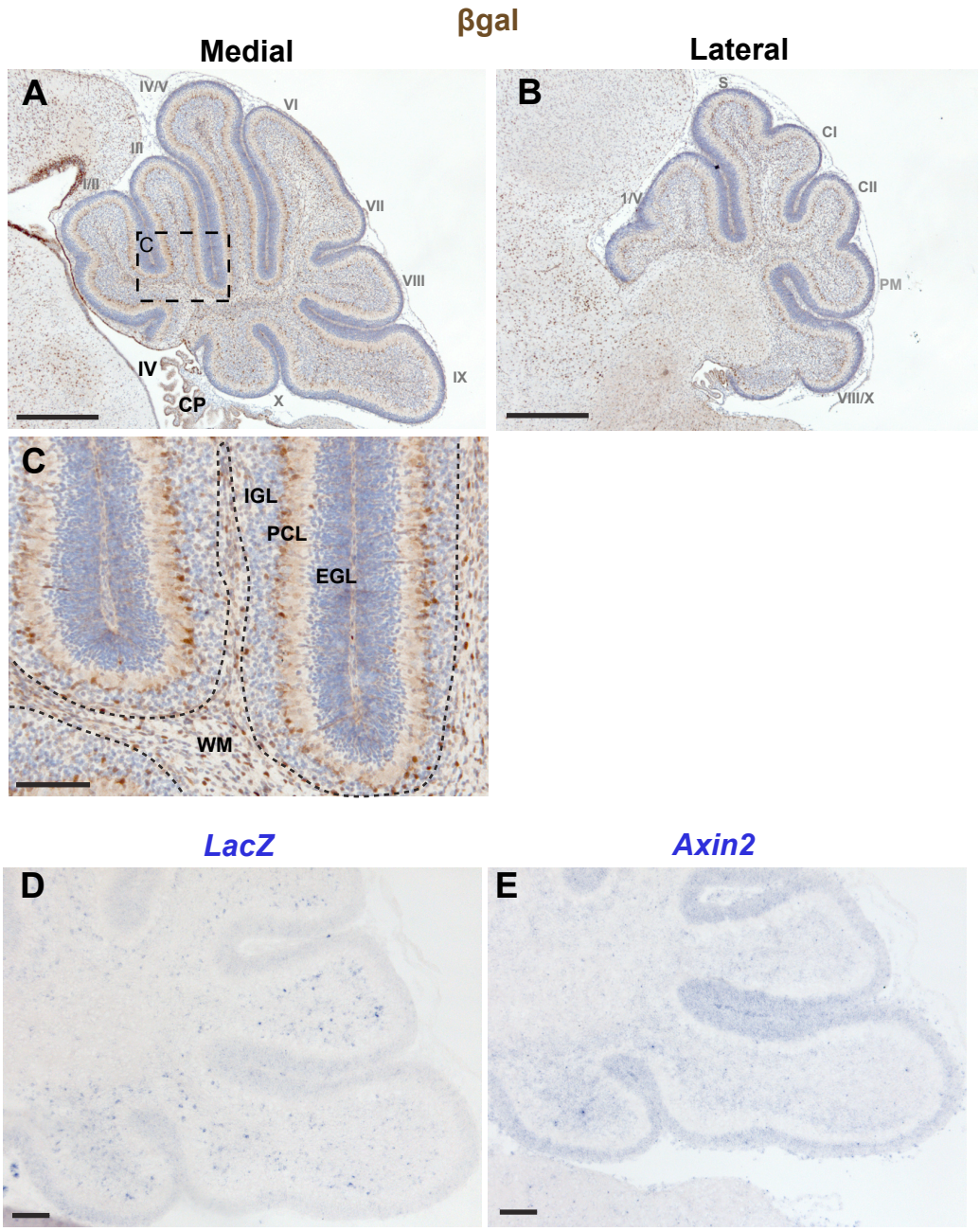

Figure 3.6 - Expression of the BAT-gal reporter and Wnt/β-catenin target gene *Axin2* in the P5 cerebellum.
DAB immunohistochemistry for β-gal on medial (A) and lateral (B) sagittal cerebellum sections revealed a widespread expression pattern with no clear anterior-posterior differences. Higher magnification (C) allowed the identification of β-gal+ cells wtihin the WM (demarcated by the dashed line), rarely within the IGL and predominating within the PCL. The EGL was void of β-gal expression. *In situ* hybridisation for *LacZ* (D) showed a more restricted pattern of expression, while *Axin2* (E) showed a fainter and more homogenous expression pattern. Scale bars: A-B = 500 µm, C-E = 100 µm. Vermis and hemisphere folia are labelled in grey.

3.5.3 Analysis of β-gal and lineage markers at P5

The P5 cerebellum is undergoing extensive growth in all key cell layers and as Wnt/β-catenin signalling is commonly associated with cell growth and proliferation I sought to determine if the β-gal expression pattern identified at P5 correlated with proliferation. Double immunofluorescence for β-gal and PCNA on sagittal sections at P5 revealed extensive PCNA expression through all cell layers, although particularly within the EGL, PCL and WM (Fig. 3.7A). However, while β-gal expression was particularly clear within the PCL and WM, very few β-gal+/PCNA+ cells were observed. These results provide little evidence for a correlation between Wnt/β-catenin signalling and proliferation in the P5 cerebellum, despite the high amount of growth occurring at this time point in the Wnt/β-catenin responsive regions identified.

As PCNA is not widely co-localised with expression of β-gal, I next looked at a number of markers to determine if the β-gal+ cells identified were of a particular cell lineage. The β-gal+ cells in the IGL, PCL and ML would be consistent with migratory post-mitotic granule cells, exiting the EGL towards their final destination in the IGL. However, double immunofluorescence between β-galactosidase and NeuN, a marker for post-mitotic granule cells (Mullen et al., 1992), did not reveal any cellular colocalisation between the two proteins in any sections analysed (Fig. 3.7B). Thus, Wnt/β-catenin signalling appears unlikely to be directly involved in the migration of post-mitotic granule cells at this stage.

The presence of β-gal+ cells within the WM, IGL and PCL would also be consistent with the pattern of multipotent glial/interneuron progenitors or lineage restricted glia/interneurons. Thus, colocalisation between Pax2 or Sox9 and β-gal would indicate which lineage was responding to a Wnt/β-catenin signal. Consistent with perinatal observations, in no case were β-gal and Pax2 observed to colocalise to the same cells (Fig. 3.7C). However, β-gal was evident exclusively within the Sox9+ cell population (Fig. 3.7D). This supports the conclusion that Wnt/β-catenin is not

involved in the development of the interneuron population at this stage but rather is active in the multipotent progenitors or in the restricted glial lineage.

3.5.4 β-gal/*LacZ* expression at P10

By P10 the cerebellum has undergone extensive proliferation and terminal differentiation of the various cell types is advanced – resulting in a fully laminated and foliated structure comparable with the adult cerebellum. However, the EGL still remains at P10 and continues to proliferate and produces GCs until approximately P21. In addition, WM progenitors are still actively generating cells of the GABAergic interneuron and glial lineages. β-gal DAB immunohistochemsitry on sagittal sections of the P10 cerebellum (Fig. 3.8A-B) revealed an expression pattern that was both reduced and restricted compared to that seen at earlier time points, likely reflective of the more advanced stage of development. Both medial (Fig. 3.8A) and lateral (Fig. 3.8B) sections displayed a consistent pattern of β-gal expression predominating within the PCL and WM. This was confirmed at higher magnification (Fig. 3.8C), which clearly shows β-gal+ cells residing in the PCL. Similar to the expression pattern observed at P5, β-gal+ cells can also be observed sporadically within the IGL and ML. Consistent with previous ages, no β-gal expression was observed within the EGL.

In situ hybridisation for *LacZ* mRNA revealed a similar pattern (Fig. 3.8D) - albeit more restricted - indicating that the β-gal protein detected at the PCL is still being produced from an actively transcribed BAT-gal transgene. This observation supports the conclusion that these cells are still actively transducing a Wnt/β-catenin signal but the restricted nature of *LacZ* expression compared to β-gal is consistent with the perdurance of β-gal protein in certain cells. *In situ* hybridisation for *Axin2* was also undertaken but no staining above background levels was detected (data not shown).

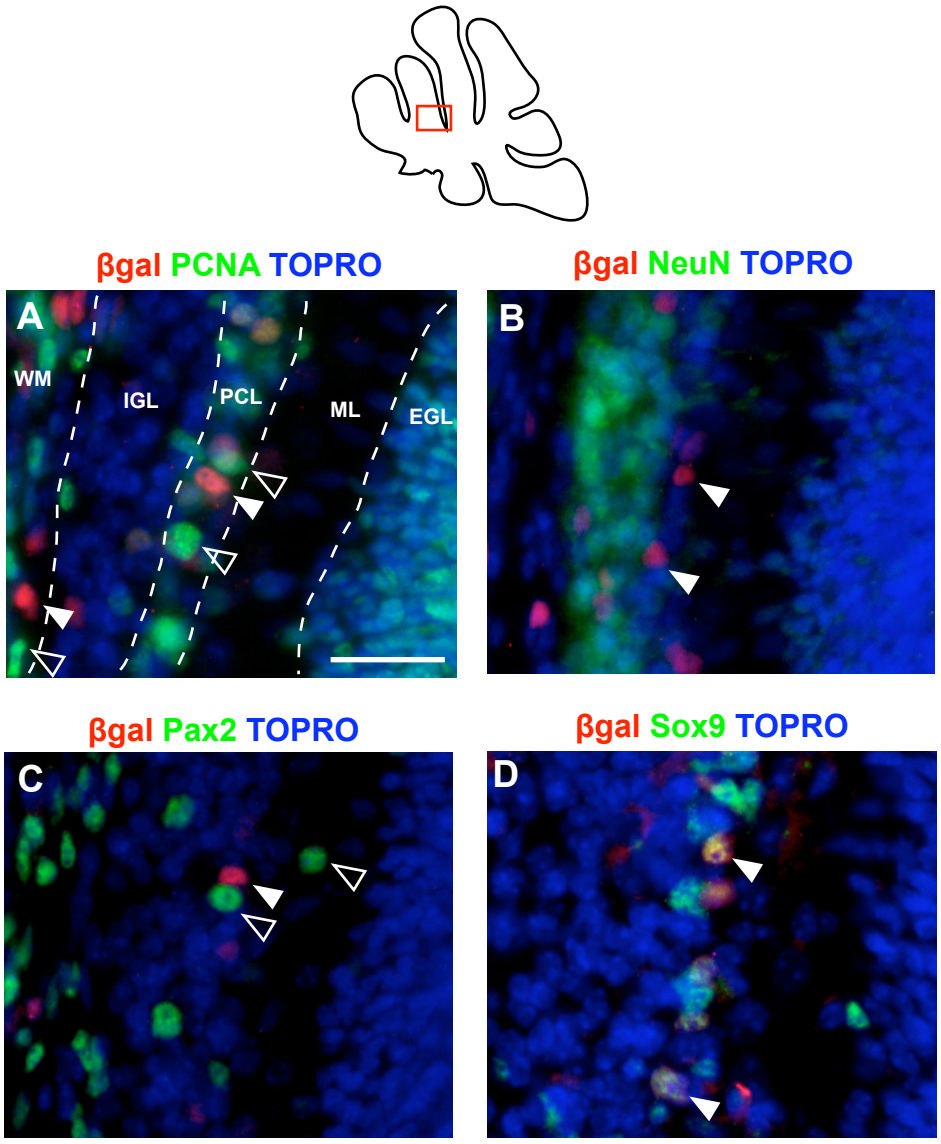

Figure 3.7 - Analysis of β-gal and cerebellar lineage markers at P5.
Double immunofluorescence for β-gal and PCNA (A) revealed the presence of β -gal+ cells within the PCL and WM (filled arrowheads, layers demarcated by dashed lines). Although β-gal+ cells were often observed in close proximity to proliferating PCNA+ cells (unfilled arrowheads) very few β-gal+/PCNA+ cells were observed. Double immunofluorescence for β-gal and NeuN (B) showed β-gal+ cells (filled arrowheads) located outwith the IGL, which displays abundant NeuN expression. Double immunofluorescence for β-gal and postmitotic interneuron marker Pax2 (C) showed the close proximity of β-gal+ (filled arrowheads) cells to Pax2+ cells (empty arrowheads) in the PCL, although no double-labelled cells were observed in any sections. Analysis with glial marker Sox9 revealed extensive nuclear colocalisation between the two proteins (white arrows, D). Images counterstained with TOPRO3. Scale bar = 50 μm.

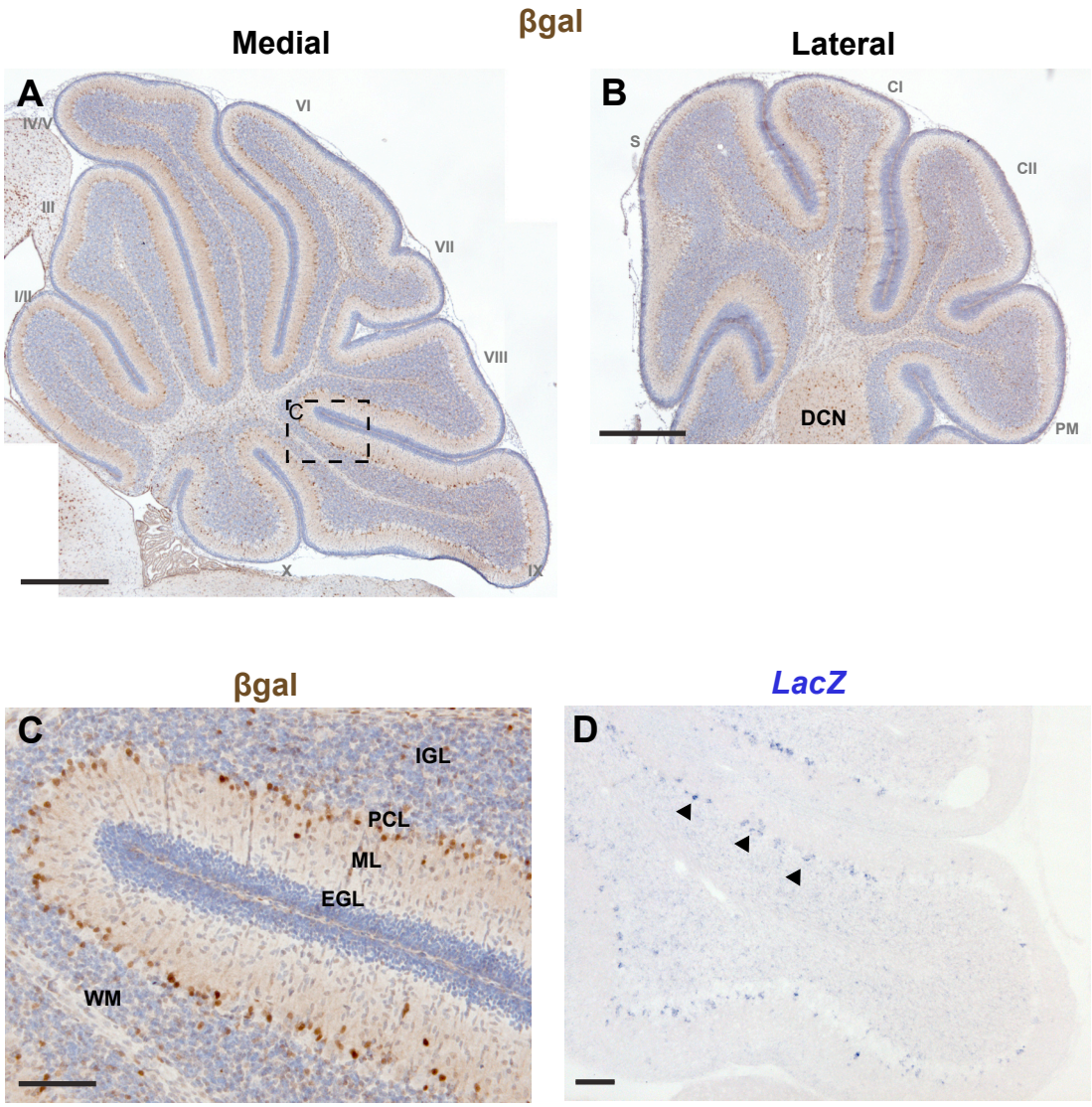

Figure 3.8 - Expression of the BAT-gal reporter in the P10 cerebellum.
DAB immunohistochemistry for β-gal on medial (A) and lateral (B) sagittal cerebellum sections at P10 revealed a widespread expression pattern with no clear anterio-posterior differences. β-gal+ cells can be observed throughout the section, including the DCN (B). Higher magnification (C) allowed the identification of β -gal+ cells sporadically within the IGL but predominating within the PCL. The EGL was void of β-gal expression. *In situ* hybridisation for *LacZ* (D) showed a more restricted pattern of expression, although clear expression was observed within the PCL (arrowheads). Scale bars: A-B = 500 µm, C-D = 100 µm. Vermis and hemisphere folia are labelled in grey.

3.5.5 Analysis of β-gal and lineage markers at P10

Double immunofluorescence of β-gal and a number of different markers was used to determine the cell type of the β-gal+ cells observed in the P10 cerebellum. Expression of PCNA at this time point illustrates the continued proliferation of GPCs in the EGL (Fig. 3.9A) and interestingly the presence of mitotic cells within the PCL – consistent with the location of β-gal+ cells observed (Fig. 3.8C). However, as was observed at P5, in no sections analysed was there evidence for colocalisation between PCNA and β-gal, indicating that the Wnt/β-catenin signal driving expression of the BAT-gal transgene is not a mitogenic signal at this stage.

Double immunofluorescence between β-gal and NeuN (Fig. 3.9B) or Pax2 (Fig. 3.9C) was also undertaken to test whether the β-gal+ cells identified were of the granule or interneuron lineages respectively. Consistent with results obtained from analysis of β-gal expression at P5, no colocalisation between β-gal and NeuN or Pax2 was identified, despite the frequent presence of β-gal+ cells in close proximity to NeuN+ or Pax2+ cells. This supports the earlier conclusion that Wnt/β-catenin signalling is not directly involved in the maturation of the interneuron or granule cell lineages.

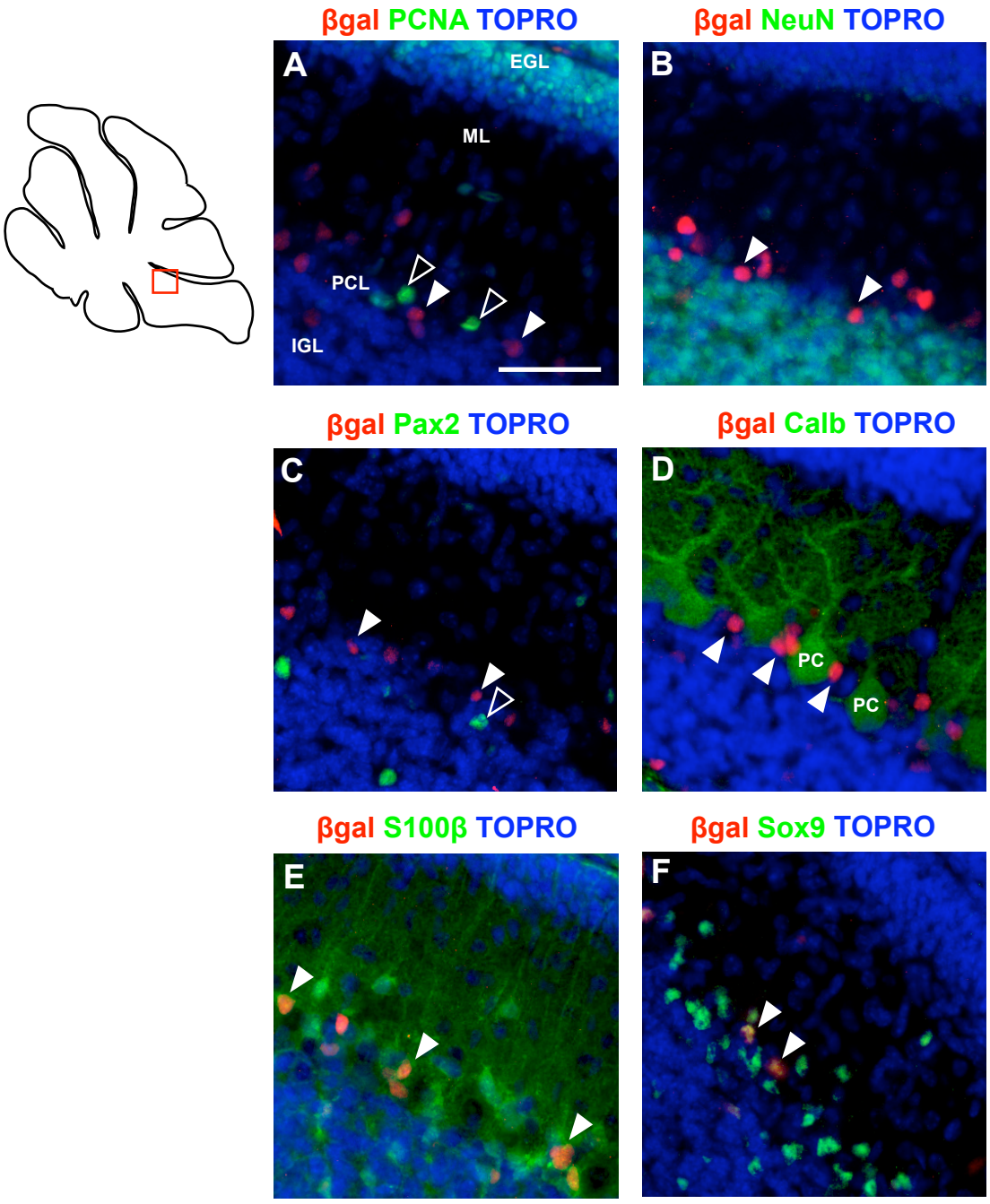

Figure 3.9 - Analysis of β-gal and cerebellar cell lineage markers at P10. Double immunofluorescence for β-gal and PCNA (A) revealed the presence of β -gal+ cells (filled arrowheads) in close proximity to PCNA+ cells (empty arrowheads) although no double-positive cells were observed in any sections. The same pattern was seen between β-gal and NeuN (B) and Pax2 (C). Interestingly, β -gal+ cells were seen clustered around Calbindin+ Purkinje cells (D) within the PCL, a location consistent with Bergmann glia. Double immunofluorescence with β-gal and glial markers s100β (E) and Sox9 (F) confirmed the identity of the β-gal+ cells as Bergmann glia. Images counterstained with TOPRO3. Scale bar = 50 μm.

The localisation of β-gal+ cells to the PCL could also be consistent with either Purkinje cells or Bergmann glia. To test the first hypothesis, double immunofluorescence for β-gal and Calbindin (Fig. 3.9D), a Purkinje cell marker only expressed at detectable levels from P10, was undertaken. β-gal+ cells can be clearly identified clustered around Purkinje cells, but in no event were Calbindin+ Purkinje cells identified with β-gal expression. The location of β-gal+ cells clustered around Purkinje cells would be consistent with Bergmann glia. This was tested by carrying out double immunofluorescence between β-gal and s100β or Sox9, both markers for Bergmann glia and other astrocytes (Landry et al., 1989). These experiments revealed extensive colocalisation between the two markers and β-gal (Fig. 3.9E-F), supporting the conclusion that the β-gal+ cell population identified within the P10 PCL consists largely of Bergmann glia. However, the β-gal+ cell population only represents a small proportion of the s100β+ or Sox9+ cell populations. Therefore the BAT-gal reporter is only active in a subset of Bergmann glia at P10.

3.5.6 β-gal expression at P21

By P21 the morphological development of the cerebellum is largely complete, with minor numbers of interneurons still being generated in the WM and the remnants of the EGL migrating through the ML into the IGL. Development of the cellular circuitry within the cerebellum is the remaining process, which proceeds well into adulthood. DAB immunohistochemsitry for β-gal at this time point revealed an expression pattern similar to that observed at P10, although notably more restricted with β-gal+ cells predominating in the PCL but also detectable sporadically within the IGL, WM and DCN (Fig. 3.10A-B). There were no differences observed between medial (Fig. 3.10A) and lateral (Fig. 3.10B) sections and the localisation of β-gal+ cells to the PCL was consistent across a single section (i.e. no anterior to posterior differences were observed). Higher magnification confirmed the presence of β-gal+ cells within the PCL (Fig. 3.10C), with limited β-gal expression observed within the WM, IGL and ML.

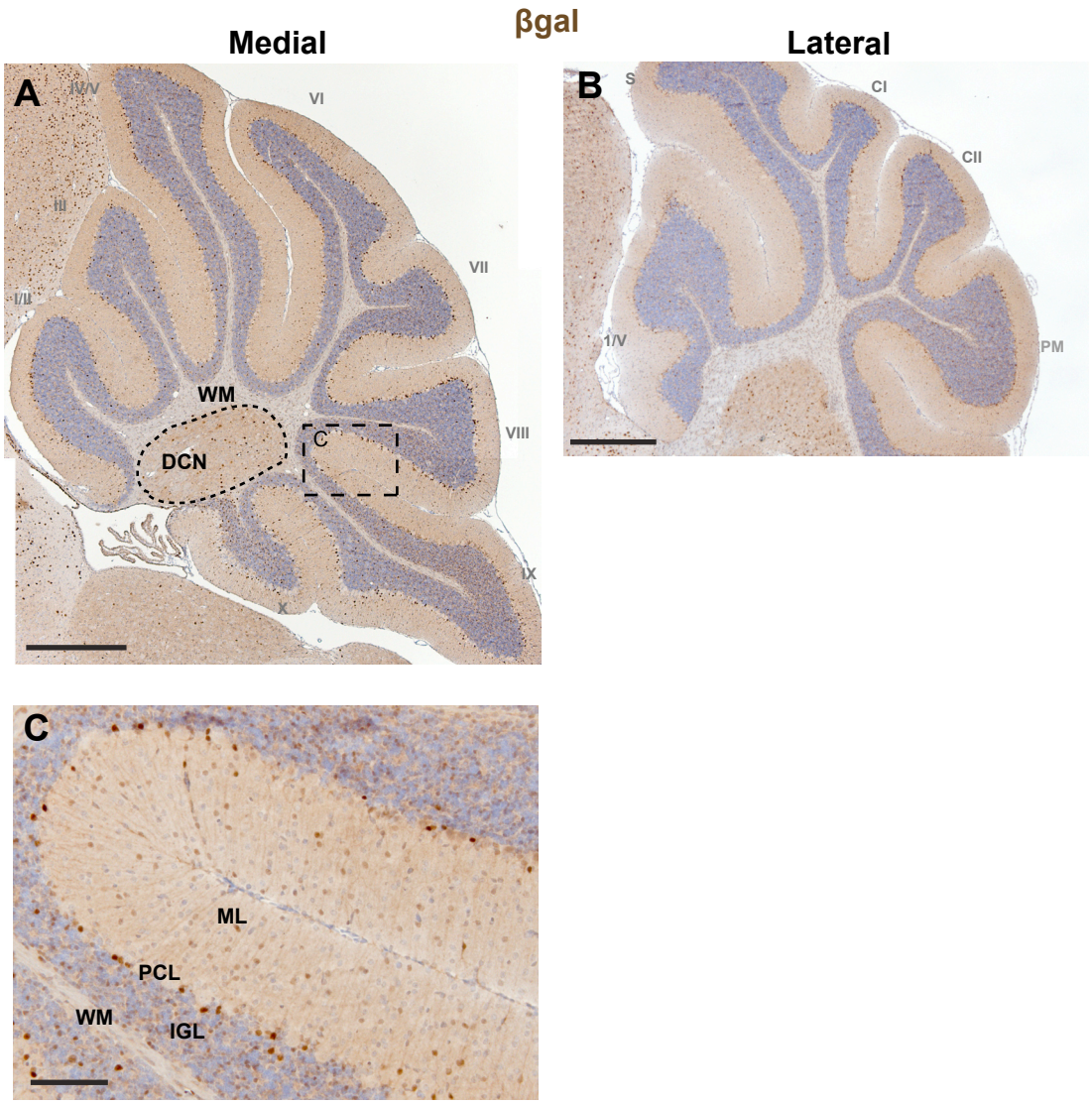

Figure 3.10 - Expression of the BAT-gal reporter in the P21 cerebellum.
DAB immunohistochemistry for β-gal on medial (A) and lateral (B) sagittal cerebellum sections at P21 revealed a restricted expression pattern with β-gal+ cells discernable within the PCL and DCN, with no apparent difference from anterior to posterior. Higher magnification (C) allowed the clear identification of β-gal+ cells within the PCL, as well as sporadic expression noted within the IGL. Scale bars: A-B = 500 µm, C = 100 µm. Vermis and hemisphere folia are labelled in grey.

Importantly, *in situ* hybridisation for *LacZ* did not reveal detectable levels of the transcript in any of the sections analysed (data not shown), indicating that active transcription of the BAT-gal transgene has likely reduced to undetectable levels by this time point but that detectable levels of the β-gal protein persist. *In situ* hybridisation for *Axin2* at P21 also revealed no staining above background levels (data not shown).

3.5.7 Analysis of β-gal and cell fate markers at P21

By P21 there is little remaining proliferation within the cerebellum, with most of the cell types having terminally differentiated. Few PCNA+ can be observed scattered in the PCL or WM, although double immunofluorescence for PCNA and β-gal did not reveal any colocalisation (data not shown) consistent with earlier time points and supporting the conclusion that the Wnt/β-catenin activity at this stage is not mitogenic. As the last remaining GCs and interneurons are produced, the expression of NeuN and Pax2 is evident. However double fluorescence immunohistochemistry revealed no colocalisation between β-gal and NeuN (Fig. 3.11A) and Pax2 (Fig. 3.11B). Consistent with the location identified through β-gal DAB detection and with the observations at P10, β-gal+ cells were identified on the fringes of the NeuN positive IGL (Fig. 3.11A) and present around Calbindin positive Purkinje cells identified with double immunofluorescence for Calbindin and β-gal (Fig. 3.11C). Double immunofluorescence for β-gal and s100β revealed a similar pattern of β-gal expression in a small subset of s100β+ Bergmann glia as that seen at P10, supporting the conclusion that the remaining β-gal+ cells at P21 are largely Bergmann glia.

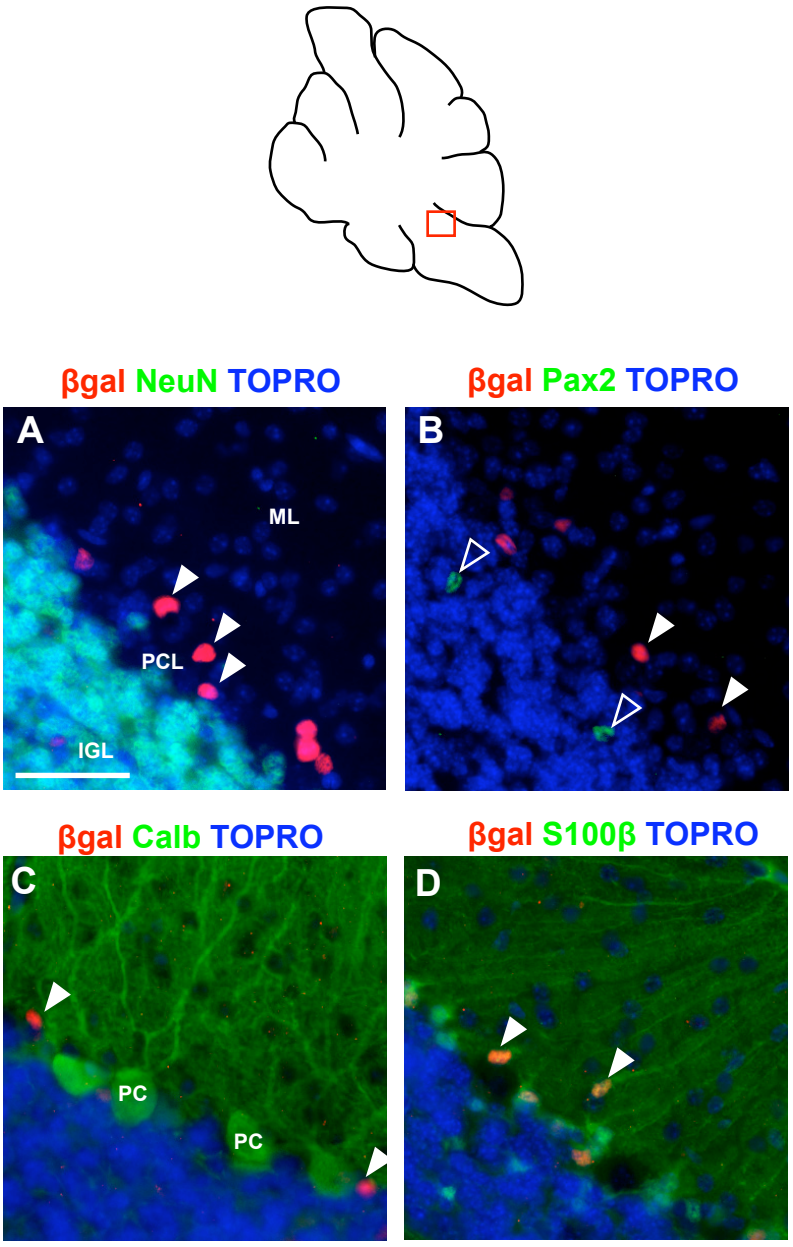

Figure 3.11 - Analysis of β-gal and cerebellar cell lineage markers at P21. Double immunofluorescence for β-gal and NeuN (A), Pax2 (B) and Calbindin (C) confirm the PCL localisation of β-gal+ cells (filled arrowheads) and demonstrate that they do not express markers of interneurons, granule neurons or PCs respectively. Colocalisation with glial marker s100β confirms the identity of these cells as Bergmann glia. Images counterstained with TOPRO3. Scale bar = 50 μm.

3.5.8 RT-PCR analysis of Wnt ligand expression during cerebellum development

As expression analysis of the BAT-gal transgene suggested active Wnt/β-catenin signalling at all time points analysed, I next carried out RT-PCR on RNA extracted from dissected cerebellum at E18.5, P1, P5, P10 and P21 (the small size of the embryonic cerebellum prohibited dissection at earlier time points) to determine which Wnt ligands were expressed and could be responsible for driving expression of the reporter[*]. Genes for analysis were selected based on published evidence (Hall et al., 2000; Lucas and Salinas, 1997; Salinas et al., 1994) or by Wnt ligands identified in the developing cerebellum according to the Allen Brain Atlas (http://www.brain-map.org). β-actin was used as a positive control for these experiments and was present in all samples (Fig. 3.12). As a general measure of Wnt/β-catenin activity over this developmental series *Axin2* expression was analysed and found to be present at all time points, although apparently reduced at P21, supporting the activity of the Wnt/β-catenin pathway at these time points.

A number of Wnt ligands showed differential expression patterns throughout the developmental series, including *Wnt3, 7a* and *11* which all appeared to increase from E18.5 to P21. *Wnt 7b* and *9a* both appeared to decrease between P1 and P21, while *Wnt1* was only identified at E18.5. Consistent levels of expression were observed by *Wnt5a* across the whole series and a more sporadic expression pattern was observed by W*nt2b, 6, 10b* and *16*. No expression of *Wnt2, 3a, 4* or *10a* was identified (Fig. 3.12).

[*] These experiments were carried out by myself and two BSc (hons) project students: Eimhear Lusbey and Mark Pringle.

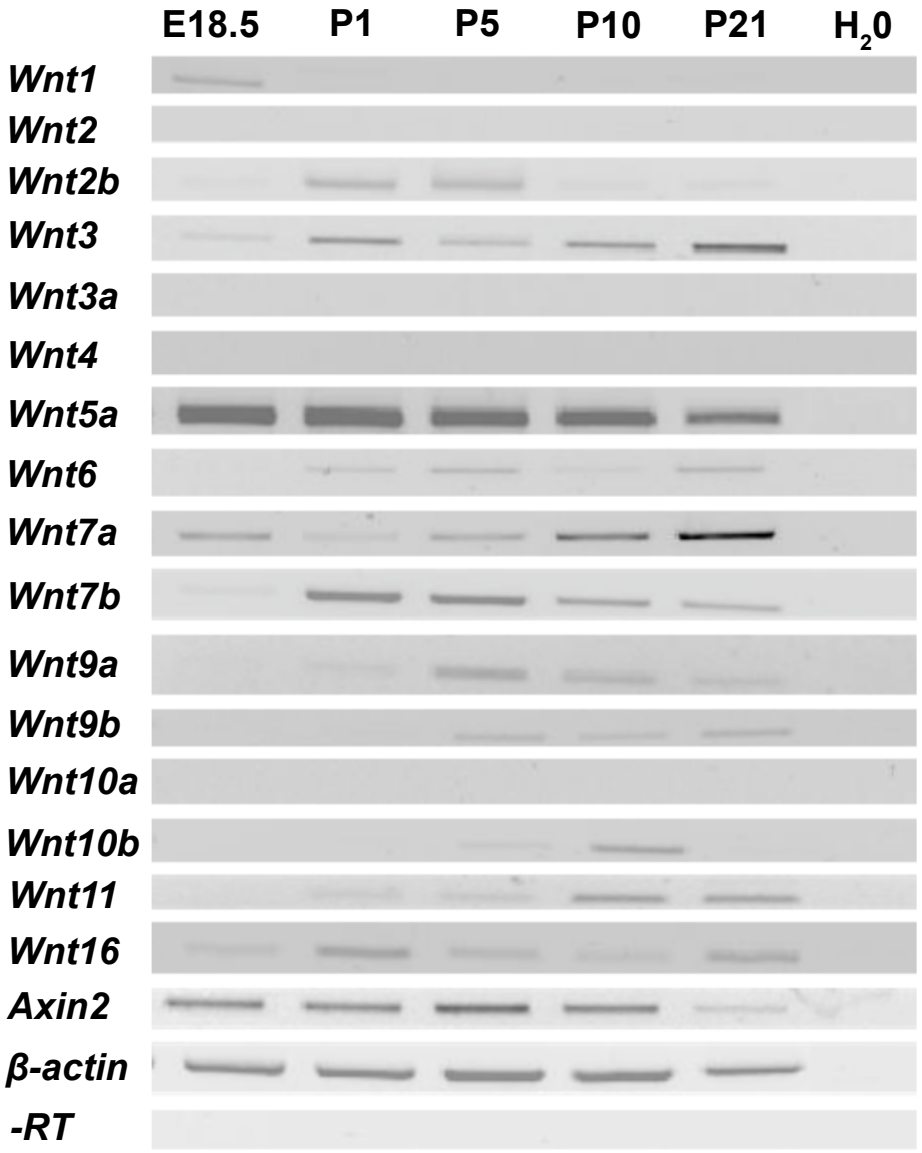

Figure 3.12 - RT-PCR analysis of Wnt ligand expression during cerebellum development.
An array of Wnt ligands were examined by RT-PCR for their expression at defined stages during cerebellum development, revealing a pattern of differential expression at each time point. The expression of *Axin2* confirms Wnt/β-catenin signalling activity at each time point. *β*-actin was used as a positive control, while reactions without reverse transcriptase (-RT) and water instead of template were used as negative controls.

3.6 Discussion

The aim of this chapter was to investigate the distribution of Wnt/β-catenin signalling during development of the cerebellum. This was undertaken from E12.5 to P21 primarily using the BAT-gal Wnt reporter mouse strain (Maretto et al., 2003). The specific roles played by Wnt/β-catenin signalling during development of the cerebellum are not yet well characterised. Here, I provide evidence for a specific and dynamic spatio-temporal pattern of Wnt/β-catenin signalling through different stages of cerebellum development (summarised in Fig. 3.13).

3.6.1 Validity of the BAT-gal transgene as an accurate reporter of Wnt/β-catenin signalling activity in the developing cerebellum

Before the results of this chapter can be interpreted, the validity of the BAT-gal transgenic reporter as a method of identifying bona fide Wnt/β-catenin signalling regions needs to be discussed in light of the data presented. The BAT-gal reporter mouse has been widely cited as a tool to study the role of Wnt/β-catenin signalling in the developing CNS (Backman et al., 2005; Bluske et al., 2009; Fancy et al., 2009; Fotaki et al., 2011a; Ivaniutsin et al., 2009; Laine et al., 2010; Liu et al., 2010; Machon et al., 2007; Mazumdar et al., 2010; Mutch et al., 2009; Selvadurai and Mason, 2011) but there are inherent limitations to the model that need to be taken into consideration.

Most downstream Wnt/β-catenin target genes display a tightly regulated and context specific expression pattern – likely the result of a complex set of cooperative regulatory elements directing expression to the right cell types at the right times (Barolo and Posakony, 2002). Transgenic reporters used to detect Wnt/β-catenin signalling (e.g. BAT-gal, TOPGAL, BAT*lacZ*, TCF/Lef-LacZ) all express a target gene with a deliberately simplistic upstream regulatory mechanism consisting of a minimal promoter coupled to multimerized TCF/LEF binding sites – the rationale behind this being that reporter gene expression should be activated in all contexts where a Wnt/β-catenin is being transduced. However, because of the artificial

regulatory construction of these reporters they cannot be considered good mechanistic models for how a Wnt/β-catenin signal is natively transduced (Barolo, 2006). Thus, while a reporter may be expressed in a similar pattern to native Wnt/β-catenin target genes, it is not being done so in the same way and as a result could cause expression that is inconsistent with Wnt/β-catenin signaling in certain contexts.

Because of this, a number of investigators choose to use *Axin2* expression as a marker for Wnt/β-catenin signalling instead of a transgenic reporter, either by analysing its endogenous mRNA expression or with available knockin *Axin2* reporter models (Lustig et al., 2002). *Axin2* encodes a negative feedback inhibitor of the Wnt/β-catenin signalling pathway and is a direct target of TCF/LEF-mediated transcription. Unlike other downstream Wnt/β-catenin targets, *Axin2* has an upstream regulatory sequence similar to that utilised by reporter models, with eight high-affinity TCF binding sites (Jho et al., 2002) that allows it to be expressed much more widely than the more tightly regulated Wnt/β-catenin target genes. Despite this, *Axin2* is still subject to the sort of native regulation that controls the expression of Wnt/β-catenin target genes (although obviously not as much as other targets). Thus, expression of *Axin2* may not indicate true levels of Wnt/β-catenin signalling in all contexts.

Combined, these caveats support the fact that no simple and consistent method of reporting Wnt/β-catenin signalling exists and the available tools need to be considered based on the context being investigated. A recent publication reached this conclusion after comparing BAT-gal, TOPGAL and *Axin2*^{LacZ} models in both developmental and pathological contexts in the lung (Al Alam et al., 2011). These authors noted differential expression patterns between all three reporters, and that the utility of each depended on whether one was investigating the up- or down-regulation of the Wnt/β-catenin pathway.

In the context of the data presented in this chapter the BAT-gal reporter also shows differential expression to *Axin2*, although the key Wnt/β-catenin signalling domains and cell lineages identified are consistent. *In situ* hybridisation for *LacZ* and *Axin2* at E12.5 and E14.5 (Fig. 3.1-2) revealed a similar expression pattern, with the key domains of the URL and IsO showing expression of both genes. However, notable differences were observed. *Axin2* showed a clear gradient of expression from the URL and LRL, particularly evident at E12.5, while the BAT-gal transgene was expressed more sporadically. The gradient of *Axin2* expression, compared to the more binary expression of *LacZ,* is likely attributable to the more subtle regulation of *Axin2* compared to the artificial BAT-gal transgene. This conclusion is supported by similar published observations made analysing BAT-gal expression in the cortex and thalamus (Bluske et al., 2009; Machon et al., 2007). In both these cases expression of the BAT-gal reporter was identified in the same domains as *Axin2* expression, although *Axin2* exhibited a much smoother gradient of expression while the BAT-gal reporter was expressed in a patchier and more mosaic manner.

Another important discrepancy between the two Wnt/β-catenin detection methods observed was the lack of detectable *Axin2* expression in postnatal cerebellum tissue where there was clear *LacZ* expression (Fig. 3.4,6,8,10). However, inability to detect expression of a gene by *in situ* hybridisation does not necessarily mean it is not present, as it could persist below the limits of detection with the given methodology. This is supported by the observation that *Axin2* is detected by RT-PCR from E18.5 to P21 (Fig. 3.12). In addition, the fallibility of *Axin2* as a marker for Wnt/β-catenin signalling activity means that we cannot rule out activity of the pathway if *Axin2* is not expressed. That said, this result is a clear limitation of these data and needs to be taken into consideration during further interpretation.

Finally, as considerable analysis has been undertaken utilising immunohistochemsitry for the β-gal protein rather than *LacZ* mRNA, it is pertinent to discuss discrepancies between these two detection methods for the BAT-gal reporter. A number of observations were made where cells were shown to express the β-gal protein but not *LacZ* mRNA, suggesting that detectable levels of the protein

persist in cells beyond the point where the cell has ceased to transduce a Wnt/β-catenin signal. At E14.5 cells in the CP were identified with β-gal but not *LacZ* expression (compare Fig. 3.2A with Fig. 3.2E), however the URL showed expression of both, consistent with the idea that β-gal+ cells migrating away from the URL and no longer responding to a Wnt/β-catenin signal may still contain detectable levels of the protein. In addition, the pattern of β-gal expression appeared more widespread at postnatal stages, compared to *LacZ* expression. By P21 *LacZ* expression was not detectable, while considerable expression of the β-gal protein was observed (Fig. 3.8). This likely represents the perdurance of β-gal protein in a certain proportion of β-gal+ cells identified, although it does not affect the conclusion that Wnt/β-catenin signalling was present during *development* of the identified cells.

The limitations of the BAT-gal reporter model obviously need to be taken into consideration. However, it is clear that there is no consistent method for universally identifying Wnt/β-catenin responding cells and as discussed different methods should be employed depending on the context. In the data presented here, differential expression between the detection methods (β-gal immunohistochemsitry, *LacZ in situ* hybridisation and *Axin2 in situ* hybridisation) exists, but the identification of key Wnt/β-catenin responding domains and cell lineages is consistent.

3.6.2 BAT-gal reporter expression at the embryonic IsO is consistent with this being a Wnt/β-catenin responsive signalling centre

Early patterning of the midbrain-hindbrain region is dependent on molecular signals released from the IsO. Formed at an expression boundary between *Gbx2* and *Otx2* (Simeone, 2000), the IsO is identified genetically through the expression of *Fgf8*, *Wnt1* and *En1*, all of which act in a positive feedback loop (Adams et al., 2000; Davis and Joyner, 1988; McMahon et al., 1992; Reifers et al., 1998). The importance of these genes in patterning the surrounding tissue, including the cerebellum, is evident when their expression is perturbed in mouse models which display severe patterning defects (Basson et al., 2008; McMahon and Bradley, 1990; Thomas and Capecchi, 1990; Wurst et al., 1994). The maintenance of *Wnt1* expression at the IsO

is therefore consistent with the observation that the BAT-gal reporter is expressed in this region and in the surrounding tissue at all embryonic ages analysed (Fig. 3.1, 3.2, 3.3). In addition to its role as a morphogenic signalling centre, the IsO is also a germinal centre that provides both the cell types and molecular signals required for fusion of the two cerebellar hemispheres (Louvi et al., 2003). A role for Wnt/β-catenin signalling in this process is demonstrated by recent evidence where loss of Jbn, a protein that has been shown to facilitate nuclear translocation of β-catenin (Lancaster et al., 2009), causes cerebellar midline fusion defects associated with a decrease in Wnt/β-catenin activity at the IsO and anterior-medial ventricular zone (Lancaster et al., 2011).

3.6.3 BAT-gal reporter expression at the embryonic RL is consistent with the early generation of GPCs but not their further development

Analysis of BAT-gal reporter expression at E12.5 and E14.5 revealed the RL as a Wnt/β-catenin signalling centre in both cases (Fig. 3.1-2) and the early EGL at E14.5 (Fig. 3.2). The rhombic lip gives birth to projection neurons of the deep cerebellar nuclei from E10.5 to E12.5 (Fink et al., 2006) followed by GPCs and unipolar brush cells from E12.5 onwards (Englund et al., 2006; Machold and Fishell, 2005; Wang et al., 2005). Because the projection neurons of the deep cerebellar nuclei are born prior to our analysis and the unipolar brush cells migrate along a different path than the dorsal stream that forms the EGL, I concluded that the BAT-gal reporter expression observed is limited to GPCs. This indicates a potential role for Wnt/β-catenin signalling in the initial specification of GPCs at E12.5 and their early migration at E14.5. Consistent with this, a number of studies have identified expression of *Wnt1* at the RL (Davis and Joyner, 1988; Dymecki and Tomasiewicz, 1998; Fischer et al., 2007; Nichols and Bruce, 2006; Wilkinson et al., 1987) and its ablation from this domain may contribute to the patterning defects in the *Wnt1* knockout mouse models (McMahon and Bradley, 1990; Thomas and Capecchi, 1990). Due to the consistency between the known expression pattern of *Wnt1*, and its important role in development of this area, it is possible that Wnt1 activity is responsible for the active Wnt/β-catenin signalling at the RL in addition to the IsO. However, it remains to be established whether additional Wnt genes are expressed in this area.

While active Wnt/β-catenin signalling was identified in the early migrating GPCs (Fig. 3.2), this was lost in the GPCs observed in the EGL during later stages of development. By E18.5, BAT-gal expression within the EGL was minimal and from P1 onwards, it was undetectable (Fig. 3.3-4). These data are consistent with a role for Wnt/β-catenin signalling during early specification of GPCs but not in their further migration or proliferation. Taken together with the fact that proliferation of this cell population during late embryogenesis and early post natal development is driven by Shh secreted by neighbouring Purkinje cells (Dahmane and Ruiz i Altaba, 1999; Wechsler-Reya and Scott, 1999), these results suggest that while Wnt/β-catenin signalling plays a role in the early specification of the GPC cell population at the embryonic rhombic lip, it does not appear to be involved in the continued development of these cells in the EGL. Interestingly, recent evidence shows that dysregulation of the Wnt/β-catenin pathway in GPCs through conditional *Apc* knockout (thereby constitutively activating the pathway) leads to a reduction in production of mature GCs and a severe reduction in cerebellar size as a result (Lorenz et al., 2011). This supports the necessity to keep Wnt/β-catenin signal transduction tightly regulated even in non-Wnt/β-catenin responsive cell lineages.

Prior to maturation of terminally differentiated GCs, they undergo migration across the presumptive ML from the EGL to the IGL. A first glance, the pattern of β-gal+ cell distribution within the postnatal cerebellum resembles the pattern that would be expected if the reporter were active in these cells. However, the absence of NeuN expression in any of the β-gal+ cells observed from P5-P21 demonstrates that this is not the case (Fig. 3.7,9,11). NeuN is abundantly expressed in most classes of neurons (Mullen et al., 1992) and has been identified in all stages of post-mitotic granule cell development (Weyer and Schilling, 2003). Thus, the lack of NeuN expression in β-gal+ cells located in these regions indicates that they are not of the granule lineage.

3.6.4 BAT-gal reporter expression at the embryonic LRL is consistent with this region as a key Wnt/β-catenin signalling centre and possible site for medulloblastoma origin

The LRL is a region that recent evidence suggests may be a site for the origin of Wnt subgroup medulloblastoma (Gibson et al., 2010). This conclusion was based on gene expression analysis which suggested the region expressed a high number of Wnt/β-catenin target genes compared to surrounding areas. Constitutive activation of the Wnt/β-catenin pathway in progenitors present in this region leads to a migration defect that eventually manifests as a tumour when tumour suppressor *TP53* is additionally knocked out. While it is somewhat controversial that the LRL is the site of origin for Wnt subtype medulloblastoma, the fact that the LRL was identified as a highly Wnt/β-catenin responsive region does support their conclusion. The data presented in this chapter demonstrate the activity of the Wnt/β-catenin signalling pathway in the LRL through both the expression of the BAT-gal reporter and Wnt/β-catenin target gene *Axin2*, supporting the conclusions of Gibson et al (2010) that the LRL is a Wnt/β-catenin responsive region and potential site for the origin of Wnt subgroup medulloblastoma.

3.6.5 BAT-gal reporter expression at the perinatal VZ supports a role for Wnt/β-catenin in regulating progenitors from this region

At E18.5, many β-gal+ cells were seen in the ventricular zone (Fig. 3.3-4), whereas at earlier stages they were less abundant (Fig. 3.1-2). This indicates that Wnt/β-catenin signalling is active in cell lineages originating at the ventricular zone from this time point. Purkinje cells are amongst the first cell lineage generated at the ventricular zone. They arise at the onset of cerebellar neurogenesis between E10.5 and E12.5 (Altman and Bayer, 1997; Hashimoto and Mikoshiba, 2003). The interneuron lineage can then be detected by the expression of Pax2 in scattered cells at the ventricular zone from E13.5 to E17.5 (Maricich and Herrup, 1999) from where they migrate dorsally into the white matter of the early cerebellum as Pax2+ lineage restricted progenitors (Maricich and Herrup, 1999; Weisheit et al., 2006). Concurrently, gliogenesis begins at the ventricular zone from E13.5, identified

through the expression of S100β, BLBP and Sox9 (Hachem et al., 2007). The early Bergmann glial population is hypothesised to exit the ventricular zone at E14.5 and follow a migratory path behind Purkinje cells (Yamada and Watanabe, 2002). Birth of the remaining cerebellar glial populations follows from this point.

The data presented here suggests that the cell populations born and migrating away from the ventricular zone between E18.5 and P1 could be doing so in response to a Wnt/β-catenin signal. Based upon the timing of known cell populations arising from the ventricular zone, we can conclude that Wnt/β-catenin signalling is active in the multipotent VZ progenitors that are responsible for generating *both* the interneuron and glial lineages. However, the identity of the β-gal+ cells within the E18.5 and P1 cerebellum is less clear. Due to the fact that multipotent VZ progenitors and glial lineage restricted WM progenitors display the same molecular markers (i.e. GFAP, Nestin, Sox9) it cannot be concluded whether these β-gal+ cells identified are lineage restricted (i.e. glial or interneuron) or not. The key finding from the data presented above (Fig. 3.5) is that the lineage restricted interneurons do not express β-gal, leading to the conclusion that Wnt/β-catenin signalling is active in multipotent progenitors and potentially within the glial lineage.

RT-PCR analysis of the E18.5 and P1 cerebellum revealed the expression of a number of different Wnt ligands (Fig. 3.12). *Wnt1*, known to be involved in early cerebellum development (see above refs), is identified at E18.5 but not P1, suggesting a possible residual role into late embryonic development.

3.6.6 BAT-gal reporter expression in the postnatal cerebellum is consistent with a role for Wnt/β-catenin signalling in developing Bergmann glia

Further to the identification of β-gal+ cells at the ventricular zone, a population of β-gal+ cells was also observed within all other layers of the cerebellum (excluding the EGL) from E18.5 through to P21. Lack of colocalisation between β-galactosidase and Pax2, NeuN and Calbindin at all postnatal stages analysed (Fig. 3.7,9,11) ruled out the possibility of the β-gal+ cell population being of the interneuron, granule or

Purkinje cell types respectively. The remaining alternative is that the β-gal+ cell population identified within the developing cerebellum are glia. Oligodendrocytes are thought to arise from extra-cerebellar tissue (Grimaldi et al., 2009), while velate and fibrous astrocytes arise from progenitors at the VZ or progenitors that have delaminated to the presumptive WM (Milosevic and Goldman, 2002; Milosevic and Goldman, 2004). Bergmann glia are thought to follow a slightly different developmental path. Rather than arising during gliogenesis from WM progenitors like the rest of the astrocyte lineage, a population of early Bergmann glia arise from the ventricular zone and migrate in close proximity to - and remain developmentally intertwined with - Purkinje cells (Yamada and Watanabe, 2002). This wave of migration occurs from E14.5 onwards, and by E18.5 these glia come to lie in a pattern similar to that seen for some of the β-gal+ cell population identified, outlining the developing folia inferior to the EGL. A β-gal+ cell population in this pattern was seen at all postnatal stages, although the number of labelled cells appears to decrease with age. Anatomical location of β-gal+ cells throughout postnatal development and colocalisation of β-gal with glial markers Sox9 and s100β at P5 (Fig. 3.7), P10 (Fig. 3.9) and P21 (Fig. 3.11) strongly supports the conclusion that the developing Bergmann glia population is responding to a Wnt/β-catenin signal. Consistent with this, a recent study revealed that dysregulated Wnt/β-catenin signalling, through loss of *Apc*, lead to a disruption of Bergmann glia cell structure resulting in the eventual degeneration of the neighbouring PC population (Wang et al., 2011).

Interestingly, the lack of β-galactosidase expression at the ventricular zone at E14.5 indicates that Wnt/β-catenin signalling is not involved in the birth of the Bergmann glia but may be potentially involved in its further development and maturation. This is consistent with the post-mitotic development of Bergmann glia occurring alongside dendritogenesis and synaptogenesis of Purkinje cells (Yamada et al., 2000; Yamada and Watanabe, 2002; Yuasa, 1996) and suggests a possible role for Wnt/β-catenin in this process. However, the presence of β-gal+ cells at the VZ of E18.5 and P1 cerebellum (Fig. 3.3-4) raises the possibility that Bergmann glia are still being

generated at this time point, or that the generation of additional cell lineages is also regulated by a Wnt/β-catenin signal.

RT-PCR analysis for the expression of Wnt ligands during postnatal cerebellum development revealed the presence of several ligands that could be responsible for driving the expression of the BAT-gal reporter (Fig. 3.12). *Wnt3, 7a* and *7b* were all identified in the postnatal cerebellum. *Wnt3* and *7a* have both been shown to be expressed in PCs and GCs respectively and, alongside *Wnt7b* are known to regulate axon remodelling, dendritogenesis and synapse formation (Hall et al., 2000; Lucas and Salinas, 1997; Rosso et al., 2005; Salinas et al., 1994). Importantly though, they have also been shown to regulate these processes independent of Wnt/β-catenin signalling (Ciani et al., 2004; Purro et al., 2008; Rosso et al., 2005). The lack of postnatal BAT-gal reporter expression in the GCs or PCs is consistent with this, although the possibility remains that the ligand expressed by these cells could be bound by the neighbouring β-gal+ Bergmann glia and cause activation of the reporter. In addition to these known Wnt ligands identified, *Wnt2b, 5a, 6, 9a, 9b, 10b, 11* and *16* were all identified with varying post natal expression patterns. These ligands have been shown to play a role in numerous developmental processes in a number of organs (see http://www.stanford.edu/group/nusselab/cgi-bin/wnt/mouse for a summary of Wnt ligands involved in organogenesis). However, a role for these ligands signalling through the Wnt/β-catenin pathway in cerebellar development (or even CNS development) remains to be determined.

3.6.7 Summary

Cerebellum development is anatomically well defined, though the molecular mechanisms that govern the generation of the complexity observed in the adult cerebellum remain to be fully resolved. In this chapter I have presented a spatio-temporal description of Wnt/β-catenin signalling activity during cerebellum development that both supports and extends previous published findings. From the data presented in this chapter I conclude that there are potential roles for Wnt/β-catenin signalling at the embryonic RL, the perinatal VZ and in the developing cerebellar glial lineage (Fig. 3.13).

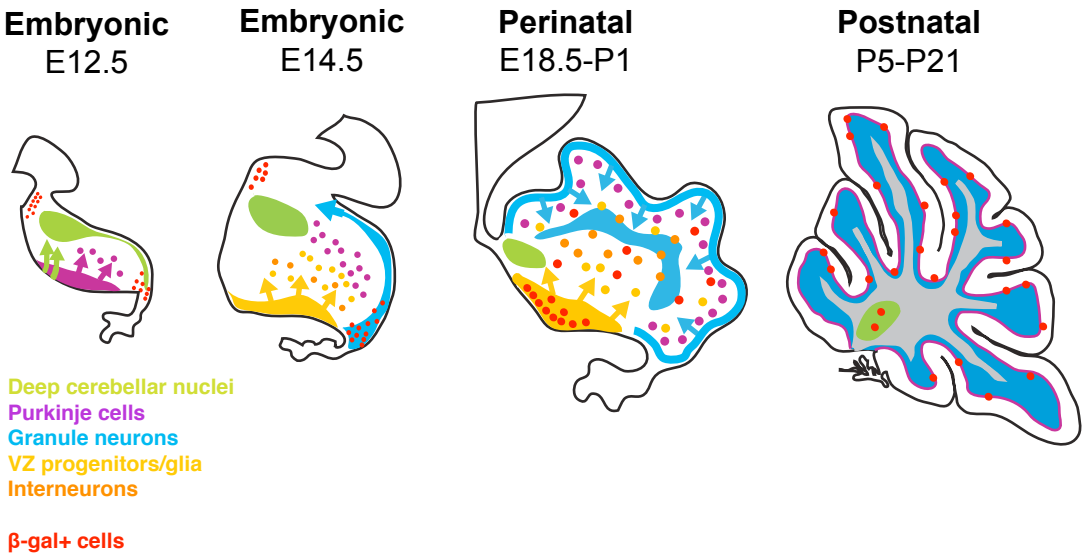

Figure 3.13 - Summary of Wnt/β-catenin activity during cerebellum development from E12.5 to P21.
Based on expression analysis of the BAT-gal reporter allele throughout cerebellum development, a dynamic pattern of Wnt/β-catenin was revealed. Initially expression was observed at the RL and the IsO at E12.5 and E14.5. By E18.5 expression had shifted to the VZ and in cells radiating from that centre, while expression in the granule lineage had ceased. During postnatal stages the expression becomes restricted to the PCL, consistent with a population of Bergmann glia.

4 Analysis of Wnt/β-catenin signalling dysregulation in cerebellar slice culture

4.1 Introduction

The novel expression of the BAT-gal reporter observed perinatally and postnatally suggests a number of possible roles for Wnt/β-catenin signalling in cerebellum development. The identification of the VZ and its tangentially radiating progeny as cells with high Wnt/β-catenin activity leads to the hypothesis that Wnt/β-catenin signalling could play a role in the regulation of VZ progenitors and in the cell lineages they give rise to. While a role for Wnt/β-catenin signalling in this process has not yet been observed, a number of hypotheses can be generated based on the understanding of the function of Wnt/β-catenin signalling elsewhere in the CNS.

Within the cortex, a growing body of literature suggests multiple roles for Wnt/β-catenin signalling in regional specification and regulation of the radial dimension by controlling progenitor and transit amplifying cell proliferation and differentiation. The ventricular zone in the developing cortex contains a population of radial glia that divide asymmetrically to produce either terminally differentiated neurons, IPCs or additional radial glial cells. IPCs then divide to produce two terminally differentiated neurons, thus amplifying the neurogenic pool (Molyneaux et al., 2007). A role for Wnt/β-catenin signalling has been identified in this process based on published evidence that shows a reduction in cortical neurogenesis after inhibition of the pathway (Zhou et al., 2006). Conversely, activation of the pathway promotes expansion of the developing cortex (Chenn and Walsh, 2002; Ivaniutsin et al., 2009). These findings support a role for Wnt/β-catenin signalling in regulating self-renewal of the radial glial population, where inhibition causes increased cell cycle exit and hence fewer neurons, and activation promotes radial glial self-renewal and an increased neurogenic pool. In addition, the Wnt/β-catenin pathway has also been shown to promote IPC differentiation (Hirabayashi et al., 2004; Munji et al., 2011).

These multiple roles of Wnt/β-catenin signalling in regulating self-renewal and differentiation in the cortex support the hypothesis that a similar mechanism could be responsible for the regulation of VZ progenitors and their progeny. To address this, a loss-of-function/gain-of-function approach was attempted using small molecule activation/inhibition of the Wnt/β-catenin pathway in organotypic cerebellar slice culture. Organotypic slice culture has been used successfully to study numerous aspects of cerebellar developmental biology (Choi et al., 2005; Dusart et al., 1997; Fink et al., 2006; Ghoumari et al., 2000; Li et al., 2006). Despite the limitations of a 2D culture system such as this, it presents an opportunity to generate useful pilot data to guide future *in vivo* experiments.

The use of small molecules to activate or inhibit cellular signalling pathways is an effective tool to generate pilot data before expensive and time consuming genetic manipulation is undertaken. The nature of the Wnt/β-catenin pathway presents an attractive target for small molecule dysregulation: it is a biochemically well-characterised pathway with multiple positive and negative regulatory components available for targeting. Wnt ligands are cysteine-rich secreted glycoproteins that act in an autocrine, paracrine or juxtacrine manner. A Wnt ligand binds and activates the Frizzled-LRP5/6 transmembrane receptor complex and activates a downstream cystoplasmic cascade that results in the dissociation of the β-catenin destruction complex – consisting of APC, GSK3β, Axin and CK1. Dissociation of this complex allows for the cytoplasmic accumulation and nuclear translocation of β-catenin where it activates a transcriptional response with TCF/LEF cotranscription factors. In this chapter, I investigated the effectiveness of several small molecules that activate or inhibit the Wnt/β-catenin pathway by targeting different components.

Inhibition of GSK3β stops the phosphorylation of β-catenin by the destruction complex and allows cytoplasmic accumulation and nuclear translocation to occur. 6-bromoindirubin (a component of Tyrian purple dye found in molluscs) and its synthetic derivative 6-bromoindirubin-3'-oxime (BIO) were shown to be potent inhibitors of GSK3β and when applied to *Xenopus* embryos resulted in ectopic activation of Wnt/β-catenin signalling (Meijer et al., 2003). This finding was further

extended to both mouse and human cells (Sato et al., 2004) and has since become routine for *in vitro* activation of Wnt/β-catenin signalling. However, indirubins are known to cross-react with numerous kinases in addition to GSK3β (Meijer et al., 2003; Zhen et al., 2007). A more selective GSK3β inhibitor CHIR99021 (CHIR) has also been identified (Ring et al., 2003) and has been shown to activate the Wnt/β-catenin pathway *in vitro* as a result (Ying et al., 2008).

Considerably more research has been undertaken in the identification of inhibitors of Wnt/β-catenin signalling due to the potential clinical applications to Wnt-dependent cancer (e.g. colon cancer). Numerous high throughput drug screens have identified a number of small molecules that cause effective inhibition of the Wnt/β-catenin pathway. Inhibitor of Wnt production-2 (IWP2) was identified in one such screen as an inhibitor of the acyltransferase Porcn. Porcn is required for palmitoylation of the Wnt ligand prior to secretion (Willert et al., 2003) and disruption of this process by IWP2 leads to a reduction in secreted Wnt ligand alongside downstream Wnt/β-catenin activity *in vitro* (Chen et al., 2009). An additional screen identified a tankyrase inhibitor XAV939 (XAV) that acts downstream of Wnt production by stabilising the β-catenin destruction complex (Huang et al., 2009). These authors demonstrate that tankyrase 1 and 2 bind directly to Axin and target it for ubiquitination, thereby providing a mechanism for the homeostatic regulation of Axin levels. Disruption of this process leads to an upregulation of Axin, which then reduces the amount of cytoplasmic β-catenin available for Wnt/β-catenin signal transduction. A further small molecule screen utilising RNAi knockdown of upstream components identified several small molecules that target the β-catenin-TCF/LEF transcription complex independent of β-catenin stabilisation (Gonsalves et al., 2011). These inhibitors of β-catenin responsive transcription (iCRT) were shown to inhibit the expression of Wnt/β-catenin target genes while cytoplasmic function of β-catenin remained unaffected. While clinical applications were the primary objective of the screens that identified these small molecules, they present a useful tool for experimental manipulation of the Wnt/β-catenin pathway.

4.2 Aim and experimental design

The aim of the work carried out in this chapter was to characterise the early effects of Wnt/β-catenin pathway dysregulation on development of the E18.5 cerebellum *ex vivo* in order to generate pilot data on its possible function. To address this, E18.5 BAT-gal+ cerebellums were cultured in the presence of GSK3β inhibitors BIO or CHIR, Porcn inhibitor IWP2, Tankyrase inhibitor XAV or β-catenin transcriptional inhibitor iCRT3 for 24 hours (Fig. 4.1A). BrdU was also added to the culture for the final two hours to give a measure of proliferation. Slices were then analysed for expression of Wnt/β-catenin pathway activation, proliferation, apoptosis and cell fate by immunohistochemistry or qRT-PCR (Fig. 4.1B).

In order to quantitate the expression of the different markers analysed by immunohistochemistry, counting frames were placed in four defined regions of the section (Fig. 4.1B): three along the anterior-posterior extent of the EGL, and one ventrally covering the VZ and the area immediately dorsal to it. The frames placed along the EGL were further partitioned to generate defined quantitation for the EGL and the internal component inferior to the EGL. Quantitation involved generating a labelling index for each of the markers by counting all Topro+ cells and then all cells expressing the marker being analysed in the ventral, internal and EGL regions. Two sections from each slice were quantitated for each marker and averaged to give a value for an individual slice. One slice was analysed from three individual animals in each experimental group (n=3). For qPCR, three slices were analysed for each experimental group (n=3). Quantitated immunohistochemistry or qRT-PCR from treated slices in all cases were compared to the relevant DMSO treated control using an unpaired two-tailed T-test and a P value of less than 0.05 was considered significant.

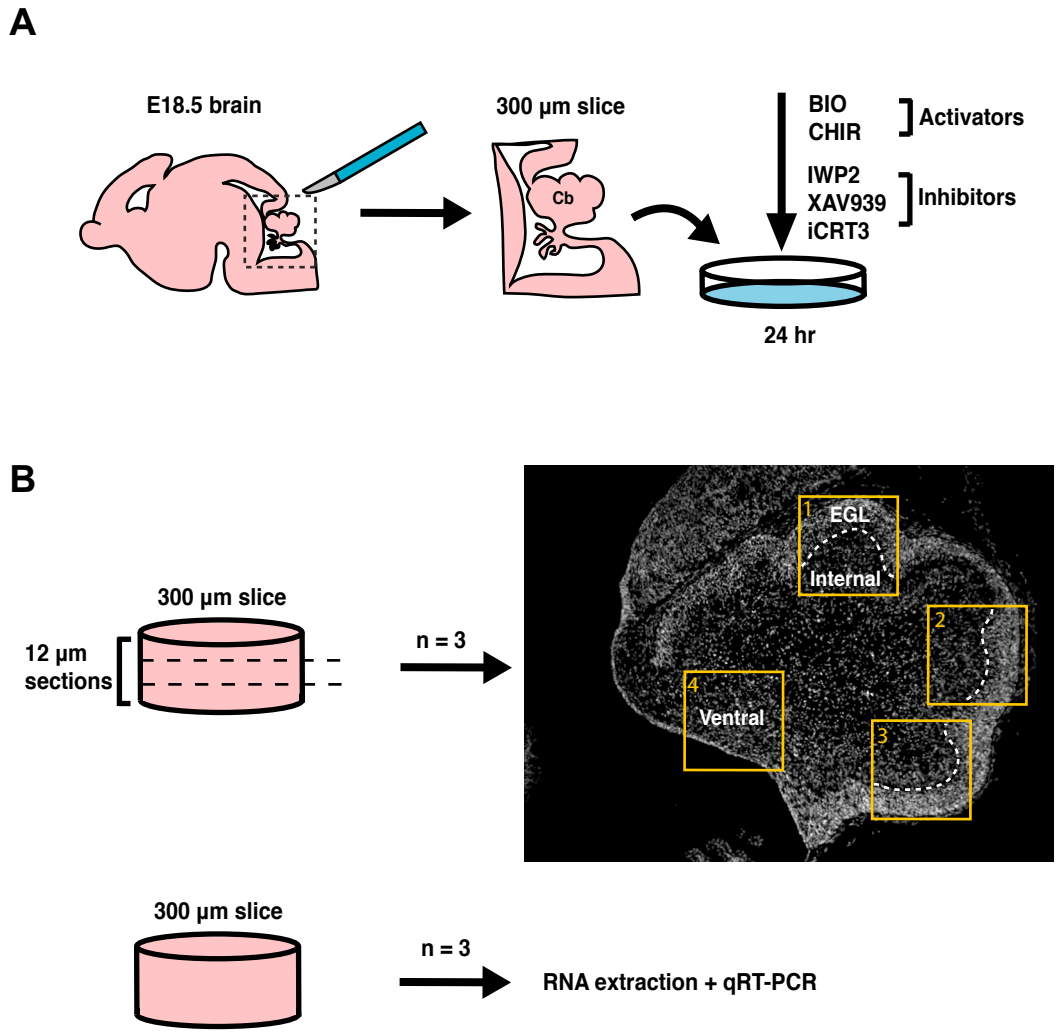

Figure 4.1 - Experimental design for *ex vivo* analysis of Wnt/β-catenin signalling in the E18.5 cerebellum.
(A) E18.5 brains were dissected and embedded in agarose before being sectioned on a vibratome into 300 µm thick slices. The explant slices were grown in culture for 24 hr in the presence of small molecule activators or inhibitors of the Wnt/β-catenin pathway. (B) Individual slices were then fixed, frozen and sectioned further on a cryostat. Two sections were tested with immunohistochemistry and quantitated for the expression of various markers at four defined regions that include the EGL, interior and ventral regions in a slice taken from three animals (n=3). Alternatively, RNA was extracted from three slices (n=3) and tested with qRT-PCR.

4.3 Establishement of a cerebellar slice culture protocol

4.3.1 Culture length and tissue preparation optimisation

In order to determine the culturing parameters, slices were cultured for between 24 and 96 hours and gross morphology was examined. In addition, two methods of post-culture processing were compared: tissue freezing followed by cryosectioning (Fig. 4.2A,C,E,G) and wax embedding followed by microtome sectioning (Fig 4.2B,D,F,H). Frozen tissue sections after 24 hours *ex vivo* had a normal morphology with an easily definable EGL (Fig. 4.2A). However, by 48 hours *ex vivo* this was lost as the EGL appeared less organised and was not as easy to differentiate from the cell layer inferior to it (Fig. 4.2C). This was also observed after 72 hours *ex vivo* (Fig. 4.2E) and by 96 hours *ex vivo* the morphology was significantly disrupted with a thickened EGL and a disruption to cell density within the internal region (Fig. 4.2G). Due to the loss of morphology from 48 hours onwards, I decided to limit my analysis to slices examined after 24 hours *ex vivo*. The changes to cell density and the disorganisation of the cell layers from 48 hours onwards would have prohibited accurate quantitation of cell numbers. Similar morphological features were observed with sections analysed after wax preparation. After 24 hours *ex vivo* the laminated structure of the cerebellum was clear (Fig. 4.2B). This became less evident with each additional day *ex vivo* (Fig. 4.2D,F,H). However, the cell sparse nature of the cerebellum after 24 hours *ex vivo* appeared to result in tearing between the ventral and dorsal aspects of the section when the wax preparation was used. Due to this, I reasoned that the frozen preparation was preferable for retaining the cellular morphology of the slice.

4.3.2 Dose response for small molecules targeting the Wnt/β-catenin pathway

A number of small molecules were trialled in the *ex vivo* cerebellar slice culture paradigm. Initially, a dose response was performed for each using concentrations based on published evidence or covering a broad range. The effect of the different concentrations was judged non-quantitatively by the extent of BrdU label retention or BAT-gal reporter expression (measured by immunohistochemistry for β-gal)

compared to DMSO treated control slices (Fig. 4.3A). Wnt/β-catenin pathway activator BIO has been shown to be effective at concentrations between 5-20 μM in *ex vivo* culture experiments (Fliniaux et al., 2008; Kuure et al., 2007; Laine et al., 2010) so I conducted a dose response at 5 μM (Fig. 4.3B), 10μM (Fig. 4.3C) and 20 μM (Fig. 4.3D). While a 5 μM concentration of BIO appeared to result in an increase in BrdU label retention, a concentration of 20 μM showed increased expression of the BAT-gal reporter, thus both these concentrations of BIO were selected for further analysis. No published evidence was found for the use of CHIR in an explant culture system, although it has been shown to be effective *in vitro* at a concentration of 3 μM (Ying et al., 2008). Thus, I trialled 0.5 μM (Fig. 4.3E), 5 μM (Fig. 4.3F) and 50 μM (Fig. 4.3G) concentrations. While none of the slices analysed contained the BAT-gal reporter transgene, a marked change in BrdU label retention was clear at 50 μM (Fig. 4.3G) therefore this concentration was selected for further analysis.

Wnt/β-catenin pathway inhibitors IWP2 and XAV have both been shown to inhibit the pathway in organotypic kidney culture (Karner et al., 2010; Karner et al., 2011) at concentrations of 5 μM and 200 μM respectively, although XAV has also been shown to function *in vitro* at a concentration of 1 μM. Thus I performed a dose response using a range from 0.5 μM-50 μM for IWP2 (Fig. 4.3H-J) and a higher range of 1 μM-100 μM for XAV (Fig. 4.3K-M). At no dose tested was a clear difference in BrdU label retention or β-gal expression evident, therefore the highest dose (50 μM and 100 μM for IWP2 and XAV respectively) was selected for further analysis. Finally, iCRT3 has only recently been identified (Gonsalves et al., 2011) so no published evidence for its use in an explant culture system exists. As it was shown to be effective in a number of different *in vitro* settings at concentrations between 25 μM and 100 μM (Gonsalves et al., 2011) I performed a dose response covering the same range (Fig. 4.3N-P). No change to the expression of β-gal was evident, although reduced BrdU label retention was observed in all cell layers from a concentration of 50 μM, therefore this dose was selected for further analysis.

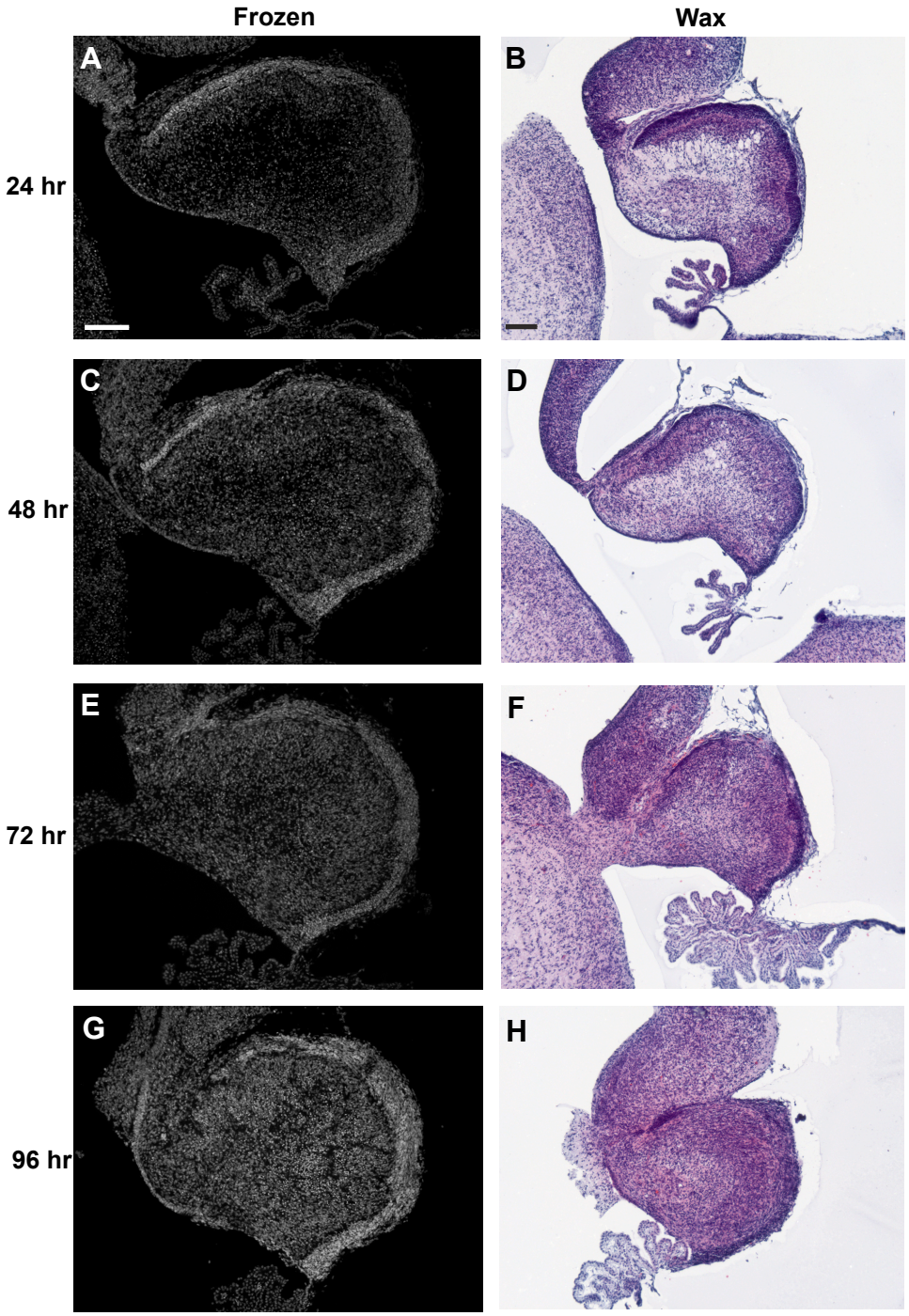

Figure 4.2 - Optimisation of culture length and tissue processing technique. Explant slices from E18.5 cerebellum were cultured for 24 (A-B), 48 (C-D), 72 (E-F) or 96 (G-H) hours and then frozen (A,C,E,G) and analysed with TOPRO3 or wax embedded (B,D,F,H) and analysed with a haematoxylin stain. Scale bars = 100 µm.

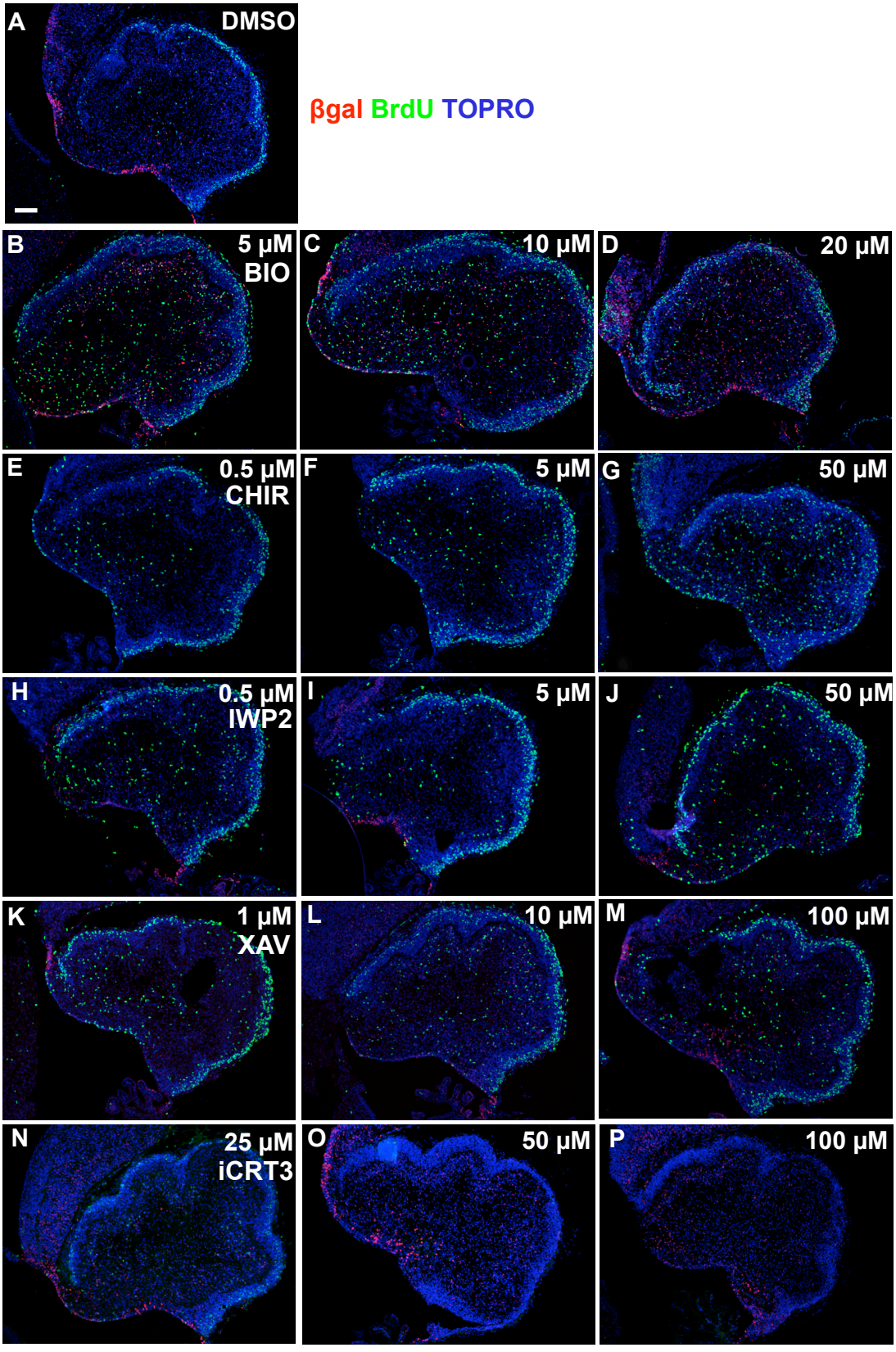

Figure 4.3 - Small molecule dose response.
Immunohistochemistry for BrdU and β-gal was undertaken on explant cerebellum slices cultured in the presence of DMSO (A) or varying concentrations of BIO (B-D), CHIR (E-G), IWP2 (H-J), XAV (K-M) or iCRT3 (N-P) in order to determine the extent of action on BAT-gal reporter expression and proliferation and select the most effective concentration for use in further experiments. Scale bar = 100 μm.

4.4 Inhibition of Wnt/β-catenin signalling was not successful in this cerebellar slice culture system

Despite the negligible changes observed with the doses of Wnt/β-catenin pathway inhibitors tested initially (Fig. 4.3), I hypothesised that closer investigation might reveal an effect that would justify further analysis. To test this, I cultured explant cerebellum slices from entire E18.5 BAT-gal+ litters and treated each with either 50 μM IWP2, 100 μM XAV or 50 μM iCRT3. β-gal expression was still evident in slices treated with IWP2 (Fig. 4.4B), XAV (Fig. 4.4C) or iCRT3 (Fig. 4.4D). However, as results in the previous chapter suggest the β-gal protein may persist for a period after pathway activity has ceased, I analysed the expression of Wnt/β-catenin downstream target *Axin2* by qPCR. This experiment showed no change in the level of *Axin2* between any of the treatment groups and the DMSO treated control slices (Fig. 4.4F). The likely explanation for these data are the limitations of the relatively short culture period in the presence of the small molecules. Due to the constraints of the culture system and the requirement for a clear morphology for accurate quantitation of cell numbers no further experiments were carried out using the Wnt/β-catenin pathway inhibitors.

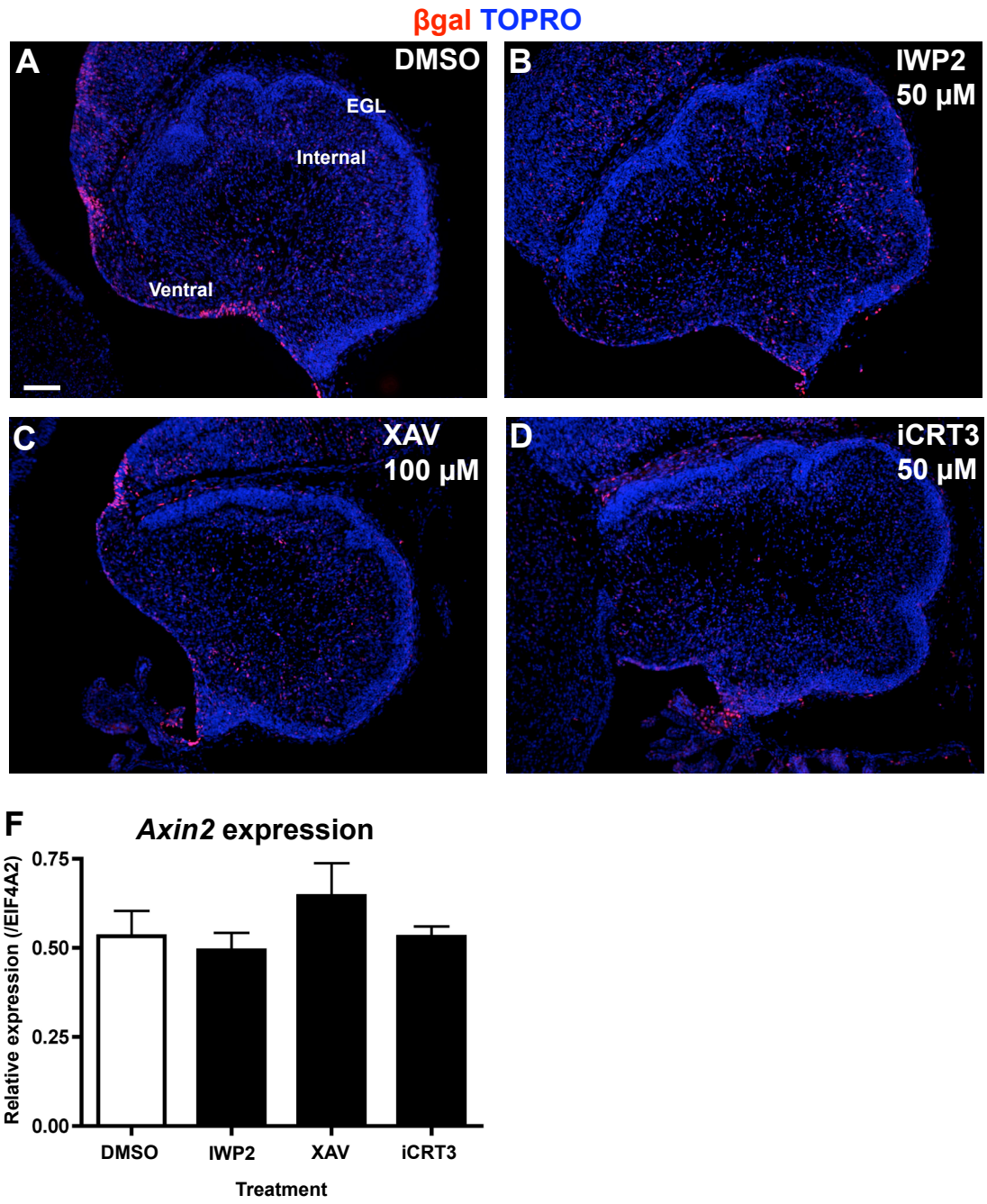

Figure 4.4 - Small molecule induced Wnt/β-catenin pathway inhibition was not successfull in the culture setting.
E18.5 BAT-gal+ cerebellum slices were cultured in the presence of DMSO (A), 50 µM IWP2 (B), 100 µM XAV (C) or 50 µM iCRT3 (D). Expression of β-gal was analysed by immunohistochemistry and compared. Expression of *Axin2* was analysed by qRT-PCR (F) and each of the treated groups (black bars) was compared to the DMSO control group (white bar) by a T-test. No signficant difference was observed (n=3, error bars = SEM). Scale bar = 100 µm.

4.5 Activation of Wnt/β-catenin signalling in cerebellar slice culture

4.5.1 Small molecule inhibition of GSK3β activates the Wnt/β-catenin pathway in cerebellar slice culture

Analysis of β-gal expression in BAT-gal+ E18.5 cerebellum slices cultures for 24 hours *ex vivo* revealed an expression pattern identical to that observed at E18.5 *in vivo* (see Chapter 3). β-gal expression was detected along the VZ and spread throughout the internal region of the slice (Fig. 4.5A). Quantitation of β-gal expression calculated by counting β-gal+ cells and expressing that as a proportion of total cell number in the EGL, internal and ventral regions reflected this observation (white bars in Fig. 4.5E). Only 1.4% (±0.4%) of cells within the EGL expressed β-gal, while 9.9% (±1.6%) and 19.4% (±3.1%) of cells within the internal and ventral regions were β-gal+ respectively (Fig. 4.5E).

Treatment of slices with 5 μM BIO for 24 hours did not appreciably increase the expression of β-gal (Fig. 4.5B). This is evident in the quantitation of β-gal+ cells (compared red bars with white bars in Fig. 4.5E). 5 μM BIO treatment resulted in 3.1% (±1.3%) of EGL cells, 15.0% (±3.8%) of internal cells and 18.6% (±3.1%) of ventral cells expressing β-gal, a result which was not significantly different to that observed in DMSO treated slices. Treatment with 20 μM BIO did result in a notable increase in the expression of β-gal (Fig. 4.5C). This was particularly evident in the EGL and internal region compared to the DMSO treated control. Quantitation reflected this (compare orange bars with white bars Fig. 4.5E). The proportion of β-gal+ cells within the EGL rose to 17.2% (±1.2%), within the internal region to 17% (±1.3%) and within the ventral region to 20.7% (±3.8%). These differences were significant between the 20 μM and DMSO treated slices within the EGL and internal regions, though not the ventral region – likely reflecting the existing Wnt/β-catenin activity in that region. Pathway activation with CHIR showed an even more pronounced effect on expression of the BAT-gal reporter. β-gal was clearly evident

within all cell layers in the slice (Fig. 4.5D). The proportion of β-gal+ cells was increased in all cell layers (compare blue bars with white bars Fig. 4.5E). β-gal+ cells made up 32.1% (±2.3%), 25% (±4%) and 31.3% (±4.4%) of the EGL, internal and ventral regions respectively.

These data are supported by qPCR for *Axin2,* which was used as an independent validation for Wnt/β-catenin pathway activation (Fig. 4.5F). Relative expression of *Axin2* compared to *EIF4A2* was not significantly increased by slice treatment with 5 μM BIO, however it was after treatment with 20 μM and further still with 50 μM CHIR. This pattern is consistent with that observed for the proportion of β-gal+ cells in the whole cerebellum (last group Fig. 4.5E), which consisted of pooled results from the EGL, internal and ventral regions. Combined, these data are consistent with activation of the Wnt/β-catenin signalling pathway in E18.5 cerebellum slices treated *ex vivo* with small molecules inhibiting GSK3β.

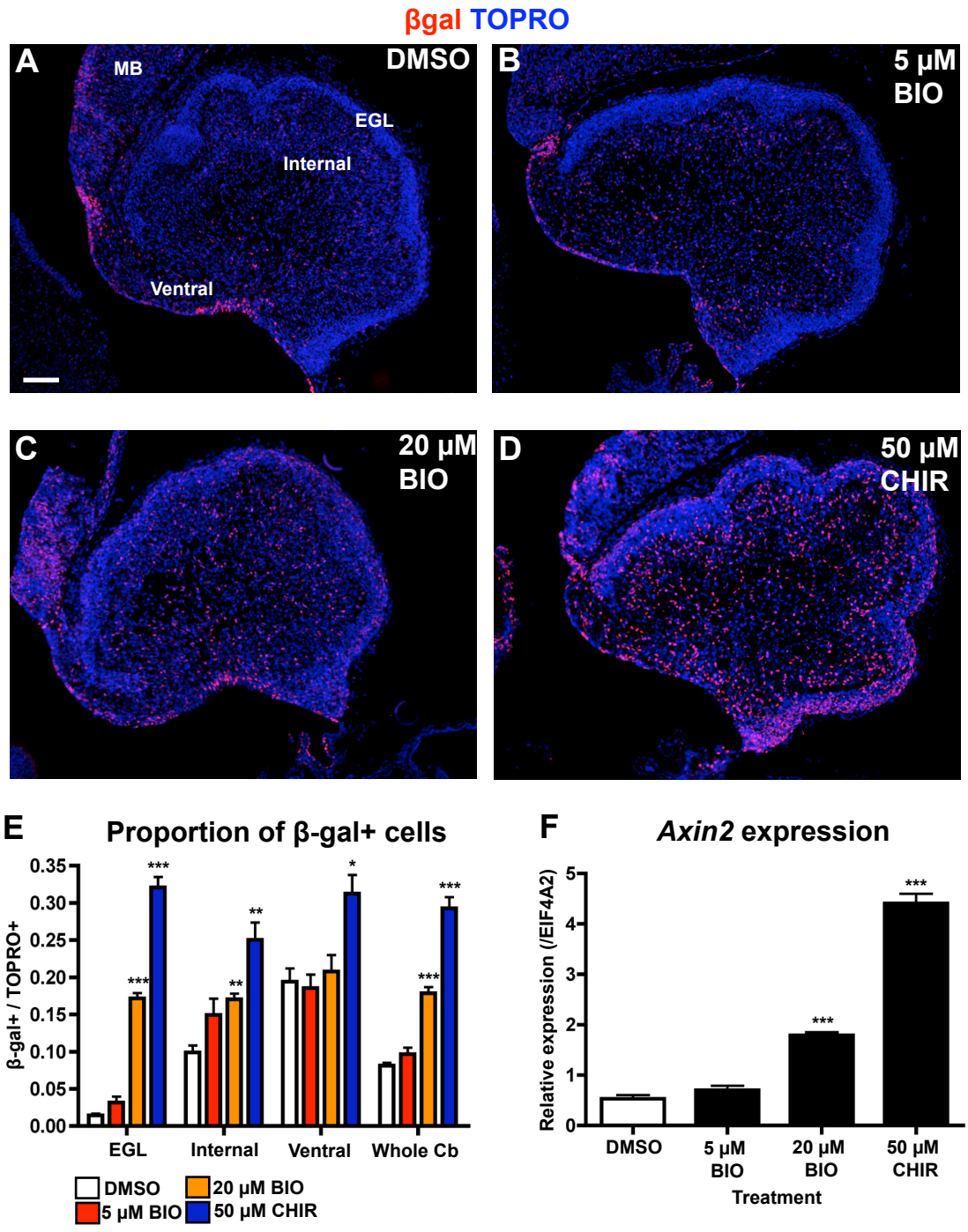

Figure 4.5 - GSK3β inhibition activates the Wnt/β-catenin signalling pathway. E18.5 BAT-gal+ cerebellum slices were cultured in the presence of DMSO (A), 5 μM BIO (B), 20 μM BIO (C) or 50 μM CHIR (D). Expression of β-gal was analysed by immunohistochemistry and quantitated (E) by counting the total proportion of β -gal+ cells in each of the defined regions. Comparisons were made between each of the treatment groups and the DMSO control group for each region by T-test. Expression of *Axin2* was analysed by qRT-PCR (F) and each of the treated groups (black bars) was compared to the DMSO control group (white bar) by a T-test. (n=3, error bars = SEM, *=p<0.05, **=p<0.01, ***=p<0.001 for E-F). Scale bar = 100 μm.

4.5.2 Wnt/β-catenin pathway activation in cerebellar slice culture increases proliferation

As Wnt/β-catenin is often associated with proliferation, the next set of experiments sought to determine the effects of Wnt/β-catenin pathway activation on proliferation within the cultured slices. BrdU was added to the cultures two hours prior to fixation and the amount of BrdU label retained by cells within the slices gives an indication of the number of cells in S-phase, which can be used to approximate proliferation. The DMSO treated control slices showed considerable BrdU label retention within the EGL, consistent with the proliferative nature of this region, and less in the internal and ventral regions of the slice (Fig. 4.6A). The number of BrdU+ cells was counted and expressed as a proportion of total cells, to give a BrdU labelling index (LI) of untreated proliferation levels of 22.5% (±1.5%) in the EGL, 6.7% (±2.8%) in the internal region and 5.9% (±1.3%) in the ventral region (white bars in Fig. 4.6E).

In slices treated with 5 μM and 20 μM BIO (Fig. 4.6B-C) an increase in the BrdU LI was observed in all cell layers (compare red/orange bars with white bars Fig. 4.6E). The BrdU LI was increased to 28.2% (±2.8%) and 24% (±4.3%) for 5 μM and 20 μM concentrations respectively in the EGL, while in the internal region the BrdU LI was 13.4% (±2.6%) and 12% (±1.8%) respectively. The BrdU LI in the ventral region was increased to 14.1% (±1.9%) and 13.8% (±4.5%) respectively. These changes were significant in all cases except for the increase in BrdU LI in the EGL of slices treated with 20 μM BIO. CHIR treatment revealed a slightly different picture of BrdU label retention (Fig. 4.6D, blue bars Fig 4.6E). Notably, the BrdU LI in the EGL was significantly reduced to 16% (±1.4%). In contrast, the BrdU LI in the internal and ventral regions were significantly increased to 15.1% (±3.2%) and 16% (±3.1%) respectively. Similar to what was observed with the expression of β-gal, BrdU label retention in CHIR treated cerebellum slices appears to become homogenous between regions, with the differences between the EGL, internal and ventral regions becoming less evident. These data support the conclusion that increased Wnt/β-catenin pathway activity results in an increase in proliferation in E18.5 cerebellum slices *ex vivo*. However, it is interesting to note that the dynamics

of BrdU label retention are different between BIO and CHIR treated slices and that proliferation does not increase in a similar pattern to that seen with expression of β-gal or *Axin2*.

In order to test if the increase in proliferation is a direct result of activated Wnt/β-catenin signalling within individual cells, the number of β-gal+ BrdU+ cells were analysed by double immunofluorescence and expressed as a proportion of total β-gal+ cells (Fig. 4.6F). Within the EGL, the low proportion of β-gal+ cells in DMSO treated control combined with an even smaller proportion that were BrdU+ (5.4% ±5.9%) created a high amount of variation within the sample group. However, the EGL of slices treated with 5 μM or 20 μM BIO showed a significantly higher proportion of BrdU+ β-gal+ cells: 31% (±5.6%) and 38.5% (±4.6%) respectively. This was not evident in CHIR treated slices, which only showed an increase to 11.6% (±1.5%). Within the internal region, only the 20 μM BIO treated slices showed a significant increase in the proportion of BrdU+ β-gal+ cells to 28.8% (±6.5%). Treatment with 5 μM BIO resulted in an increase to 24.8% (±7%) and treatment with CHIR resulted in an increase to 18.9% (±4.9%) compared to the control treated level of 12.6% (±4.4%). Within the ventral region, 5 μM BIO treatment showed a significant difference, with 22% (±1.4%) of β-gal+ cells also being BrdU+ compared to 5.4% (±7.5%) of cells in control treated slices. 20 μM BIO and CHIR treated slices were not significantly different, although showed an increase to 19.9% (±6.7%) and 14.2% (±2.9%) respectively. These data do not provide conclusive evidence for a cell autonomous or non-autonomous affect on proliferation of Wnt/β-catenin pathway activation.

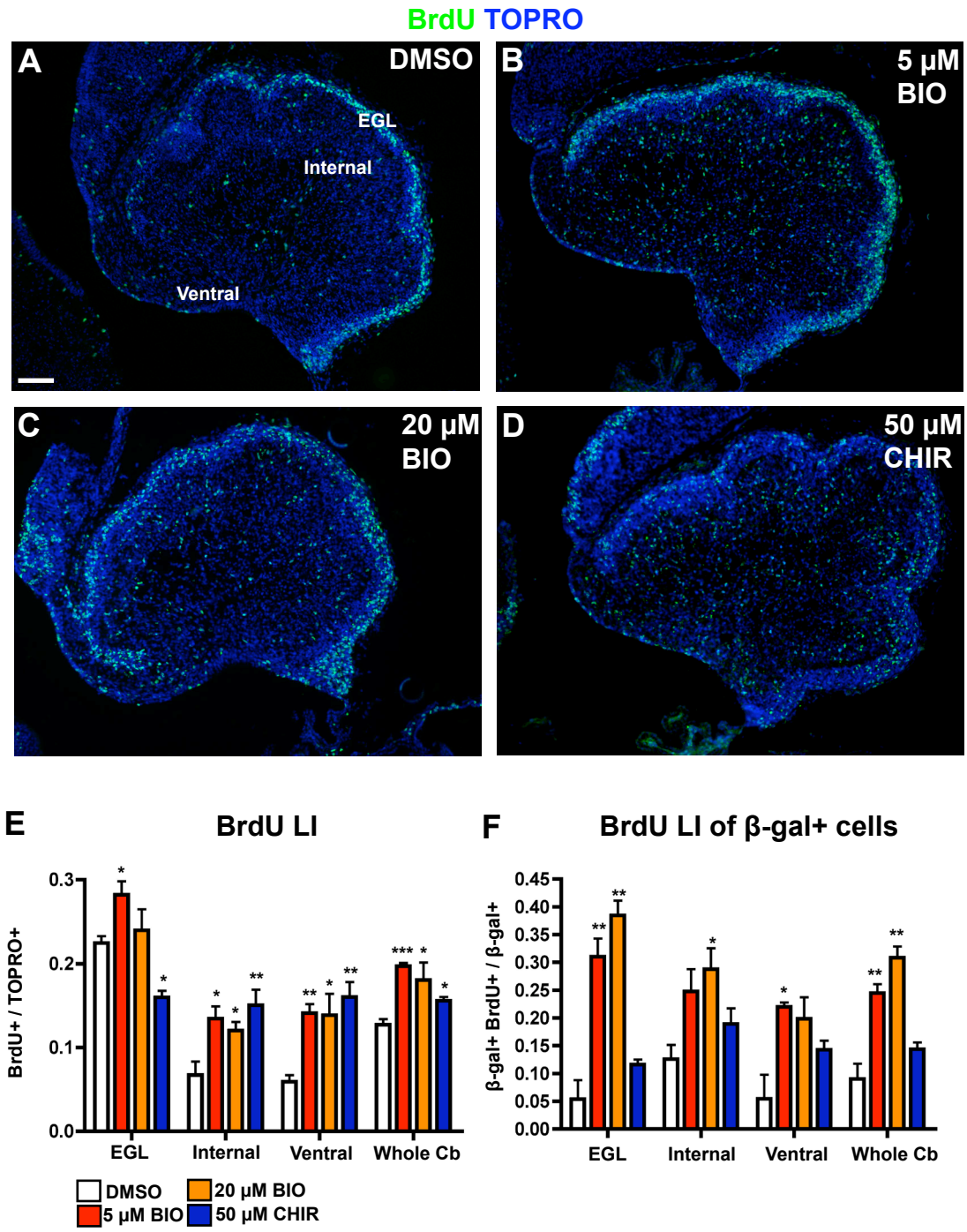

Figure 4.6 - Wnt/β-catenin pathway activation induces proliferation *ex vivo*. E18.5 BAT-gal+ cerebellum slices were cultured in the presence of DMSO (A), 5 µM BIO (B), 20 µM BIO (C) or 50 µM CHIR (D) and treated with BrdU two hours prior to fixation. Expression of BrdU was analysed by immunohistochemistry and quantitated (E) by counting the total proportion of BrdU+ cells in each of the defined regions (generating a LI). A BrdU LI was generated for the β-gal+ cell population (F) in the same way but using double immunofluorescnece for BrdU and β-gal. Comparisons were made between each of the treatment groups and the DMSO control group for each region by T-test (n=3, error bars = SEM, *=p<0.05, **=p<0.01, ***=p<0.001 for E-F). Scale bar = 100 µm.

4.5.3 Wnt/β-catenin pathway activation in cerebellar slice culture does not affect apoptosis

Wnt/β-catenin signalling is known to be an important regulator of cell survival and apoptosis, although whether it acts to promote cell survival (Chen et al., 2001; He et al., 2004; You et al., 2002) or apoptosis (Kim et al., 2000; Olmeda et al., 2003) appears to be context dependent (Benchabane and Ahmed, 2009). To test how activation of Wnt/β-catenin signalling in cerebellar slice culture affects apoptosis, I analysed the expression of cleaved Caspase 3 (Casp3), a pro-apoptotic protein (Jänicke et al., 1998), by immunohistochemistry in slices treated with 5 μM or 20 μM BIO, 50 μM CHIR or DMSO.

In control DMSO treated slices (Fig. 4.7A), Casp3 can be observed throughout the slice though it appears to predominate in the internal and ventral regions rather than within the EGL. Quantitation of Casp3+ cells per μm^2 confirms this observation (white bars Fig. 4.7E). Comparison with Casp3 expression in slices treated with 5 μM BIO (Fig. 4.7B), 20 μM BIO (Fig. 4.7C) or 50 μM CHIR (Fig. 4.7D) did not reveal any obvious differences. Quantitation of Casp3+ cell numbers did not result in any significant differences between DMSO control or treated slices in any of the regions analysed, or in the cerebellum slice as a whole (Fig. 4.7E). These data show that activation of Wnt/β-catenin signalling in cerebellum slice culture neither promotes or inhibits apoptosis.

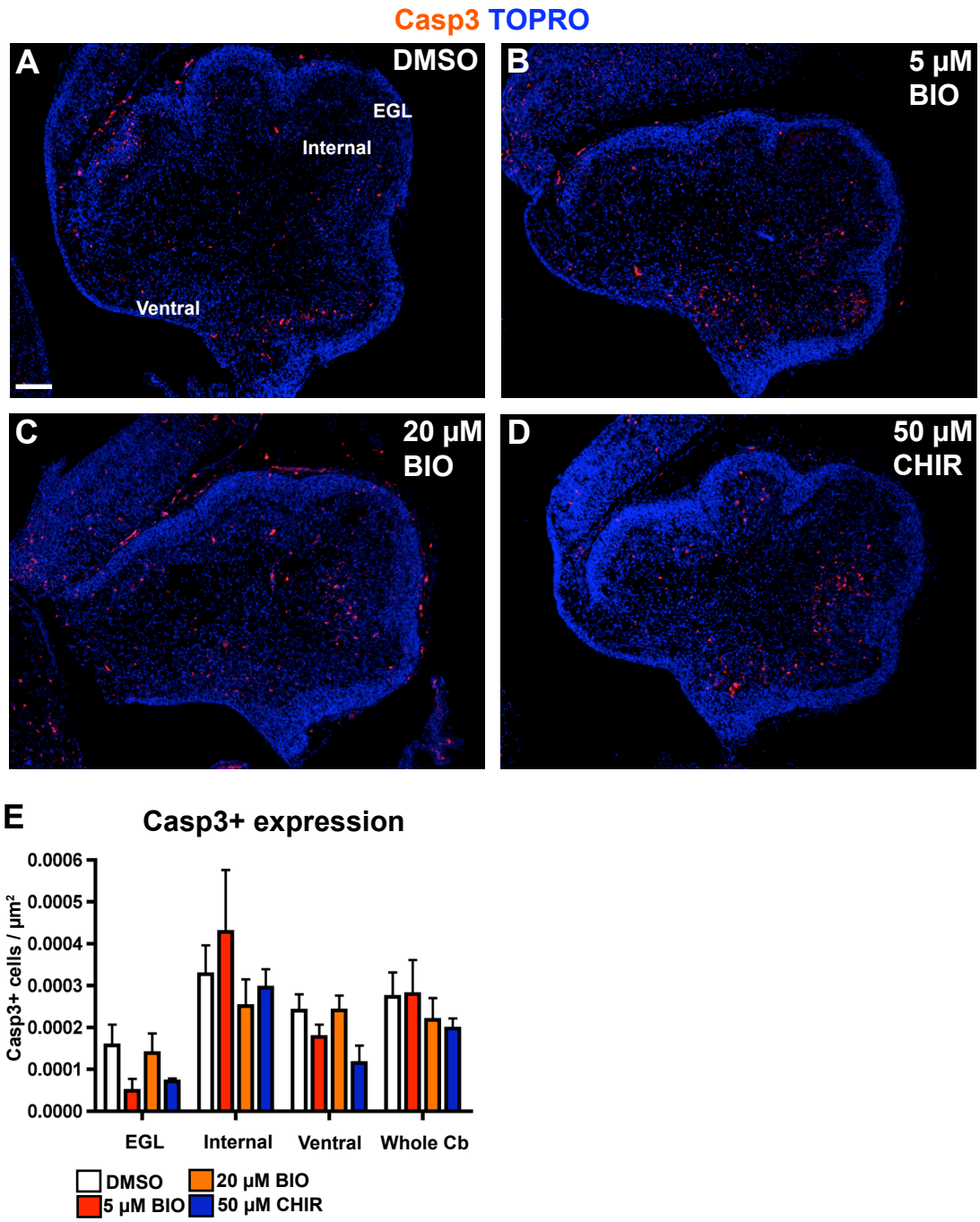

Figure 4.7 - Wnt/β-catenin pathway activation has no effect on apoptosis. E18.5 cerebellum slices were cultured in the presence of DMSO (A), 5 µM BIO (B), 20 µM BIO (C) or 50 µM CHIR (D). Apoptosis was analysed by immunohistochemistry for Casp3 and quantitated (E) by counting the total Casp3+ cells in each of the defined regions and expressing this in terms of area. Comparisons were made between each of the treatment groups and the DMSO control group for each region by T-test (n=3, error bars = SEM). No significant differences were observed. Scale bar = 100 µm.

4.5.4 Wnt/β-catenin pathway activation in cerebellar slice culture restricts the expression of interneuron lineage progenitor marker Pax2

As I have previously identified the activity of wnt/β-catenin signalling at the perinatal VZ (Chapter 3), I reasoned that ectopic activation of the pathway may disrupt the generation of cell lineages arising from there. The interneuron lineage is first identified by the expression of Pax2 (Maricich and Herrup, 1999), which is transiently activated in lineage restricted interneuron progenitors born from multipotent VZ or WM progenitors before their terminal differentiation and maturation (Milosevic and Goldman, 2002; Milosevic and Goldman, 2004) – a process that begins embryonically and continues until adulthood. In order to examine the effects of Wnt/β-catenin activation on development of the interneuron population, I analysed the expression of Pax2 in treated and control slices and quantitated the proportion of Pax2+ cells in the previously defined regions (with the exception of the EGL, since no Pax2+ cells are observed there).

Control DMSO treated slices showed a pattern of widespread Pax2 expression within the internal and ventral regions of the cerebellum (Fig. 4.8A), consistent with cells of the early interneuron population born at the VZ and migrating radially throughout the cerebellum. Quantitation of Pax2+ cells revealed a higher proportion ventrally (21% (±2.2%)) compared to the internal region (14% (±1.7%)) (white bars fig. 4.8E), consistent with Pax2 expression being activated initially and then lost during later development as the cells migrate away from the VZ. Treatment of slices with 5 μM BIO (Fig. 4.8B) did not result in any observable difference in expression of Pax2. Quantitation of the proportion of Pax2+ cells demonstrated 11.5% (±2%) internally and 15.5% (±5.7%) ventrally (red bars Fig. 4.8E), which were not significantly different to the proportion of Pax2+ cells observed in these regions in the DMSO treated control slices. Treatment with 20 μM BIO showed an interesting restriction of Pax2 expression within the internal region (Fig. 4.8C) compared to the DMSO treated control slices, with the limits of Pax2 expression not reaching as far towards the EGL. However, quantitation revealed that 8.5% (±3%) of cells internally and 21.4% (±6.8%) of cells ventrally were Pax2+, a result that was not significantly

different from the control (orange bars Fig. 4.8E). Treatment of the slices with CHIR resulted in a similar pattern of Pax2 expression (Fig. 4.8D) to that observed with 20 μM BIO treatment. Namely, the expression of Pax2 did not extend as far towards the EGL as the control slices. This observation is consistent with quantitation that showed 18.4% (±1.8%) of cells in the ventral region were Pax2+, a result that was not significantly different from control slices, while internally the proportion of Pax2+ cells was significantly reduced with only 9.2% (±0.7%) of cells expressing Pax2.

These results support the conclusion that the expression of Pax2 ventrally, and thus the generation of Pax2+ interneurons, is not affected by activation of the Wnt/β-catenin signalling pathway. However, the extent of Pax2+ expression within the cerebellum is affected. Pax2 expression displays a more restricted pattern in slices treated with 20 μM BIO or 50 μM CHIR, resulting in significantly fewer Pax2+ cells towards the periphery of the CHIR treated slices.

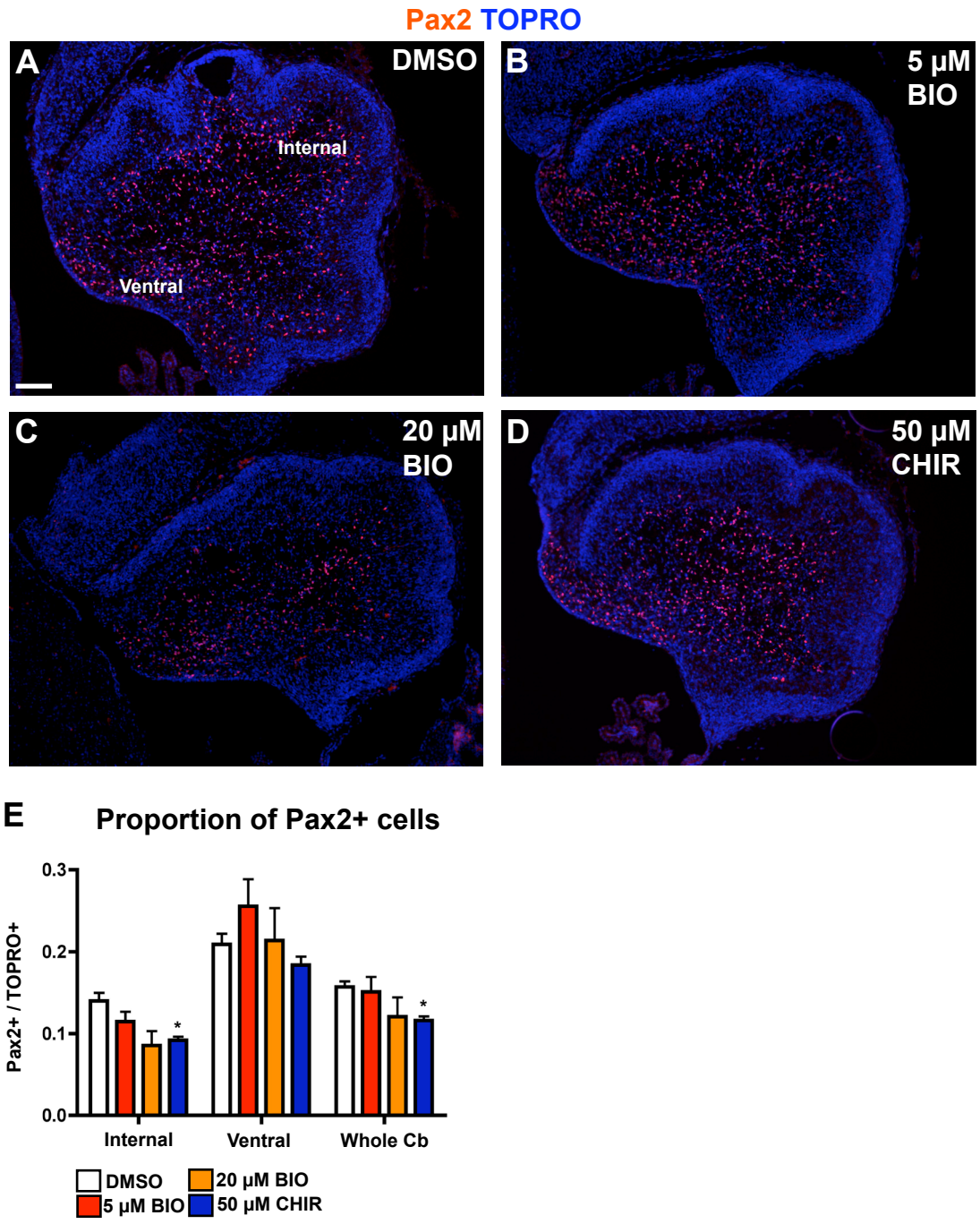

Figure 4.8 - Wnt/β-catenin pathway activation restrictes the expression of interneuron lineage marker Pax2.
E18.5 cerebellum slices were cultured in the presence of DMSO (A), 5 µM BIO (B), 20 µM BIO (C) or 50 µM CHIR (D). Expression of Pax2 was analysed by immunohistochemistry and quantitated (E) by counting the total proportion of Pax2+ cells in each of the defined regions. Comparisons were made between each of the treatment groups and the DMSO control group for each region by T-test (n=3, error bars = SEM,*=$p<0.05$). Scale bar = 100 µm.

4.5.5 Wnt/β-catenin pathway activation in cerebellar slice culture inhibits the expression of Sox9

The other key cell lineage generated from the VZ at E18.5 is the glial lineage. Glia become lineage restricted upon delamination from the VZ or from multipotent WM progenitors and migrate radially in a similar fashion to the interneuron lineage. Sox9 is expressed in cells at the VZ progenitors during this period (Kordes et al., 2005; Pompolo and Harley, 2001) and is known to have a function in glial/neuronal fate determination in other systems (Stolt et al., 2003). Interestingly, Sox9 expression is also maintained in mature glia of the cerebellum (Kordes et al., 2005; Sottile et al., 2006). As Wnt/β-catenin signalling is active at the VZ, I reasoned that it could play a role in regulation of the glial lineage and that its modulation could therefore alter the expression of Sox9.

DMSO treated control E18.5 cerebellum slices (Fig. 4.9A and white bars Fig. 4.9E) revealed a Sox9 expression pattern consistent with previously published evidence (Kordes et al., 2005; Pompolo and Harley, 2001). Expression of Sox9 within the EGL is minimal, with only 3.3% (±0.5%) of cells Sox9+. Expression is more widespread within the internal and ventral regions, with 25.5% (±3.2%) and 37.1% (±3.4) of cells expressing Sox9 respectively. This is consistent with a high expression of Sox9 along the VZ and in cells radiating out from it. Treatment of slices with 5 μM BIO did not affect the expression of Sox9 (Fig. 4.9B). Immunohistochemistry revealed expression along the VZ and within the internal region consistent with that observed in control slices treated with DMSO. Quantitation of Sox9+ cell numbers (red bars, Fig. 4.9E) was consistent with this, with 2.5% (±0.3), 26.3% (±2.4) and 30.4% (±3.6) of cells within the EGL, internal and ventral regions respectively expressing Sox9. These values were not significantly different from those observed in control slices.

Treatment with 20 μM BIO resulted in an apparent reduction in Sox9 expression (Fig. 4.9C and orange bars Fig. 4.9E). While the low expression within the EGL was consistent with control slices (4.2% ±2.1%), the expression within the VZ and in the

internal region appeared reduced. Quantitation revealed a significant reduction in Sox9 expression within the internal region to 16.1% (±3%). Ventrally the proportion of Sox9+ cells was reduced to 25% (±1%), a significant reduction from what was observed with control slices. The most striking result was observed in slices treated with CHIR (Fig. 4.9D). A clear reduction in the expression of Sox9 is evident along the VZ and within the internal region. Quantitation of Sox9+ cell numbers revealed a significant reduction in all regions compared to the DMSO treated control slices (blue bars Fig. 4.9E). No Sox9+ cells were observed within the EGL, while only 2.5% (±0.5%) of cells within the internal region were Sox9+. Within the ventral region the proportion of Sox9+ cells was reduced to 9.6% (±6.1%).

These data are supported by qRT-PCR analysis for the expression of Sox9 in the cultured slices (Fig. 4.9F). These experiments confirmed the significant reduction in Sox9 expression after treatment with CHIR and are consistent with the significant reduction in Sox9+ cells observed in the slice as a whole (Fig. 4.9E). While qRT-PCR analysis of slices treated with 5 μM BIO or 20 μM BIO did not reveal a significant difference with control slices, a general trend was evident that is consistent with the number of Sox9+ cells observed in the slice as a whole. Combined, these data support the conclusion that activation of the Wnt/β-catenin signalling pathway in E18.5 cerebellum slices *ex vivo* causes a reduction in the expression of Sox9 with greater pathway activation (as seen with CHIR in Fig. 4.5) leading to a greater reduction in Sox9 expression.

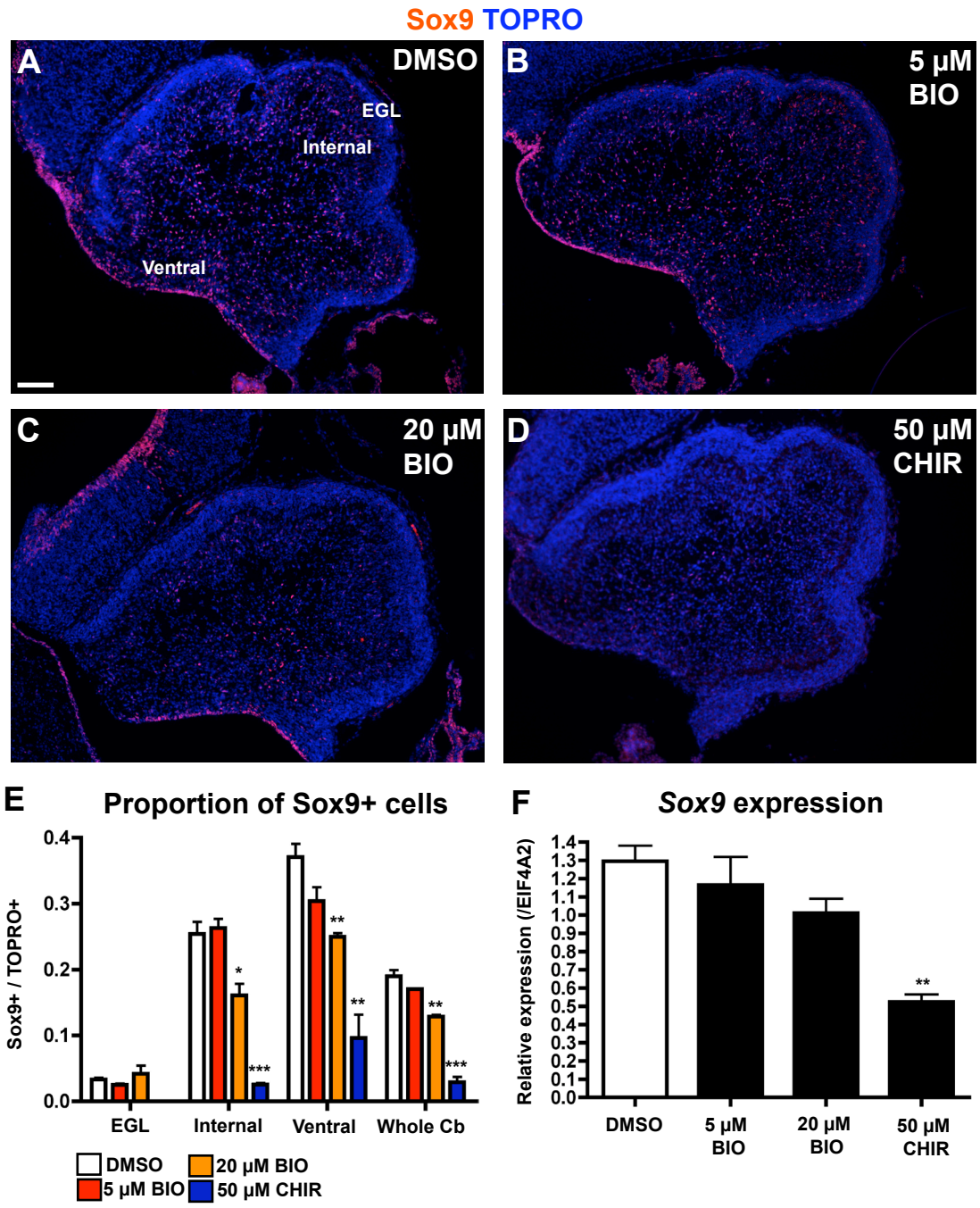

Figure 4.9 - Wnt/β-catenin pathway activation reduces expression of VZ progenitor and astrocyte marker Sox9.
E18.5 cerebellum slices were cultured in the presence of DMSO (A), 5 µM BIO (B), 20 µM BIO (C) or 50 µM CHIR (D). Expression of Sox9 was analysed by immunohistochemistry and quantitated (E) by counting the total proportion of Sox9+ cells in each of the defined regions. Comparisons were made between each of the treatment groups and the DMSO control group for each region by T-test. *Sox9* mRNA expression was analysed by qRT-PCR (F). Comparisons were made between each of the treatment groups and the DMSO control group by T-test (n=3, error bars = SEM, *=p<0.05, **=p<0.01, ***=p<0.001 for E-F). Scale bar = 100 µm.

4.5.6 Wnt/β-catenin pathway activation in cerebellar slice culture inhibits the expression of GFAP

Similar to Sox9, GFAP is expressed in the VZ monolayer and also in mature Bergmann glia and astrocytes (Levitt and Rakic, 1980; Nolte et al., 2001; Yuasa, 1996). Based on the finding that activated Wnt/β-catenin signalling affects the expression of glial marker Sox9, I sought to determine the effects on an additional glial marker GFAP. Immunohistochemistry for GFAP on DMSO treated control slices revealed a pattern of high expression ventrally, with considerable expression along the ventricular zone and glial processes evident radiating away from the VZ towards the pial surface of the cerebellum (Fig. 4.10A). This is consistent with expression of GFAP in the VZ progenitors. Treatment with 5 μM BIO (Fig. 4.10B), 20 μM BIO (Fig. 4.10C) or 50 μM CHIR (Fig. 4.10D) all revealed a considerable restriction of GFAP staining in the cerebellum. While clear staining was observed along the length of the VZ in control slices, this was not evident in any of the treated slices. The staining appeared patchier and less intense. In addition, the extent of staining radiating from the VZ into the internal region was notably reduced. GFAP in control slices can be observed almost reaching the EGL in places, whereas this was not observed in any of the treated slices.

As GFAP is a cytoplasmic protein, cell numbers were unable to be quantified. However, the qualitative reduction in GFAP immunoreactivity was consistent with qRT-PCR data, which revealed a significant reduction in GFAP expression after treatment with 20 μM BIO and 50 μM CHIR (Fig. 4.10F). These data support the conclusion that activation of the Wnt/β-catenin signalling pathway in E18.5 cerebellum slices affects the expression of glial markers at the VZ and within the developing cerebellum.

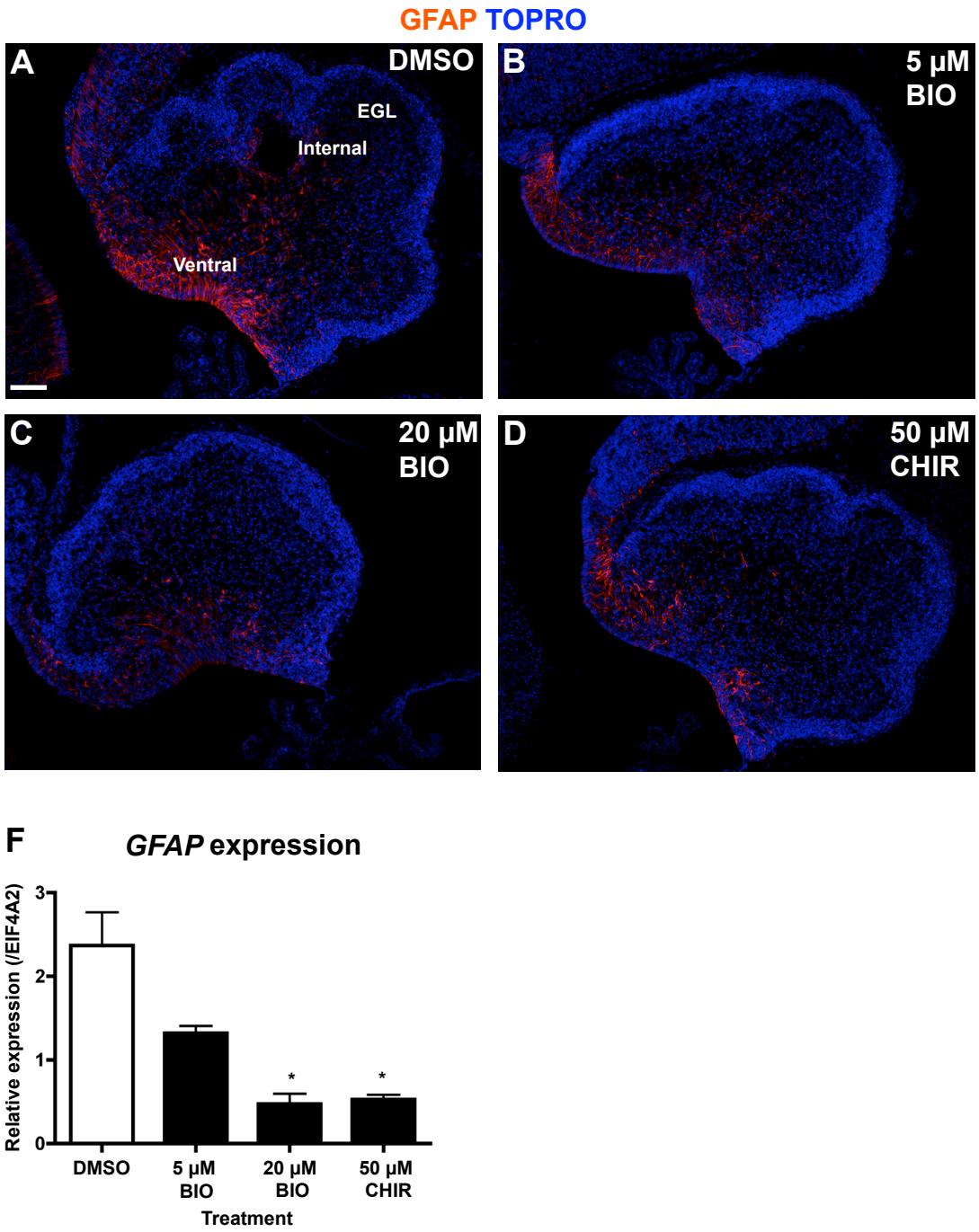

Figure 4.10 - Wnt/β-catenin pathway activation reduces expression of VZ progenitor and astrocyte marker GFAP.
E18.5 cerebellum slices were cultured in the presence of DMSO (A), 5 µM BIO (B), 20 µM BIO (C) or 50 µM CHIR (D). Expression of GFAP was analysed by immunohistochemistry. GFAP mRNA expression was analysed by qRT-PCR (F). Comparisons were made between each of the treatment groups and the DMSO control group by T-test (n=3, error bars = SEM, *=$p<0.05$). Scale bar = 100 µm.

4.6 Discussion

The aim of this chapter was to establish an *ex vivo* culture system to characterise the early effects of small molecule mediated Wnt/β-catenin pathway modulation on perinatal cerebellum development. In particular, I sought to gain insight into the function of Wnt/β-catenin signalling at the VZ, as I had previously identified this as a domain of Wnt/β-catenin activity (Chapter 3). The results presented in this chapter demonstrate that activation of the Wntβ-catenin signalling pathway *ex vivo* in E18.5 cerebellum slices results in a general increase in proliferation, no change to apoptosis and importantly affects the expression of markers for VZ progenitors and their progeny.

4.6.1 Limitations of the experimental system and analysis

Before the observations made in this chapter can be discussed, there are a number of limitations to the experiments and analyses carried out that need to be addressed. The most obvious of these was the short length of time that slices could be grown in culture. The cerebellum undergoes considerable growth at E18.5, with expansion of the GPC population within the EGL causing a dramatic increase in the extent of foliation by P1. The restrictions of the agarose surrounding the slice and the two-dimensional nature of the culture mean that cell migration is unable to proceed normally and thus the morphology of the cerebellum is notably disrupted from 48 hours *ex vivo* onwards to the extent that the individual layers (i.e. EGL vs the internal region) could not be accurately defined. Thus, experiments were limited to 24 hours *ex vivo*.

While small molecule upregulation of the Wnt/β-catenin signalling pathway was successfully achieved after 24 hours *ex vivo*, this was not the case for inhibitors of the pathway (Fig. 4.4). All of the small molecules used have been shown previously to be effective *in vitro* and *ex vivo* in some cases at dosages within the range tested in these experiments (Chen et al., 2009; Gonsalves et al., 2011; Huang et al., 2009; Karner et al., 2010; Karner et al., 2011). Hence, it is likely that 24 hours was not sufficient for the compounds to act on their targets and elicit an observable effect.

Further experiments are therefore required to optimise this culture paradigm in order to test inhibition of the Wnt/β-catenin signalling pathway.

Another limitation was the small number (n=3) of samples used for the analysis. The amount of confocal microscopy and manual cell counting required for the quantitation of cell numbers expressing β-gal, BrdU, Casp3, Pax2 and Sox9 for each of the treatment groups meant that undertaking this on a sample size of greater than three would not have been realistic within the time frame of this project. Thus, it is conceivable that some of the effects observed may not be entirely representative of a larger population of cultured slices.

Lastly, while the small molecules used to activate the Wnt/β-catenin pathway caused an upregulation of both the BAT-gal reporter and independent Wnt reporter Axin2 (Fig. 4.5), the possibility of non-specific action causing some of the observed effects cannot be excluded. Firstly, GSK3β is known to be involved in a number of cellular processes and signalling pathways independent of the Wnt/β-catenin signalling pathway. Evidence suggests that alternative GSK3β substrates include Creb (Grimes and Jope, 2001), Nfat (Beals et al., 1997; Neal and Clipstone, 2001), Neurogenin-2 (Ma et al., 2008), Smad1 (Fuentealba et al., 2007) and c-Jun (de Groot et al., 1993). Secondly, it is important to reiterate the fact that BIO is known to act on other kinases other than GSK3β (Meijer et al., 2003; Zhen et al., 2007). Taken together, the published evidence argues that multiple cellular pathways are being affected in this culture system. A necessary follow up experiment to provide confidence that the findings from this chapter are a result of activated Wnt/β-catenin signalling alone is to use an independent method of pathway activation (i.e. genetic or molecular targeting of another component of the destruction complex).

4.6.2 GSK3β inhibition successfully activates Wnt/β-catenin signalling *ex vivo*

The data presented in this chapter confirm that inhibition of GSK3β results in the activation of Wnt/β-catenin signalling in cerebellar slice culture *ex vivo* (Fig. 4.5). GSK3β inhibitors BIO and CHIR have been shown to activate the pathway in a

number of *in vitro* and *ex vivo* settings (Meijer et al., 2003; Sato et al., 2004; Ying et al., 2008). Here I have demonstrated the success of GSK3β inhibition as an activator of Wnt/β-catenin signalling in the context of organotypic cerebellar slice culture. Without GSK3β inhibition expression of the BAT-gal reporter was observed primarily along the VZ and within the internal region – consistent with the observations made in Chapter 3. Treatment with a high concentration of BIO or CHIR resulted in a significant increase in BAT-gal reporter expression, which was particularly evident in the regions that had low levels of Wnt/β-catenin activity (primarily the EGL). This suggests that cells within all key domains in the E18.5 cerebellum are competent to transduce a Wnt/β-catenin signal. qRT-PCR for endogenous Wnt/β-catenin target gene *Axin2* on RNA extracted from whole slices validated these findings.

4.6.3 Wnt/β-catenin activation is mitogenic but does not affect apoptosis

Activation of the Wnt/β-catenin signalling pathway is often associated with an increase in proliferation. This is largely due to observations from mice (Megason and McMahon, 2002; Yamaguchi et al., 1999) and *Drosophila* (Giraldez and Cohen, 2003) where loss of Wnt/β-catenin signalling causes a reduction in tissue growth. In addition, induction of Wnt/β-catenin signalling in cancer has been shown to increase proliferation. Consistent with this, cell cycle regulators c-myc and cyclin-D1 have been identified as targets of the pathway in colon cancer (He et al., 1998; Shtutman et al., 1999). In cerebellum slices treated with BIO (at either concentration tested) or CHIR, a significant increase in BrdU label retention was observed in all layers except the EGL (Fig. 4.6E). This is likely due to the already high levels of proliferation within the EGL. Interestingly, the addition of CHIR to the slices resulted in a decrease in the BrdU LI within the EGL – supporting a potential inhibitory role of Wnt/β-catenin signalling on the generation of GPCs (a process known to be primarily driven by Shh signalling) with a high concentration of a specific GSK3β inhibitor as opposed to BIO which is known to act on other kinases. However, further evidence is required to determine the mechanism behind the

reduced BrdU LI in the EGL of CHIR treated slices (i.e. whether the observation is a result of slower cell cycling or premature terminal differentiation).

Within the other regions analysed, BIO or CHIR treatment both resulted in an increased BrdU LI. However, the BrdU LI observed between the different treatments did not reflect the progressive increase in Wnt/β-catenin activity previously observed from 5 μM BIO to 20 μM BIO and then 50 μM CHIR (Fig. 4.5). Instead, the BrdU LI within the internal and ventral regions after any treatment appeared similar, suggesting a possible limit to the capacity for proliferation as a response to Wnt/β-catenin induced proliferation in the culture conditions. However, further experiments would be needed to test this.

If the increase in BrdU label retention observed after all three small molecule treatments were being driven in a cell autonomous fashion by increased Wnt/β-catenin signalling, then we would also expect to see an increase in the proportion of β-gal+ cells that are BrdU+ above control levels. This is the case for all three regions measured. However, the three treatments show quite different patterns. In addition, the variation within sample groups means that the increases observed in most cases are not significantly different. Thus, while it is clear that activation of the Wnt/β-catenin signalling pathway in cerebellar slice culture increases proliferation, these data are not sufficient to support the conclusion that it is driving increased proliferation in a consistently cell-autonomous manner.

Alongside an increase in proliferation, it could be hypothesised that an increase in cell survival (i.e. a reduction in apoptosis) would also be observed. However, no effects on apoptosis were observed in any of the treated slices, suggesting that no change in cell survival occurs as a result of Wnt/β-catenin pathway activation in E18.5 cerebellum slice culture (Fig. 4.7). This is consistent with the opposing and context dependent evidence of Wnt/β-catenin signalling both promoting cell survival (Chen et al., 2001; He et al., 2004; You et al., 2002) and apoptosis (Kim et al., 2000; Olmeda et al., 2003).

4.6.4 Wnt/β-catenin activation affects VZ cell fate markers

The previous identification of Wnt/β-catenin signalling at the perinatal VZ suggests a potential role in regulating the genesis of the two lineages generated in this region at this time point: interneurons and glia. The dual and opposing roles of Wnt/β-catenin signalling driving self renewal of radial glia (Chenn and Walsh, 2002; Ivaniutsin et al., 2009; Zhou et al., 2006) or promoting the differentiation of IPCs down the neuronal lineage (Hirabayashi et al., 2004; Munji et al., 2011) supports a potential role for Wnt/β-catenin signalling in regulating the behaviour of VZ progenitors and the lineages that are derived from them. To test this hypothesis I analysed the expression of interneuron fate marker Pax2, which labels lineage restricted early born interneurons (Maricich and Herrup, 1999; Milosevic and Goldman, 2002; Milosevic and Goldman, 2004), alongside GFAP and Sox9, which label the VZ progenitors and their glial restricted progeny (Kordes et al., 2005; Levitt and Rakic, 1980; Nolte et al., 2001; Pompolo and Harley, 2001; Sottile et al., 2006; Yuasa, 1996).

If Wnt/β-catenin signalling were driving the production of the interneuron lineage, it could be hypothesised that an increase in activity of the pathway would promote more cells to enter the lineage and express Pax2. However, these results suggest the opposite: that increased Wnt/β-catenin pathway activity inhibits the expression of Pax2 (Fig. 4.8). This decrease, however, was only observed in the internal region of the cerebellum, nearer to the EGL than the VZ. These data support the conclusion that activation of the Wnt/β-catenin signalling pathway affects the expression of Pax2 in differentiating interneurons, rather than during their genesis at the VZ, and leads to the hypothesis that Wnt/β-catenin signalling may promote the early differentiation of interneurons from Pax2+ progenitors.

Conversely, if Wnt/β-catenin signalling were driving the production of glia or promoting the expansion of the VZ progenitor pool, then one would expect an expansion of the glial population as a result of activation of the pathway. The observation made in Chapter 3 that Wnt/β-catenin signalling is active at the VZ and

in the developing Bergmann glia population supports this. However, this was again not the case (Fig. 4.9-10). Activation of the Wnt/β-catenin pathway by 20 μM BIO or 50 μM CHIR resulted in a significant reduction in the expression of Sox9 within the internal and ventral regions of the slice. In particular, treatment with CHIR caused a marked reduction of Sox9 expression along the length of the VZ (Fig. 4.9D). Expression of GFAP was also observed by immunohistochemistry and qRT-PCR in all treated slices. Initially, these data are contrary to the hypothesis that Wnt/β-catenin signalling promotes the production of glia in the developing cerebellum. However, the possibility of a strong negative feedback mechanism being promoted by the dysregulation of the Wnt/β-catenin signalling pathway could explain this inconsistency. Analysis of these markers after inhibition of the pathway would certainly help resolve the function of Wnt/β-catenin signalling in cerebellum development and, as pointed out, is a significant limitation to the data presented in this chapter.

4.6.5 Summary

The aim of this chapter was to investigate the early effects of Wnt/β-catenin pathway dysregulation on development of the E18.5 cerebellum and to generate pilot data on its function. While the limitations of the culture system discussed make it difficult to draw any meaningful conclusions beyond the immediate observations made within this chapter, it is clear that activation of the Wnt/β-catenin signalling pathway has a profound effect on the development of cell lineages arising from the VZ – suggesting a potential role for Wnt/β-catenin signalling in regulating the behaviour of VZ progenitors and the lineages they generate. An analysis of dysregulated Wnt/β-catenin signalling *in vivo* is now required to both support these findings and extend the conclusions further to the function of Wnt/β-catenin signalling during cerebellum development.

5 Genetic activation of Wnt/β-catenin signalling during cerebellum development *in vivo*

5.1 Introduction

Work presented in the previous two chapters confirms the presence of Wnt/β-catenin activity during cerebellum development and indicates a potential role in regulating cell behaviour at the VZ and in the lineages arising from there. In order to investigate this potential role further I used a genetic approach to constitutively activate the pathway during cerebellum development.

In addition to utilising standard gene knockout mouse models, the rapid uptake in Cre/*lox* inducible gene targeting in developmental biology over the past decade has presented a useful tool to probe the function of different signalling pathways during brain development. The bacteriophage-P1 *cre* gene codes for a Cre-recombinase enzyme that efficiently recombines DNA between two *LoxP* sites. By floxing an integral sequence of a particular gene and using a Cre under the control of a tissue specific promoter it is possible to carry out spatio-temporal specific gene ablation (Sauer, 1998). Furthermore, the generation of a Cre-recombinase fused to a mutant form of the estrogen receptor (ER) ligand binding domain (CreER) allows for more precise temporal regulation of Cre activation by the addition of tamoxifen to the system (Hayashi and McMahon, 2002).

A number of mouse models have been generated that utilise this technology to study developmental signalling pathways during cerebellum development, but little has been revealed about the nature of Wnt/β-catenin signalling. Constitutive activation of Wnt/β-catenin signalling in GPCs (Lorenz et al., 2011) utilising a *Math1-Cre* (Matei et al., 2005) addition transgene expressed in GPCs crossed to a floxed *Apc* allele (Miclea et al., 2009) revealed severe developmental abnormalities in GC generation. The reduced cerebellum size and disrupted cytoarchitecture observed was primarily the result of premature GC differentiation, although this effect was only

observed in the anterior of the cerebellum – suggesting uneven *Math1-Cre* expression across the GPC population. That said, this study reveals a potential link between Wnt/β-catenin signalling and neuronal differentiation, although only in the granule lineage. Gibson et al (Gibson et al., 2010) generated mice with a constitutively active *Ctnnb1*$^{lox(ex3)}$ allele (Harada et al., 1999) under the control of an addition *BLBP-Cre* transgene, expressed in MHB progenitors (including the VZ, RL and LRL) from E10.5 (Hegedus et al., 2007). While no abnormalities were observed in the cerebellum from these mice, the analysis was limited to proliferation (Ki67) and apoptosis (TUNEL) markers. Importantly, a developmental analysis of cells arising from the VZ and RL was not carried out. Thus, the conclusions we can draw from this study about the role of Wnt/β-catenin signalling during cerebellum development are limited. Combined, these limited studies do not provide a functional explanation for the role of Wnt/β-catenin signalling during cerebellum development consistent with what has been presented in the previous two chapters. An explanation for Wnt/β-catenin signalling at the VZ and in the developing glial population in particular is lacking.

5.2 Aims and experimental design

The aim of the work presented in this chapter was to investigate the functional consequences of Wnt/β-catenin pathway activation *in vivo* during cerebellum development. To this end, I used a combination of mouse models to remove *Apc* function (and thus constitutively activate the pathway) during cerebellum development and investigated the effects. Initially the *Apc*^{min} mouse (Moser et al., 1990) was used as it contains a loss-of-function *Apc* allele and as mutations in human *APC* are known to predispose to medulloblastoma (Hamilton et al., 1995), I hypothesised that mice with the *Apc*^{min} mutation may also develop cerebellar abnormalities in addition to intestinal neoplasia. Thus, I collected cerebellum tissue from *Apc*$^{mi/+}$ mice and analysed the histology for any signs of gross pathology that may result from constitutively activated Wnt/β-catenin signalling.

Secondly, I sought to use a conditional genetic approach to remove both *Apc* alleles in a defined cell type at defined points in development. To achieve this, a mouse line containing a *Nestin-Cre*ER^{T2} (hereinafter referred to as *Nestin-Cre)* addition transgene (Carlén et al., 2006) was obtained in order to target recombination of a floxed *Apc* allele (Shibata et al., 1997) in the Nestin+ progenitor population at different stages of cerebellum development. As Nestin is expressed in both the VZ and RL progenitor domains (Dahlstrand et al., 1995; Zimmerman et al., 1994), utilising this Cre-recombinase line allowed the targeting of *Apc* mutations to all progenitors in order to investigate the effects of Wnt/β-catenin pathway activation in all cell lineages during development. The approach I took with these experiments was to first cross the *Nestin-Cre* onto a *Rosa26 eYFP (R26YFP)* reporter line (Srinivas et al., 2001) to validate the Cre-recombinase activity at different points during development (Fig. 5.1A). Secondly, I crossed the *Nestin-Cre* line onto a line carrying an Apc^{lox} allele (Shibata et al., 1997) that contains two *LoxP* sites and a Neomycin cassette flanking exon 14 of the mouse *Apc* gene. Tamoxifen induced Cre-recombinase activation in mice homozogous for the Apc^{lox} allele should generate non-functional APC protein after recombination of exon 14 in the cell types targeted (Fig. 5.1B).

Finally, I sought to upscale and optimise these experiments for a full analysis by generating triple transgenic animals with $Nestin\text{-}Cre^{+/-}$; $Apc^{lox/lox}$; $R26YFP^{+/-}$ genotype (Fig. 5.1C). To achieve this I generated mice homozygous for both the Apc^{lox} and *R26YFP* alleles, crossed these to $Nestin\text{-}Cre^{+/-}$; $Apc^{lox/lox}$ mice and treated the offspring with tamoxifen. The aim of this set of experiments was to optimise the tamoxifen dosage that gave the highest Cre-recombinase induction as measured by YFP expression and to enable $Apc^{lox/lox}$ cells to be tracked over a developmental time course.

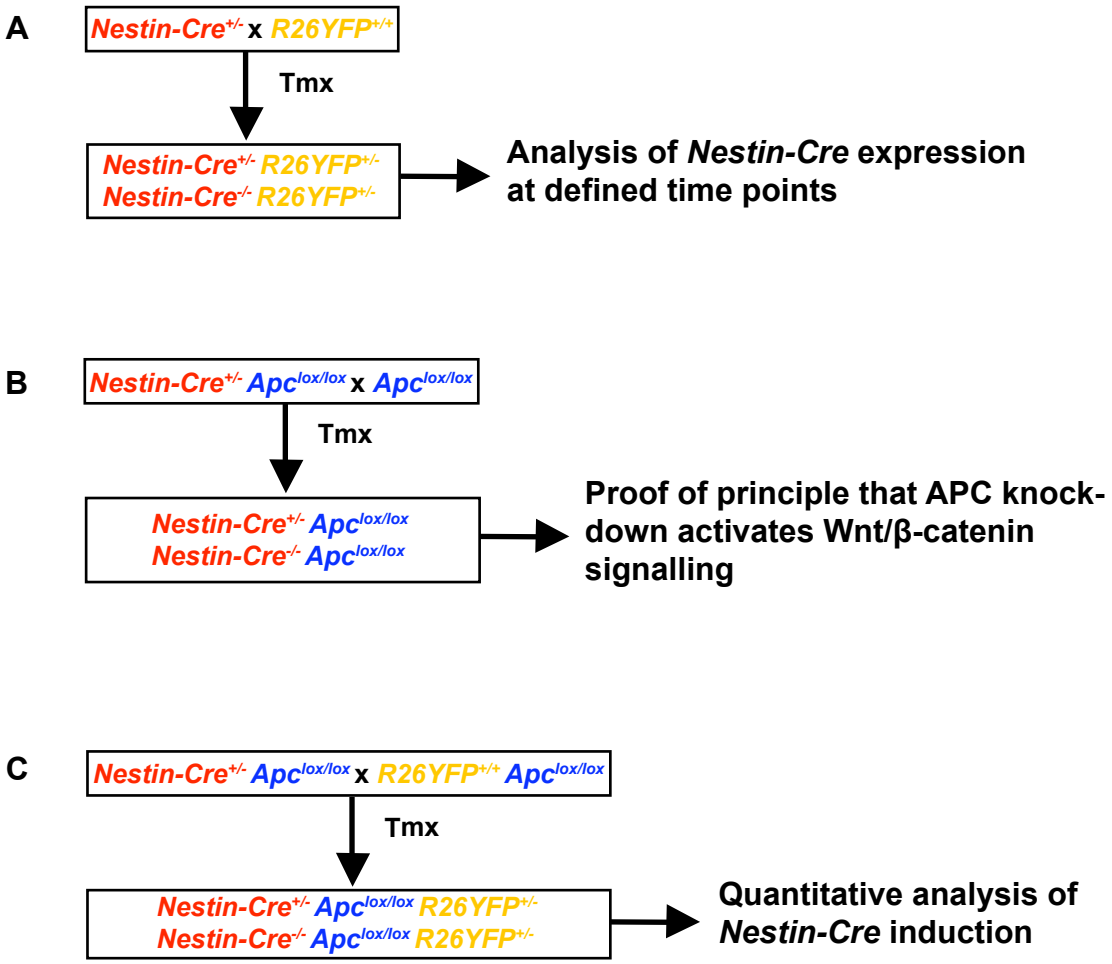

Figure 5.1 - Breeding strategy and experimental summary.
In order to test the expression of the *Nestin-Cre* transgene, heterozygous mice were crossed to mice homozygous for the *R26YFP* reporter. Offspring were treated with tamoxifen (Tmx) at defined points and analysed for YFP expression (A). *Nestin-Cre* mice were then crossed to mice carrying the Apc^{lox} allele and offspring were treated with Tmx in order to validate Wnt/β-catenin pathway activation in *Nestin-Cre* expressing cells (B). Finally, the *R26YFP* reporter allele was crossed onto the conditional knockout line in order to scale up the experiments and quantitate the extent of *Nestin-Cre* induction (C).

5.3 Analysis of the *Apc*^{min} mouse cerebellum revealed no pathology

The *Apc*^{min} mouse model of intestinal neoplasia was identified after an ethylnitrosourea (ENU) screen generated a mutant mouse predisposed to multiple intestinal neoplasia (Min) (Moser et al., 1990). Linkage analysis and DNA sequencing revealed a point mutation in the *Apc* gene was responsible (Su et al., 1992). As the *Apc*^{min} mutation causes intestinal polyposis throughout the intestinal tract in young adult mice the oldest age possible for analysis was 13 weeks, beyond this point the neoplasia normally develops to a point that requires the animals to be culled for humane reasons. Sagittal sections from *Apc*$^{+/+}$ (Fig. 5.2A-B) and *Apc*$^{min/+}$ (Fig. 5.2C-D) mice (n=3 of each) were stained with hematoxylin in order to identify any histological differences. However, no sections analysed revealed any differences in gross morphology or lamination of the *Apc*$^{min/+}$ cerebellum (Fig. 5.2C-D). In addition, no obvious ectopic growth that would be consistent with a preneoplastic lesion was identified. These data support the conclusion that the required second hit of the *Apc* gene necessary for constitutive activation of the Wnt/β-catenin pathway is a considerably rare event in the cerebellum and would likely require a high number of animals to be observed before any effects of pathway activation could be observed.

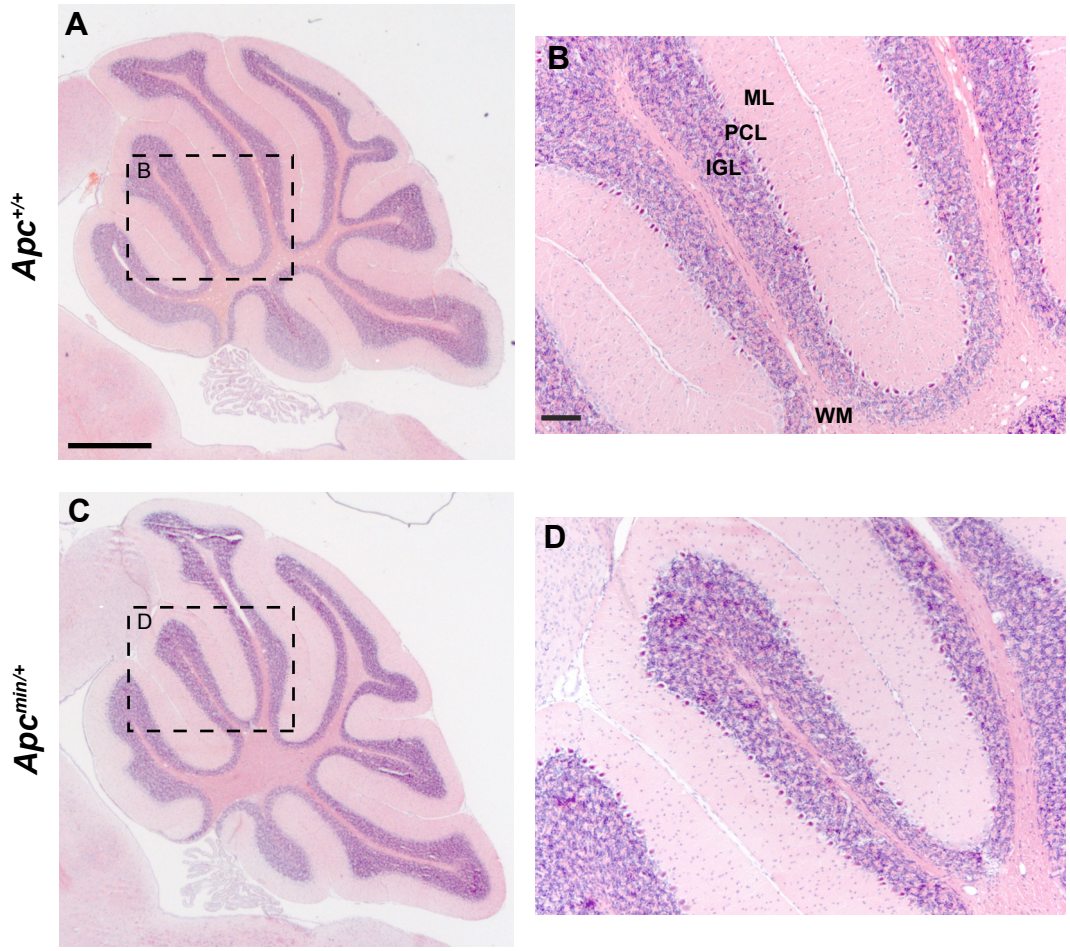

Figure 5.2 - The *Apc*^{min} mouse cerebellum shows no evidence of gross pathology. Sagittal cerebellum sections from 13 week old *Apc*$^{+/+}$ (A-B) and *Apc*$^{min/+}$ (C-D) mice were stained with Hematoxylin and Eosin and examined for evidence of gross pathology. No obvious differences were observed between the two groups. Scale bars = 500 µm (A,C), 100 µm (B,D).

5.4 *Nestin-Cre* induction of an $Apc^{lox/lox}$ mutation

In order to constitutively activate the Wnt/β-catenin pathway *in vivo* I utilised an inducible *Nestin-Cre* addition transgene (Carlén et al., 2006) and a floxed *Apc* allele (Shibata et al., 1997) to remove APC function in the progenitor population at defined stages during cerebellum development.

5.4.1 Nestin is expressed at key stages during cerebellum development

I first sought to validate the expression pattern of Nestin by immunohistochemistry at various stages in early cerebellum development. At E14.5, Nestin can be observed along the length of the VZ (Fig. 5.3A). At higher magnification Nestin fibres can be observed radiating out from the VZ (Fig. 5.3B). Outside of the VZ Nestin expression remains relatively low. By E18.5 considerable Nestin expression can be observed throughout the cerebellum, with Nestin fibres evident extending from the EGL down into the tissue (Fig. 5.3C). Nestin is also evident within the developing cerebellum, although appears stronger in the anterior (Fig. 5.3D). At P1 the expression appears more restricted. Nestin fibres can be seen extending from the EGL into the PCL (Fig. 5.3E), and also within WM (Fig. 5.3F). This pattern is also seen at P5, though appears considerably more restricted (Fig. 5.3G-H). These data support the continued yet differential expression of Nestin within the developing cerebellum from E14.5 to P5.

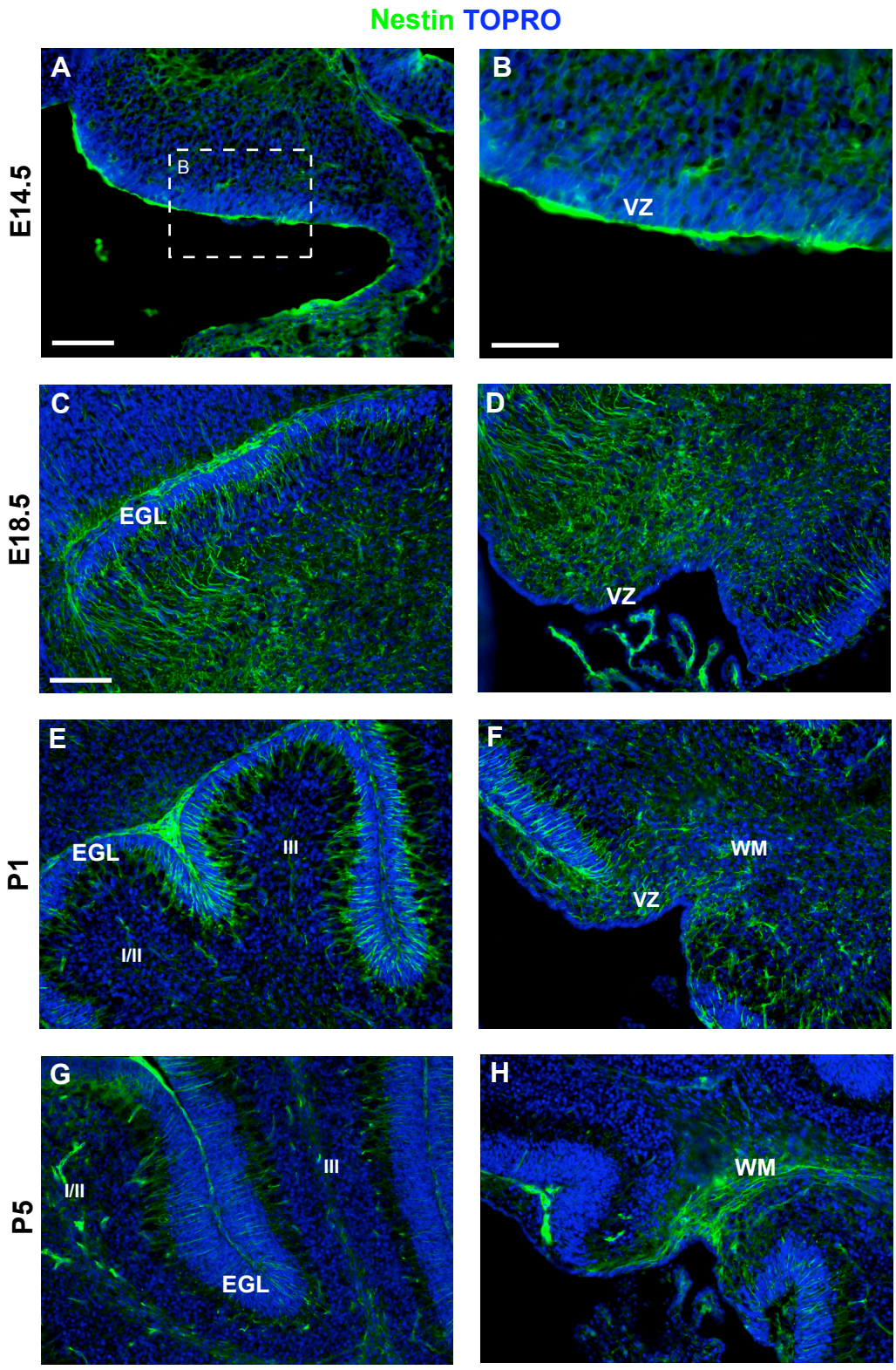

Figure 5.3 - Nestin is expressed in the developing cerebellum.
Sagittal cerebellum sections from E14.5 (A-B), E18.5(C-D), P1 (E-F) and P5 (G-H) mice were tested by immunohistochemistry for the expression of Nestin. Scale bars = 100 µm (A,C-H), 50 µm (B). Folia identified by roman numerals.

5.4.2 Induction of the *Nestin-Cre* transgene activates a *R26YFP* reporter

While Nestin expression is evident in the developing cerebellum, the *Nestin-Cre* transgene is an artificial construct driven by a single Nestin enhancer element (Kawaguchi et al., 2001; Zimmerman et al., 1994), thus the dynamics of its expression are unlikely to be entirely consistent with that of endogenous Nestin. For this reason, I next sought to validate the activity of the *Nestin-Cre* transgene. To do this I crossed heterozygous *Nestin-Cre* mice with homozygous *R26YFP* reporter mice to generate offspring that were heterozygous for both *Nestin-Cre* and *R26YFP*. These litters were treated with established concentrations of tamoxifen at two embryonic and two postnatal time points to induce the Cre-recombinase and thereby activate expression of the *R26YFP* reporter. Expression of YFP was then analysed by immunohistochemistry.

Induction of Cre-recombinase activity at E13.5 by a single injection of 10 mg tamoxifen to a pregnant mother followed by a chase of three days resulted in a mosaic activation of the *R26YFP* reporter throughout the developing cerebellum (Fig. 5.4A). YFP expression was observed in numerous patches along the VZ, in cells apparently radiating out from the VZ, and also in scattered cells in the anterior EGL and immediately below it. No YFP expression was observed in the posterior EGL. A slightly later embryonic induction (E15.5) with the same dose followed by a three day chase resulted in a similar pattern of expression (Fig. 5.4B), with YFP expression again observed along the VZ and in cells radiating outward towards the EGL. Again, a notable lack of YFP expression was observed in the EGL. SC injections of tamoxifen postnatally also resulted in detectable YFP expression. Injections at P1 (1.5 mg) followed by a two day chase resulted in expression predominating in the PCL with scattered expression throughout the WM and occasionally in the EGL (Fig. 5.4C). SC tamoxifen injection at P5 followed by a four day chase gave a similar pattern of *R26YFP* expression, with YFP detected almost exclusively in the PCL and WM, with scattered expression through the IGL. No expression was observed in the EGL (Fig. 5.4D). Combined, these data confirm the activity of the *Nestin-Cre* transgene at numerous points through development, though

the restriction of the reporter expression compared to the expression of endogenous Nestin protein suggests *Nestin-Cre* is not active in all Nestin expressing cells at the dosages of tamoxifen used. In particular, Nestin expression at P1 and P5 was observed throughout the PCL and WM while expression of the *R26YFP* reporter appeared considerably more restricted.

5.4.3 Potential linkage between the *Nestin-Cre* and *Apc* alleles caused difficulty in generating the *Nestin-Cre* $Apc^{lox/lox}$ mouse model

To constitutively activate Wnt/β-catenin signalling in the *Nestin-Cre* expressing cells during cerebellum development I crossed the *Nestin-Cre* line to the Apc^{lox} line. However, a number of crosses were required to obtain *Nestin-*$Cre^{+/-}$ *;* $Apc^{lox/lox}$ individuals and the genotype ratios obtained indicated a potential linkage between the *Nestin-Cre* and *Apc* alleles. Offspring from three separate pairs were genotyped and the observed genotype frequencies were compared to the expected genotype frequencies (Table 5.1). In all three crosses carried out, the *Nestin-Cre* allele and the Apc^{lox} alleles from the two parents rarely ended up in the same offspring (i.e. the *Nestin-Cre* and *Apc* alleles appear to segregate together more often than would be expected). A two-tailed Chi^2 test to analyse the difference between the observed and expected offspring genotypes revealed a significant difference in all three crosses. This suggests that the aberrant segregation of the two alleles observed is likely the result of them both being present on the same chromosome, though far enough apart that several rare offspring were obtained with the *Nestin-*$Cre^{+/-}$ *;* $Apc^{lox/lox}$ genotype required for further breeding.

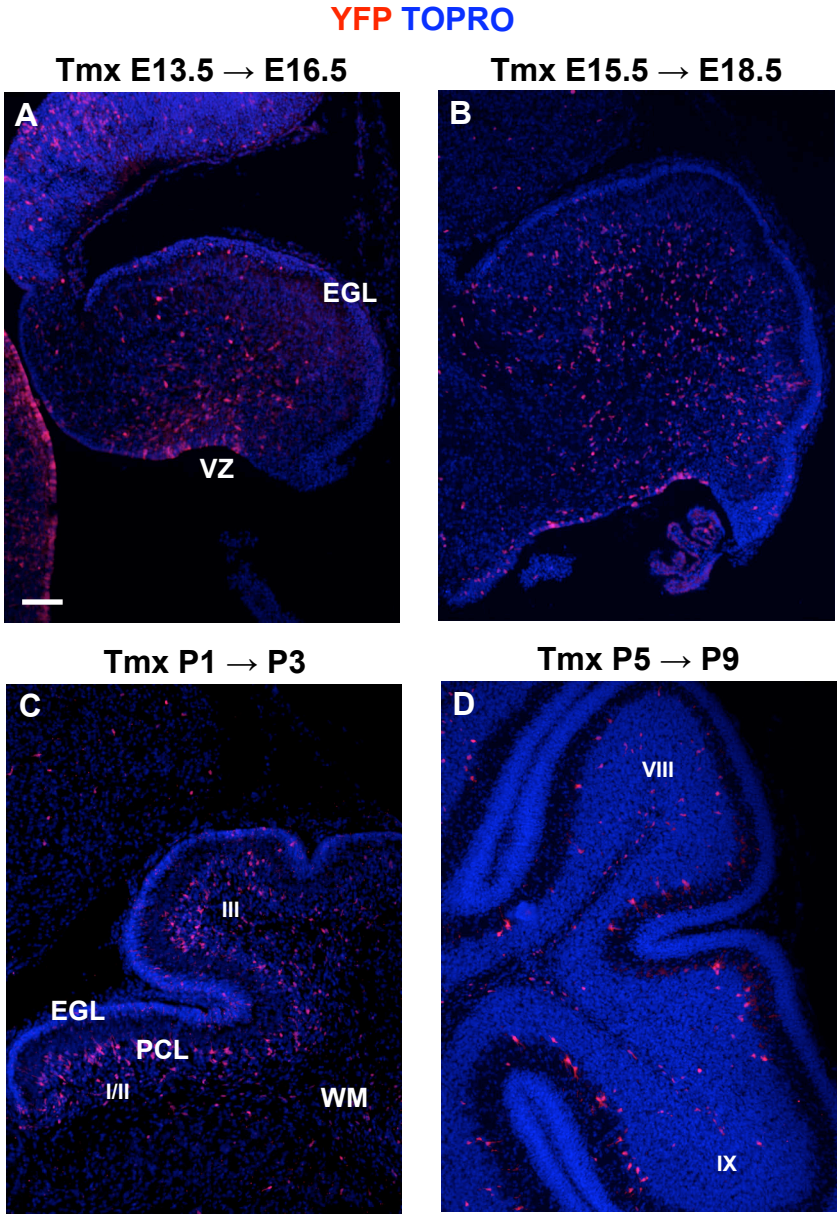

Figure 5.4 - *R26YFP* reporter expression induced after tamoxifen induction of *Nestin-Cre* activity.
Nestin-Cre+ ; R26YFP+ animals were injected with tamoxifen *in utero* or early postnatally to induce *Nestin-Cre* activity at E13.5 (A), E15.5 (B), P1 (C) and P5 (D). Expression of the *R26YFP* reporter was analysed by immunohistochemistry between two and four days later on sagittal cerebellum sections.Scale bar = 100 µm. Folia identified by roman numerals.

Table 5.1 - Chi^2 tests for the segregation of *Nestin-Cre* and *Apc* alleles

Cross	Offspring genotypes	Observed numbers	Expected numbers (frequency)	Chi^2 / P value
Cre$^{+/-}$ *Apc*$^{lox/+}$	*Cre*$^{+/}$ *Apc*$^{lox/lox-}$	1	3.25 (25%)	
x	*Cre*$^{+/-}$*Apc*$^{lox/+}$	7	3.25 (25%)	
Cre$^{-/-}$ *Apc*$^{lox/lox}$	*Cre*$^{-/-}$*Apc*$^{lox/lox}$	4	3.25 (25%)	
	Cre$^{-/-}$.*Apc*$^{lox/+}$	1	3.25 (25%)	**7.62 / 0.019 (3df)**
Cre$^{+/-}$ *Apc*$^{lox/+}$	*Cre*$^{+/}$ *Apc*$^{lox/lox-}$	0	4.75 (12.5%)	
x	*Cre*$^{+/-}$*Apc*$^{lox/+}$	11	4.75 (12.5%)	
Cre$^{-/-}$ *Apc*$^{lox/+}$	*Cre*$^{+/-}$*Apc*$^{+/+}$	7	9.5 (25%)	
	Cre$^{-/-}$ *Apc*$^{lox/lox-}$	8	9.5 (25%)	
	Cre$^{-/-}$*Apc*$^{lox/+}$	11	4.75 (12.5%)	
	Cre$^{-/-}$*Apc*$^{+/+}$	1	4.75 (12.5%)	**25.05 / 0.00136 (5df)**
Cre$^{+/-}$ *Apc*$^{lox/+}$	*Cre*$^{+/-}$*Apc*$^{lox/+}$	3	14.75 (25%)	
x	*Cre*$^{+/-}$*Apc*$^{+/+}$	31	14.75 (25%)	
Cre$^{-/-}$ *Ap*$^{+/+}$	*Cre*$^{-/-}$*Apc*$^{lox/+}$	20	14.75 (25%)	
	Cre$^{-/-}$*Apc*$^{+/+}$	5	14.75 (25%)	**35.58 / <0.0001 (3df)**

5.4.4 *Nestin-Cre ; APC$^{lox/lox}$* mutant mice display ectopic β-catenin, confirming activation of the Wnt/β-catenin pathway

Once adequate numbers of *Nestin-Cre$^{+/-}$; Apc$^{lox/lox}$* males were obtained I began a series of proof of principle experiments to test the activity of the *Nestin-Cre* transgene on the *Apc^{lox}* allele at defined embryonic and postnatal stages of development. *Nestin-Cre$^{+/-}$; Apc$^{lox/lox}$* males were crossed to *Apc$^{lox/lox}$* females in order to generate offspring that were either *Nestin-Cre$^{+/-}$; Apc$^{lox/lox}$* for analysis or *Nestin-Cre$^{-/-}$; Apc$^{lox/lox}$* as controls. These offspring were treated with tamoxifen embryonically by a gavage delivered to the pregnant mother, or by early postnatal SC injection.

10 mg of tamoxifen in total was delivered (in 200 μl corn oil) to E14.5 pregnant *Apc$^{lox/lox}$* females that had been set up in timed matings with *Nestin-Cre$^{+/-}$; Apc$^{lox/lox}$* males. The embryos were first collected at E18.5 and sagittal sections taken from the resulting *Cre+* and *Cre-* embryos were analysed by immunohistochemsitry for the ectopic localisation of β-catenin as a marker for loss of APC (as APC is an abundantly expressed cytoplasmic protein, detecting its lack of expression in few cells spread amidst a high number of APC+ cells was too difficult). While no effect was observed in the *Cre-* sections (Fig. 5.5A), a small proportion of cells were identified in the *Cre+* embryos, particularly along the VZ, that displayed ectopic nuclear localisation of β-catenin protein (Fig. 5.5B-C). This indicated that Cre-mediated recombination of the *Apc$^{lox/lox}$* allele had occurred and that the Wnt/β-catenin pathway had become upregulated as a result.

In order to analyse the long term consequences of Wnt/β-catenin pathway activation in the cerebellum at this stage, a second litter was left to term and then analysed after six weeks postnatal growth. Initially, a cresyl violet (CV) stain was carried out on sagittal sections and gross morphology of the *Cre-* (Fig. 5.5D) and *Cre+* (Fig. 5.5E) cerebellums were compared, although no obvious differences were observed between the two groups. Consistent with this, further immunohistochemistry for β-catenin

revealed a lack of ectopic expression (Fig. 5.5F-G) in the *Cre+* cerebellums. These data suggest that the complement of mutant cells generated by E18.5 have either died out by this time point, or that recombination of the Apc^{lox} allele was not successful in this litter.

1.5 mg tamoxifen (delivered in 50 μl corn oil) was injected SC to each pup from the same cross at P1. Animals were then culled and cerebella dissected at P10. Sagittal sections from each *Cre-* (Fig. 5.6A) and *Cre+* (Fig. 5.6B) cerebellum were then analysed by immunohistochemistry for the expression of β-catenin. These experiments revealed ectopic expression of β-catenin throughout each lobe of the cerebellum (Fig. 5.6B-C), with particularly extensive expression within the developing ML and PCL – consistent with the glia and interneuron populations. However, in an additional litter analysed after six weeks postnatal development no differences were observed at the gross morphological level between the *Cre-* (Fig. 5.6D) and *Cre+* (Fig. 5.6E) cerebellums, nor was there any evidence for ectopic expression of β-catenin (Fig. 5.6F-G). Again, this could be due to either the death of the mutant cells generated earlier, or the failure of recombination to take place.

Interestingly, in a litter that was allowed to develop for six months one of the *Cre+* animals developed intestinal adenomas and was subsequently culled. Sagittal sections from the dissected cerebellum of this animal were compared to a *Cre-* littermate (Fig. 5.7A) and a small amount of ectopic β-catenin localisation was observed (Fig. 5.7B-C). These results indicate that in this individual Cre-mediated recombination of the Apc^{lox} allele was successful, though this either occurred in a small proportion of cells or the survival of the mutant cells was limited. Indeed, no developmental defects were observed in these sections alongside the ectopic β-catenin expression. Multiple intestinal adenomas were present in this animal, predominating in the distal portion of the large intestine. The *Cre-* littermate showed normal large intestine morphology and β-catenin expression (Fig. 5.7D,F), while the Cre+ adenoma displayed extensive disorganisation and ectopic β-catenin expression consistent with an intestinal adenoma driven by Wnt/β-catenin signalling (personal

communication – Dr. O. Faluyi, Queens Medical Research Institute, University of Edinburgh, UK).

Induction of *Apc*^{lox} recombination was also tested at an additional postnatal time point. 1.5 mg tamoxifen was injected SC (in 50 μl corn oil) to a P5 litter, which was then left until P21 before analysis. At this point animals were culled and the cerebella dissected and processed. Immunohistochemistry for β-catenin in *Cre*- (Fig. 5.8A) and *Cre*+ animals (Fig. 5.8B-C) revealed a number of cells with ectopic nuclear β-catenin throughout the layers of the cerebellum, although again predominance in the PCL and ML was evident. This is likely the result of the glia and interneuron progenitors being the remaining Nestin expressing cells at P5. An additional litter was treated with tamoxifen at P5 and left until six weeks. While no gross morphological differences were observed between *Cre*- (Fig. 5.8D) and *Cre*+ individuals (Fig. 5.8E), immunohistochemistry for β-catenin revealed considerable ectopic expression (Fig. 5.8F-H).

The limited data obtained from these experiments confirm the activity of the *Nestin-Cre* transgene on the *Apc*^{lox} allele during cerebellum development from the observation of ectopic β-catenin expression shortly after induction of the *Cre*-recombinase at E14.5, P1 and P5. However, a number of inconsistencies were observed in the full data set. Namely, no expression of β-catenin was observed after six weeks in the cerebellum of animals injected with tamoxifen at E14.5 or P1, while this was observed in animals injected at P1 after six months and after six weeks and six months in animals injected with tamoxifen at P5. These confounding results suggest that the protocol for Cre induction by tamoxifen injection was not consistently successful and warranted a more thorough optimisation of these experiments in order to draw any solid conclusions from the data.

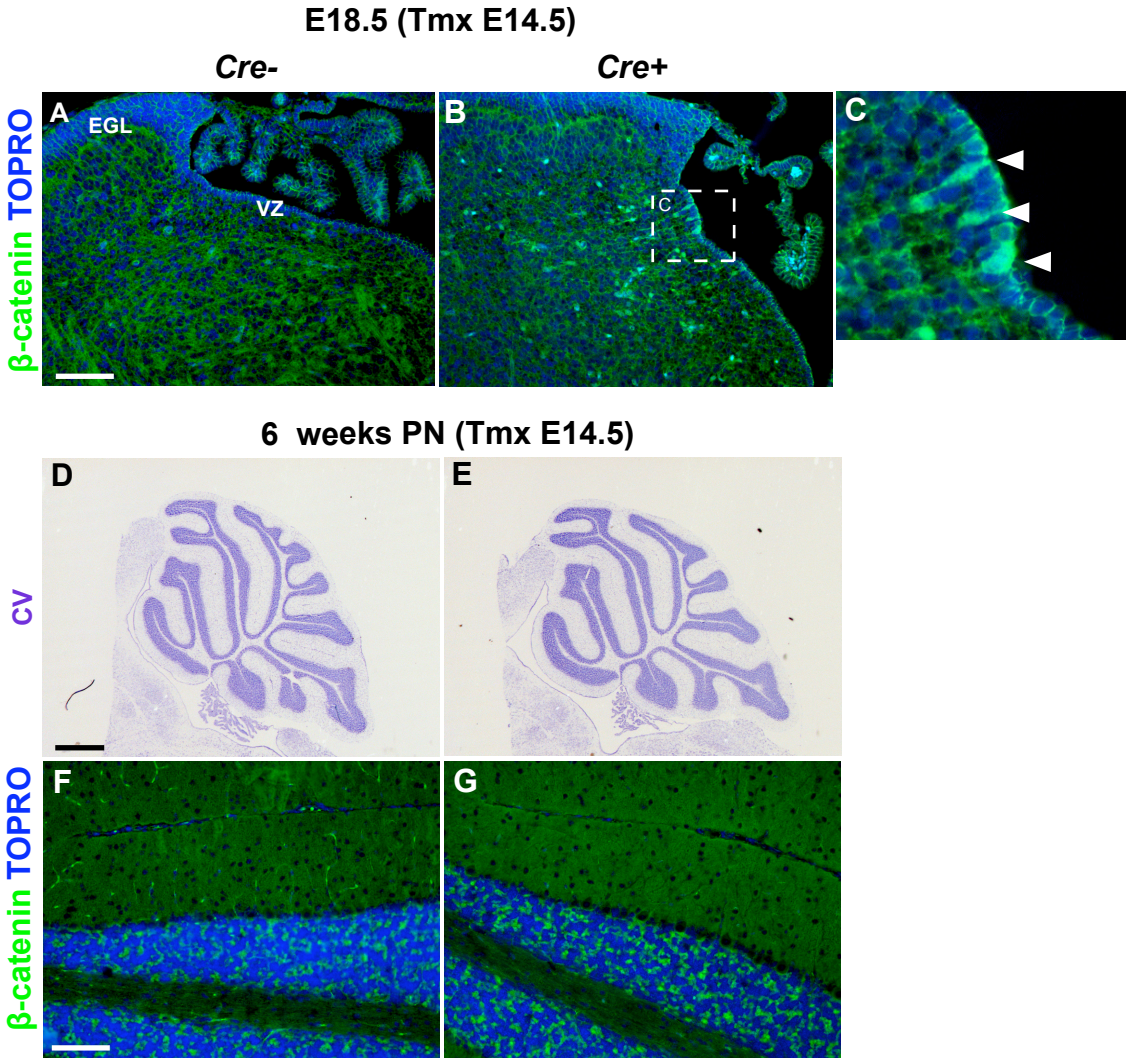

Figure 5.5 - *Nestin-Cre* induced loss of APC at E14.5 led to ectopic accumulation of β-catenin.

Nestin-Cre+ ; Apc$^{lox/lox}$ x *Nestin-Cre- ; Apc*$^{lox/lox}$ crosses were set up and pregnant females were injected with Tmx at E14.5. Resulting *Cre-* (A) and *Cre+* (B) embryos were identified and ectopic accumulation of β-catenin was observed in the Cre+ embryos (B-C). An additional litter was left to develop normally for six weeks (D-G), but no gross pathology was observed (D-E) through cresyl violet (CV) staining. No ectopic accumulation of β-catenin was observed (F-G). Scale bars = 100 μm (A-B, F-G), 500 μm (D-E).

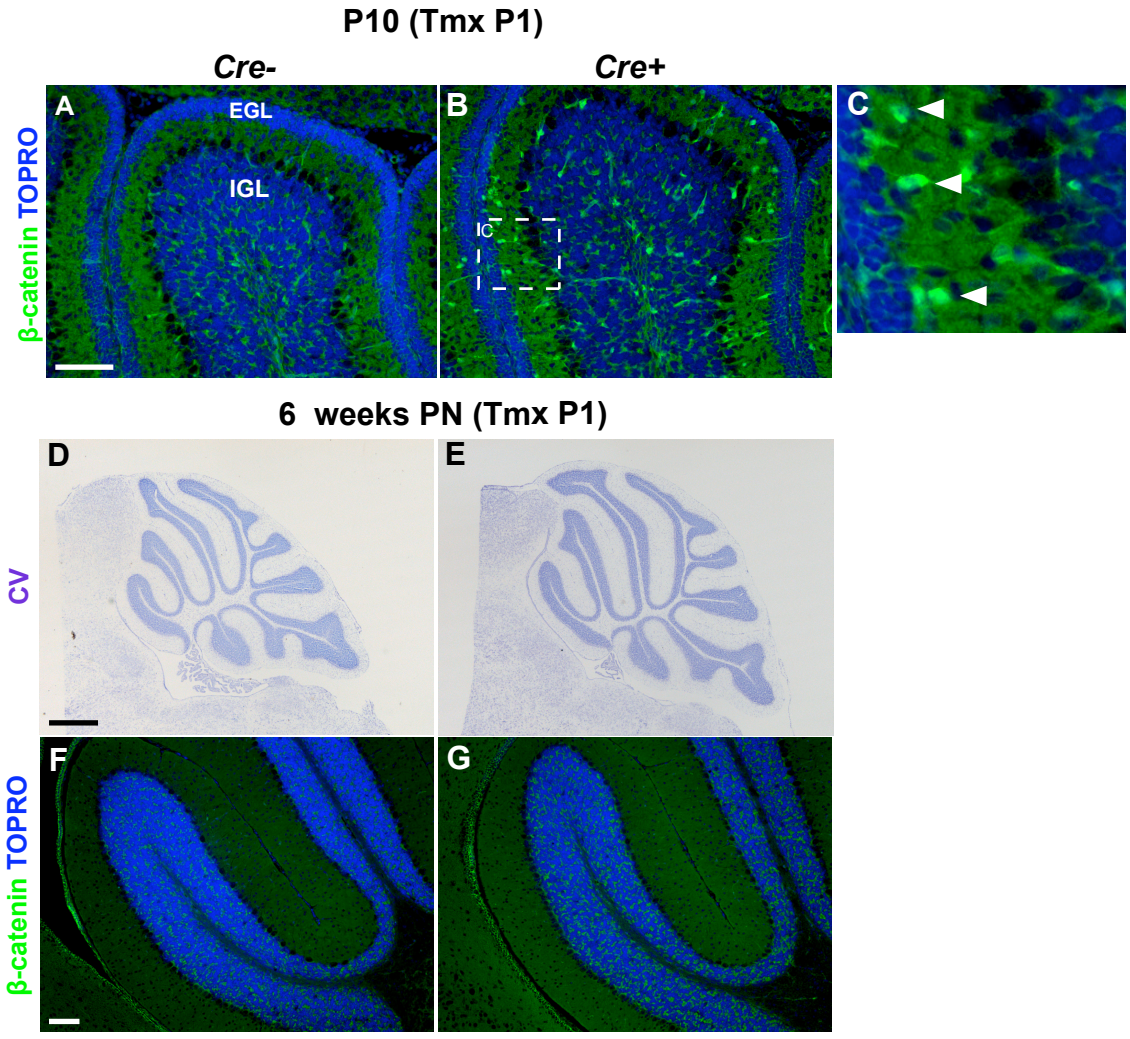

Figure 5.6 - *Nestin-Cre* induced loss of APC at P1 led to ectopic accumulation of β-catenin.
Pups from *Nestin-Cre+ ; Apc*$^{lox/lox}$ x *Nestin-Cre- ; Apc*$^{lox/lox}$ crosses were injected with Tamoxifen at P1. *Cre-* (A) and *Cre+* (B) animals were identified at P10 and ectopic accumulation of β-catenin was observed in sagittal sections from *Cre+* embryos (B-C). An additional litter was left to develop normally for six weeks (D-G), but no gross pathology was observed (D-E). No ectopic accumulation of β-catenin was observed either (F-G). Scale bars = 100 µm (A-B, F-G), 500 µm (D-E).

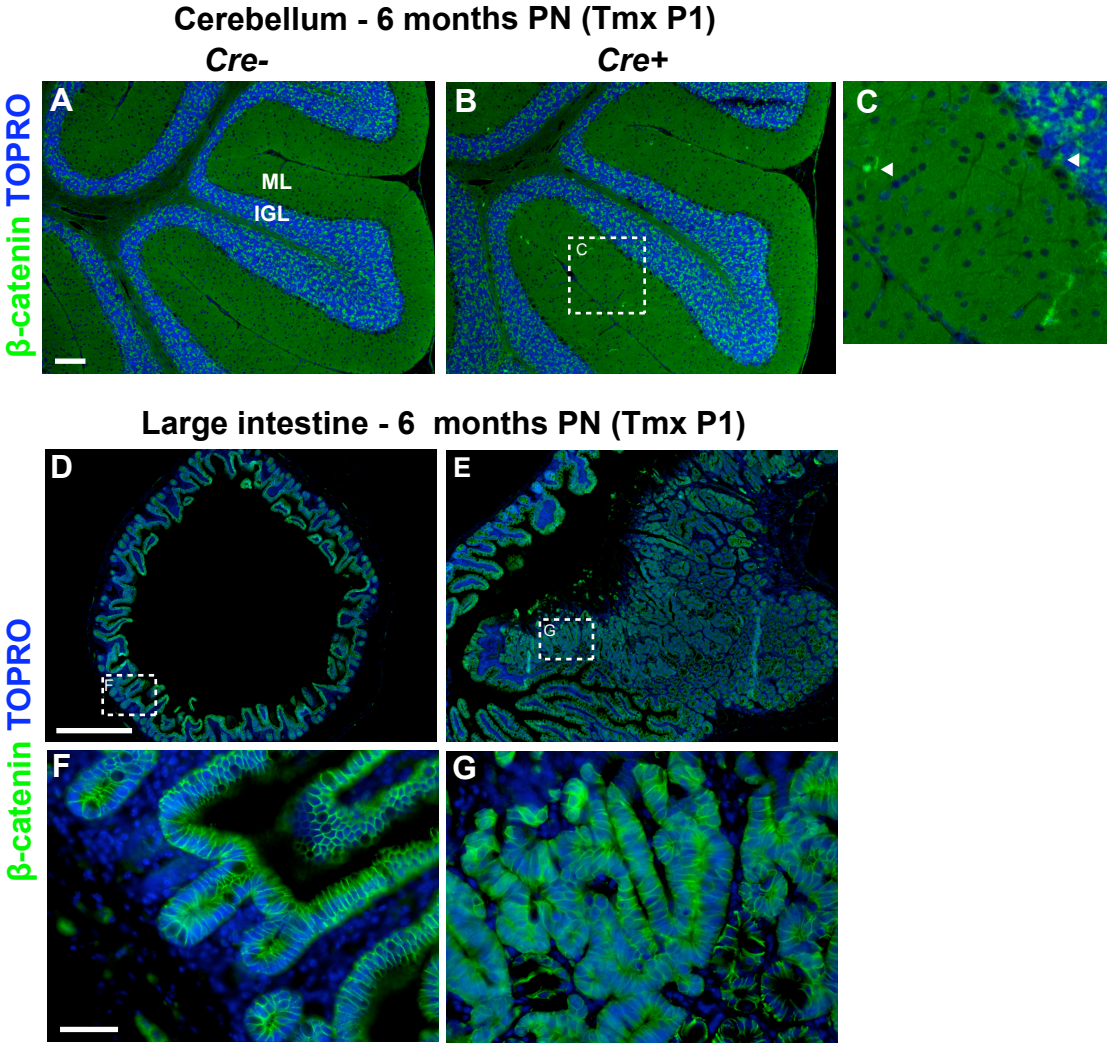

Figure 5.7 - *Nestin-Cre* induced loss of APC at P1 led to ectopic accumulation of β-catenin and intestinal adenoma after six months in one case.
Nestin-Cre- ; Apc$^{lox/lox}$ (A,D,F) and *Nestin-Cre+ ; Apc*$^{lox/lox}$ (B,E,G) pups were injected with tamoxifen at P1. Ectopic accumulation of β-catenin was observed in the cerebellum of one *Cre+* animal (B-C) after six months. The same animal developed an intestinal adenoma (E) which displayed considerable disorganisation and ectopic accumulation of β-catenin (G) compared to the epithelia of a *Cre-* intestine (F). Scale bars = 100 µm (A-B, F-G), 500 µm (D-E).

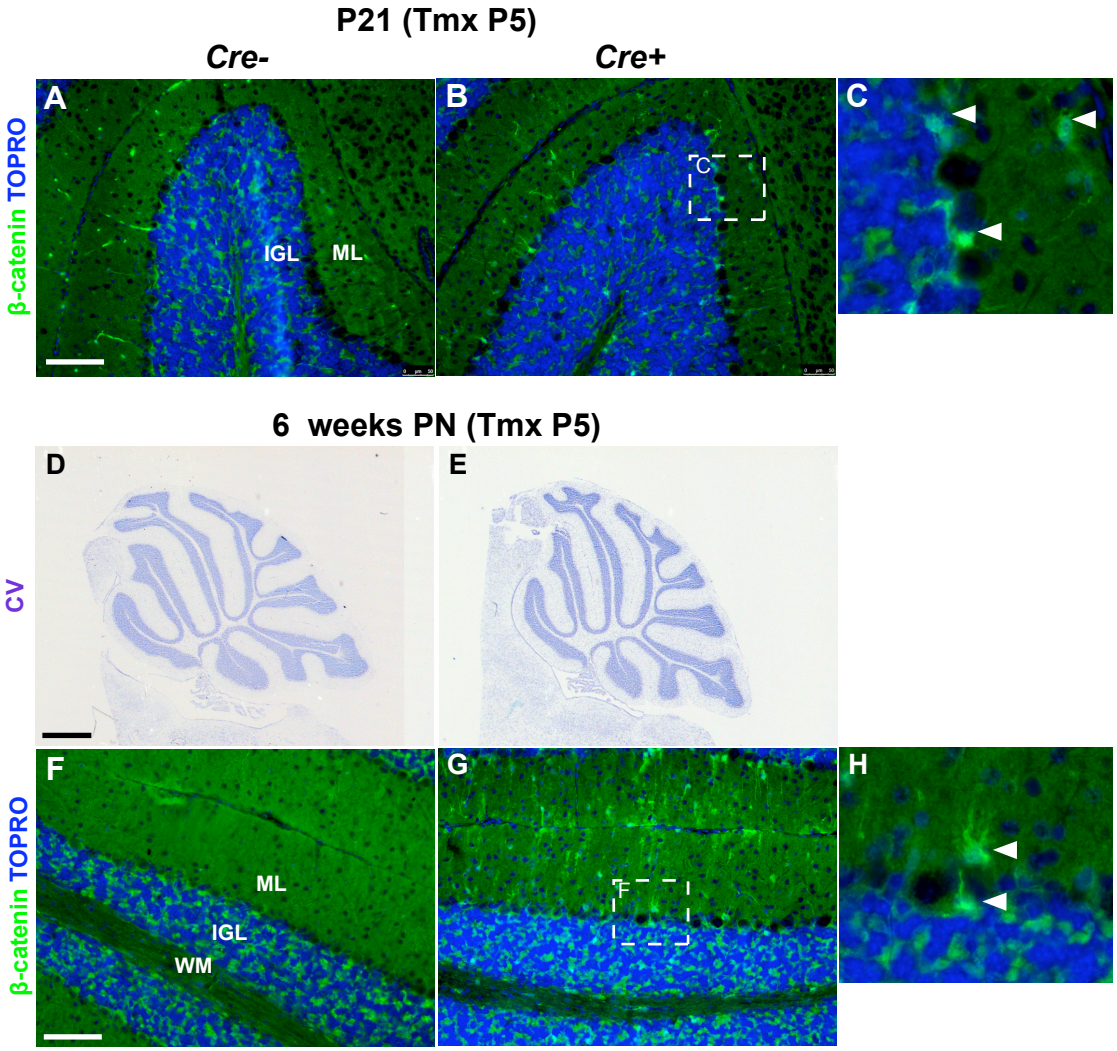

Figure 5.8 - *Nestin-Cre* induced loss of APC at P5 led to ectopic accumulation of β-catenin.
Pups from *Nestin-Cre+ ; Apc*$^{lox/lox}$ x *Nestin-Cre- ; Apc*$^{lox/lox}$ crosses were injected with Tamoxifen at P5. *Cre-* (A) and *Cre+* (B) animals were identified at P21 and ectopic accumulation of β-catenin was observed in sagittal sections from *Cre+* embryos (B-C). An additional litter was left to develop normally for six weeks (D-G), but no gross pathology was observed (D-E). However, ectopic accumulation of β-catenin was observed (F-H) throughout the cerebellum. Scale bars = 100 μm (A-B, F-G), 500 μm (D-E).

5.4.5 Generation of a *Nestin-Cre+ ; Apc$^{lox/lox}$; R26YFP+* triple transgenic model for experimental optimisation

In order to investigate the phenotype of constitutive Wnt/β-catenin activation in the developing cerebellum, I next sought to optimise the induction protocol by creating triple transgenic mice with the *Nestin-Cre, Apc^{lox}* and *R26YFP* alleles. To obtain mice with this genotype, I generated *Apc$^{lox/lox}$; R26YFP$^{+/+}$* double homozygous animals and crossed them with the previously generated *Nestin-Cre$^{+/-}$; Apc$^{lox/lox}$* animals. With these mice generated, I planned to quantify the extent of recombination (by counting YFP+ cells in the tamoxifen treated cerebella) with different tamoxifen doses at the different time points. In addition, I investigated the use of 4-hydroxy (4-OH) tamoxifen – the metabolically active form of the drug (tamoxifen itself requires processing in the liver for conversion to its active state).

Initially, *Nestin-Cre$^{+/-}$; Apc$^{lox/lox}$* males were crossed to *Apc$^{lox/lox}$; R26YFP$^{+/+}$* females and the offspring were treated with 10.5 mg or 12 mg of tamoxifen by gavage delivered to the pregnant mother at E14.5 or E16.5 respectively. In addition, P1 stage pups were injected SC with either 1.5 mg tamoxifen or 0.05 mg 4-OH tamoxifen. Offspring induced embryonically were collected at E18.5 for analysis and offspring induced at P1 were collected for analysis at P7 (Fig. 5.9A). The cerebellum of *Cre+* individuals (approximately half the total offspring) were sectioned and analysed by immunohistochemistry for YFP and β-catenin expression. In addition, the cortex of these animals was collected and DNA extracted in order to test for presence of the recombined *Apc* allele (*ApcΔ)* by PCR.

These experiments revealed that in all cases little to no YFP or ectopic β-catenin expression was observed (Fig. 5.9B-C) in stark contrast to the induction of YFP or ectopic expression of β-catenin observed previously (Fig. 5.4-5.7). In no case was the *ApcΔ* allele identified. A total of 37 *Cre+* individuals (out of a total of 72 individuals) were treated with tamoxifen in the four dosing regimes, none of which displayed any YFP expression above one or two rare cells per section. To confirm that the tamoxifen preparation was not causing this lack of *Nestin-Cre* activation, a

separate experiment was carried out where the offpsing from an *Emx1-Cre* x *R26YFP* cross were treated with 10.5 mg tamoxifen by gavage to the pregnant mother at E14.5 followed by analysis at E18.5. In all *Cre+* individuals from this experiment, considerable induction of the YFP reporter was evident throughout the cortex (the region of *Emx1* expression) (Fig. 5.9D-E). This confirmed that both the reporter transgene and the tamoxifen preparation were functional and that the lack of YFP expression or ectopic β-catenin expression observed is likely due to loss of *Nestin-Cre* transgene function.

A

Optimisation of Tmx induction

Dose and delivery	Induction age	Analysis age	n (*Cre+*)
10.5 mg Gavage	E14.5	E18.5	16 (8)
12 mg Gavage	E16.5	E18.5	10 (5)
1.5 mg SC	P1	P7	30 (15)
0.05 mg SC (4-OH)	P1	P7	16 (8)

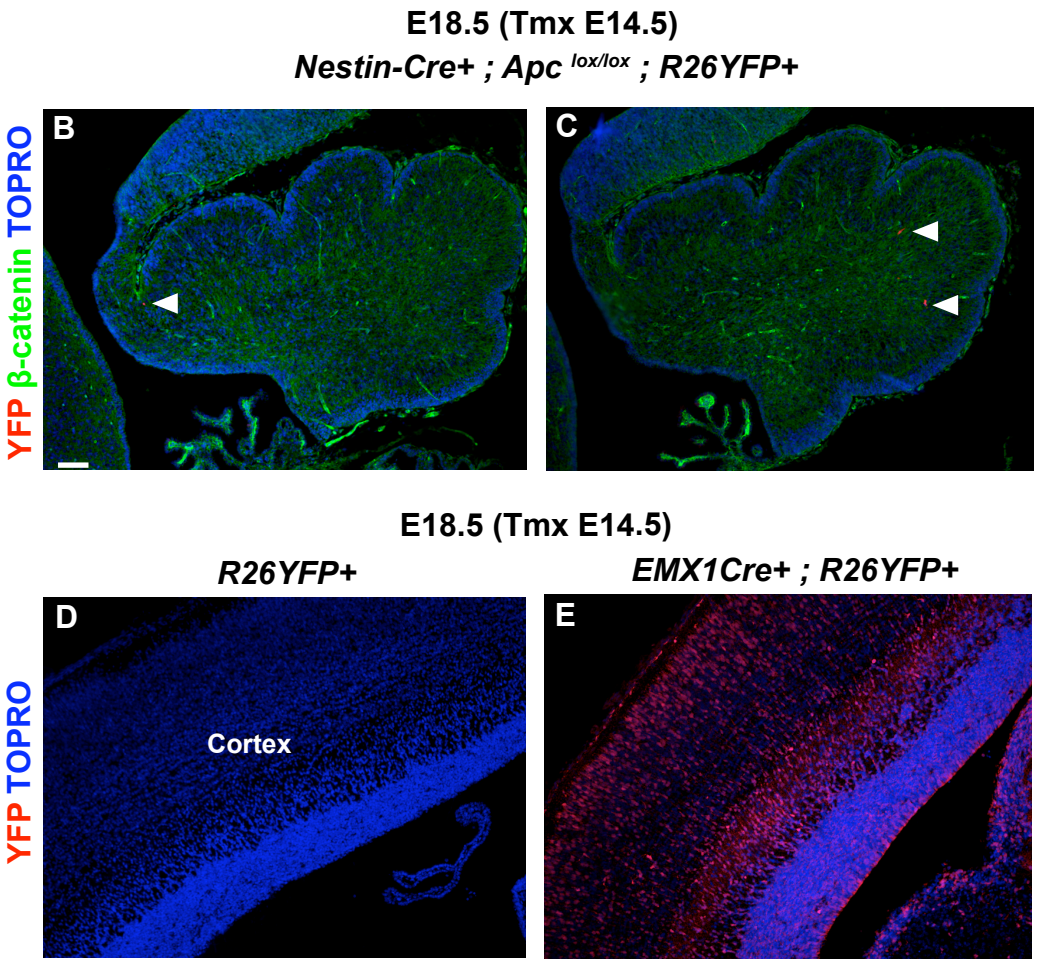

Figure 5.9 - Loss of *Nestin-Cre* activity despite effectiveness of tamoxifen preparation on other models.
To optimise the tamoxifen induction protocol, a *R26YFP* reporter was crossed onto *Nestin-Cre ; Apc*$^{lox/lox}$ animals and a series of tamoxifen or 4-hydroxy (OH) tamoxifen injections were carried out at E14.5, E16.5 and P1 followed by analysis at E18.5 or P7 (A). Only rarely were YFP+ cells observed in sagittal sections taken from these animals (white arrows B-C, representative images). The tamoxifen preparation was trialed on an independent Cre line (*EMX1Cre*), which revealed expected expression of the same *R26YFP* reporter (D-E) in the cortex (Cx). Scale bar = 100 µm (A-E).

5.5 Discussion

The aim of this chapter was to investigate the consequences of constitutively activating the Wnt/βcatenin pathway *in vivo* at defined points during development. To address this I utilised existing mouse models with targeted mutations to the *Apc* gene. Results from these experiments revealed either a lack of aberrant phenotype, or were unsuccessful.

5.5.1 The *Apc^{min}* mouse does not model medulloblastoma

The *Apc^{min}* mouse contains a point mutation in the *Apc* gene resulting in a truncated and non-functional protein being produced (Moser et al., 1990; Su et al., 1992). Mice heterozygous for the *Apc^{min}* allele exhibit loss of heterozygosity (LOH) and develop intestinal polyposis and eventual multiple adenomas after 10 weeks. As such, they are frequently used to model the human condition FAP. As FAP patients are 90 times more likely to develop medulloblastoma than the general population (Hamilton et al., 1995) I reasoned that early preneoplastic lesions may be evident in the cerebellum of mice with the *Apc^{min}* mutation. However, no such lesions nor any gross developmental defects were evident. This is most likely due to the requirement for *Apc* LOH in order for Wnt/β-catenin signalling to become constitutively active. While the continuous turnover of cells within the intestinal crypts allows for the gradual accumulation of mutation (such as the second hit required for *Apc* LOH), the limited amount of cell division during cerebellum development in comparison means that this event would be exceedingly rare. Thus, a large cohort of mice would have to be analysed in order to find any abnormality resulting from *Apc* LOH in the cerebellum. In addition, as the Wnt subgroup of paediatric medulloblastoma is known to be less aggressive and to develop relatively late in childhood (Kool et al., 2008) it is also possible that the timescale for these experiments was not long enough for any lesions to become evident.

5.5.2 Attempts to constitutively activate the Wnt/β-catenin pathway during cerebellum development mediated by the *Nestin-Cre* transgene were not successful

Conditional gene targeting allows for the effects of a gene knockout to be studied in a spatio-temporal specific manner. In this context, I chose a *Nestin-CreER*^{T2} trasngene (Carlén et al., 2006) to knockout the *Apc* gene (Shibata et al., 1997) in the cerebellum progenitor population (Dahlstrand et al., 1995; Zimmerman et al., 1994) at defined stages in cerebellum development. Thus, while a full knockout of *Apc* function would not be viable, this approach would allow a functional investigation on the consequences of Wnt/β-catenin pathway activation in progenitors at different stages of development.

Initially, validation of the *Nestin-Cre* trasngene using a *R26YFP* reporter allele revealed widespread expression of the reporter following tamoxifen induction at E13.5 or E15.5 (Fig. 5.4) throughout the cerebellum. Furthermore, reporter activation was observed after postnatal induction at both P1 and P5, albeit in a more restricted manner consistent with the expression of endogenous Nestin (Fig. 5.2). Combined, these experiments provided the rationale for using the *Nestin-Cre* trasngene to knockout *Apc* function at these stages of cerebellum development. Proof of principle experiments testing the conditional knockout of *Apc* at E14.5, P1 and P5 revealed ectopic accumulation of β-catenin after a period of four to 15 days (Fig. 5.5-5.8). However, inconsistencies were evident between experimental groups after attempts to leave injected animals for periods of six weeks to six months. To resolve these, and to launch a more thorough investigation of the functional effects of conditional *Apc* knockout in the developing cerebellum, I carried out further breeding in order to generate *Nestin-Cre Apc*$^{lox/lox}$ *R26YFP* transgenic animals. However, experiments carried out on animals at this point revealed an almost complete loss of *Nestin-Cre* activity. From these data I conclude that attempts to optimise and scale up the experiments resulted in a heritable loss of *Nestin-Cre* function and thus alternative methods of *in vivo* modelling would be required to address the aims for this chapter.

6 Activation of Wnt/β-catenin signalling *in vivo* using *in utero* electroporation

6.1 Introduction

The aim of the work presented in the previous chapter was to investigate the functional consequences of Wnt/β-catenin pathway activation *in vivo* at defined stages during cerebellum development. Attempts to address this aim using an inducible genetic knockout mouse model were not successful and due to the time constraints of generating further mouse models I decided to pursue *in utero* electroporation as an alternative method of *in vivo* genetic manipulation. Briefly, the technique involves exposing embryos *in utero* and microinjecting DNA into the embryonic tissue of interest followed by passing a current through the tissue with external electrodes so that the DNA is taken into cells within the region (Saito and Nakatsuji, 2001).

There are a number of examples of *in utero* electroporation being used as a technique for studying cerebellum development that demonstrate its advantages over traditional genetic approaches. Core to this is the ability to more precisely control the spatio-temporal extent of the genetic change being introduced by choosing when a DNA injection is carried out and defining the region to take up the DNA by positioning the electrodes accordingly. This has allowed a descriptive fate map of the brain stem nuclei to be generated by targeting a YFP encoding plasmid to the LRL and following the migration of YFP+ cells over a developmental window (Kawauchi et al., 2006). This approach has also been used to investigate the role of different transcription factors and signalling pathways in the generation of LRL derived lineages (Dipietrantonio and Dymecki, 2009; Gibson et al., 2010; Kalinovsky et al., 2011). Of particular interest is the study by Gibson et al. that demonstrated LRL cells with activated Wnt/β-catenin signalling were unable to migrate appropriately and formed ectopic clusters of mutant cells in the DHB (Gibson et al., 2010).

In addition to targeting mutations to the LRL, *in utero* electroporation has also been used in gain/loss of function experiments to study development from the VZ (Grimaldi et al., 2009) and URL (Kawauchi and Saito, 2008). Grimaldi et al. used *in utero* electroporation to demonstrate the role of *Ascl1* in the generation of GABAergic interneurons from the VZ by electroporating *Ascl1* expression vectors to induce overexpression of the gene. Kawauchi and Saito demonstrated that Bar-class homeobox transcription factors *Mbh1* and *Mbh2* lie downstream of GPC marker *Math1* and are required for differentiation of GCs from GPCs by electroporating constructs to over or under express all three genes (Kawauchi and Saito, 2008). These studies highlight the ease of gene transfer with multiple constructs to study a developmental process without resorting to time consuming and costly generation of multiple knockout mouse models. Combined, these studies highlight the ease, efficiency, specificity and ability to target multiple genes using *in utero* electroporation in order to study cerebellum development, making it a feasible alternative method to address the aims that were not successfully achieved in the previous chapter.

6.2 Aims and experimental design

As with the previous chapter, the aim of the work presented here was to investigate the functional consequences of Wnt/β-catenin pathway activation *in vivo* during cerebellum development. To achieve this I conducted a series of experiments using *in utero* electroporation to deliver Cre-reombinase encoding DNA directly to the progenitors surrounding the fourth ventricle of $Apc^{lox/lox}$ and $Apc^{lox/+}$ embryos. Some embryos carrying the *R26YFP* reporter allele were also generated in order to better track the extent of electroporation (these cases are specified in the proceeding sections). This was followed by an analysis of the effects over a developmental window from E14.5 to E18.5.

E13.5 was chosen as the time point for electroporation as a compromise between two key limiting factors. Unlike the lateral ventricles, the fourth ventricle is not an evenly

shaped space with a simple surrounding tissue. Early in development (between E10.5-E12.5) it takes up considerable space and is easily identifiable from a dorsal view of the MHB region. However, it becomes progressively restricted in size during development and becomes obscured under the growing cerebellar anlage, making access for injection more difficult. Another confounding factor is the thickness of the uterine wall. During early embryogenesis (from conception to E12.5) the thickness of the uterus makes it difficult to visualise the gross anatomy of each embryo, whereas from E13.5 onwards this becomes much easier. Thus, I chose E13.5 as the best time point to carry out electroporations as the uterine wall is thin enough to see the embryo yet the fourth ventricle is large enough to allow access for the injection procedure. In addition, electroporation at E13.5 enabled the plasmid to be targeted to the VZ at a relatively early period of cerebellum development, allowing the effects of Wnt/β-catenin pathway activation to be observed in the multiple cell lineages that develop from that point onwards.

pCAG-Cre-IRES2-EGFP plasmid DNA (Woodhead et al., 2006) containing coding sequence for Cre-recombinase and GFP was injected (>1.5 μg/μl) in a solution containing Fast Green dye into the fourth ventricle of the exposed E13.5 embryos (Fig. 6.1A). Accumulation of the dye in the fourth ventricle was used to judge the success of the injection. Electrodes were then placed over the MHB region on a medial-lateral axis with the positive electrode on the right so that the negatively charged DNA would only be taken up by cells surrounding the right side of the ventricle (Fig. 6.1B). While orientation of the positive electrode directly over the right cerebellar hemisphere would potentially lead to a more successful plasmid uptake in the VZ, orienting the electrodes along the medial-lateral axis is more reproducible and also allowed for electroporation of cells within the LRL and DHB. Analysis was carried out on the cerebellum and HB tissue from $Apc^{lox/lox}$ and $Apc^{lox/+}$ embryos at E14.5, E15.5, E16.5 and E18.5 (Fig. 6.1C). Initially I sought to determine the extent of electroporation based on the expression of GFP and the activation of Wnt/β-catenin signalling based on the ectopic expression of β-catenin. A more thorough comparison between the two genotypes was carried out at E18.5 in order to allow a reasonable amount of time for any effects to manifest.

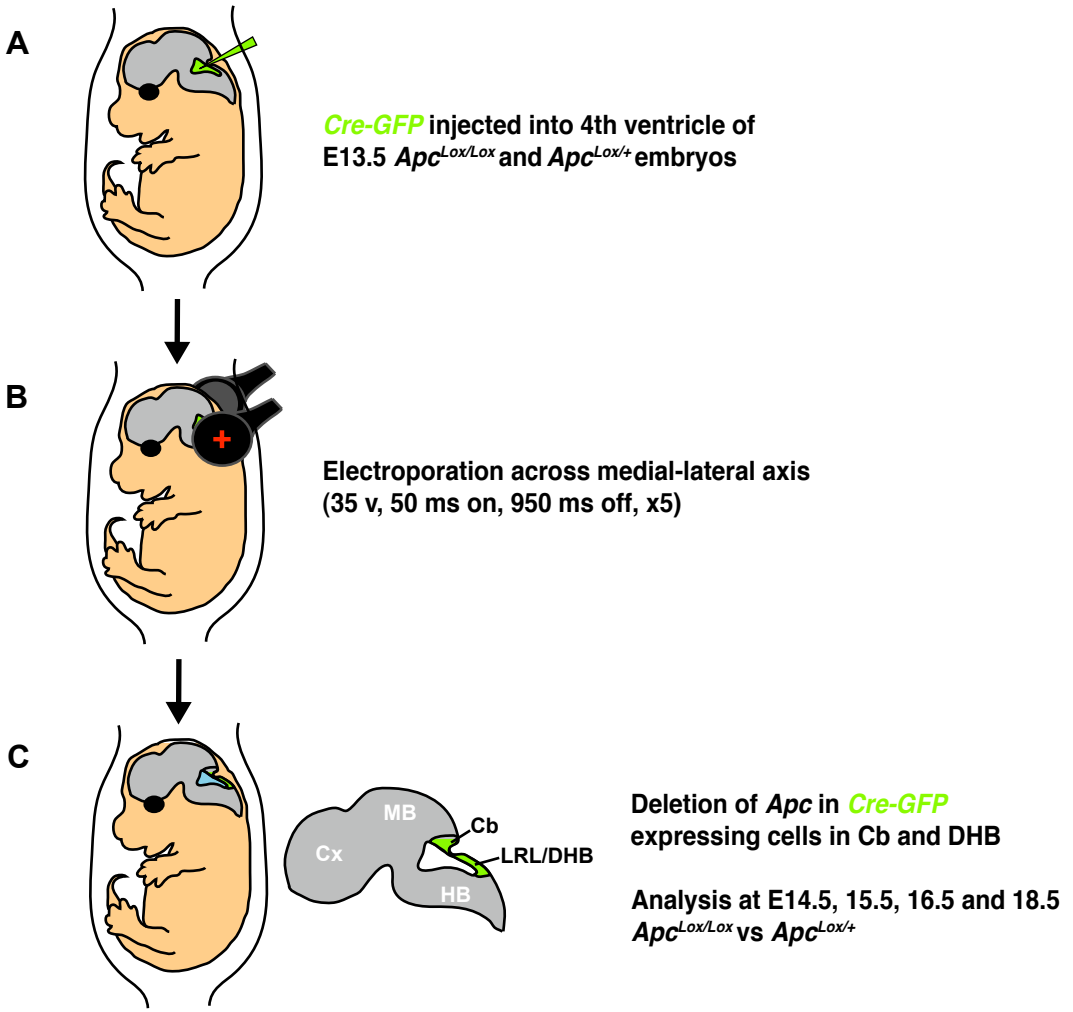

Figure 6.1 - Experimental procedure
Apc$^{lox/lox}$ males were crossed to *Apc*$^{lox/+}$ females and embryos were injected in the 4th ventricle with *Cre-GFP* plasmid (A) before being electroporated (B). Embryos were then allowed to develop *in vivo* before being analysed (C).

6.3 Early effects of *Cre-GFP* electroporation to E13.5 *Apc*$^{lox/lox}$ embryos

I first sought to analyse the extent of GFP expression after electroporation at E13.5 and to show evidence for activation of the Wnt/β-catenin pathway in these cells. To this end I chose to analyse cerebella from electroporated embryos after 24 and 48 hours.

6.3.1 Electroporation of *Cre-GFP* plasmid was evident at E14.5 and E15.5, but no activation of the Wnt/β-catenin pathway was observed

A total of 44 embryos were electroporated with *Cre-GFP* plasmid at E13.5 for collection at E14.5. Of these, 35 survived giving an 80% survival rate. 11 embryos were identified as GFP+ upon dissection, giving an electroporation success rate of 25%. Immunohistochemistry on sagittal sections from the right cerebellar hemisphere in GFP+ embryos analysed at E14.5 revealed widespread expression of GFP along the length of the VZ and in cells and processes radiating out from the VZ, indicating the successful uptake of plasmid DNA by the cells surrounding the ventricle (Fig. 6.2A-B). GFP+ cells were also evident within the URL, EGL and DHB. It is worth noting that this expression pattern was not always consistent between embryos, as minor changes in the volume of plasmid DNA injected, the site of injection and the orientation of the electrodes leads to more or less plasmid uptake in different regions surrounding the ventricle (Appendix 4). Sections from *Apc*$^{lox/lox}$ embryos were also analysed for β-catenin expression in order to determine if electroporation of the plasmid DNA had led to Cre expression, the recombination of *Apc* and the subsequent activation of Wnt/β-catenin signalling. However, in all sections analysed by immunohistochemistry β-catenin expression was normal (Fig. 6.2C-D) and no ectopic nuclear expression was observed despite the abundance of GFP expression (compare Fig. 6.2B and Fig. 6.2D). This result suggests the possibility that, despite the fact GFP expression was activated, 24 hours may not have been sufficient for *Apc* recombination and subsequent Wnt/β-catenin pathway activation to occur.

To test this assumption I analysed sections taken from the right cerebellar hemisphere of embryos collected at E15.5 after electroporation at E13.5, allowing 48 hours for the effects of *Cre-GFP* plasmid electroporation to manifest. Of the 72 embryos electroporated for collection at E15.5, 53 had survived giving a survival rate of 74%. Of all these embryos 13 were identified as GFP+, giving a success rate of 18%. Immunohistochemistry revealed a similar pattern of GFP expression to that observed at E14.5, with GFP+ cells identified at the VZ and in the cells and processes radiating away (Fig. 6.2E-F). Variation was also observed between embryos, with some showing expression of GFP within the DHB, RL and in differing patterns along the VZ (Appendix 4). Immunohistochemistry for β-catenin was also carried out on these sections of E15.5 cerebellum but results were similar to what was observed at E14.5 with no ectopic nuclear localisation detected (Fig. 6.2G-H). Cells that expressed GFP (Fig. 6.2F) did not show any evidence of ectopic β-catenin expression (Fig. 6.2H), suggesting that activation of the Wnt/β-catenin pathway had not occurred in electroporated cells after 48 hours.

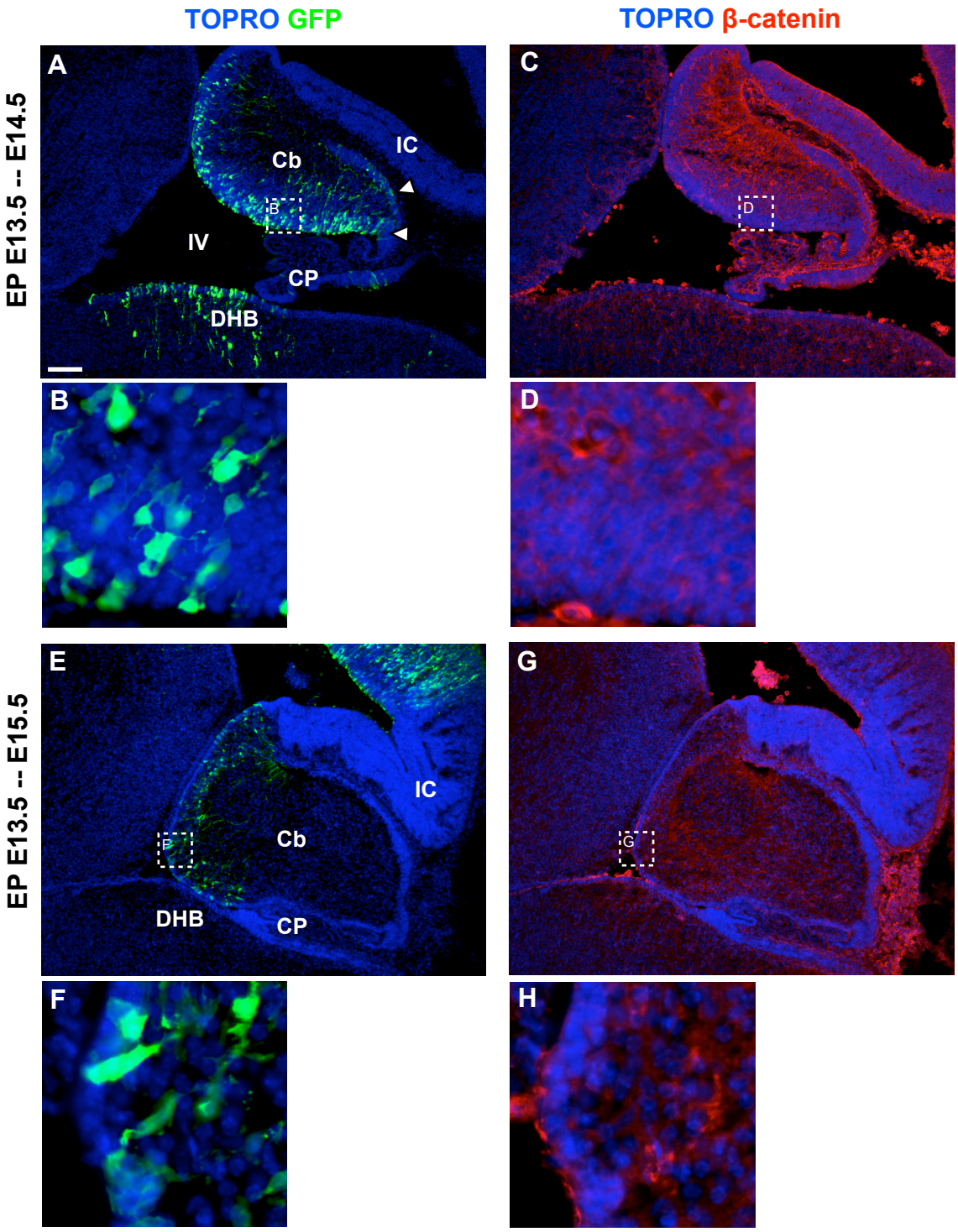

Figure 6.2 - Electroporation of *Cre-GFP* plasmid into E13.5 cerebellum did not result in Wnt/β-catenin pathway activation at E14.5 or E15.5.
Apc$^{lox/lox}$ embryos were electroporated (EP) with *Cre-GFP* plasmid at E13.5 and analysed for the expression of GFP and β-catenin at E14.5 (A-F) and E15.5 (E-H). While widespread GFP expression along the VZ and sporadically in the URL and EGL (white arrows) is evident at E14.5 (A-B) and E15.5 (E-F), indicating successful electroporation, no ectopic expression of β-catenin is observed at either age (C-D, G-H). Scale bar = 100 μm.

6.3.2 Electroporation of *Cre-GFP* plasmid to $Apc^{lox/lox}$ embryos causes Wnt/β-catenin pathway activation by E16.5

A total of 62 embryos were electroporated with *Cre-GFP* plasmid at E13.5 and analysed at E16.5. Of these 58 survived, giving a survival rate of 93.5% and 20 were identified as GFP+, giving a success rate of 32.2%. GFP+ embryos were analysed by immunohistochemistry to determine the extent of GFP expression. By this time point the GFP expression within all cerebellum sections analysed had extended well beyond the initial domains in contact with the fourth ventricle. In the cerebellum GFP+ cells could be clearly observed at the VZ and in a widely dispersed population of cells radiating away from the VZ (Fig. 6.3A), consistent with the developing glial and interneuron cell lineages. GFP expression was also observed in cells at the LRL and within the DHB (Fig. 6.3B). Consistent with observations at earlier time points, there was a certain amount of variation between each of the embryos analysed with regards to the extent of GFP expression in the cerebellum and DHB as a result of minor differences between the injection and electroporation between embryos (Appendix 4).

From a gross perspective expression of β-catenin within the cerebellum and DHB of $Apc^{lox/lox}$ embryos appeared normal (Fig. 6.3A-B), but higher magnification revealed the nuclear localisation of β-catenin in a majority of the GFP+ cells. GFP can be observed clearly in the nuclei of cells within the VZ (Fig. 6.3C) and the ectopic nuclear expression of β-catenin could be seen in a very similar pattern, with a majority of the GFP+ cells showing nuclear localisation of β-catenin (Fig. 6.3 D-E). This was also observed in the DHB, where the pattern of GFP expression (Fig. 6.3F) was strikingly similar to the pattern of nuclear β-catenin expression (Fig. 6.3G-H). These data support the activation of Wnt/β-catenin signalling in electroporated cells at E16.5. Combined with the above data (Fig. 6.2), this suggests that the sequence of events required between electroporation of the *Cre-GFP* plasmid into an $Apc^{lox/lox}$ cell and the subsequent activation of the Wnt/β-catenin pathway takes up to 72 hours in this model system.

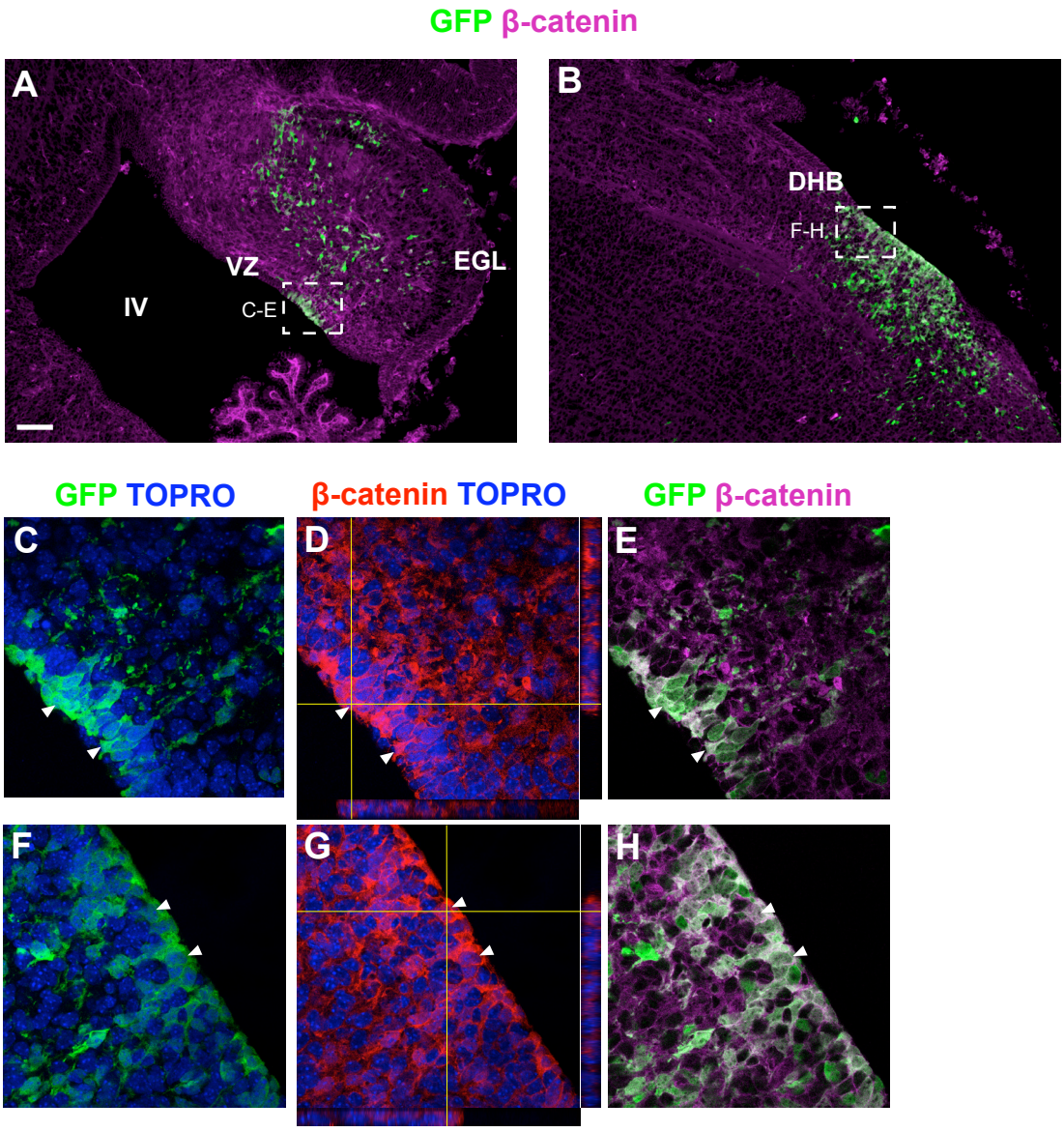

Figure 6.3 - Ectopic β-catenin localisation in E16.5 cerebellum and DHB of *Apc*$^{lox/lox}$ embryos electroporated with *Cre-GFP* plasmid at E13.5.
E13.5 embryos were injected with *Cre-GFP* plasmid at E13.5 and the cerebellum (A, C-E) and DHB (B, F-H) were analysed for the expression of GFP and β-catenin. GFP expression was evident in cells at the VZ and migrating away (C). Nuclear β -catenin was also observed in cells in this region (D) colocalising with GFP expression (E, white arrows in C-E). This was also observed in the DHB (F-G). Scale bar = 100 µm.

6.4 Late embryonic effects of *Cre-GFP* electroporation to E13.5 $Apc^{lox/lox}$ embryos

With activation of the Wnt/β-catenin pathway established in $Apc^{lox/lox}$ cells 72 hours after electroporation with *Cre-GFP* plasmid, I next sought to determine the effects of pathway upregulation in electroporated cells during late embryogenesis. While a larger developmental window would potentially allow longer for any potential effects to become manifest, E18.5 represents a point in development where a number of the key cerebellar lineages are going through important developmental processes including cell specification, proliferation, differentiation and migration. Thus, focusing my analysis at this point allows for the identification of a phenotype with regards to these processes as they occur, rather than looking for an end result.

6.4.1 Electroporation of *Cre-GFP* plasmid results in widespread GFP expression by E18.5 regardless of *Apc* genotype

A total of 106 embryos were electroporated with *Cre-GFP* plasmid at E13.5 and left until E18.5. Of these 80 survived, giving a survival rate of 75.5%, and 32 were GFP+, giving a success rate of 30.2%. Immunohistochemistry for GFP in sagittal section taken from the entire MHB region revealed a pattern of widespread GFP expression within the cerebellum, DHB and PGN. $Apc^{lox/+}$ and $Apc^{lox/lox}$ embryos were compared and few differences were observed between them. In both cases, GFP expression was evident in the ventral region of the cerebellum and in a widely dispersed pattern throughout consistent with developing interneuron and glial lineages radiating from the VZ (Fig. 6.4A-B). Interestingly, few GFP+ cells were observed within the EGL of any sections analysed except for one of the $Apc^{lox/lox}$ embryos, which showed several clusters of GFP+ cells within the EGL. There also appeared to be clustering of GFP+ cells within the cerebellum to a greater extent than in $Apc^{lox/+}$ embryos (white arrows in Fig. 6.4B).

In addition to GFP expression within the cerebellum, it was also evident within the DHB of both $Apc^{lox/+}$ and $Apc^{lox/lox}$ embryos (Fig. 6.4C-D). GFP expression can be

observed within the LRL and in cells migrating through the DHB from the LRL. While subtle differences were evident between all embryos analysed (Appendix 5), the extent of GFP+ cell migration through the DHB appeared reduced in the $Apc^{lox/lox}$ embryos compared to the $Apc^{lox/+}$ embryos. However, the identification of GFP+ cells in the PGN of both $Apc^{lox/+}$ (Fig. 6.4E) and $Apc^{lox/lox}$ (Fig. 6.4F) embryos suggests that migration from the LRL is not impaired following electroporation.

It is also important to note that there was no detectable difference in the total number of GFP+ cells per section between the two *Apc* genotypes (Table 6.1). The four $Apc^{lox/lox}$ embryos analysed revealed an average number of GFP+ cells/section of 115.7 (±38.4), while $Apc^{lox/+}$ embryos revealed 161 GFP+ cells/section (±71.9). A student's T-test between these two data sets did not reveal a significant difference (p=0.309). However, an added complication to address is that a number of the mice in each of these genotype groups also contained the *R26YFP* reporter allele. This reporter should become stably expressed in cells that have undergone Cre-mediated recombination and in any progeny that arise from them. In addition, the YFP protein is detected with the immunohistochemistry methods used to detect GFP. Thus, animals carrying the *R26YFP* allele might be expected to contain more GFP+ cells than those without (because expression of the activated *R26YFP* allele is permanent whereas expression of the electroporated *Cre-IRES-GFP* is likely to be transient). Quantitation of GFP expressing cells in the animals used above but compared between *R26YFP* genotype instead revealed that this was indeed the case (Table 6.1). Animals with the reporter had an average of 150.8 (±84.9) GFP+ cells/section, while animals without had 84.9 (±11.5), a significant difference (p=0.030, student's T-test). Taken together, we can conclude that mice with the reporter allele contain more GFP expressing cells. However, mice of each *R26YFP* genotype were present in both *Apc* genotype groups (Appendix 6).

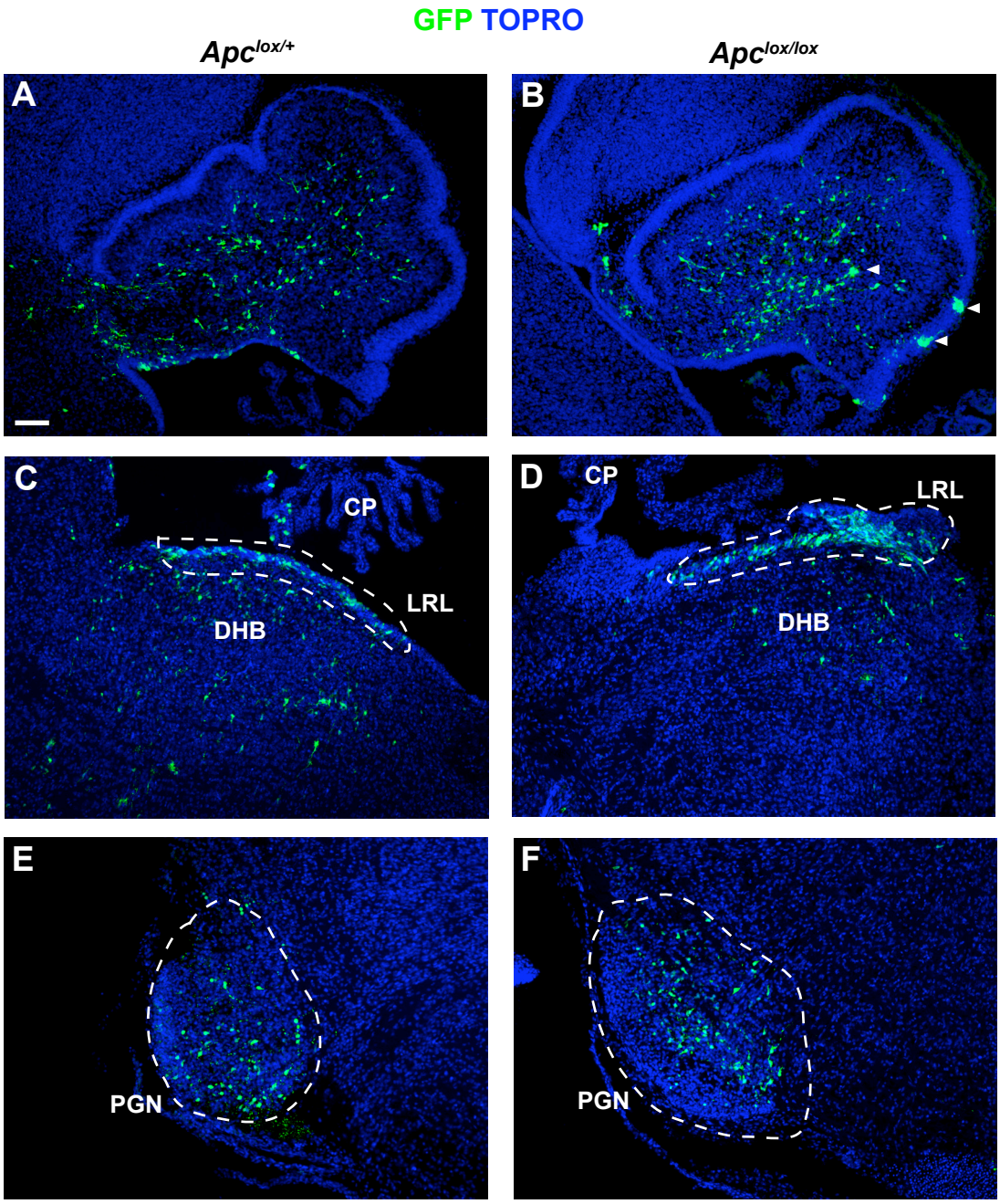

Figure 6.4 - Distribution of GFP+ electroporated cells in the E18.5 cerebellum and HB of embryos electroporated with *Cre-GFP* plasmid at E13.5.
Apc$^{lox/+}$ and *Apc*$^{lox/lox}$ E13.5 embryos were injected with *Cre-GFP* plasmid and GFP expression was analysed at E18.5. In both *Apc*$^{lox/+}$ (A) and *Apc*$^{lox/lox}$ (B) embryos GFP+ cells can be observed dispersed throughout the cerebellum from the VZ. In the *Apc*$^{lox/lox}$ cerebellum small clusters of GFP+ cells were also seen (white arrows). GFP expression was also observed in the DHB in both *Apc*$^{lox/+}$ (C) and *Apc*$^{lox/lox}$ (D) embryos, though *Apc*$^{lox/lox}$ embryos consistently showed clustering of GFP+ cells at the LRL while *Apc*$^{lox/+}$ embryos had a more dispersed pattern. Both genotypes displayed GFP expression at the PGN (pontine grey nucleus, E-F), a result of electroporated cells migrating from the LRL. Scale bar - 100 µm.

Table 6.1 - Comparison of total GFP+ cells/slice between *Apc* and *R26YFP* genotypes

Genotype	n	Mean	SD	T-test
$Apc^{lox/lox}$	4	115.7	38.4	
$Apc^{lox/+}$	4	160.9	71.9	
				0.309
$R26YFP^{+/-}$	5	150.8	28.5	
$R26YFP^{-/-}$	3	84.9	11.5	
				0.030

6.4.2 Activation of the Wnt/β-catenin pathway is evident at E18.5 after electroporation with *Cre-GFP* plasmid.

Having established the extent of GFP expression within the electroporated embryos at E18.5, I next sought to determine if the activation of the Wnt/β-catenin signalling pathway observed at E16.5 persists until E18.5. Sections from the cerebellum (Fig. 6.5A) and DHB (Fig. 6.5B) were analysed by immunohistochemistry for the expression of GFP and β-catenin. High magnification of GFP expressing regions in the cerebellum (Fig. 6.3C) revealed the extent of ectopic nuclear β-catenin expression (Fig. 6.5D), which colocalised with GFP in a majority of cells (white arrows, Fig. 6.5E). Areas of GFP expression in the DHB (Fig. 6.5F) also exhibited considerable nuclear localisation of β-catenin (Fig. 6.5G) that colocalised with GFP (white arrows, Fig. 6.5H). Quantitation of VZ and LRL high magnification images (e.g. Fig. 6.5 C-H) from 10 individual $Apc^{lox/lox}$ embryos revealed that an average of 82% (±6.2%) of GFP+ cells also showed evidence for nuclear localisation of β-catenin.

In addition, I utilised these data to determine if there was a difference in the extent of nuclear β-catenin localisation between the two *R26YFP* genotypes (Table 6.2). Comparing the proportion of GFP+ cells with nuclear β-catenin expression between $R6YFP^{+/-}$ (n=3) and $R6YFP^{-/-}$ (n=7) individuals importantly revealed that there was no difference between the two (p=0.221). Thus, for the remaining experiments I carried out quantitation of GFP+ (i.e. electroporated) cells under that assumption that the majority of GFP+ cells demonstrated activated Wnt/β-catenin signalling and that the presence or lack of the *R26YFP* reporter allele did not affect the extent of the mutation in the electroporated cell population.

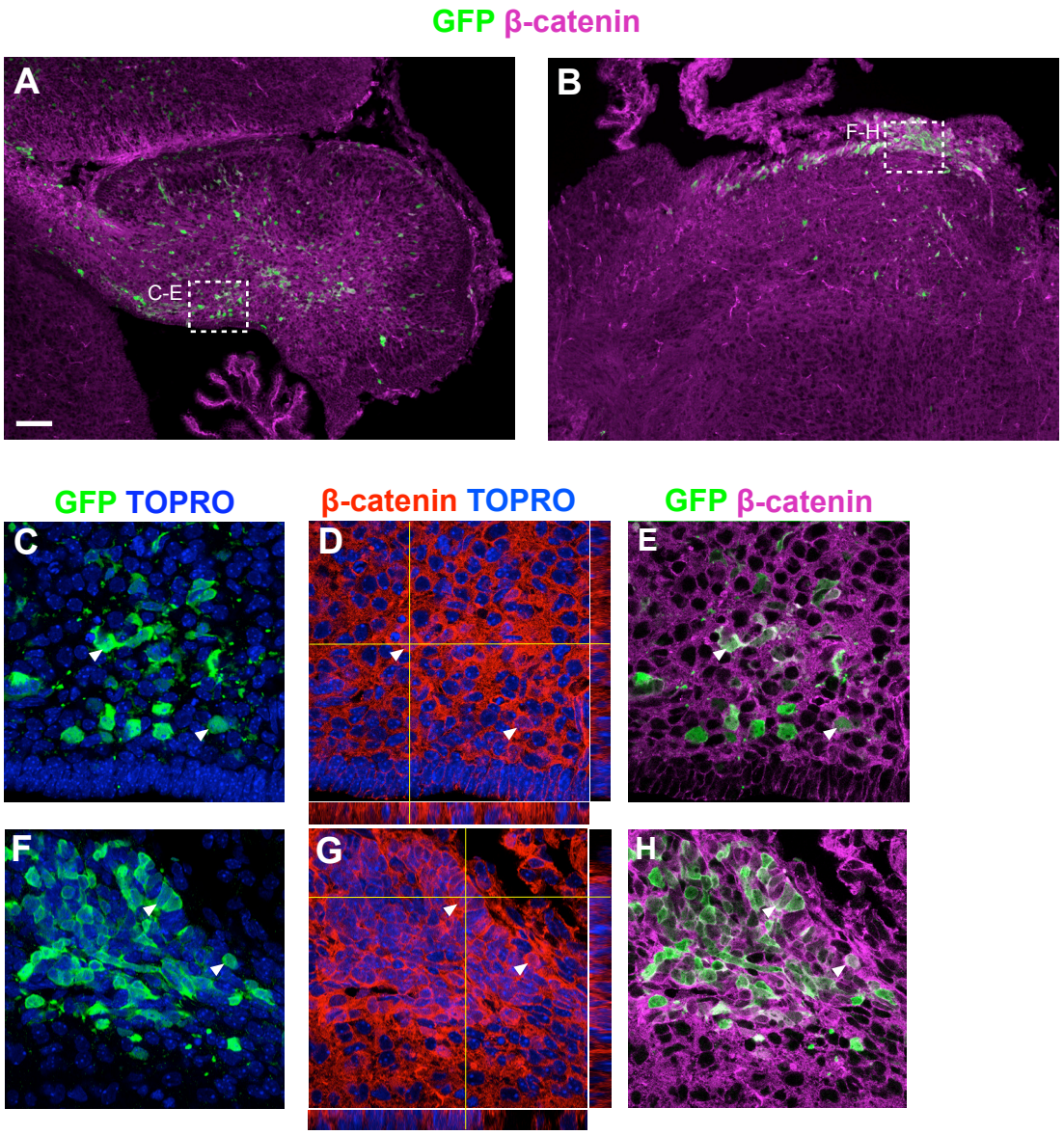

Figure 6.5 - Electroporation of *Cre-GFP* plasmid into E13.5 *Apc*^{loxlox} embryos causes ectopic localisation of β-catenin in the cerebellum and DHB at E18.5. Embryos were injected with *Cre-GFP* plasmid at E13.5 and the cerebellum (A, C-E) and DHB (B, F-H) were analysed for the expression of GFP and β-catenin. GFP expression was evident in cells migrating from the VZ (C). Nuclear β-catenin was also observed in cells in this region (D, crosshairs) colocalising with GFP expression (E, white arrows in C-E). This was also observed in the DHB (F-G). Scale bar = 100 μm.

Table 6.2 - Comparison of GFP+ cells with nuclear β-catenin expression between *R26YFP* genotypes

Genotype	n	Mean (%)	SD (%)	T-test
R26YFP$^{+/-}$	3	78.7	2.2	
R26YFP$^{-/-}$	7	84.2	6.8	
				0.221

6.4.3 The PGN does not show evidence for activated Wnt/β-catenin signalling in electroporated cells

An exception to the conclusion that a majority of electroporated cells show evidence for activated Wnt/β-catenin signalling was found after closer examination of the GFP+ cell population within the PGN (Fig. 6.6A). Consistent with the hypothesis that activated Wnt/β-catenin signalling acts to impair the migration of PGN neurons from the LRL (Gibson et al., 2010), few - if any - GFP+ cells were identified with nuclear localisation of β-catenin (Fig. 6.6B-D).

6.4.4 Activation of the Wnt/β-catenin pathway results in reduced proliferation of mutant cells

Consistent with published findings that Wnt/β-catenin signalling drives proliferation in certain contexts (Megason and McMahon, 2002; Yamaguchi et al., 1999), the results presented in Chapter 4 showed that increased Wnt/β-catenin signalling caused an increase in proliferation *ex vivo*. To determine if this was also the case *in vivo* I first administered BrdU to E18.5 $Apc^{lox/lox}$ and $Apc^{lox/+}$ embryos electroporated with *Cre-GFP* plasmid at E13.5 two hours prior to fixation in order to generate a BrdU LI for each that could be used as a measure of proliferation. However, the proportion of BrdU+/GFP+ cells generated was too small for analysis. As an alternative measure, I compared PCNA expression between the two groups. PCNA expression is considerably more widespread, and while not as specific to a particular point in the cell cycle, gives a broad indication of proliferation as evident in Chapter 3.

Immunohistochemistry for PCNA on cerebellum sections taken from E18.5 embryos revealed no immediate differences between the $Apc^{lox/+}$ (Fig. 6.7A-B) and $Apc^{lox/lox}$ (Fig. 6.7C-D) embryos. PCNA was, in both cases, observed in a pattern indicating high proliferation within the EGL and scattered proliferation throughout the rest of the cerebellum. In order to determine the effects of electroporation on proliferation more specifically, I quantitated PCNA expression in just the GFP+ (i.e. electroporated) cells. The total number of GFP+ cells was counted in three sections

from four individuals per genotype (n=4) and the proportion of PCNA+ cells was established (Fig. 6.7E). This revealed a surprising reduction in PCNA expression within the electroporated cell population of $Apc^{lox/lox}$ embryos (13.4%±3.5%) compared to the $Apc^{lox/+}$ embryos (31.1%±4.2%), suggesting that *in vivo* the activation of Wnt/β-catenin signalling has an inhibitory effect on proliferation of cells in the developing cerebellum.

6.4.5 Activation of the Wnt/β-catenin pathway results in reduced expression of Pax2 in mutant cells

The entire complement of cerebellar interneurons are generated sequentially from progenitors at the VZ and within the WM from E13.5 onwards (Hoshino et al., 2005; Leto et al., 2009; Pascual et al., 2007; Sudarov et al., 2011). As *ex vivo* results indicated a potential inhibitory effect on the expression of interneuron lineage marker Pax2 (see Chapter 4) I sought to determine the effects of *Cre-GFP* plasmid electroporation on the expression of Pax2 in $Apc^{lox/lox}$ embryos at E18.5. Immunohistochemistry on cerebellum sections from both $Apc^{lox/+}$ (Fig. 6.8A-B) and $Apc^{lox/lox}$ (Fig. 6.8 C-D) embryos revealed extensive Pax2 expression within the developing cerebellum, consistent with the developing interneuron lineage. Quantitative analysis revealed a reduction in the extent of Pax2 expression within the GFP+ cell population in the $Apc^{lox/lox}$ embryos (Fig. 6.8E). While $Apc^{lox/+}$ embryos displayed Pax2 expression in 47.9%(±12.5%) of GFP+ cells, this was reduced to 20.5% (±3.4%) in $Apc^{lox/lox}$ embryos. These data corroborate the finding in Chapter 4 that activation of the Wnt/β-catenin signalling pathway inhibits the expression of Pax2.

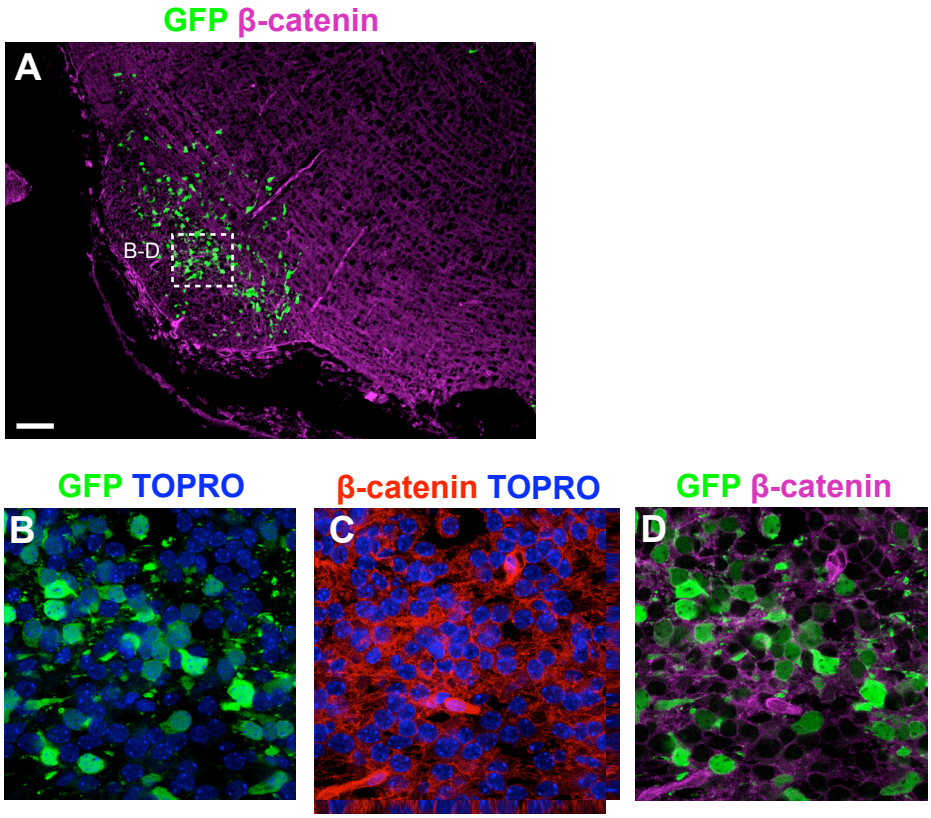

Figure 6.6 - Electroporation of *Cre-GFP* plasmid into E13.5 *Apc*^{loxlox} embryos does not result in ectopic localisation of β-catenin in the PGN at E18.5.
Embryos were injected with *Cre-GFP* plasmid at E13.5 and the PGN of *Apc*^{loxlox} embryos was analysed for expression of GFP and β-catenin (A). While extensive GFP expression was observed (B), there was little to no ectopic nuclear localisation of β-catenin (C) or colocalisation between the two (D). Scale bar = 100 μm.

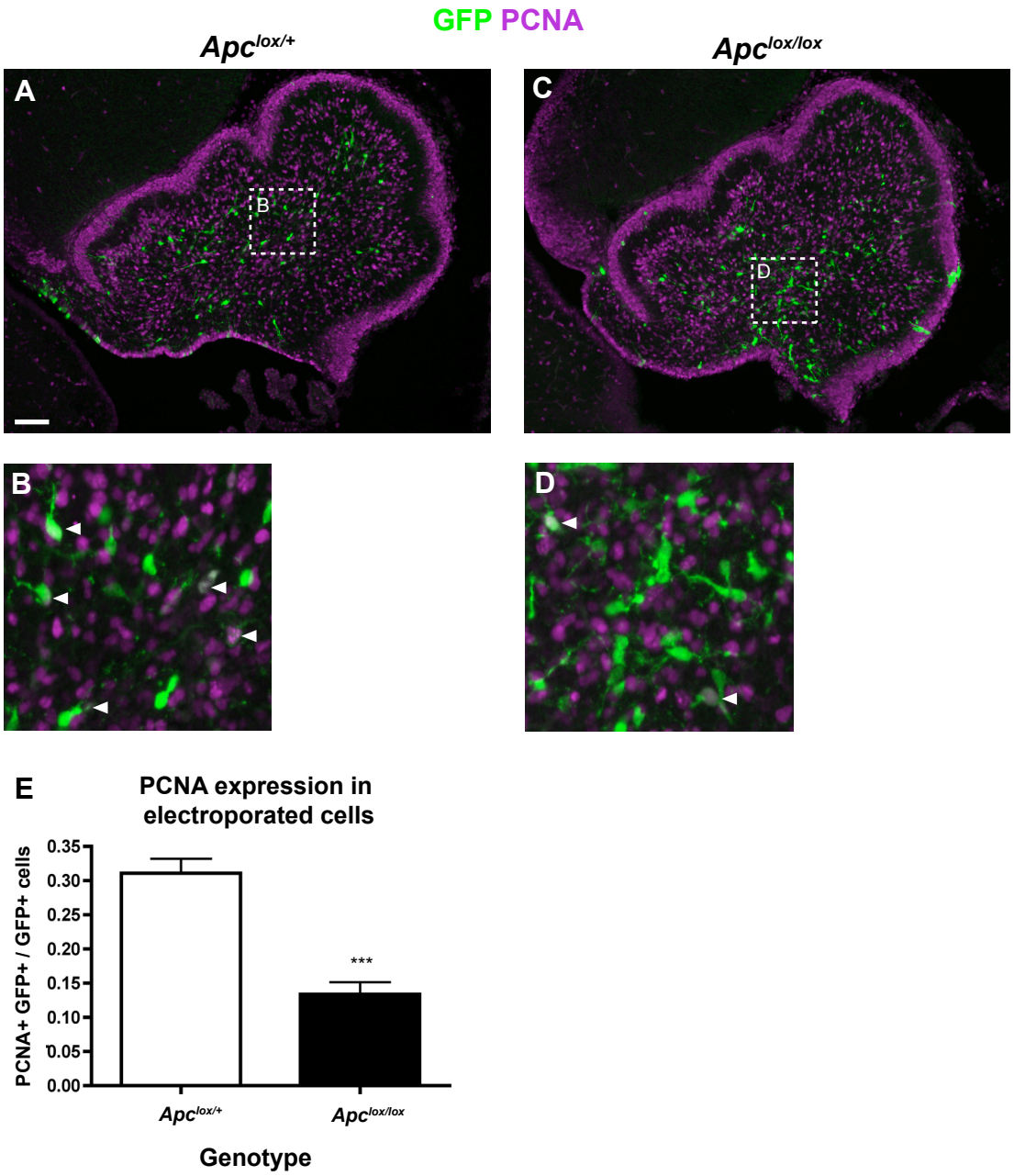

Figure 6.7 - Activation of Wnt/β-catenin signalling causes reduced proliferation in mutant cells at E18.5.
Embryos were injected with *Cre-GFP* plasmid at E13.5 and the expression of GFP and PCNA was compared between the $Apc^{lox/+}$ (A-B) and $Apc^{lox/lox}$ (C-D) cerebellum at E18.5. Quantitation of GFP+ cells also expressing PCNA (white arrows) is consistent with a reduction in proliferation of GFP+ cells in the $Apc^{lox/lox}$ cerebellum (E) (***=P<0.001, n=4, error bars = SEM). Scale bar = 100 μm.

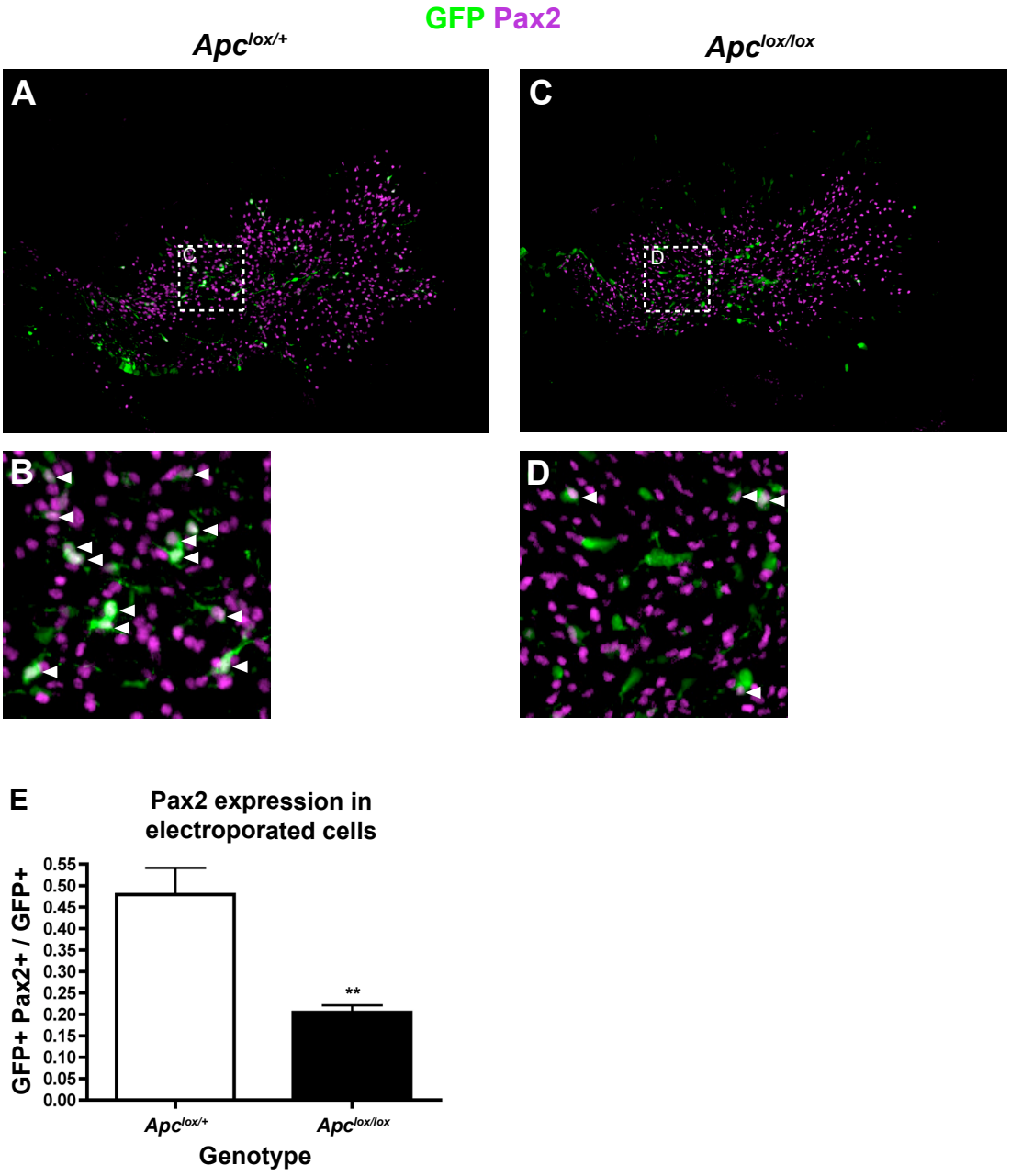

Figure 6.8 - Activation of Wnt/β-catenin signalling causes reduced Pax2 expression in mutant cells at E18.5.
Embryos were injected with *Cre-GFP* plasmid at E13.5 and the expression of GFP and Pax2 was compared between the $Apc^{lox/+}$ (A-B) and $Apc^{lox/lox}$ (C-D) cerebellum at E18.5. Quantitation of GFP+ cells also expressing Pax2 is consistent with a reduction in expression of Pax2 in GFP+ cells in the $Apc^{lox/lox}$ cerebellum (E) (** = P<0.01, n=4, error bars = SEM). Scale bar = 100 μm.

6.4.6 Activation of the Wnt/β-catenin pathway results in reduced expression of Sox9 in mutant cells

Sox9 is expressed by the VZ progenitors lining the fourth ventricle and those that have delaminated from the VZ into the WM (Kordes et al., 2005; Pompolo and Harley, 2001). It is also expressed in the cerebellar glial lineage (Kordes et al., 2005; Sottile et al., 2006). As *ex vivo* experiments revealed a reduction in Sox9 expression after activation of the Wnt/β-catenin signalling pathway (see Chapter 4), I sought to determine if this finding also applied *in vivo*.

Cerebellum sections were analysed by immunohistochemistry from E18.5 $Apc^{lox/+}$ (Fig. 6.9A-B) and $Apc^{lox/lox}$ (Fig. 6.9C-D) embryos electroporated with *Cre-GFP* plasmid at E13.5. Consistent with *ex vivo* data presented in Chapter 4, there was a reduction in Sox9 expression in the GFP+ cell population in $Apc^{lox/lox}$ embryos compared to $Apc^{lox/+}$ embryos. While 34.7% (±4.8%) of GFP+ cells in $Apc^{lox/+}$ embryos expressed Sox9, this was reduced to 6.3% (±0.2%) in $Apc^{lox/lox}$ embryos (Fig. 6.9E). In addition, non-quantitative analysis of GFP and Sox9 expression in the DHB revealed a similar finding. Clusters of GFP+ cells void of Sox9 expression were evident, despite the expression of Sox9 in the surrounding cells (Fig. 6.9F-G). These results support the conclusion that increased Wnt/β-catenin signalling in cells derived from the VZ and LRL has an inhibitory effect on the expression of Sox9.

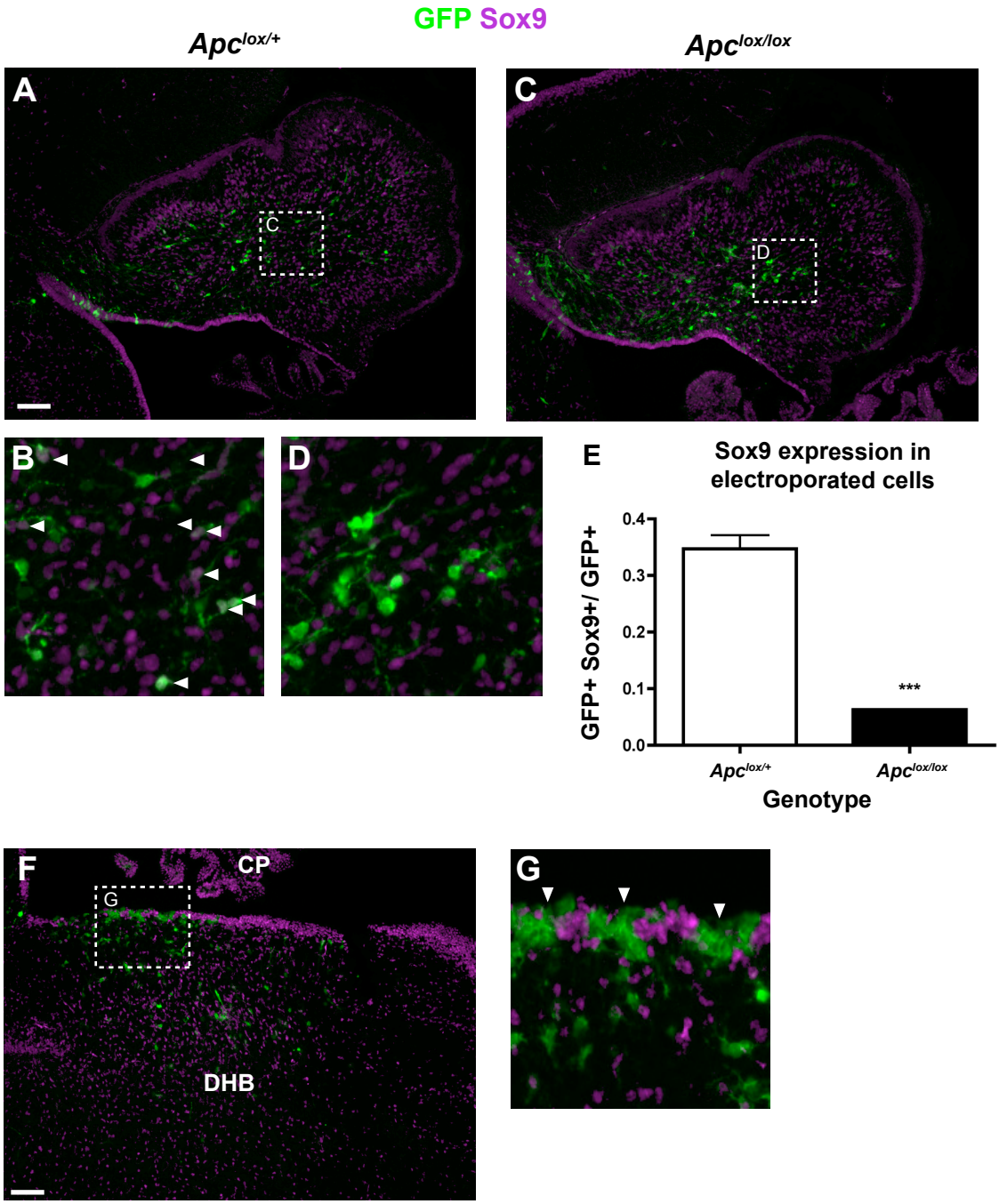

Figure 6.9 - Activation of Wnt/β-catenin signalling causes reduced Sox9 expression in mutant cells at E18.5.
Embryos were injected with *Cre-GFP* plasmid at E13.5 and the expression of GFP and Sox9 was compared between the $Apc^{lox/+}$ (A-B) and $Apc^{lox/lox}$ (C-D) cerebellum at E18.5. Quantitation of GFP+ cells also expressing Sox9 is consistent with a reduction in expression of Sox9 in GFP+ cells in the $Apc^{lox/lox}$ cerebellum (E).This phenomenon was also observed within GFP+ patches in the Sox9 expressing DHB domain (F-G, white arrows) (*** = P<0.001, n=4, error bars = SEM). Scale bar = 100 μm.

6.5 Discussion

In Chapters 3 and 4 I presented evidence for Wnt/β-catenin pathway activity during cerebellum development that, based on *ex vivo* data, potentially plays a role in development of the VZ-derived cerebellar lineages (interneurons and glia). Thus, the aim of the work presented in this chapter was to investigate the functional consequences of Wnt/β-catenin pathway activation *in vivo* during cerebellum development. To this end, I used mice with a floxed *Apc* allele and targeted a *Cre-GFP* encoding plasmid to cells lining the fourth ventricle using *in utero* electroporation early in development. The data presented in this chapter confirm the validity of this procedure in activating the Wnt/β-catenin pathway, and support the conclusions made in Chapter 4 that activated Wnt/β-catenin signalling affects the development of lineages from the VZ.

6.5.1 Electroporation in the E13.5 fourth ventricle successfully targets VZ and DHB progenitors

In utero electroporation has been demonstrated as an effective tool for precise spatio-temporal genetic modification of the developing cerebellum and DHB (Dipietrantonio and Dymecki, 2009; Gibson et al., 2010; Grimaldi et al., 2009; Kalinovsky et al., 2011; Kawauchi and Saito, 2008). Similar to the study performed by Grimaldi et al. (2009), I used *in utero* electroporation in order to target a mutation to the VZ of the developing cerebellum. However, I was also able to target the LRL and DHB with this technique by adjusting the orientation of the electrodes as described by Gibson et al. (2010). After electroporation of *Cre-GFP* encoding plasmid to the fourth ventricle of E13.5 embryos, widespread GFP expression was observed at E14.5 indicating the successful plasmid uptake and expression in cells lining the ventricle (Fig. 6.2A). At this time point GFP expression was observed along the length of the VZ and in a number of delaminated cells migrating from the VZ, in the CP and also within the DHB. This pattern was also observed in the E15.5 cerebellum (Fig. 6.2E). By E16.5 electroporation that had targeted the VZ (Fig. 6.3A) or DHB (Fig. 6.3B) resulted in a pattern of GFP expression consistent with cell migration from these two sites. Within the cerebellum GFP+ cells could be

observed spreading throughout the developing tissue from the VZ (Fig. 6.3A), while in the DHB cells could be observed lining the ventricle and migrating ventrally through the tissue (Fig. 6.3B). This was consistent with the pattern of GFP expression observed at E18.5, which demonstrated a well-dispersed GFP+ cell population from the VZ throughout the developing cerebellum (Fig. 6.4A). GFP expression was also evident at the DHB in the cells lining the ventricle and in ventrally migrating cells (Fig. 6.4C). In addition, GFP expression was observed within the PGN (Fig. 6.4E), suggesting DHB cells electroporated at E13.5 had since migrated to the PGN by E18.5.

An important point for consideration before judging the success of this technique is the level of consistency observed between electroporated embryos. Subtle differences in the plasmid injection and positioning of the electrodes for the subsequent electroporation can create considerable differences in plasmid uptake and GFP expression (Appendix 4-5). In order to circumvent the effects of this variability on further analysis, I undertook electroporations on a considerable sample size. A total of 284 individual embryos were electroporated, consisting of 44 for analysis at E14.5, 72 for analysis at E15.5, 62 for analysis at E16.5 and 106 for analysis at E18.5. From this pool of electroporated embryos, suitable consistency was obtained to minimise the effects of variability on further analysis.

An additional limitation of *in utero* electroporation observed is the level of efficiency achieved. Despite the high number of embryos electroporated, only 226 survived, giving an overall survival rate of 79.6%. From this, a minority of embryos demonstrated levels of GFP expression detectable under a dissection microscope. Of all the embryos injected, 25% analysed at E14.5, 18.1% at E15.5, 32.2% at E16.5 and 30.2% of embryos analysed at E18.5 were identified as GFP+. This gave a total electroporation efficiency rate of 26.8%. As above, I attempted to work around the relatively low survival rate and considerably lower efficiency rate of electroporated embryos by carrying out a high number of electroporations.

Limitations aside, the technique of *in utero* electroporation represents an effective tool for targeting mutations or labelling cells in a precise spatio-temporal manner during cerebellum development. By carrying out the procedure on a large number of embryos, and importantly by refining the technique over time, I was able to generate a pool of successfully electroporated embryos that demonstrated plasmid uptake in the cells surrounding the fourth ventricle and GFP expression in the cell lineages derived from them.

6.5.2 Electroporation of *Cre-GFP* plasmid DNA into $Apc^{lox/lox}$ embryos activated the Wnt/β-catenin signalling pathway after 72 hours

In order to identify cells where Wnt/β-catenin signalling had become activated, I looked for the ectopic nuclear localisation of β-catenin protein by immunohistochemistry in $Apc^{lox/lox}$ embryos. Interestingly, this was not observed at E14.5 (Fig. 6.2C-D) or E15.5 (Fig. 6.2G-H) after electroporation at E13.5. However, analysis at E16.5 revealed extensive ectopic expression of β-catenin within the electroporated VZ (Fig. 6.3C-E) and DHB (Fig. 6.3F-H). From these data I conclude that activation of the Wnt/β-catenin signalling pathway through Cre-recombinase mediated loss of a floxed *Apc* allele requires up to 72 hours in the developing cerebellum and DHB. This is consistent with previous findings that Cre mediated knockout of *Apc* in the cortex requires at least 48 hours for any effect to be observed (Ivaniutsin et al., 2009).

The reasons for this are unclear but could potentially be due to the chain of events required to take place between electroporation and Wnt/β-catenin pathway activation. Firstly, the plasmid must be taken into the cell where the Cre-recombinase then gets transcribed and translated. The identification of GFP+ cells at E14.5 indicates transcription and translation of the coding plasmid DNA does not take more than 24 hours. At this point the enzyme needs to locate the floxed DNA sequence and carry out recombination between the two sites – a process dependent on the efficiency of the enzyme. After this has been achieved the cytoplasmic levels of APC need to fall to a certain threshold to allow levels of β-catenin to reach a point where

translocation to the nucleus occurs. Thus, depending on the half-life of the APC protein itself, it is not unreasonable to assume that the concordant reduction and increase in cytoplasmic APC and β-catenin levels respectively are likely to be the key rate limiting steps for Wnt/β-catenin pathway activation to occur.

By E18.5 a widely dispersed GFP expression pattern was observed within the cerebellum and DHB. β-catenin immunohistochemitsry on this cell population revealed the maintenance of ectopic β-catenin expression indicating sustained Wnt/β-catenin pathway upregulation from E16.5. Analysis of high magniication images taken from the VZ and DHB of 10 $Apc^{lox/lox}$ embryos revealed that 82% (±6.2%) of GFP+ (i.e. electroporated) cells also expressed detectable levels of nuclear β-catenin. Thus, while it is evident that a majority of GFP+ cells were mutant in terms of Wnt/β-catenin pathway activation, not all of the electroporated cells were. The competency of cells to respond to a Wnt/β-catenin signal, and the efficiency of the Cre enzyme are two potential explanations for this result.

The ability of a cell or tissue to respond to particular external signals has long been recognised as an important mechanism for generating a heterogeneous cell population from relatively few inductive signals (Waddington, 1940). Thus, it is possible that in the cerebellum or DHB not all cells have the capacity to respond to the loss of *Apc* in the same way. However, the specific factors that could be contributing to this heterogeneity remain to be defined. Secondly, the efficiency of the Cre-recombinase enzyme itself is also likely to affect the proportion of electroporated cells that activate the Wnt/β-catenin pathway. Cre-recombinase efficiency in this case is unknown, but it is possible that it does not successfully recombine the floxed *Apc* allele in 100% of cells it is produced in. These confounding factors aside, the evidence presented in this chapter still suggests that a majority of $Apc^{lox/lox}$ cells electroporated with Cre-recombinase do respond by eventually activating the Wnt/β-catenin signalling pathway. Having established this, I next sought to determine what the effects of this pathway activation were on development of the cerebellum and DHB.

6.5.3 Effects of *in vivo* Wnt/β-catenin pathway activation on migration and proliferation of VZ derived cell lineages at E18.5

The work presented in Chapters 3 and 4 suggests a potential role for Wnt/β-catenin signalling in development of VZ derived cell lineages. However, there is little published evidence to support this and to allow further hypotheses on the specific function to be generated. Gibson et al. presented the only published study that attempts to dysregulate Wnt/β-catenin signalling in VZ derived cells but did not observe any effects (Gibson et al., 2010). Thus, it was not immediately clear what the effects of Wnt/β-catenin pathway activation would be in these cells after Cre-induced loss of *Apc*. However, based on the various cellular processes known to be controlled by Wnt/β-catenin signalling I would have hypothesised that effects on migration and proliferation of the VZ cell lineages could arise.

APC is known to be an important regulator of cell migration through the Wnt/β-catenin pathway in the context of intestinal epithelia (Sansom et al., 2004). APC has also been long established as a regulator of neuronal migration in a Wnt-independent manner (Näthke et al., 1996). These studies suggest that either through Wnt/β-catenin signalling or not, loss of *Apc* would impair migration of the electroporated cells from the VZ. However, comparison of GFP expression between $Apc^{lox/+}$ and $Apc^{lox/lox}$ embryos did not reveal any gross differences in the extent electroporated cells had migrated through the developing cerebellum (Fig. 6.4A-B). Interestingly, a number of GFP+ cell clusters were observed in Apc^{loxlox} embryos that were not evident in any $Apc^{lox/+}$ embryos, which could be suggestive of a migratory or adhesion defect in some cells. Ultimately though, the variability between electroporated embryos did not allow for a quantitative comparison in cell migration between the two genotypes and further work using a different *in vivo* model would be required to more thoroughly test the effects of Wnt/β-catenin pathway activation on migration of VZ derived cell lineages.

Wnt/β-catenin signalling is known to drive proliferation in certain contexts (Giraldez and Cohen, 2003; He et al., 1998; Megason and McMahon, 2002; Shtutman et al.,

1999; Yamaguchi et al., 1999) and the results presented in Chapter 4 suggest that activation of the pathway in cerebellar slice culture promotes proliferation. However, comparison of PCNA expression in the GFP+ cell population revealed a reduction in $Apc^{lox/lox}$ embryos compared to $Apc^{lox/+}$ embryos, suggesting that activation of the Wnt/β-catenin pathway in this context has an inhibitory effect on proliferation. Interestingly, Gibson et al. did not observe any change in proliferation after activation of β-catenin in their *Blbp-Cre* mouse model. However, it is important to note that the markers used to detect proliferation were different (BrdU label retention compared to PCNA expression used here) and the nature of the mutation was different. Importantly though, Gibson et al. limited their analysis to the VZ monolayer only and not the mutant VZ-derived cells within the cerebellum. Thus, it is possible that the reduction in PCNA expression identified here represents a reduction in the proliferation or premature cell cycle exit of progenitors that have delaminated from the VZ monolayer.

One confounding limitation is the observation that total numbers of GFP+ cells within the cerebellum does not differ between the two genotypes. One could hypothesise that the reduction in proliferation of electroporated cells observed in $Apc^{lox/lox}$ embryos should result in fewer GFP+ cells being present. However, this was not evident. It is possible that the reduction in proliferation had not manifest in a significant reduction in the GFP+ population over the developmental window used for these experiments. That is, the time from detectable Wnt/β-catenin pathway activation (E16.5) to this analysis (E18.5) may not have been sufficient to allow the reduction in proliferation identified through PCNA expression to have an effect on the total pool of GFP+ cells. A longer chase after the electroporation would therefore be required to test this.

6.5.4 Effects of *in vivo* Wnt/β-catenin pathway activation on the expression of VZ derived cell lineage markers at E18.5

The data presented in Chapter 4 supports the hypothesis that activation of the Wnt/β-catenin pathway in the E18.5 cerebellum, *ex vivo* at least, causes a reduction in the expression of interneuron and astrocyte lineage markers Pax2 and Sox9 respectively,

suggesting a potential dysregulation of cell lineages generated at the VZ. Thus, after electroporation of *Cre-GFP* plasmid to the cerebellum of $Apc^{lox/lox}$ mice I hypothesised that the electroporated cells would display a similar reduction in the expression of these two markers. Consistent with this, the expression of both Pax2 (Fig. 6.8) and Sox9 (Fig. 6.9) in GFP+ cells was significantly reduced in $Apc^{lox/lox}$ compared to $Apc^{lox/+}$ embryos. These findings suggest that, while the generation and migration of GFP+ cells from the VZ appears to be relatively unaffected, activated Wnt/β-catenin signalling in these cells could be driving a transcriptional change that appears to be consistent with an altered cell fate. Parallels can be drawn between this conclusion and the established role of Wnt/β-catenin signalling in regulation of the self renewal and differentiation of cell lineages arising from radial glia during cortical development (Chenn and Walsh, 2002; Hirabayashi et al., 2004; Munji et al., 2011; Zhou et al., 2006). However, further modelling of Wnt/β-catenin pathway activation and inhibition at the VZ during cerebellum development is now required to test this further.

6.5.5 Effects of *in vivo* Wnt/β-catenin pathway activation on LRL derived cell lineages at E18.5

While trying to establish the developmental origins of medulloblastoma, Gibson et al. revealed that activated Wnt/β-catenin signalling in the LRL during development resulted in impaired migration of LRL-derived neurons and the resulting formation of preneoplastic lesions on the surface of the DHB (Gibson et al., 2010). As *in utero* electroporation has been previously shown to successfully target plasmid uptake to the LRL (Dipietrantonio and Dymecki, 2009; Gibson et al., 2010; Kalinovsky et al., 2011; Kawauchi et al., 2006), this presented an opportunity to undertake a complementary analysis of the effects of Wnt/β-catenin pathway upregulation by targeting the *Cre-GFP* plasmid to the LRL of $Apc^{lox/lox}$ embryos.

After *Cre-GFP* plasmid electroporation targeted to the LRL and DHB at E13.5, GFP+ cells were evident persisting within the LRL, spread through DHB and in the LRL-derived neurons of the PGN by E18.5 in both $Apc^{lox/+}$ and $Apc^{lox/lox}$ embryos (Fig. 6.4). Interestingly, and consistent with the findings from Gibson et al., the LRL

in *Apc*$^{lox/lox}$ embryos appeared to retain more GFP expression compared to the *Apc*$^{lox/+}$ embryos which showed a more dispersed pattern of GFP expression through the DHB. In addition, while GFP was observed in the PGN of both genotypes, suggesting that differentiation and migration of PGN neurons from the LRL had taken place, there was no detectable nuclear expression of β-catenin within the GFP+ cell population in the *Apc*$^{lox/lox}$ PGN (Fig. 6.6). This is consistent with the normal development of a population of electroporated cells expressing GFP but - for reasons alluded to above - not showing evidence for *Apc* recombination having taken place. Furthermore, the identification of clusters of GFP+ cells within the DHB that did not express Sox9 (Fig. 6.9F-G), even though the DHB is a Sox9 expression domain, suggests that Wnt/β-catenin pathway activation may be having a similar transcriptional effect to that observed in the VZ-derived cells within the cerebellum.

Ultimately, while some evidence from these experiments supports the findings from Gibson et al., the technique and subsequent analysis was insufficient to test the hypothesis thoroughly. The aforementioned variability between electroporated embryos, and the ability to only target a small percentage of the total LRL cell population likely precluded the ability to detect obvious changes similar to those observed by Gibson et al.

6.5.6 Summary

Combined, the data presented here builds on the findings from previous chapters. I have demonstrated that the technique of *in utero* electroporation can be successfully used to activate the Wnt/β-catenin signalling pathway in the developing cerebellum. After activation of the pathway in a subset of cells within the VZ at E16.5, subsequent defects are observed in proliferation of the cells derived from the VZ along with a reduction in expression of interneuron and glial lineage markers Pax2 and Sox9. In addition, a potential migratory defect was observed in electroporated cells within the LRL. These data provide validation to extend this work to a further *in vivo* analysis of the effects of activated Wnt/β-catenin signalling in cells derived from the VZ and LRL.

7 Final discussion

7.1 Summary of findings presented in this thesis

The work presented in this thesis encompasses a descriptive analysis of Wnt/β-catenin signalling pathway activity throughout cerebellum development and a functional investigation into its role. Here I discuss the results presented in the context of the aims outlined in Chapter 1.

7.1.1 Wnt/β-catenin signalling activity is present transiently in discrete progenitor populations during cerebellum development

In order to investigate the dynamics of Wnt/β-catenin signalling activity during cerebellum development, I utilised mice carrying a BAT-gal Wnt reporter allele (Maretto et al., 2003). As discussed in Chapter 3, the complexities of the Wnt/β-catenin signalling pathway, particularly the context specificity of the transcriptional response, poses difficulties for using endogenous reporters of the pathway. Thus, the BAT-gal transgenic reporter allele, despite its limitations (Barolo, 2006), presents a useful tool for generating an informative preliminary data set on the activity of the Wnt/β-catenin signalling pathway in an unknown system.

The early cerebellum contains three domains important to its future development: the IsO, the VZ and the RL. The IsO is specified first (around E7.5) at the MHJ as a gene expression boundary and maintains a self-regulating gene expression circuit that provides the inductive cues for the development of the surrounding tissue. Following the establishment of this centre, the early cerebellar cell lineages are then generated from around E10.5 from the VZ, which extends caudally from the IsO lining the dorsal aspect of the fourth ventricle, and the RL, which is a transient region forming the interface between the most caudal aspect of the VZ and the roof plate (Fig. 1.4). Consistent with published findings that demonstrate the function of Wnt1 as a key IsO signalling factor (McMahon and Bradley, 1990; McMahon et al.,

1992; Thomas and Capecchi, 1990), I have identified expression of the BAT-gal reporter allele in this region from E12.5 onwards supporting the conclusion that Wnt1 in this event is likely signalling through the Wnt/β-catenin pathway (Lancaster et al., 2011). From this point, the expression of the BAT-gal begins to regress with the diminishing activity of the IsO as a functional signalling centre.

The RL is a transient germinal centre that can be divided into two domains, the URL to the anterior and the LRL to the posterior. While the former generates all glutamatergic cell lineages in the cerebellum from E10.5, the lower generates neurons of the various pre-cerebellar nuclei that reside in the HB. Expression of the BAT-gal reporter in both these domains at E12.5 and E14.5 supports a role for Wnt/β-catenin signalling in development of the cell lineages that arise from there. This is consistent with the identification of Wnt1 and Wnt3a expression in both the URL and LRL (Davis and Joyner, 1988; Dymecki and Tomasiewicz, 1998; Fischer et al., 2007; Louvi et al., 2007; Nichols and Bruce, 2006; Wilkinson et al., 1987). The pattern of BAT-gal reporter expression observed from E12.5-E14.5 at the URL is consistent with the specification and early migration of GPCs. While this could overlap with the DCN neurons (which are born up until E12.5), the lack of BAT-gal expression within the SPS supports the conclusion that this cell lineage is not responding to a Wnt/β-catenin signal. By E18.5 a striking reduction of BAT-gal expression was evident within the newly formed EGL, suggesting that while Wnt/β-catenin signalling was active during the specification of GPCs, it is not involved in their continued expansion. This is consistent with numerous lines of evidence that conclude expansion of the GPC population within the EGL occurs in response to alternative signalling pathways (Dahmane and Ruiz i Altaba, 1999; Dakubo et al., 2006; Solecki et al., 2001; Wechsler-Reya and Scott, 1999).

Illustrating the well-established dynamic nature of Wnt/β-catenin signalling during development, the VZ, which was void of BAT-gal reporter expression at E12.5 and E14.5, demonstrated a considerable induction of the reporter from E18.5 onwards. The VZ is the birth place of GABAergic neurons and glia for the cerebellum. From E10.5 to E14.5 the VZ generates GABAergic DCN neurons, PCs, Bergmann glia and

an early cohort of Pax2+ interneuron progenitors. From this point on, the VZ shifts solely to the production of interneurons and astrocytes, both of which derive from progenitors that delaminate from the VZ and multiply in the WM (Leto et al., 2006; Milosevic and Goldman, 2002; Milosevic and Goldman, 2004; Sudarov et al., 2011; Zhang and Goldman, 1996). However, the potency of these progenitors is not yet established (i.e. whether or not the interneuron and glial lineages arise from two separate pools of WM progenitors or if they arise from asymmetric division within a single progenitor pool). The observation of BAT-gal reporter expression along the VZ and within the developing cerebellar anlage during the perinatal time points would be consistent with its expression in multipotent progenitors or a lineage restricted population. Double immunofluorescence at this time point between β-gal and Pax2 or Sox9, which labels interneurons and progenitors/glia respectively, ruled out the presence of β-gal expression within lineage-restricted interneurons (Fig. 3.5). Due to the fact Sox9 is expressed in both multipotent progenitors and the glial lineage, I am unable to determine if the β-gal+ cells observed in the cerebellum at this time point represents a multipotent progenitor population, a glial restricted population or both. Given the recent identification of a multipotent cerebellar stem cell population that persists throughout adulthood (Lee et al., 2005), it is tempting to speculate that Wnt/β-catenin signalling could be somehow involved.

Analysis at later time points revealed that expression of the BAT-gal reporter was sustained until P21 in a progressively restricted pattern consistent with the Bergmann glia. Double immunofluorescence with Sox9 and s100β within the PCL confirmed this (Fig. 3.7,9,11). This is interesting given the findings that Bergmann glia are born at the VZ shortly following the PCs and closely follow their migration (Sudarov et al., 2011; Yamada and Watanabe, 2002). The observations presented here, that the BAT-gal reporter is not expressed within the VZ at E14.5 but is expressed within the developing cerebellum from E18.5 onwards are consistent with Bergmann glia activating a response to the Wnt/β-catenin signalling pathway after their birth and during their subsequent migration and maturation and/or the additional birth of subsequent Bergmann glia from a population of WM progenitors.

7.1.2 A possible role for Wnt/β-catenin signalling in development of glial and interneuron lineages from the VZ

Based on the findings from analysis of BAT-gal Wnt/β-catenin reporter expression during the late embryonic and early postnatal time points, I hypothesised a potential role for the pathway in development of the glial lineage from progenitors at the VZ and within the WM. Numerous lines of evidence suggest Wnt/β-catenin signalling plays a role in regulating the proliferation, self-renewal and differentiation of radial glia within the developing cortex (Chenn and Walsh, 2002; Hirabayashi et al., 2004; Ivaniutsin et al., 2009; Munji et al., 2011; Zhou et al., 2006) so it is not unreasonable to anticipate a similar mechanism occurring within the developing cerebellum. However, there are considerable limitations to our knowledge of cerebellum progenitor activity compared to the comparatively well-characterised system in the cortex, which makes comparison difficult.

In order to test this hypothesis and to investigate the function of Wnt/β-catenin signalling during cerebellum development, I took both an *ex vivo* and *in vivo* approach to constitutively activate the pathway and characterise the effects on generation of cell lineages derived from the VZ. Using a GSK3β inhibitor to constitutively activate the Wnt/β-catenin signalling pathway *ex vivo* in slices of E18.5 cerebellum revealed that, while cell death was unaffected, a reduction in the expression of interneuron lineage marker Pax2 and, strikingly, the progenitor/glial markers Sox9 and GFAP (Fig. 4.8,9,10). Interestingly, the reduction in Pax2 was limited to the distal regions of the slice, while the reduction in Sox9 and GFAP was considerably more widespread and to a much greater extent – as revealed through both immunohistochemistry and qRT-PCR. In order to investigate this further, I carried out genetic activation of the Wnt/β-catenin signalling pathway *in vivo* during cerebellum development. By electroporating a *Cre-GFP* expressing plasmid into the VZ of $Apc^{lox/lox}$ embryos at E13.5 I was able to induce constitutive Wnt/β-catenin signalling in a subset of VZ-derived cells. Consistent with the effects observed after pathway activation *ex vivo*, embryos analysed at E18.5 (five days after electroporation and two days after activation of the pathway was observed) displayed

a reduction in the expression of Pax2 and Sox9 in the electroporated cells. Importantly, these results suggest that activating the Wnt/β-catenin signalling pathway did not force the balance of interneuron or glial generation from a single multipotent progenitor pool in any one direction. This is in contrast to the observation of BAT-gal reporter expression exclusively in the Sox9 and s100β expressing population, which would suggest a role in glial development.

Taking into consideration the activity of the Wnt/β-catenin pathway observed through expression of the BAT-gal reporter, and the effects on VZ-derived lineage marker expression after constitutive activation both *ex vivo* and *in vivo*, I propose a model where the Wnt/β-catenin pathway could regulate multiple steps in the progression from VZ radial glia to fully differentiated interneurons and astrocytes (Fig. 7.1). Firstly, the observation made in Chapter 3 that BAT-gal reporter expression is expressed from the VZ and within the developing cerebellum by E18.5 in an exclusively Sox9+ cell population suggests a potential role in the development of a VZ-derived cell lineage. Furthermore, the observation that BAT-gal reporter expression is maintained at levels detectable by immunohistochemistry through until P21 in a cell population that becomes progressively restricted to the Bergmann glia would be consistent with the hypothesis that Wnt/β-catenin signalling is involved in the development and maturation of this cell lineage. While little evidence exists to support this, a recent study by Wang et al. (2011) has demonstrated that dysregulation of Wnt/β-catenin signalling in Bergmann glia is associated with a disruption in their morphology and cerebellar localisation. Given this finding, it might be assumed that activation of the Wnt/β-catenin signalling pathway during development would promote the generation of glia from VZ or WM progenitors. However, *ex vivo* and *in vivo* activation of the pathway by inhibiting GSK3β or APC respectively resulted in a quantifiable reduction in the expression of glial markers Sox9 and GFAP, in addition to a reduction in interneuron marker Pax2. These data would be consistent with experimental manipulation of the pathway blocking the differentiation of VZ-derived progenitors into either lineage and instead promoting a modified cell fate – either increased self-renewal of a progenitor population of differentiation into an alternative cell lineage.

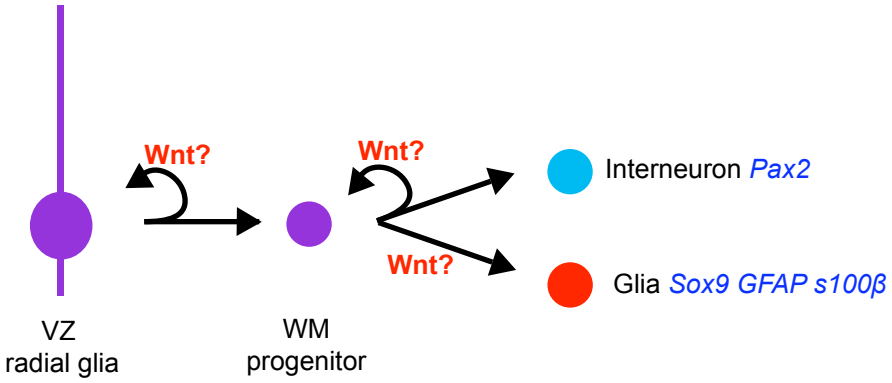

Figure 7.1 - Model for Wnt/β-catenin signalling function in development of cell lineages from the VZ.
Based on the observations that Wnt/β-catenin activity was observed in the developing glial population and that constitutive activation of the pathway led to a reduction in the expression of Sox9 and Pax2 *in vivo* I propose a model whereby multiple steps in the progression from VZ radial glia to fully differentiated interneurons and glia could be regulated by Wnt/β-catenin activity. The observation of Wnt/β-catenin activity in the Bergmann glia population suggests a potential role in maturation of this cell population. In addition, the reduction in expression of both interneuron and glial markers after pathway deregulation would be consistent with an additional role in promoting stem/progenitor cell self-renewal.

7.1.3 Contribution of activated Wnt/β-catenin signalling to the aetiology of medulloblastoma

The final aim of this thesis was to reconcile the descriptive and functional analyses of Wnt/β-catenin signalling with a potential hypothesis for the aetiology of medulloblastoma. While a subset of medulloblastomas with activated Wnt/β-catenin signalling is well defined (Ellison et al., 2005; Kool et al., 2008; Schwalbe et al., 2011; Thompson et al., 2006), a potential developmental origin of this class of disease has only recently been identified (Gibson et al., 2010). It has been hypothesised in the past that, as opposed to the induction of Shh subtype medulloblastoma within the EGL, the Wnt subtype arises from the dysregulation of development at the VZ (Gilbertson and Ellison, 2008). Consistent with this hypothesis, I have observed the activation of Wnt/β-catenin signalling within the VZ and in cell lineages arising from there in a temporally regulated manner. The observations made here that constitutive activation of the pathway in these cells leads to changes in proliferation and expression of cell fate markers is consistent with activated Wnt/β-catenin signalling promoting a number of phenotypic changes to these cells that could potentially induce a neoplastic progression.

This hypothesis is at odds with recent findings by Gibson et al. (2010), who propose that the Wnt molecular subtype of medulloblastom arises from a migration defect arising in the LRL progenitors. The observations made in Chapter 3 that the BAT-gal reporter and downstream Wnt target gene *Axin2* are both expressed in the LRL support the conclusion that Wnt/β-catenin signalling is a developmental regulator for this region. The further observation in Chapter 6 that LRL $Apc^{lox/lox}$ cells electroporated with a *Cre*-expressing plasmid tend to cluster on the DHB surface and do not migrate to the PGN is consistent with similar observations made by Gibson et al. (2010). However, as discussed in Chapter 1, the results presented in this study fall short of conclusively excluding the potential for medulloblastoma from other germinal centres and thus further clarification is required in order to reconcile the results presented in this thesis with those of Gibson et al. (2010).

7.2 Future directions

The limited scope of the work presented in this thesis and the assumptions made in my proposed model have generated a number of questions that need to be addressed in order to more convincingly appreciate the role Wnt/β-catenin signalling plays in development of the cerebellum and to more conclusively test the ideas proposed for the developmental origins of Wnt subtype medulloblastoma.

7.2.1 Further descriptive analysis of Wnt/β-catenin signalling during cerebellum development

The data presented in Chapter 3 represents a descriptive analysis of Wnt/β-catenin activity throughout cerebellum development. This information has not been described previously and thus presents a novel set of pilot information on which to build a more thorough analysis. Firstly, although the laminar structure of the cerebellum is homogenous throughout, analysis of gene expression and input/output fibre organization reveals additional levels of cerebellar organization (Sillitoe and Joyner, 2007). A number of molecules are known to be expressed in distinct parasagittal domains in the adult cerebellum, most notable among these is the aldolase ZebrinII (Brochu et al., 1990), which is expressed by PCs and displays a characteristic zebra-like pattern of sagittal stripes on the surface of the cerebellum. The development of this organization is known to take place during the first two postnatal weeks and has been linked to the developmental regulator En2 (Millen et al., 1995). As an abundance of BAT-gal reporter expression has been observed in the cerebellum during this early postnatal time point, a logical progression would be to determine a more accurate spatial map of its expression across the anterior-posterior and medial-lateral axes, paying particular attention to the possibility of its expression in parasagittal domains. This would allow the potential role of Wnt/β-catenin signalling in the development of the cerebellar circuitry to be explored.

In addition to a more precise spatial analysis of Wnt/β-catenin activity during cerebellum development, a quantitative analysis on the extent of BAT-gal reporter expression over time would allow further conclusions on the temporal nature of

Wnt/β-catenin pathway activity to be generated. From the data presented in Chapter 3 it is clear that the extent of BAT-gal expression reduces over time, though it is not clear at what point expression peaks and how fast it ceases after that point. A combination of immunohistochemistry and quantitative qRT-PCR should address this adequately.

In order to probe the mechanism of Wnt/β-catenin pathway activity further, I propose an additional line of experiments examining the extent of Wnt ligand and Fz receptor expression over a developmental time course, similar to that undertaken by Yaguchi et al. describing the spatiotemporal expression pattern of different FGF genes during cerebellum development (Yaguchi et al., 2009). There are 19 different Wnt ligands and 10 Fz receptors, all of which have been associated with different processes and diseases (Logan and Nusse, 2004). Importantly, a number of Wnt ligands (e.g. Wnt5A) are thought to signal through β-catenin independent pathways. The RT-PCR analysis of Wnt ligand expression presented in Chapter 3 is a starting point for this analysis.

Lastly, insight into the downstream mechanism of the pathway could be achieved through a transcriptional investigation into the Wnt responding cells identified at the different time points during development. Use of a fluorogenic LacZ substrate can be used to isolate live LacZ+ cells for subsequent sorting and transcriptional profiling after dissociation of the cerebellum at defined points in development. This experiment would add an important dimension of information to the identification of active Wnt/β-catenin signalling already observed during development.

7.2.2 Determining the cell fate of Wnt responding cells during cerebellum development

One of the key findings from the data presented within this thesis is the identification of Wnt/β-catenin signalling in the RL and VZ, both defined germinal centres, at different points during development. While the data presented in Chapter 3 would suggest that the pathway is playing a role in the specification of GPCs within the RL and in development of the glial lineage from the VZ, a fate mapping approach would

offer definitive evidence for the fate of the cells responding to the Wnt/β-catenin signal in these germinal centres. This approach has been demonstrated previously using a Cre recombinase driven by a specific Wnt gene (Dymecki and Tomasiewicz, 1998; Louvi et al., 2007; Rodriguez and Dymecki, 2000) to activate a reporter gene such as *LacZ*. However, the limitation of these studies is that all cells expressing the Cre throughout development will become labelled. Alternatively, genetic inducible fate mapping provides a method for tracing the development of cells that express a known marker at a particular point in time (Joyner and Zervas, 2006). In short, engineering a Wnt-specific inducible Cre would allow for only the cells expressing the Cre during the period of induction to activate reporter expression and thus the temporal generation of different cell lineages from these germinal centres could be characterised. This would be particularly advantageous in determining the potency of the Wnt/β-catenin responsive cells at the VZ (i.e. are they able to generate both interneurons and glia or is the expression of the Wnt reporter limited to a glial restricted progenitor?).

7.2.3 Clarification of Wnt/β-catenin function by reduction of signalling activity during development.

In order to fully characterise the function of Wnt/β-catenin signalling during cerebellum development, an investigation into the effects of spatiotemporal inhibition of the pathway needs to be carried out. In Chapter 4 and 6 I presented data that suggests a possible link between the Wnt/β-catenin signalling pathway and development of VZ-derived cell lineages, potentially in the form of progenitor cell regulation (Fig. 7.1). Analysing the effects of Wnt/β-catenin pathway inhibition in the same model systems would test the validity of these results and provide further evidence into the function of Wnt/β-catenin signalling during development.

As an extension from the work presented here, two key experiments can be undertaken. Firstly, an optimisation of the *ex vivo* culture conditions to allow adequate time for a Wnt/β-catenin pathway inhibitor to take effect would allow the effects of inhibition in this system to be investigated. The key observation from

activation of the pathway in this system was the striking reduction in Sox9 and GFAP expression, thus I would hypothesis that inhibition of the pathway would cause the opposite effect – an increase in Sox9/GFAP expression. A rescue experiment could also be attempted, where a pathway inhibitor is added to the culture after treatment with an activator. Secondly, the effects of pathway activation observed *in vivo* after electroporation of a *Cre* expressing plasmid into the fourth ventricle of $Apc^{lox/lox}$ embryos could be validated by additional electroporation experiments where a dominant-negative *Tcf* expressing plasmid (Tetsu and McCormick, 1999) is administered. Again, based on the observations made in Chapter 6, I would hypothesis that an inhibition of the pathway in this manner would result in an increase in Sox9 expression.

While these experiments would provide a valuable data set for the interpretation of data presented in this thesis, an inducible *in vivo* system would provide a more thorough analysis of Wnt/β-catenin pathway inhibition during cerebellum development. A number of different Cre alleles have been described with activity in different progenitor populations during cerebellum development, including *Math1-Cre* expressed in the RL (Matei et al., 2005), *Ptf1a-Cre* expressed in the VZ (Yamada et al., 2007), and *Nestin-* , *Blbp-* and *GFAP-Cre* transgenes expressed in a wider pool of progenitors comprising the RL and VZ (Carlén et al., 2006; Hegedus et al., 2007; Marino et al., 2000). To carry out genetic inhibition of the Wnt/β-catenin signalling pathway, I would propose using the *Ptf1a-Cre* in order to target the VZ. However, suitable candidate genes to target with LoxP mediated recombination in order to inhibit the pathway without affecting other cellular functions are few. In addition, targeting specific Wnt ligands for mutation would be dependent on a better understanding of which ligands are expressed during cerebellum development. An alternative would be to use viral mediated introduction of a specific pathway inhibitor such as dominant-negative *Tcf* (Tetsu and McCormick, 1999). This approach would allow precise temporal inhibition of the pathway, but would be spatially limited to the VZ monolayer. Ultimately, the hypothesis that Wnt/β-catenin regulates the generation of cell lineages from the VZ requires an analysis of this nature to be tested appropriately.

7.2.4 Extended analysis on the effects of Wnt/β-catenin constitutive activation in different cell lineages during cerebellum development

In order to extend the functional characterisation of Wnt/β-catnein signalling in cerebellum development and to investigate the developmental origins of Wnt subtype medulloblastoma further, a more detailed analysis into the effects of pathway activation on development of VZ-derived cell lineages needs to be carried out. The data presented in Chapters 4 to 6 demonstrate a potential role for Wnt/β-catenin signalling in the development of VZ-derived cell lineages and the hypothesis from this is that dysregulation of the VZ progenitors could contribute to tumourigenesis. Unlike inhibition of the pathway, conditional genetics presents a readily available tool in this case.

Several studies have been reported investigating the effects of Wnt/β-catenin pathway activation in different progenitor populations during cerebellum development. Most notably the recent studies by Lorenz et al. (2011) and Gibson et al. (2010) that used a combination of floxed *Apc* or constitutively active β-catenin alleles targeted by *Math1-* or *Blbp-Cre* tansgenes. However, neither of these studies utilised inducible *Cre* alleles, meaning there was limited temporal control over the induction of the mutation. In addition, the results from these studies do not reconcile with each other. In particular, the long term analysis of VZ-derived cells that were subject to constitutive Wnt/β-catenin signalling was not carried out by Gibson et al. (2010). Importantly, activation of Wnt/β-catenin signalling through loss of APC in Bergmann glia (a VZ-derived cell lineage) resulted in progressive degeneration during postnatal life (Wang et al., 2011), suggesting there are long term effects to the mutation. Thus, I propose using an inducible Cre recombinase to target constitutive activation of the Wnt/β-catenin signalling pathway to the VZ at defined developmental stages. These experiments would offer additional insight into the role Wnt/β-catenin signalling plays in the aetiology of medulloblastoma and help to clarify the findings of the small number of studies that have so far investigated this question.

7.3 Concluding remarks

The development of highly complex structures such as the CNS relies on the precisely coordinated spatiotemporal activity of different developmental signalling pathways. While a number of different pathways are known to regulate various processes in cerebellum development, the role of Wnt/β-catenin signalling has not yet been fully explored. Importantly, ectopic activation of the pathway predisposes to a well-defined subtype of medulloblastoma. Based on observations made in other tissues, there is a clear link between a role for Wnt/β-catenin signalling in stem/progenitor cell regulation and its dysregulation in cancer. Thus, I hypothesised that Wnt/β-catenin signalling is involved in cerebellum development and that dysregulation of its normal function contributes to medulloblastoma. Utilising a transgenic Wnt reporter I have shown a highly dynamic pattern of Wnt/β-catnein activity in defined cell lineages during cerebellum development, including two key progenitor populations within the RL and VZ – supporting a role for Wnt/β-catenin signalling as a developmental regulator in the cerebellum. Functional investigation revealed a potential link with the developing glial and interneuron lineages from the VZ, though further work is now required in order to more accurately determine the extent and nature of Wnt/β-catenin activity during cerebellum development and to clarify its function in the different cell lineages. While a mechanism for the pathogenesis of Wnt/β-catenin induced medulloblastoma still eludes us, a better understanding of the role the pathway plays in development will reveal how dysregulation of its function contributes to cancer.

8 Bibliography

Aberle, H., Bauer, A., Stappert, J., Kispert, A. and Kemler, R. (1997). beta-catenin is a target for the ubiquitin-proteasome pathway. *EMBO J*. **16**, 3797-804.

Adams, K. A., Maida, J. M., Golden, J. A. and Riddle, R. D. (2000). The transcription factor Lmx1b maintains Wnt1 expression within the isthmic organizer. *Development* **127**, 1857-67.

Al Alam, D., Green, M., Tabatabai Irani, R., Parsa, S., Danopoulos, S., Sala, F. G., Branch, J., El Agha, E., Tiozzo, C., Voswinckel, R. et al. (2011). Contrasting Expression of Canonical Wnt Signaling Reporters TOPGAL, BATGAL and Axin2 during Murine Lung Development and Repair. *PLoS ONE* **6**, e23139.

Alder, J., Cho, N. K. and Hatten, M. E. (1996). Embryonic precursor cells from the rhombic lip are specified to a cerebellar granule neuron identity. *Neuron* **17**, 389-99.

Altman, J. and Bayer, S. A. (1997). Development of the Cerebellar System in Relation to its Evolution, Structure, and Functions. New York: CRC Press.

Anderson, S. A., Qiu, M., Bulfone, A., Eisenstat, D. D., Meneses, J., Pedersen, R. and Rubenstein, J. L. (1997). Mutations of the homeobox genes Dlx-1 and Dlx-2 disrupt the striatal subventricular zone and differentiation of late born striatal neurons. *Neuron* **19**, 27-37.

Andressen, C., Blümcke, I. and Celio, M. R. (1993). Calcium-binding proteins: selective markers of nerve cells. *Cell Tissue Res*. **271**, 181-208.

Argenti, B., Gallo, R., Di Marcotullio, L., Ferretti, E., Napolitano, M., Canterini, S., De Smaele, E., Greco, A., Fiorenza, M. T., Maroder, M. et al. (2005). Hedgehog antagonist REN(KCTD11) regulates proliferation and apoptosis of developing granule cell progenitors. *J. Neurosci*. **25**, 8338-46.

Aruga, J., Inoue, T., Hoshino, J. and Mikoshiba, K. (2002). Zic2 controls cerebellar development in cooperation with Zic1. *J. Neurosci*. **22**, 218-25.

Aruga, J., Minowa, O., Yaginuma, H., Kuno, J., Nagai, T., Noda, T. and Mikoshiba, K. (1998). Mouse Zic1 is involved in cerebellar development. *J. Neurosci*. **18**, 284-93.

Ashwell, K. W. and Zhang, L. L. (1992). Ontogeny of afferents to the fetal rat cerebellum. *Acta Anat. (Basel)*. **145**, 17-23.

Backman, M., Machon, O., Mygland, L., van den Bout, C. J., Zhong, W., Taketo, M. M. and Krauss, S. (2005). Effects of canonical Wnt signaling on dorso-ventral specification of the mouse telencephalon. *Dev. Biol*. **279**, 155-68.

Baeza, N., Masuoka, J., Kleihues, P. and Ohgaki, H. (2003). AXIN1 mutations but not deletions in cerebellar medulloblastomas. *Oncogene* **22**, 632-6.

Bänziger, C., Soldini, D., Schütt, C., Zipperlen, P., Hausmann, G. and Basler, K. (2006). Wntless, a conserved membrane protein dedicated to the secretion of Wnt proteins from signaling cells. *Cell* **125**, 509-22.

Baptista, C. A., Hatten, M. E., Blazeski, R. and Mason, C. A. (1994). Cell-cell interactions influence survival and differentiation of purified Purkinje cells in vitro. *Neuron* **12**, 243-60.

Barolo, S. (2006). Transgenic Wnt/TCF pathway reporters: all you need is Lef? *Oncogene* **25**, 7505-11.

Barolo, S. and Posakony, J. W. (2002). Three habits of highly effective signaling pathways: principles of transcriptional control by developmental cell signaling. *Genes Dev.* **16**, 1167-81.

Basson, M. A., Echevarria, D., Ahn, C. P., Sudarov, A., Joyner, A. L., Mason, I. J., Martinez, S. and Martin, G. R. (2008). Specific regions within the embryonic midbrain and cerebellum require different levels of FGF signaling during development. *Development* **135**, 889-98.

Beals, C. R., Sheridan, C. M., Turck, C. W., Gardner, P. and Crabtree, G. R. (1997). Nuclear export of NF-ATc enhanced by glycogen synthase kinase-3. *Science* **275**, 1930-4.

Behesti, H. and Marino, S. (2008). Cerebellar granule cells: Insights into proliferation, differentiation, and role in medulloblastoma pathogenesis. *Int. J. Biochem. Cell Biol.* **41**, 435-45.

Ben-Arie, N., Bellen, H. J., Armstrong, D. L., McCall, A. E., Gordadze, P. R., Guo, Q., Matzuk, M. M. and Zoghbi, H. Y. (1997). Math1 is essential for genesis of cerebellar granule neurons. *Nature* **390**, 169-72.

Ben-Arie, N., McCall, A. E., Berkman, S., Eichele, G., Bellen, H. J. and Zoghbi, H. Y. (1996). Evolutionary conservation of sequence and expression of the bHLH protein Atonal suggests a conserved role in neurogenesis. *Hum. Mol. Genet.* **5**, 1207-16.

Benchabane, H. and Ahmed, Y. (2009). The adenomatous polyposis coli tumor suppressor and Wnt signaling in the regulation of apoptosis. *Adv. Exp. Med. Biol.* **656**, 75-84.

Bhanot, P., Brink, M., Samos, C. H., Hsieh, J. C., Wang, Y., Macke, J. P., Andrew, D., Nathans, J. and Nusse, R. (1996). A new member of the frizzled family from Drosophila functions as a Wingless receptor. *Nature* **382**, 225-30.

Bluske, K., Kawakami, Y., Koyano-Nakagawa, N. and Nakagawa, Y. (2009). Differential activity of Wnt/beta-catenin signaling in the embryonic mouse thalamus. *Dev. Dyn.* **238**, 3297-309.

Bovolenta, P., Esteve, P., Ruiz, J. M., Cisneros, E. and Lopez-Rios, J. (2008). Beyond Wnt inhibition: new functions of secreted Frizzled-related proteins in development and disease. *J. Cell Sci.* **121**, 737-46.

Brand, M., Heisenberg, C. P., Jiang, Y. J., Beuchle, D., Lun, K., Furutani-Seiki, M., Granato, M., Haffter, P., Hammerschmidt, M., Kane, D. A. et al. (1996). Mutations in zebrafish genes affecting the formation of the boundary between midbrain and hindbrain. *Development* **123**, 179-90.

Brochu, G., Maler, L. and Hawkes, R. (1990). Zebrin II: a polypeptide antigen expressed selectively by Purkinje cells reveals compartments in rat and fish cerebellum. *J. Comp. Neurol.* **291**, 538-52.

Bryja, V., Andersson, E. R., Schambony, A., Esner, M., Bryjová, L., Biris, K. K., Hall, A. C., Kraft, B., Cajanek, L., Yamaguchi, T. P. et al. (2009). The extracellular domain of Lrp5/6 inhibits noncanonical Wnt signaling in vivo. *Mol. Biol. Cell* **20**, 924-36.

Caneparo, L., Huang, Y. L., Staudt, N., Tada, M., Ahrendt, R., Kazanskaya, O., Niehrs, C. and Houart, C. (2007). Dickkopf-1 regulates gastrulation movements by coordinated modulation of Wnt/beta catenin and Wnt/PCP activities, through interaction with the Dally-like homolog Knypek. *Genes Dev.* **21**, 465-80.

Carlén, M., Meletis, K., Barnabé-Heider, F. and Frisén, J. (2006). Genetic visualization of neurogenesis. *Exp. Cell Res.* **312**, 2851-9.

Casper, K. B. and McCarthy, K. D. (2006). GFAP-positive progenitor cells produce neurons and oligodendrocytes throughout the CNS. *Mol. Cell. Neurosci.* **31**, 676-84.

Chamorro, M. N., Schwartz, D. R., Vonica, A., Brivanlou, A. H., Cho, K. R. and Varmus, H. E. (2005). FGF-20 and DKK1 are transcriptional targets of beta-catenin and FGF-20 is implicated in cancer and development. *EMBO J.* **24**, 73-84.

Chan, E. F., Gat, U., McNiff, J. M. and Fuchs, E. (1999). A common human skin tumour is caused by activating mutations in beta-catenin. *Nat. Genet.* **21**, 410-3.

Chan-Palay, V. and Palay, S. (1972). The form of velate astrocytes in the cerebellar cortex of monkey and rat: high voltage electron microscopy of rapid Golgi preparations. *Z. Anat. Entwicklungsgesch.* **138**, 1-19.

Chen, B., Dodge, M. E., Tang, W., Lu, J., Ma, Z., Fan, C.-W., Wei, S., Hao, W., Kilgore, J., Williams, N. S. et al. (2009). Small molecule-mediated disruption of Wnt-dependent signaling in tissue regeneration and cancer. *Nat Chem Biol* **5**, 100-7.

Chen, S., Guttridge, D. C., You, Z., Zhang, Z., Fribley, A., Mayo, M. W., Kitajewski, J. and Wang, C. Y. (2001). Wnt-1 signaling inhibits apoptosis by activating beta-catenin/T cell factor-mediated transcription. *J. Cell Biol.* **152**, 87-96.

Chenn, A. and Walsh, C. A. (2002). Regulation of cerebral cortical size by control of cell cycle exit in neural precursors. *Science* **297**, 365-9.

Choi, Y., Borghesani, P. R., Chan, J. A. and Segal, R. A. (2005). Migration from a mitogenic niche promotes cell-cycle exit. *J. Neurosci.* **25**, 10437-45.

Ciani, L., Krylova, O., Smalley, M. J., Dale, T. C. and Salinas, P. C. (2004). A divergent canonical WNT-signaling pathway regulates microtubule dynamics: dishevelled signals locally to stabilize microtubules. *J. Cell Biol.* **164**, 243-53.

Clevers, H. (2006). Wnt/beta-catenin signaling in development and disease. *Cell* **127**, 469-80.

Crossley, P. H. and Martin, G. R. (1995). The mouse Fgf8 gene encodes a family of polypeptides and is expressed in regions that direct outgrowth and patterning in the developing embryo. *Development* **121**, 439-51.

Crossley, P. H., Martinez, S. and Martin, G. R. (1996). Midbrain development induced by FGF8 in the chick embryo. *Nature* **380**, 66-8.

D'Arcangelo, G., Miao, G. G., Chen, S. C., Soares, H. D., Morgan, J. I. and Curran, T. (1995). A protein related to extracellular matrix proteins deleted in the mouse mutant reeler. *Nature* **374**, 719-23.

Dahlstrand, J., Lardelli, M. and Lendahl, U. (1995). Nestin mRNA expression correlates with the central nervous system progenitor cell state in many, but not all, regions of developing central nervous system. *Brain Res. Dev. Brain Res.* **84**, 109-29.

Dahmane, N. and Ruiz i Altaba, A. (1999). Sonic hedgehog regulates the growth and patterning of the cerebellum. *Development* **126**, 3089-100.

Dakubo, G. D., Mazerolle, C. J. and Wallace, V. A. (2006). Expression of Notch and Wnt pathway components and activation of Notch signaling in medulloblastomas from heterozygous patched mice. *J. Neurooncol.* **79**, 221-7.

Danielian, P. S. and McMahon, A. P. (1996). Engrailed-1 as a target of the Wnt-1 signalling pathway in vertebrate midbrain development. *Nature* **383**, 332-4.

Daniels, D. L. and Weis, W. I. (2005). Beta-catenin directly displaces Groucho/TLE repressors from Tcf/Lef in Wnt-mediated transcription activation. *Nat Struct Mol Biol* **12**, 364-71.

DasGupta, R. and Fuchs, E. (1999). Multiple roles for activated LEF/TCF transcription complexes during hair follicle development and differentiation. *Development* **126**, 4557-68.

Davis, C. A. and Joyner, A. L. (1988). Expression patterns of the homeo box-containing genes En-1 and En-2 and the proto-oncogene int-1 diverge during mouse development. *Genes Dev.* **2**, 1736-44.

de Groot, R. P., Auwerx, J., Bourouis, M. and Sassone-Corsi, P. (1993). Negative regulation of Jun/AP-1: conserved function of glycogen synthase kinase 3 and the Drosophila kinase shaggy. *Oncogene* **8**, 841-7.

de Lau, W., Barker, N., Low, T. Y., Koo, B. K., Li, V. S., Teunissen, H., Kujala, P., Haegebarth, A., Peters, P. J., van de Wetering, M. et al. (2011). Lgr5 homologues associate with Wnt receptors and mediate R-spondin signalling. *Nature* **476**, 293-7.

Dipietrantonio, H. J. and Dymecki, S. M. (2009). Zic1 levels regulate mossy fiber neuron position and axon laterality choice in the ventral brain stem. *Neuroscience* **162**, 560-73.

Dusart, I., Airaksinen, M. S. and Sotelo, C. (1997). Purkinje cell survival and axonal regeneration are age dependent: an in vitro study. *J. Neurosci.* **17**, 3710-26.

Dymecki, S. M. and Tomasiewicz, H. (1998). Using Flp-recombinase to characterize expansion of Wnt1-expressing neural progenitors in the mouse. *Dev. Biol.* **201**, 57-65.

Eberhart, C. G., Tihan, T. and Burger, P. C. (2000). Nuclear localization and mutation of beta-catenin in medulloblastomas. *J. Neuropathol. Exp. Neurol.* **59**, 333-7.

Edwards, M. A., Yamamoto, M. and Caviness, V. S. (1990). Organization of radial glia and related cells in the developing murine CNS. An analysis based upon a new monoclonal antibody marker. *Neuroscience* **36**, 121-44.

Ellison, D. W., Onilude, O. E., Lindsey, J. C., Lusher, M. E., Weston, C. L., Taylor, R. E., Pearson, A. D., Clifford, S. and Committee, U. K. C. s. C. S. G. B. T. (2005). beta-Catenin status predicts a favorable outcome in childhood medulloblastoma: the United Kingdom Children's Cancer Study Group Brain Tumour Committee. *J. Clin. Oncol.* **23**, 7951-7.

Englund, C., Kowalczyk, T., Daza, R. A., Dagan, A., Lau, C., Rose, M. F. and Hevner, R. F. (2006). Unipolar brush cells of the cerebellum are produced in the rhombic lip and migrate through developing white matter. *J. Neurosci.* **26**, 9184-95.

Esteve, P., Sandonìs, A., Ibañez, C., Shimono, A., Guerrero, I. and Bovolenta, P. (2011). Secreted frizzled-related proteins are required for Wnt/β-catenin signalling activation in the vertebrate optic cup. *Development* **138**, 4179-84.

Fancy, S. P., Baranzini, S. E., Zhao, C., Yuk, D. I., Irvine, K. A., Kaing, S., Sanai, N., Franklin, R. J. and Rowitch, D. H. (2009). Dysregulation of the Wnt pathway inhibits timely myelination and remyelination in the mammalian CNS. *Genes Dev.* **23**, 1571-85.

Farndon, P. A., Del Mastro, R. G., Evans, D. G. and Kilpatrick, M. W. (1992). Location of gene for Gorlin syndrome. *Lancet* **339**, 581-2.

Fink, A. J., Englund, C., Daza, R. A., Pham, D., Lau, C., Nivison, M., Kowalczyk, T. and Hevner, R. F. (2006). Development of the deep cerebellar nuclei: transcription factors and cell migration from the rhombic lip. *J. Neurosci.* **26**, 3066-76.

Fischer, T., Guimera, J., Wurst, W. and Prakash, N. (2007). Distinct but redundant expression of the Frizzled Wnt receptor genes at signaling centers of the developing mouse brain. *Neuroscience* **147**, 693-711.

Fliniaux, I., Mikkola, M. L., Lefebvre, S. and Thesleff, I. (2008). Identification of dkk4 as a target of Eda-A1/Edar pathway reveals an unexpected role of ectodysplasin as inhibitor of Wnt signalling in ectodermal placodes. *Dev. Biol.* **320**, 60-71.

Fogarty, M., Emmenegger, B. A., Grasfeder, L. L., Oliver, T. G. and Wechsler-Reya, R. J. (2007). Fibroblast growth factor blocks Sonic hedgehog signaling in neuronal precursors and tumor cells. *Proc Natl Acad Sci USA* **104**, 2973-8.

Fotaki, V., Larralde, O., Zeng, S., Mclaughlin, D., Nichols, J., Price, D. J., Theil, T. and Mason, J. O. (2010). Loss of Wnt8b has no overt effect on hippocampus development but leads to altered Wnt gene expression levels in dorsomedial telencephalon. *Dev. Dyn.* **239**, 284-96.

Fotaki, V., Price, D. J. and Mason, J. O. (2011a). Wnt/β-catenin signaling is disrupted in the extra-toes (Gli3(Xt/Xt)) mutant from early stages of forebrain development, concomitant with anterior neural plate patterning defects. *J. Comp. Neurol.* **519**, 1640-57.

Fotaki, V., Price, D. J. and Mason, J. O. (2011b). Wnt/β-catenin signalling is disrupted in the extratoes (Gli3Xt/Xt) mutant from early stages of forebrain development, concomitant with anterior neural plate patterning defects. *J. Comp. Neurol.* ***in press***.

Fuentealba, L. C., Eivers, E., Ikeda, A., Hurtado, C., Kuroda, H., Pera, E. M. and De Robertis, E. M. (2007). Integrating patterning signals: Wnt/GSK3 regulates the duration of the BMP/Smad1 signal. *Cell* **131**, 980-93.

Gao, W. O., Heintz, N. and Hatten, M. E. (1991). Cerebellar granule cell neurogenesis is regulated by cell-cell interactions in vitro. *Neuron* **6**, 705-15.

Gat, U., DasGupta, R., Degenstein, L. and Fuchs, E. (1998). De Novo hair follicle morphogenesis and hair tumors in mice expressing a truncated beta-catenin in skin. *Cell* **95**, 605-14.

Gebbia, M., Ferrero, G. B., Pilia, G., Bassi, M. T., Aylsworth, A., Penman-Splitt, M., Bird, L. M., Bamforth, J. S., Burn, J., Schlessinger, D. et al. (1997). X-linked situs abnormalities result from mutations in ZIC3. *Nat. Genet.* **17**, 305-8.

Ghoumari, A. M., Wehrlé, R., Bernard, O., Sotelo, C. and Dusart, I. (2000). Implication of Bcl-2 and Caspase-3 in age-related Purkinje cell death in murine organotypic culture: an in vitro model to study apoptosis. *Eur. J. Neurosci.* **12**, 2935-49.

Gibson, P., Tong, Y., Robinson, G., Thompson, M., Currle, D. S., Eden, C., Kranenburg, T. A., Hogg, T., Poppleton, H., Martin, J. et al. (2010). Subtypes of medulloblastoma have distinct developmental origins. *Nature* **468**, 1095-1099.

Gilbertson, R. J. and Ellison, D. W. (2008). The origins of medulloblastoma subtypes. *Annu. Rev. Pathol.* **3**, 341-65.

Giraldez, A. J. and Cohen, S. M. (2003). Wingless and Notch signaling provide cell survival cues and control cell proliferation during wing development. *Development* **130**, 6533-43.

Glinka, A., Wu, W., Delius, H., Monaghan, A. P., Blumenstock, C. and Niehrs, C. (1998). Dickkopf-1 is a member of a new family of secreted proteins and functions in head induction. *Nature* **391**, 357-62.

Gonsalves, F. C., Klein, K., Carson, B. B., Katz, S., Ekas, L. A., Evans, S., Nagourney, R., Cardozo, T., Brown, A. M. and Dasgupta, R. (2011). Feature Article: An RNAi-based chemical genetic screen identifies three small-molecule inhibitors of the Wnt/wingless signaling pathway. *Proc Natl Acad Sci USA*.

Goodrich, L. V., Milenković, L., Higgins, K. M. and Scott, M. P. (1997). Altered neural cell fates and medulloblastoma in mouse patched mutants. *Science* **277**, 1109-13.

Grimaldi, P., Parras, C., Guillemot, F., Rossi, F. and Wassef, M. (2009). Origins and control of the differentiation of inhibitory interneurons and glia in the cerebellum. *Dev. Biol.* **328**, 422-33.

Grimes, C. A. and Jope, R. S. (2001). CREB DNA binding activity is inhibited by glycogen synthase kinase-3 beta and facilitated by lithium. *J. Neurochem.* **78**, 1219-32.

Grove, E. A., Tole, S., Limon, J., Yip, L. and Ragsdale, C. W. (1998). The hem of the embryonic cerebral cortex is defined by the expression of multiple Wnt genes and is compromised in Gli3-deficient mice. *Development* **125**, 2315-25.

Guger, K. A. and Gumbiner, B. M. (1995). beta-Catenin has Wnt-like activity and mimics the Nieuwkoop signaling center in Xenopus dorsal-ventral patterning. *Dev. Biol.* **172**, 115-25.

Gunhaga, L., Marklund, M., Sjödal, M., Hsieh, J. C., Jessell, T. M. and Edlund, T. (2003). Specification of dorsal telencephalic character by sequential Wnt and FGF signaling. *Nat. Neurosci.* **6**, 701-7.

Hachem, S., Laurenson, A. S., Hugnot, J. P. and Legraverend, C. (2007). Expression of S100B during embryonic development of the mouse cerebellum. *BMC Dev Biol* **7**, 17.

Hahn, H., Wicking, C., Zaphiropoulous, P. G., Gailani, M. R., Shanley, S., Chidambaram, A., Vorechovsky, I., Holmberg, E., Unden, A. B., Gillies, S. et al. (1996). Mutations of the human homolog of Drosophila patched in the nevoid basal cell carcinoma syndrome. *Cell* **85**, 841-51.

Hall, A. C., Lucas, F. R. and Salinas, P. C. (2000). Axonal remodeling and synaptic differentiation in the cerebellum is regulated by WNT-7a signaling. *Cell* **100**, 525-35.

Hall, P. A., Levison, D. A., Woods, A. L., Yu, C. C.-W., Kellock, D. B., Watkins, J. A., Barnes, D. M., Gillett, C. E., Camplejohn, R., Dover, R., Waseem, N. H and Lane, D. P. (1990). Proliferating cell nuclear antigen (PCNA) immunolocalization in paraffin sections: An index of cell proliferation with evidence of deregulated expression in some, neoplasms. *J. Pathol.* **162**, 285-294.

Hamilton, S. R., Liu, B., Parsons, R. E., Papadopoulos, N., Jen, J., Powell, S. M., Krush, A. J., Berk, T., Cohen, Z. and Tetu, B. (1995). The molecular basis of Turcot's syndrome. *N. Engl. J. Med.* **332**, 839-47.

Hanahan, D. and Weinberg, R. (2011). Hallmarks of Cancer: The Next Generation. *Cell* **144**, 646-674.

Hanahan, D. and Weinberg, R. A. (2000). The hallmarks of cancer. *Cell* **100**, 57-70.

Harada, N., Tamai, Y., Ishikawa, T., Sauer, B., Takaku, K., Oshima, M. and Taketo, M. M. (1999). Intestinal polyposis in mice with a dominant stable mutation of the beta-catenin gene. *EMBO J.* **18**, 5931-42.

Hashimoto, M. and Mikoshiba, K. (2003). Mediolateral compartmentalization of the cerebellum is determined on the "birth date" of Purkinje cells. *J. Neurosci.* **23**, 11342-51.

Hatten, M. and Roussel, M. F. (2011). Development and cancer of the cerebellum. *Trends Neurosci.* **34**, 134-42.

Hatten, M. E. and Heintz, N. (1995). Mechanisms of neural patterning and specification in the developing cerebellum. *Annu. Rev. Neurosci.* **18**, 385-408.

Hatten, M. E. and Mason, C. A. (1990). Mechanisms of glial-guided neuronal migration in vitro and in vivo. *Experientia* **46**, 907-16.

Hayashi, S. and McMahon, A. P. (2002). Efficient recombination in diverse tissues by a tamoxifen-inducible form of Cre: a tool for temporally regulated gene activation/inactivation in the mouse. *Dev. Biol.* **244**, 305-18.

He, B., You, L., Uematsu, K., Xu, Z., Lee, A. Y., Matsangou, M., McCormick, F. and Jablons, D. M. (2004). A monoclonal antibody against Wnt-1 induces apoptosis in human cancer cells. *NEO* **6**, 7-14.

He, T. C., Sparks, A. B., Rago, C., Hermeking, H., Zawel, L., da Costa, L. T., Morin, P. J., Vogelstein, B. and Kinzler, K. W. (1998). Identification of c-MYC as a target of the APC pathway. *Science* **281**, 1509-12.

He, X., Saint-Jeannet, J. P., Woodgett, J. R., Varmus, H. E. and Dawid, I. B. (1995). Glycogen synthase kinase-3 and dorsoventral patterning in Xenopus embryos. *Nature* **374**, 617-22.

Hegedus, B., Dasgupta, B., Shin, J. E., Emnett, R. J., Hart-Mahon, E. K., Elghazi, L., Bernal-Mizrachi, E. and Gutmann, D. H. (2007). Neurofibromatosis-1 regulates neuronal and glial cell differentiation from neuroglial progenitors in vivo by both cAMP- and Ras-dependent mechanisms. *Cell Stem Cell* **1**, 443-57.

Hendriksen, J., Jansen, M., Brown, C. M., van der Velde, H., van Ham, M., Galjart, N., Offerhaus, G. J., Fagotto, F. and Fornerod, M. (2008). Plasma membrane recruitment of dephosphorylated beta-catenin upon activation of the Wnt pathway. *J. Cell Sci.* **121**, 1793-802.

Hirabayashi, Y., Itoh, Y., Tabata, H., Nakajima, K., Akiyama, T., Masuyama, N. and Gotoh, Y. (2004). The Wnt/beta-catenin pathway directs neuronal differentiation of cortical neural precursor cells. *Development* **131**, 2791-801.

Hoshino, M., Nakamura, S., Mori, K., Kawauchi, T., Terao, M., Nishimura, Y., Fukuda, A., Fuse, T., Matsuo, N., Sone, M. et al. (2005). Ptf1a, a bHLH Transcriptional Gene, Defines GABAergic Neuronal Fates in Cerebellum. *Neuron* **47**, 201-213.

Hovanes, K., Li, T. W., Munguia, J. E., Truong, T., Milovanovic, T., Lawrence Marsh, J., Holcombe, R. F. and Waterman, M. L. (2001). Beta-catenin-sensitive isoforms of lymphoid enhancer factor-1 are selectively expressed in colon cancer. *Nat. Genet.* **28**, 53-7.

Huang, H., Mahler-Araujo, B. M., Sankila, A., Chimelli, L., Yonekawa, Y., Kleihues, P. and Ohgaki, H. (2000). APC mutations in sporadic medulloblastomas. *Am. J. Pathol.* **156**, 433-7.

Huang, S., Mishina, Y., Liu, S., Cheung, A., Stegmeier, F., Michaud, G., Charlat, O., Wiellette, E., Zhang, Y., Wiessner, S. et al. (2009). Tankyrase inhibition stabilizes axin and antagonizes Wnt signalling. *Nature* **461**, 614-20.

Itoh, M. (1984). The Cerebellum and Neural Control. New York: Raven.

Ivaniutsin, U., Chen, Y., Mason, J. O., Price, D. J. and Pratt, T. (2009). Adenomatous polyposis coli is required for early events in the normal growth and differentiation of the developing cerebral cortex. *Neural Dev* **4**, 3.

Jänicke, R. U., Sprengart, M. L., Wati, M. R. and Porter, A. G. (1998). Caspase-3 is required for DNA fragmentation and morphological changes associated with apoptosis. *J. Biol. Chem.* **273**, 9357-60.

Jho, E. H., Zhang, T., Domon, C., Joo, C. K., Freund, J. N. and Costantini, F. (2002). Wnt/beta-catenin/Tcf signaling induces the transcription of Axin2, a negative regulator of the signaling pathway. *Mol. Cell. Biol.* **22**, 1172-83.

Joyner, A. L. and Zervas, M. (2006). Genetic inducible fate mapping in mouse: establishing genetic lineages and defining genetic neuroanatomy in the nervous system. *Dev. Dyn.* **235**, 2376-85.

Kalani, M. Y., Cheshier, S. H., Cord, B. J., Bababeygy, S. R., Vogel, H., Weissman, I. L., Palmer, T. D. and Nusse, R. (2008). Wnt-mediated self-renewal of neural stem/progenitor cells. *Proc Natl Acad Sci USA* **105**, 16970-5.

Kalinovsky, A., Boukhtouche, F., Blazeski, R., Bornmann, C., Suzuki, N., Mason, C. and Scheiffele, P. (2011). Development of axon-target specificity of ponto-cerebellar afferents. *PLoS Biol* **9**, e1001013.

Karner, C., Merkel, C., Dodge, M., Ma, Z., Lu, J., Chen, C., Lum, L. and Carroll, T. (2010). Tankyrase is necessary for canonical Wnt signaling during kidney development. *Dev. Dyn.* **239**, 2014-23.

Karner, C. M., Das, A., Ma, Z., Self, M., Chen, C., Lum, L., Oliver, G. and Carroll, T. J. (2011). Canonical Wnt9b signaling balances progenitor cell expansion and differentiation during kidney development. *Development* **138**, 1247-57.

Kawaguchi, A., Miyata, T., Sawamoto, K., Takashita, N., Murayama, A., Akamatsu, W., Ogawa, M., Okabe, M., Tano, Y., Goldman, S. A. et al. (2001). Nestin-EGFP transgenic mice: visualization of the self-renewal and multipotency of CNS stem cells. *Mol. Cell. Neurosci.* **17**, 259-73.

Kawauchi, D. and Saito, T. (2008). Transcriptional cascade from Math1 to Mbh1 and Mbh2 is required for cerebellar granule cell differentiation. *Dev. Biol.* **322**, 345-54.

Kawauchi, D., Taniguchi, H., Watanabe, H., Saito, T. and Murakami, F. (2006). Direct visualization of nucleogenesis by precerebellar neurons: involvement of ventricle-directed, radial fibre-associated migration. *Development* **133**, 1113-23.

Kazanskaya, O., Glinka, A., del Barco Barrantes, I., Stannek, P., Niehrs, C. and Wu, W. (2004). R-Spondin2 is a secreted activator of Wnt/beta-catenin signaling and is required for Xenopus myogenesis. *Developmental Cell* **7**, 525-34.

Kiecker, C. and Niehrs, C. (2001). A morphogen gradient of Wnt/beta-catenin signalling regulates anteroposterior neural patterning in Xenopus. *Development* **128**, 4189-201.

Kim, J. Y., Nelson, A. L., Algon, S. A., Graves, O., Sturla, L. M., Goumnerova, L. C., Rowitch, D. H., Segal, R. A. and Pomeroy, S. L. (2003). Medulloblastoma tumorigenesis diverges from cerebellar granule cell differentiation in patched heterozygous mice. *Dev. Biol.* **263**, 50-66.

Kim, K., Pang, K. M., Evans, M. and Hay, E. D. (2000). Overexpression of beta-catenin induces apoptosis independent of its transactivation function with LEF-1 or the involvement of major G1 cell cycle regulators. *Mol. Biol. Cell* **11**, 3509-23.

Kimelman, D. and Xu, W. (2006). beta-catenin destruction complex: insights and questions from a structural perspective. *Oncogene* **25**, 7482-91.

Kinzler, K. W., Nilbert, M. C., Su, L. K., Vogelstein, B., Bryan, T. M., Levy, D. B., Smith, K. J., Presinger, A. C., Hedge, P. and McKechnie, D. (1991a). identification of FAP locus genes from chromosome 5q21. *Science* **253**, 661-5.

Kinzler, K. W., Nilbert, M. C., Vogelstein, B., Bryan, T. M., Levy, D. B., Smith, K. J., Preisinger, A. C., Hamilton, S. R., Hedge, P. and Markham, A. (1991b). Identification of a gene located at chromosome 5q21 that is mutated in colorectal cancers. *Science* **251**, 1366-70.

Kinzler, K. W. and Vogelstein, B. (1996). Lessons from hereditary colorectal cancer. *Cell* **87**, 159-70.

Komine, O., Nagaoka, M., Watase, K., Gutmann, D. H., Tanigaki, K., Honjo, T., Radtke, F., Saito, T., Chiba, S. and Tanaka, K. (2007). The monolayer formation of Bergmann glial cells is regulated by Notch/RBP-J signaling. *Dev. Biol.* **311**, 238-50.

Kool, M., Koster, J., Bunt, J., Hasselt, N., Lakeman, A., Van Sluis, P., Troost, D., Meeteren, N., Caron, H., Cloos, J. et al. (2008). Integrated genomics identifies five medulloblastoma subtypes with distinct genetic profiles, pathway signatures and clinicopathological features. *PLoS ONE* **3**, e3088.

Kordes, U., Cheng, Y.-C. and Scotting, P. J. (2005). Sox group E gene expression distinguishes different types and maturational stages of glial cells in developing chick and mouse. *Brain Res. Dev. Brain Res.* **157**, 209-13.

Korinek, V., Barker, N., Morin, P. J., van Wichen, D., de Weger, R., Kinzler, K. W., Vogelstein, B. and Clevers, H. (1997). Constitutive transcriptional activation by a beta-catenin-Tcf complex in APC-/- colon carcinoma. *Science* **275**, 1784-7.

Koyabu, Y., Nakata, K., Mizugishi, K., Aruga, J. and Mikoshiba, K. (2001). Physical and functional interactions between Zic and Gli proteins. *J. Biol. Chem.* **276**, 6889-92.

Kratz, J. E., Stearns, D., Huso, D. L., Slunt, H. H., Price, D. L., Borchelt, D. R. and Eberhart, C. G. (2002). Expression of stabilized beta-catenin in differentiated neurons of transgenic mice does not result in tumor formation. *BMC Cancer* **2**, 33.

Kroboth, K., Newton, I. P., Kita, K., Dikovskaya, D., Zumbrunn, J., Waterman-Storer, C. M. and Näthke, I. S. (2007). Lack of adenomatous polyposis coli protein correlates with a decrease in cell migration and overall changes in microtubule stability. *Mol. Biol. Cell* **18**, 910-8.

Kuure, S., Popsueva, A., Jakobson, M., Sainio, K. and Sariola, H. (2007). Glycogen synthase kinase-3 inactivation and stabilization of beta-catenin induce nephron differentiation in isolated mouse and rat kidney mesenchymes. *J. Am. Soc. Nephrol.* **18**, 1130-9.

Laine, H., Sulg, M., Kirjavainen, A. and Pirvola, U. (2010). Cell cycle regulation in the inner ear sensory epithelia: role of cyclin D1 and cyclin-dependent kinase inhibitors. *Dev. Biol.* **337**, 134-46.

Lancaster, M., Gopal, D., Kim, J., Saleem, S., Silhavy, J., Louie, C., Thacker, B., Williams, Y., Zaki, M. and Gleeson, J. (2011). Defective Wnt-dependent cerebellar midline fusion in a mouse model of Joubert syndrome. *Nat. Med.* **17**, 726-31.

Lancaster, M., Louie, C., Silhavy, J., Sintasath, L., Decambre, M., Nigam, S. K., Willert, K. and Gleeson, J. (2009). Impaired Wnt-beta-catenin signaling disrupts adult renal homeostasis and leads to cystic kidney ciliopathy. *Nat. Med.* **15**, 1046-54.

Landry, C. F., Ivy, G. O., Dunn, R. J., Marks, A. and Brown, I. R. (1989). Expression of the gene encoding the beta-subunit of S-100 protein in the developing rat brain analyzed by in situ hybridization. *Brain Res. Mol. Brain Res.* **6**, 251-62.

Landsberg, R. L., Awatramani, R. B., Hunter, N. L., Farago, A. F., DiPietrantonio, H. J., Rodriguez, C. I. and Dymecki, S. M. (2005). Hindbrain rhombic lip is comprised of discrete progenitor cell populations allocated by Pax6. *Neuron* **48**, 933-47.

Larsell, O. (1970). The Comparative Anatomy and Histology of the Cerebellum from Monotremes through Apes. Minneapolis: University of Monnesota Press.

Lee, A., Kessler, J. D., Read, T. A., Kaiser, C., Corbeil, D., Huttner, W. B., Johnson, J. and Wechsler-Reya, R. J. (2005). Isolation of neural stem cells from the postnatal cerebellum. *Nat. Neurosci.* **8**, 723-9.

Lee, E., Salic, A., Krüger, R., Heinrich, R. and Kirschner, M. (2003). The roles of APC and Axin derived from experimental and theoretical analysis of the Wnt pathway. *PLoS Biol* **1**, E10.

Leto, K., Bartolini, A., Yanagawa, Y., Obata, K., Magrassi, L., Schilling, K. and Rossi, F. (2009). Laminar fate and phenotype specification of cerebellar GABAergic interneurons. *J. Neurosci.* **29**, 7079-91.

Leto, K., Carletti, B., Williams, I. M., Magrassi, L. and Rossi, F. (2006). Different types of cerebellar GABAergic interneurons originate from a common pool of multipotent progenitor cells. *J. Neurosci.* **26**, 11682-94.

Levitt, P. and Rakic, P. (1980). Immunoperoxidase localization of glial fibrillary acidic protein in radial glial cells and astrocytes of the developing rhesus monkey brain. *J. Comp. Neurol.* **193**, 815-40.

Li, J., Imitola, J., Snyder, E. Y. and Sidman, R. L. (2006). Neural stem cells rescue nervous purkinje neurons by restoring molecular homeostasis of tissue plasminogen activator and downstream targets. *J. Neurosci.* **26**, 7839-48.

Liu, A. and Joyner, A. L. (2001). EN and GBX2 play essential roles downstream of FGF8 in patterning the mouse mid/hindbrain region. *Development* **128**, 181-91.

Liu, W., Lagutin, O., Swindell, E., Jamrich, M. and Oliver, G. (2010). Neuroretina specification in mouse embryos requires Six3-mediated suppression of Wnt8b in the anterior neural plate. *J. Clin. Invest.* **120**, 3568-77.

Logan, C. and Nusse, R. (2004). The Wnt signaling pathway in development and disease. *Annu. Rev. Cell Dev. Biol.* **20**, 781-810.

Lorenz, A., Deutschmann, M., Ahlfeld, J., Prix, C., Koch, A., Smits, R., Fodde, R., Kretzschmar, H. A. and Schüller, U. (2011). Severe alterations of cerebellar cortical development after constitutive activation of Wnt signaling in granule neuron precursors. *Mol. Cell. Biol.* **31**, 3326-38.

Louis, D. N., Ohgaki, H., Wiester, O. D. and Cavenee, W. K. (2007). WHO Classification of tumours of the central nervous system. Lyon: IARC.

Louvi, A., Alexandre, P., Métin, C., Wurst, W. and Wassef, M. (2003). The isthmic neuroepithelium is essential for cerebellar midline fusion. *Development* **130**, 5319-30.

Louvi, A., Yoshida, M. and Grove, E. A. (2007). The derivatives of the Wnt3a lineage in the central nervous system. *J. Comp. Neurol.* **504**, 550-69.

Lucas, F. R. and Salinas, P. C. (1997). WNT-7a induces axonal remodeling and increases synapsin I levels in cerebellar neurons. *Dev. Biol.* **192**, 31-44.

Luo, W., Peterson, A., Garcia, B. A., Coombs, G., Kofahl, B., Heinrich, R., Shabanowitz, J., Hunt, D. F., Yost, H. J. and Virshup, D. M. (2007). Protein phosphatase 1 regulates assembly and function of the beta-catenin degradation complex. *EMBO J.* **26**, 1511-21.

Lustig, B., Jerchow, B., Sachs, M., Weiler, S., Pietsch, T., Karsten, U., van de Wetering, M., Clevers, H., Schlag, P. M., Birchmeier, W. et al. (2002). Negative feedback loop of Wnt signaling through upregulation of conductin/axin2 in colorectal and liver tumors. *Mol. Cell. Biol.* **22**, 1184-93.

Lütolf, S., Radtke, F., Aguet, M., Suter, U. and Taylor, V. (2002). Notch1 is required for neuronal and glial differentiation in the cerebellum. *Development* **129**, 373-85.

Ma, Y. C., Song, M. R., Park, J. P., Henry Ho, H. Y., Hu, L., Kurtev, M. V., Zieg, J., Ma, Q., Pfaff, S. L. and Greenberg, M. E. (2008). Regulation of motor neuron specification by phosphorylation of neurogenin 2. *Neuron* **58**, 65-77.

MacDonald, B. T., Tamai, K. and He, X. (2009). Wnt/beta-catenin signaling: components, mechanisms, and diseases. *Developmental Cell* **17**, 9-26.

Machold, R. and Fishell, G. (2005). Math1 Is Expressed in Temporally Discrete Pools of Cerebellar Rhombic-Lip Neural Progenitors. *Neuron* **48**, 17-24.

Machon, O., Backman, M., Machonova, O., Kozmik, Z., Vacik, T., Andersen, L. and Krauss, S. (2007). A dynamic gradient of Wnt signaling controls initiation of neurogenesis in the mammalian cortex and cellular specification in the hippocampus. *Dev. Biol.* **311**, 223-37.

Mao, J., Wang, J., Liu, B., Pan, W., Farr, G. H., Flynn, C., Yuan, H., Takada, S., Kimelman, D., Li, L. et al. (2001). Low-density lipoprotein receptor-related protein-5 binds to Axin and regulates the canonical Wnt signaling pathway. *Mol. Cell* **7**, 801-9.

Maretto, S., Cordenonsi, M., Dupont, S., Braghetta, P., Broccoli, V., Hassan, A. B., Volpin, D., Bressan, G. M. and Piccolo, S. (2003). Mapping Wnt/beta-catenin signaling during mouse development and in colorectal tumors. *Proc Natl Acad Sci USA* **100**, 3299-304.

Maricich, S. M. and Herrup, K. (1999). Pax-2 expression defines a subset of GABAergic interneurons and their precursors in the developing murine cerebellum. *J. Neurobiol.* **41**, 281-94.

Marino, S., Vooijs, M., van Der Gulden, H., Jonkers, J. and Berns, A. (2000). Induction of medulloblastomas in p53-null mutant mice by somatic inactivation of Rb in the external granular layer cells of the cerebellum. *Genes Dev.* **14**, 994-1004.

Martinez, S., Crossley, P. H., Cobos, I., Rubenstein, J. L. and Martin, G. R. (1999). FGF8 induces formation of an ectopic isthmic organizer and isthmocerebellar development via a repressive effect on Otx2 expression. *Development* **126**, 1189-200.

Martínez, S., Marín, F., Nieto, M. A. and Puelles, L. (1995). Induction of ectopic engrailed expression and fate change in avian rhombomeres: intersegmental boundaries as barriers. *Mech. Dev.* **51**, 289-303.

Martinez, S., Wassef, M. and Alvarado-Mallart, R. M. (1991). Induction of a mesencephalic phenotype in the 2-day-old chick prosencephalon is preceded by the early expression of the homeobox gene en. *Neuron* **6**, 971-81.

Matei, V., Pauley, S., Kaing, S., Rowitch, D., Beisel, K. W., Morris, K., Feng, F., Jones, K., Lee, J. and Fritzsch, B. (2005). Smaller inner ear sensory epithelia in Neurog 1 null mice are related to earlier hair cell cycle exit. *Dev. Dyn.* **234**, 633-50.

Mazumdar, J., O'Brien, W. T., Johnson, R. S., Lamanna, J. C., Chavez, J. C., Klein, P. S. and Simon, M. C. (2010). O2 regulates stem cells through Wnt/β-catenin signalling. *Nature cell biology* **12**, 1007-13.

McMahon, A. P. and Bradley, A. (1990). The Wnt-1 (int-1) proto-oncogene is required for development of a large region of the mouse brain. *Cell* **62**, 1073-85.

McMahon, A. P., Joyner, A. L., Bradley, A. and McMahon, J. A. (1992). The midbrain-hindbrain phenotype of Wnt-1-/Wnt-1- mice results from stepwise deletion of engrailed-expressing cells by 9.5 days postcoitum. *Cell* **69**, 581-95.

McMahon, A. P. and Moon, R. T. (1989). Ectopic expression of the proto-oncogene int-1 in Xenopus embryos leads to duplication of the embryonic axis. *Cell* **58**, 1075-84.

Megason, S. G. and McMahon, A. P. (2002). A mitogen gradient of dorsal midline Wnts organizes growth in the CNS. *Development* **129**, 2087-98.

Meijer, L., Skaltsounis, A., Magiatis, P., Polychronopoulos, P., Knockaert, M., Leost, M., Ryan, X., Vonica, C., Brivanlou, A., Dajani, R. et al. (2003). GSK-3-selective inhibitors derived from Tyrian purple indirubins. *Chem. Biol.* **10**, 1255-66.

Meyers, E. N., Lewandoski, M. and Martin, G. R. (1998). An Fgf8 mutant allelic series generated by Cre- and Flp-mediated recombination. *Nat. Genet.* **18**, 136-41.

Miale, I. L. and Sidman, R. L. (1961). An autoradiographic analysis of histogenesis in the mouse cerebellum. *Exp. Neurol.* **4**, 277-96.

Miclea, R. L., Karperien, M., Bosch, C. A., van der Horst, G., van der Valk, M. A., Kobayashi, T., Kronenberg, H. M., Rawadi, G., Akçakaya, P., Löwik, C. W. et al. (2009). Adenomatous polyposis coli-mediated control of beta-catenin is essential for both chondrogenic and osteogenic differentiation of skeletal precursors. *BMC Dev Biol* **9**, 26.

Millen, K. J., Hui, C. C. and Joyner, A. L. (1995). A role for En-2 and other murine homologues of Drosophila segment polarity genes in regulating positional information in the developing cerebellum. *Development* **121**, 3935-45.

Milosevic, A. and Goldman, J. E. (2002). Progenitors in the postnatal cerebellar white matter are antigenically heterogeneous. *J. Comp. Neurol.* **452**, 192-203.

Milosevic, A. and Goldman, J. E. (2004). Potential of progenitors from postnatal cerebellar neuroepithelium and white matter: lineage specified vs. multipotent fate. *Mol. Cell. Neurosci.* **26**, 342-53.

Miyazawa, K., Himi, T., Garcia, V., Yamagishi, H., Sato, S. and Ishizaki, Y. (2000). A role for p27/Kip1 in the control of cerebellar granule cell precursor proliferation. *J. Neurosci.* **20**, 5756-63.

Mizuhara, E., Minaki, Y., Nakatani, T., Kumai, M., Inoue, T., Muguruma, K., Sasai, Y. and Ono, Y. (2010). Purkinje cells originate from cerebellar ventricular zone progenitors positive for Neph3 and E-cadherin. *Dev. Biol.* **338**, 202-14.

Mohamed, O. A., Clarke, H. J. and Dufort, D. (2004). Beta-catenin signaling marks the prospective site of primitive streak formation in the mouse embryo. *Dev. Dyn.* **231**, 416-24.

Molyneaux, B. J., Arlotta, P., Menezes, J. R. and Macklis, J. D. (2007). Neuronal subtype specification in the cerebral cortex. *Nat Rev Neurosci* **8**, 427-37.

Morin, P. J., Sparks, A. B., Korinek, V., Barker, N., Clevers, H., Vogelstein, B. and Kinzler, K. W. (1997). Activation of beta-catenin-Tcf signaling in colon cancer by mutations in beta-catenin or APC. *Science* **275**, 1787-90.

Moser, A. R., Pitot, H. C. and Dove, W. F. (1990). A dominant mutation that predisposes to multiple intestinal neoplasia in the mouse. *Science* **247**, 322-4.

Mukhopadhyay, M., Shtrom, S., Rodriguez-Esteban, C., Chen, L., Tsukui, T., Gomer, L., Dorward, D. W., Glinka, A., Grinberg, A., Huang, S. P. et al. (2001). Dickkopf1 is required for embryonic head induction and limb morphogenesis in the mouse. *Developmental Cell* **1**, 423-34.

Mullen, R. J., Buck, C. R. and Smith, A. M. (1992). NeuN, a neuronal specific nuclear protein in vertebrates. *Development* **116**, 201-11.

Munji, R. N., Choe, Y., Li, G., Siegenthaler, J. A. and Pleasure, S. J. (2011). Wnt signaling regulates neuronal differentiation of cortical intermediate progenitors. *J. Neurosci.* **31**, 1676-87.

Mutch, C. A., Funatsu, N., Monuki, E. S. and Chenn, A. (2009). Beta-catenin signaling levels in progenitors influence the laminar cell fates of projection neurons. *J. Neurosci.* **29**, 13710-9.

Nagai, T., Aruga, J., Takada, S., Günther, T., Spörle, R., Schughart, K. and Mikoshiba, K. (1997). The expression of the mouse Zic1, Zic2, and Zic3 gene suggests an essential role for Zic genes in body pattern formation. *Dev. Biol.* **182**, 299-313.

Nakaya, M.-a., Biris, K., Tsukiyama, T., Jaime, S., Rawls, J. A. and Yamaguchi, T. P. (2005). Wnt3a links left-right determination with segmentation and anteroposterior axis elongation. *Development* **132**, 5425-36.

Näthke, I. (2004). APC at a glance. *J. Cell Sci.* **117**, 4873-5.

Näthke, I. S., Adams, C. L., Polakis, P., Sellin, J. H. and Nelson, W. J. (1996). The adenomatous polyposis coli tumor suppressor protein localizes to plasma membrane sites involved in active cell migration. *J. Cell Biol.* **134**, 165-79.

Neal, J. W. and Clipstone, N. A. (2001). Glycogen synthase kinase-3 inhibits the DNA binding activity of NFATc. *J. Biol. Chem.* **276**, 3666-73.

Nichols, D. H. and Bruce, L. L. (2006). Migratory routes and fates of cells transcribing the Wnt-1 gene in the murine hindbrain. *Dev. Dyn.* **235**, 285-300.

Nolte, C., Matyash, M., Pivneva, T., Schipke, C. G., Ohlemeyer, C., Hanisch, U. K., Kirchhoff, F. and Kettenmann, H. (2001). GFAP promoter-controlled EGFP-expressing transgenic mice: a tool to visualize astrocytes and astrogliosis in living brain tissue. *Glia* **33**, 72-86.

Noordermeer, J., Klingensmith, J., Perrimon, N. and Nusse, R. (1994). dishevelled and armadillo act in the wingless signalling pathway in Drosophila. *Nature* **367**, 80-3.

Northcott, P. A., Korshunov, A., Witt, H., Hielscher, T., Eberhart, C. G., Mack, S., Bouffet, E., Clifford, S. C., Hawkins, C. E., French, P. et al. (2010). Medulloblastoma Comprises Four Distinct Molecular Variants. *J. Clin. Oncol.* **29**, 1408-14.

Nusse, R. and Varmus, H. E. (1982). Many tumors induced by the mouse mammary tumor virus contain a provirus integrated in the same region of the host genome. *Cell* **31**, 99-109.

Oliver, T. G., Read, T. A., Kessler, J. D., Mehmeti, A., Wells, J. F., Huynh, T. T., Lin, S. M. and Wechsler-Reya, R. J. (2005). Loss of patched and disruption of granule cell development in a pre-neoplastic stage of medulloblastoma. *Development* **132**, 2425-39.

Olmeda, D., Castel, S., Vilaró, S. and Cano, A. (2003). Beta-catenin regulation during the cell cycle: implications in G2/M and apoptosis. *Mol. Biol. Cell* **14**, 2844-60.

Parsons, D. W., Li, M., Zhang, X., Jones, S., Leary, R. J., Lin, J. C., Boca, S. M., Carter, H., Samayoa, J., Bettegowda, C. et al. (2011). The genetic landscape of the childhood cancer medulloblastoma. *Science* **331**, 435-9.

Pascual, M., Abasolo, I., Mingorance-Le Meur, A., Martínez, A., Del Rio, J. A., Wright, C. V., Real, F. X. and Soriano, E. (2007). Cerebellar GABAergic progenitors adopt an

external granule cell-like phenotype in the absence of Ptf1a transcription factor expression. *Proc Natl Acad Sci USA* **104**, 5193-8.

Peifer, M., McCrea, P. D., Green, K. J., Wieschaus, E. and Gumbiner, B. M. (1992). The vertebrate adhesive junction proteins beta-catenin and plakoglobin and the Drosophila segment polarity gene armadillo form a multigene family with similar properties. *J. Cell Biol.* **118**, 681-91.

Pinson, K. I., Brennan, J., Monkley, S., Avery, B. J. and Skarnes, W. C. (2000). An LDL-receptor-related protein mediates Wnt signalling in mice. *Nature* **407**, 535-8.

Pomeroy, S. L., Tamayo, P., Gaasenbeek, M., Sturla, L. M., Angelo, M., McLaughlin, M. E., Kim, J. Y., Goumnerova, L. C., Black, P. M., Lau, C. et al. (2002). Prediction of central nervous system embryonal tumour outcome based on gene expression. *Nature* **415**, 436-42.

Pompolo, S. and Harley, V. R. (2001). Localisation of the SRY-related HMG box protein, SOX9, in rodent brain. *Brain Res.* **906**, 143-8.

Purro, S. A., Ciani, L., Hoyos-Flight, M., Stamatakou, E., Siomou, E. and Salinas, P. C. (2008). Wnt regulates axon behavior through changes in microtubule growth directionality: a new role for adenomatous polyposis coli. *J. Neurosci.* **28**, 8644-54.

Raffel, C., Jenkins, R. B., Frederick, L., Hebrink, D., Alderete, B., Fults, D. W. and James, C. D. (1997). Sporadic medulloblastomas contain PTCH mutations. *Cancer Res.* **57**, 842-5.

Reifenberger, J., Wolter, M., Weber, R. G., Megahed, M., Ruzicka, T., Lichter, P. and Reifenberger, G. (1998). Missense mutations in SMOH in sporadic basal cell carcinomas of the skin and primitive neuroectodermal tumors of the central nervous system. *Cancer Res.* **58**, 1798-803.

Reifers, F., Böhli, H., Walsh, E. C., Crossley, P. H., Stainier, D. Y. and Brand, M. (1998). Fgf8 is mutated in zebrafish acerebellar (ace) mutants and is required for maintenance of midbrain-hindbrain boundary development and somitogenesis. *Development* **125**, 2381-95.

Rice, D. S. and Curran, T. (2001). Role of the reelin signaling pathway in central nervous system development. *Annu. Rev. Neurosci.* **24**, 1005-39.

Rijsewijk, F., Schuermann, M., Wagenaar, E., Parren, P., Weigel, D. and Nusse, R. (1987). The Drosophila homolog of the mouse mammary oncogene int-1 is identical to the segment polarity gene wingless. *Cell* **50**, 649-57.

Ring, D. B., Johnson, K. W., Henriksen, E. J., Nuss, J. M., Goff, D., Kinnick, T. R., Ma, S. T., Reeder, J. W., Samuels, I., Slabiak, T. et al. (2003). Selective glycogen synthase kinase 3 inhibitors potentiate insulin activation of glucose transport and utilization in vitro and in vivo. *Diabetes* **52**, 588-95.

Rios, I., Alvarez-Rodríguez, R., Martí, E. and Pons, S. (2004). Bmp2 antagonizes sonic hedgehog-mediated proliferation of cerebellar granule neurones through Smad5 signalling. *Development* **131**, 3159-68.

Rodriguez, C. I. and Dymecki, S. M. (2000). Origin of the precerebellar system. *Neuron* **27**, 475-86.

Rorke, L. (1983). The cerebellar medulloblastoma and its relationship to primitive neuroectodermal tumors. *J. Neuropathol. Exp. Neurol.* **42**, 1-15.

Rosso, S. B., Sussman, D., Wynshaw-Boris, A. and Salinas, P. C. (2005). Wnt signaling through Dishevelled, Rac and JNK regulates dendritic development. *Nat. Neurosci.* **8**, 34-42.

Rubinfeld, B., Albert, I., Porfiri, E., Fiol, C., Munemitsu, S. and Polakis, P. (1996). Binding of GSK3beta to the APC-beta-catenin complex and regulation of complex assembly. *Science* **272**, 1023-6.

Saito, T. and Nakatsuji, N. (2001). Efficient gene transfer into the embryonic mouse brain using in vivo electroporation. *Dev. Biol.* **240**, 237-46.

Salinas, P. C., Fletcher, C., Copeland, N. G., Jenkins, N. A. and Nusse, R. (1994). Maintenance of Wnt-3 expression in Purkinje cells of the mouse cerebellum depends on interactions with granule cells. *Development* **120**, 1277-86.

Sansom, O. J., Reed, K. R., Hayes, A. J., Ireland, H., Brinkmann, H., Newton, I. P., Batlle, E., Simon-Assmann, P., Clevers, H., Nathke, I. S. et al. (2004). Loss of Apc in vivo immediately perturbs Wnt signaling, differentiation, and migration. *Genes Dev.* **18**, 1385-90.

Sato, N., Meijer, L., Skaltsounis, L., Greengard, P. and Brivanlou, A. H. (2004). Maintenance of pluripotency in human and mouse embryonic stem cells through activation of Wnt signaling by a pharmacological GSK-3-specific inhibitor. *Nat. Med.* **10**, 55-63.

Sauer, B. (1998). Inducible gene targeting in mice using the Cre/lox system. *Methods* **14**, 381-92.

Schüller, U., Heine, V. M., Mao, J., Kho, A. T., Dillon, A. K., Han, Y. G., Huillard, E., Sun, T., Ligon, A. H., Qian, Y. et al. (2008). Acquisition of granule neuron precursor identity is a critical determinant of progenitor cell competence to form Shh-induced medulloblastoma. *Cancer Cell* **14**, 123-34.

Schwalbe, E. C., Lindsey, J. C., Straughton, D., Hogg, T. L., Cole, M., Megahed, H., Ryan, S. L., Lusher, M. E., Taylor, M., Gilbertson, R. J. et al. (2011). Rapid diagnosis of medulloblastoma molecular subgroups. *Clin. Cancer Res.* **17**, 1883-94.

Selvadurai, H. J. and Mason, J. O. (2011). Wnt/β-catenin Signalling Is Active in a Highly Dynamic Pattern during Development of the Mouse Cerebellum. *PLoS ONE* **6**, e23012.

Semënov, M. V., Tamai, K., Brott, B. K., Kühl, M., Sokol, S. and He, X. (2001). Head inducer Dickkopf-1 is a ligand for Wnt coreceptor LRP6. *Curr. Biol.* **11**, 951-61.

Shibata, H., Toyama, K., Shioya, H., Ito, M., Hirota, M., Hasegawa, S., Matsumoto, H., Takano, H., Akiyama, T., Toyoshima, K. et al. (1997). Rapid colorectal adenoma formation initiated by conditional targeting of the Apc gene. *Science* **278**, 120-3.

Shimizu, H., Julius, M. A., Giarré, M., Zheng, Z., Brown, A. M. and Kitajewski, J. (1997). Transformation by Wnt family proteins correlates with regulation of beta-catenin. *Cell Growth Differ*. **8**, 1349-58.

Shtutman, M., Zhurinsky, J., Simcha, I., Albanese, C., D'Amico, M., Pestell, R. and Ben-Ze'ev, A. (1999). The cyclin D1 gene is a target of the beta-catenin/LEF-1 pathway. *Proc Natl Acad Sci USA* **96**, 5522-7.

Silbereis, J., Cheng, E., Ganat, Y. M., Ment, L. R. and Vaccarino, F. M. (2009). Precursors with glial fibrillary acidic protein promoter activity transiently generate GABA interneurons in the postnatal cerebellum. *Stem Cells* **27**, 1152-63.

Sillitoe, R. V. and Joyner, A. L. (2007). Morphology, molecular codes, and circuitry produce the three-dimensional complexity of the cerebellum. *Annu. Rev. Cell Dev. Biol.* **23**, 549-77.

Simeone, A. (2000). Positioning the isthmic organizer where Otx2 and Gbx2meet. *Trends Genet*. **16**, 237-40.

Slusarski, D. C., Yang-Snyder, J., Busa, W. B. and Moon, R. T. (1997). Modulation of embryonic intracellular Ca2+ signaling by Wnt-5A. *Dev. Biol.* **182**, 114-20.

Solecki, D. J., Liu, X. L., Tomoda, T., Fang, Y. and Hatten, M. E. (2001). Activated Notch2 signaling inhibits differentiation of cerebellar granule neuron precursors by maintaining proliferation. *Neuron* **31**, 557-68.

Sottile, V., Li, M. and Scotting, P. J. (2006). Stem cell marker expression in the Bergmann glia population of the adult mouse brain. *Brain Res*. **1099**, 8-17.

Srinivas, S., Watanabe, T., Lin, C. S., William, C. M., Tanabe, Y., Jessell, T. M. and Costantini, F. (2001). Cre reporter strains produced by targeted insertion of EYFP and ECFP into the ROSA26 locus. *BMC Dev Biol* **1**, 4.

Stolt, C. C., Lommes, P., Sock, E., Chaboissier, M.-C., Schedl, A. and Wegner, M. (2003). The Sox9 transcription factor determines glial fate choice in the developing spinal cord. *Genes Dev*. **17**, 1677-89.

Su, L. K., Kinzler, K. W., Vogelstein, B., Preisinger, A. C., Moser, A. R., Luongo, C., Gould, K. A. and Dove, W. F. (1992). Multiple intestinal neoplasia caused by a mutation in the murine homolog of the APC gene. *Science* **256**, 668-70.

Sudarov, A. and Joyner, A. L. (2007). Cerebellum morphogenesis: the foliation pattern is orchestrated by multi-cellular anchoring centers. *Neural Dev* **2**, 26.

Sudarov, A., Turnbull, R. K., Kim, E. J., Lebel-Potter, M., Guillemot, F. and Joyner, A. L. (2011). Ascl1 genetics reveals insights into cerebellum local circuit assembly. *J. Neurosci*. **31**, 11055-69.

Tahinci, E., Thorne, C. A., Franklin, J. L., Salic, A., Christian, K. M., Lee, L. A., Coffey, R. J. and Lee, E. (2007). Lrp6 is required for convergent extension during Xenopus gastrulation. *Development* **134**, 4095-106.

Takada, R., Satomi, Y., Kurata, T., Ueno, N., Norioka, S., Kondoh, H., Takao, T. and Takada, S. (2006). Monounsaturated fatty acid modification of Wnt protein: its role in Wnt secretion. *Developmental Cell* **11**, 791-801.

Tamai, K., Zeng, X., Liu, C., Zhang, X., Harada, Y., Chang, Z. and He, X. (2004). A mechanism for Wnt coreceptor activation. *Mol. Cell* **13**, 149-56.

Tan, K. and Le Douarin, N. M. (1991). Development of the nuclei and cell migration in the medulla oblongata. Application of the quail-chick chimera system. *Anat. Embryol. (Berl).* **183**, 321-43.

Taylor, M., Liu, L., Raffel, C., Hui, C., Mainprize, T., Zhang, X., Agatep, R., Chiappa, S., Gao, L., Lowrance, A. et al. (2002). Mutations in SUFU predispose to medulloblastoma. *Nat. Genet.* **31**, 306-10.

Taylor, M., Mainprize, T. G. and Rutka, J. (2000). Molecular insight into medulloblastoma and central nervous system primitive neuroectodermal tumor biology from hereditary syndromes: a review. *Neurosurgery* **47**, 888-901.

Tetsu, O. and McCormick, F. (1999). Beta-catenin regulates expression of cyclin D1 in colon carcinoma cells. *Nature* **398**, 422-6.

Thomas, K. R. and Capecchi, M. R. (1990). Targeted disruption of the murine int-1 proto-oncogene resulting in severe abnormalities in midbrain and cerebellar development. *Nature* **346**, 847-50.

Thompson, M., Fuller, C., Hogg, T. L., Dalton, J., Finkelstein, D., Lau, C. C., Chintagumpala, M., Adesina, A., Ashley, D. M., Kellie, S. J. et al. (2006). Genomics identifies medulloblastoma subgroups that are enriched for specific genetic alterations. *J. Clin. Oncol.* **24**, 1924-31.

Tomoda, T., Bhatt, R. S., Kuroyanagi, H., Shirasawa, T. and Hatten, M. E. (1999). A mouse serine/threonine kinase homologous to C. elegans UNC51 functions in parallel fiber formation of cerebellar granule neurons. *Neuron* **24**, 833-46.

Truett, G., E., Heeger, P., Mynatt, R., L., Truett, A., A., Walker, J., A. and Warman, M., L. (2000). Preparation of PCR-quality mouse genomic DNA with hot sodium hydroxide and tris (HotSHOT). *Biotechniques* **29**, 52-54.

Tyrrell, T. and Willshaw, D. (1992). Cerebellar cortex: its simulation and the relevance of Marr's theory. *Philos Trans R Soc Lond, B, Biol Sci* **336**, 239-57.

van Amerongen, R. and Nusse, R. (2009). Towards an integrated view of Wnt signaling in development. *Development* **136**, 3205-14.

van de Wetering, M., Sancho, E., Verweij, C., de Lau, W., Oving, I., Hurlstone, A., van der Horn, K., Batlle, E., Coudreuse, D., Haramis, A. P. et al. (2002). The beta-catenin/TCF-4 complex imposes a crypt progenitor phenotype on colorectal cancer cells. *Cell* **111**, 241-50.

Vinson, C. R. and Adler, P. N. (1987). Directional non-cell autonomy and the transmission of polarity information by the frizzled gene of Drosophila. *Nature* **329**, 549-51.

Waddington, C. H. (1940). Organisers and Genes. Cambridge: Cambridge University Press.

Wallace, V. A. and Raff, M. C. (1999). A role for Sonic hedgehog in axon-to-astrocyte signalling in the rodent optic nerve. *Development* **126**, 2901-9.

Wallingford, J. B. and Habas, R. (2005). The developmental biology of Dishevelled: an enigmatic protein governing cell fate and cell polarity. *Development* **132**, 4421-36.

Wang, V. Y., Rose, M. F. and Zoghbi, H. Y. (2005). Math1 expression redefines the rhombic lip derivatives and reveals novel lineages within the brainstem and cerebellum. *Neuron* **48**, 31-43.

Wang, V. Y. and Zoghbi, H. Y. (2001). Genetic regulation of cerebellar development. *Nat Rev Neurosci* **2**, 484-91.

Wang, X., Imura, T., Sofroniew, M. and Fushiki, S. (2011). Loss of adenomatous polyposis coli in Bergmann glia disrupts their unique architecture and leads to cell nonautonomous neurodegeneration of cerebellar Purkinje neurons. *Glia* **59**, 857-68.

Wechsler-Reya, R. J. and Scott, M. P. (1999). Control of neuronal precursor proliferation in the cerebellum by Sonic Hedgehog. *Neuron* **22**, 103-14.

Weisheit, G., Gliem, M., Endl, E., Pfeffer, P. L., Busslinger, M. and Schilling, K. (2006). Postnatal development of the murine cerebellar cortex: formation and early dispersal of basket, stellate and Golgi neurons. *Eur. J. Neurosci.* **24**, 466-78.

Wexler, E. M., Paucer, A., Kornblum, H. I., Palmer, T. D., Plamer, T. D. and Geschwind, D. H. (2009). Endogenous Wnt signaling maintains neural progenitor cell potency. *Stem Cells* **27**, 1130-41.

Weyer, A. and Schilling, K. (2003). Developmental and cell type-specific expression of the neuronal marker NeuN in the murine cerebellum. *J. Neurosci. Res.* **73**, 400-9.

Wilkinson, D. G., Bailes, J. A. and McMahon, A. P. (1987). Expression of the proto-oncogene int-1 is restricted to specific neural cells in the developing mouse embryo. *Cell* **50**, 79-88.

Willert, K., Brown, J. D., Danenberg, E., Duncan, A. W., Weissman, I. L., Reya, T., Yates, J. R. and Nusse, R. (2003). Wnt proteins are lipid-modified and can act as stem cell growth factors. *Nature* **423**, 448-52.

Wingate, R. J. (2001). The rhombic lip and early cerebellar development. *Curr. Opin. Neurobiol.* **11**, 82-8.

Wingate, R. J. and Hatten, M. E. (1999). The role of the rhombic lip in avian cerebellum development. *Development* **126**, 4395-404.

Woodhead, G. J., Mutch, C. A., Olson, E. C. and Chenn, A. (2006). Cell-autonomous beta-catenin signaling regulates cortical precursor proliferation. *J. Neurosci.* **26**, 12620-30.

Wurst, W., Auerbach, A. B. and Joyner, A. L. (1994). Multiple developmental defects in Engrailed-1 mutant mice: an early mid-hindbrain deletion and patterning defects in forelimbs and sternum. *Development* **120**, 2065-75.

Xu, Q., Wang, Y., Dabdoub, A., Smallwood, P. M., Williams, J., Woods, C., Kelley, M. W., Jiang, L., Tasman, W., Zhang, K. et al. (2004). Vascular development in the retina and inner ear: control by Norrin and Frizzled-4, a high-affinity ligand-receptor pair. *Cell* **116**, 883-95.

Yaguchi, Y., Yu, T., Ahmed, M., Berry, M., Mason, I. and Basson, M. A. (2009). Fibroblast growth factor (FGF) gene expression in the developing cerebellum suggests multiple roles for FGF signaling during cerebellar morphogenesis and development. *Dev. Dyn.* **238**, 2058-72.

Yamada, K., Fukaya, M., Shibata, T., Kurihara, H., Tanaka, K., Inoue, Y. and Watanabe, M. (2000). Dynamic transformation of Bergmann glial fibers proceeds in correlation with dendritic outgrowth and synapse formation of cerebellar Purkinje cells. *J. Comp. Neurol.* **418**, 106-20.

Yamada, K. and Watanabe, M. (2002). Cytodifferentiation of Bergmann glia and its relationship with Purkinje cells. *Anat Sci Int* **77**, 94-108.

Yamada, M., Terao, M., Terashima, T., Fujiyama, T., Kawaguchi, Y., Nabeshima, Y. and Hoshino, M. (2007). Origin of climbing fiber neurons and their developmental dependence on Ptf1a. *J. Neurosci.* **27**, 10924-34.

Yamaguchi, T. P., Bradley, A., McMahon, A. P. and Jones, S. (1999). A Wnt5a pathway underlies outgrowth of multiple structures in the vertebrate embryo. *Development* **126**, 1211-23.

Yamashita, Y. M., Jones, D. L. and Fuller, M. T. (2003). Orientation of asymmetric stem cell division by the APC tumor suppressor and centrosome. *Science* **301**, 1547-50.

Ying, Q., Wray, J., Nichols, J., Batlle-Morera, L., Doble, B., Woodgett, J., Cohen, P. and Smith, A. (2008). The ground state of embryonic stem cell self-renewal. *Nature* **453**, 519-23.

You, Z., Saims, D., Chen, S., Zhang, Z., Guttridge, D. C., Guan, K.-L., MacDougald, O. A., Brown, A. M. C., Evan, G., Kitajewski, J. et al. (2002). Wnt signaling promotes oncogenic transformation by inhibiting c-Myc-induced apoptosis. *J. Cell Biol.* **157**, 429-40.

Yu, T., Yaguchi, Y., Echevarria, D., Martinez, S. and Basson, M. A. (2011). Sprouty genes prevent excessive FGF signalling in multiple cell types throughout development of the cerebellum. *Development* **138**, 2957-68.

Yuasa, S. (1996). Bergmann glial development in the mouse cerebellum as revealed by tenascin expression. *Anat Embryol* **194**, 223-34.

Zeng, X., Huang, H., Tamai, K., Zhang, X., Harada, Y., Yokota, C., Almeida, K., Wang, J., Doble, B., Woodgett, J. et al. (2008). Initiation of Wnt signaling: control of Wnt coreceptor Lrp6 phosphorylation/activation via frizzled, dishevelled and axin functions. *Development* **135**, 367-75.

Zeng, X., Tamai, K., Doble, B., Li, S., Huang, H., Habas, R., Okamura, H., Woodgett, J. and He, X. (2005). A dual-kinase mechanism for Wnt co-receptor phosphorylation and activation. *Nature* **438**, 873-7.

Zervas, M., Millet, S., Ahn, S. and Joyner, A. L. (2004). Cell behaviors and genetic lineages of the mesencephalon and rhombomere 1. *Neuron* **43**, 345-57.

Zhang, L. and Goldman, J. E. (1996). Generation of cerebellar interneurons from dividing progenitors in white matter. *Neuron* **16**, 47-54.

Zhang, N., Wei, P., Gong, A., Chiu, W. T., Lee, H. T., Colman, H., Huang, H., Xue, J., Liu, M., Wang, Y. et al. (2011a). FoxM1 Promotes β-Catenin Nuclear Localization and Controls Wnt Target-Gene Expression and Glioma Tumorigenesis. *Cancer Cell* **20**, 427-42.

Zhang, X., Santuccione, A., Leung, C. and Marino, S. (2011b). Differentiation of postnatal cerebellar glial progenitors is controlled by Bmi1 through BMP pathway inhibition. *Glia* **59**, 1118-31.

Zhen, Y., Sørensen, V., Jin, Y., Suo, Z. and Wiedłocha, A. (2007). Indirubin-3'-monoxime inhibits autophosphorylation of FGFR1 and stimulates ERK1/2 activity via p38 MAPK. *Oncogene* **26**, 6372-85.

Zhou, C. J., Borello, U., Rubenstein, J. L. and Pleasure, S. J. (2006). Neuronal production and precursor proliferation defects in the neocortex of mice with loss of function in the canonical Wnt signaling pathway. *Neuroscience* **142**, 1119-31.

Zimmerman, L., Parr, B., Lendahl, U., Cunningham, M., McKay, R., Gavin, B., Mann, J., Vassileva, G. and McMahon, A. (1994). Independent regulatory elements in the nestin gene direct transgene expression to neural stem cells or muscle precursors. *Neuron* **12**, 11-24.

Zumbrunn, J., Kinoshita, K., Hyman, A. A. and Näthke, I. S. (2001). Binding of the adenomatous polyposis coli protein to microtubules increases microtubule stability and is regulated by GSK3 beta phosphorylation. *Curr. Biol.* **11**, 44-9.

Zurawel, R. H., Chiappa, S. A., Allen, C. and Raffel, C. (1998). Sporadic medulloblastomas contain oncogenic beta-catenin mutations. *Cancer Res.* **58**, 896-9.

9 Appendices

Appendix 1 – Reference gene selection

qRT-PCR data for *EIF4A2* vs *18s* across all samples and biological replicates.

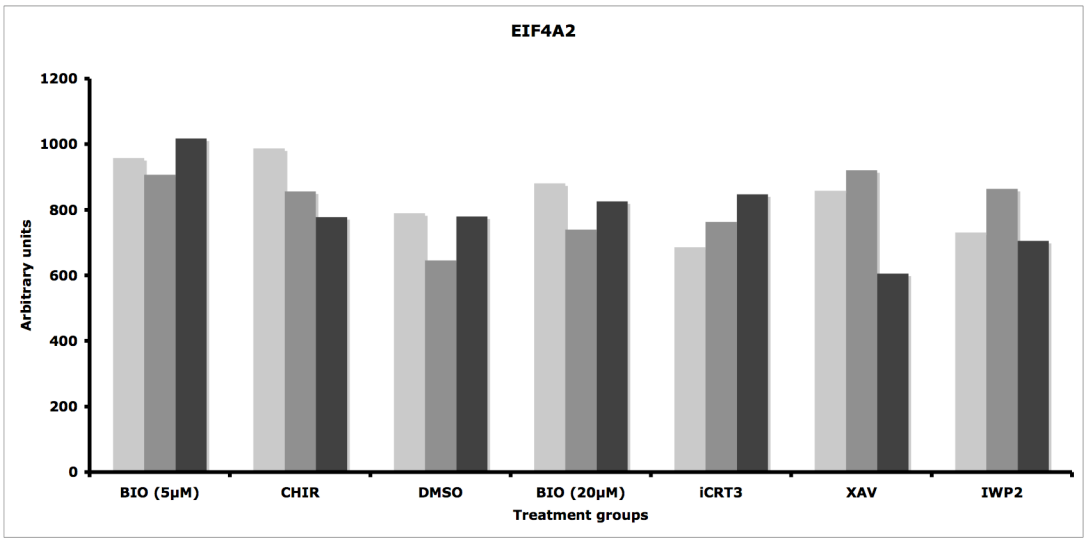

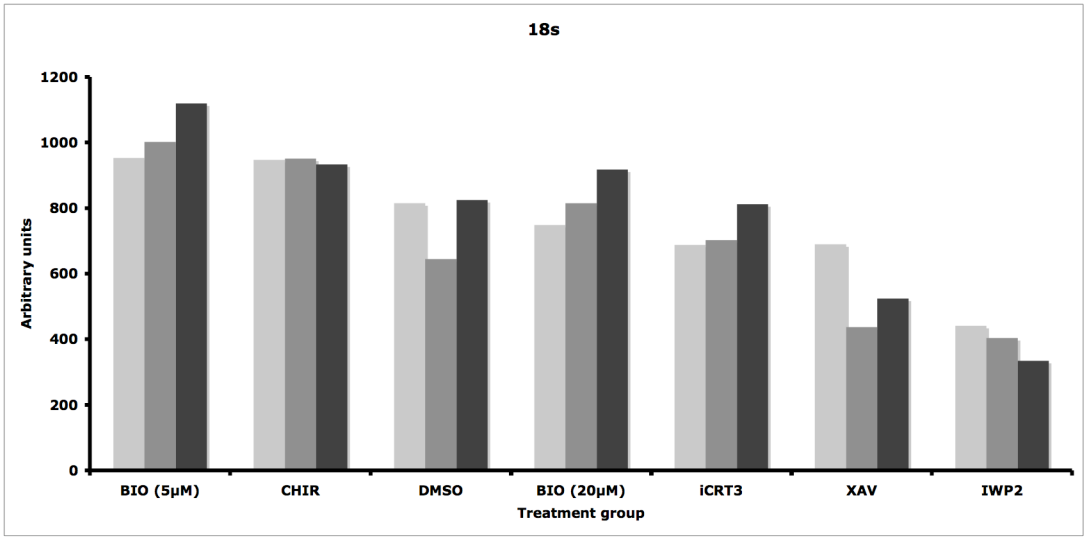

Appendix 2 – Phenol-chloroform isoamyl alcohol DNA precipitation

1. Add one volume of phenol-chloroform isoamyl alcohol (1:1) to linearised plasmid

2. Mix till emulsion forms

3. Centrifuge >13,000 RPM for five minutes, keep supernatant

4. Add 0.1 volume NaAc (3M). Mix

5. Add two volumes -20°C absolute ethanol. Mix, leave at -20°C for >1hr

6. Centrifuge ten minutes, discard supernatant

7. Add one volume 80% ethanol, centrifuge five minutes, discard supernatant

8. Dry pellet, resuspend in 50 μl nuclease free H_2O. Store at -20°C

Appendix 3 – Solutions used for RNA *in situ* hybridisation

Hybridisation buffer

50% formamide	(Fisher)
10% dextran sulfate	(Sigma)
1 mg/ml yeast RNA	(BM)
1x Denhardt's	(Invitrogen)
1x Salt	

Wash buffer

50% formamide	(Fisher)
1x SSC	
0.1% Tween-20	(Sigma)

MABT

100 mM maleic acid	
150 mM NaCl (pH 7.5)	
0.1% Tween-20	(Sigma)

Blocking solution

MABT	
20% Sheep serum	(Sigma)
2% Blocking reagent	(BM)

Pre-staining buffer (pH 9.5)

100 mM NaCl	
50 mM $MgCl_2$	
100 mM Tris	
0.1% Tween-20	(Sigma)

NBT/BCIP staining buffer

100 mM NaCL

50 mM $MgCl_2$

100 mM Tris-HCl (pH 9.5)

0.1% Tween-20	(Sigma)
10% Polyvinyl alcohol	(Sigma)
2% NBT/BCIP	(Roche)

Appendix 4 – Additional electroporation data at E14.5-E16.5

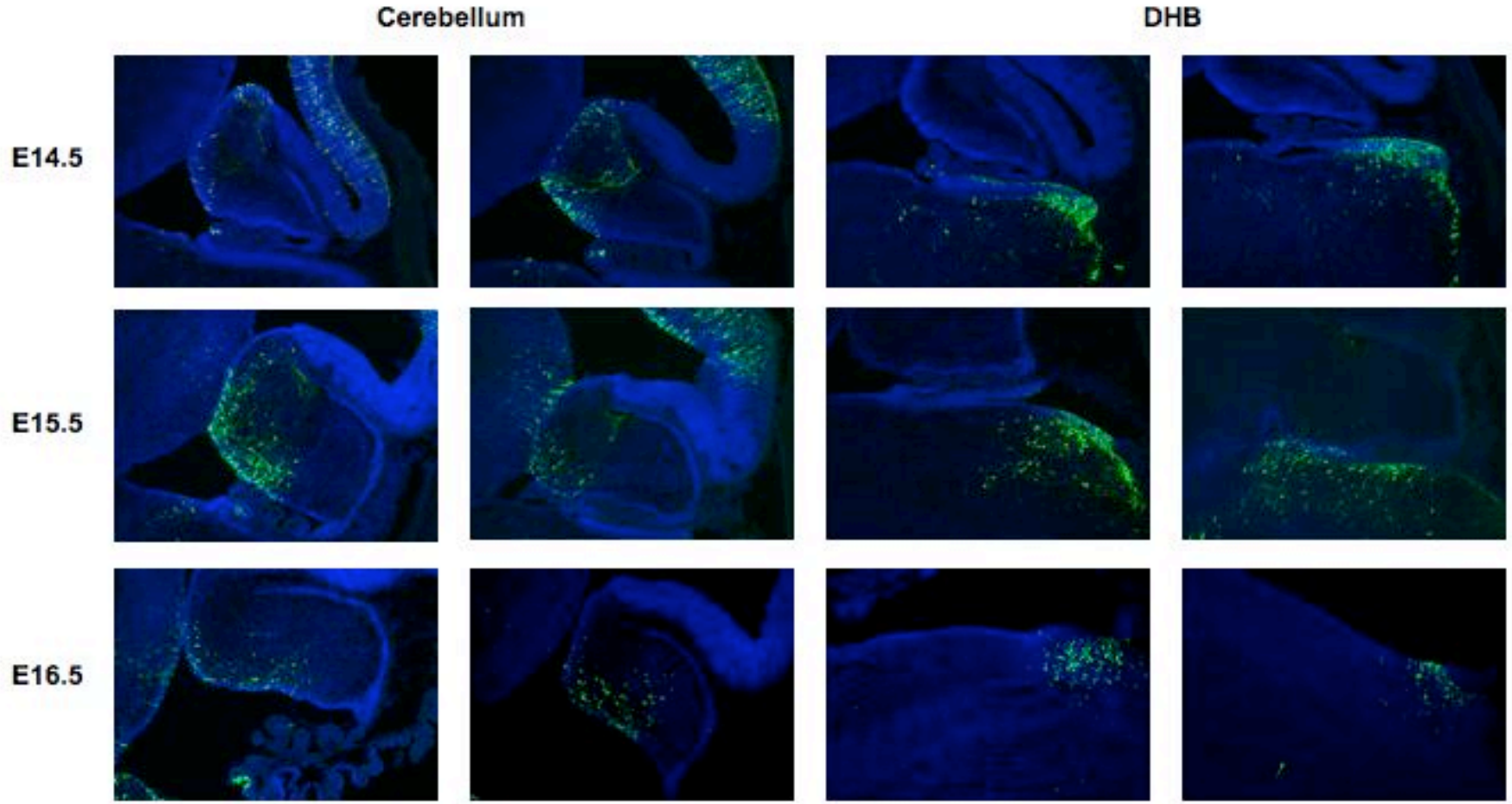

Appendix 5 – Additional electroporation data at E18.5

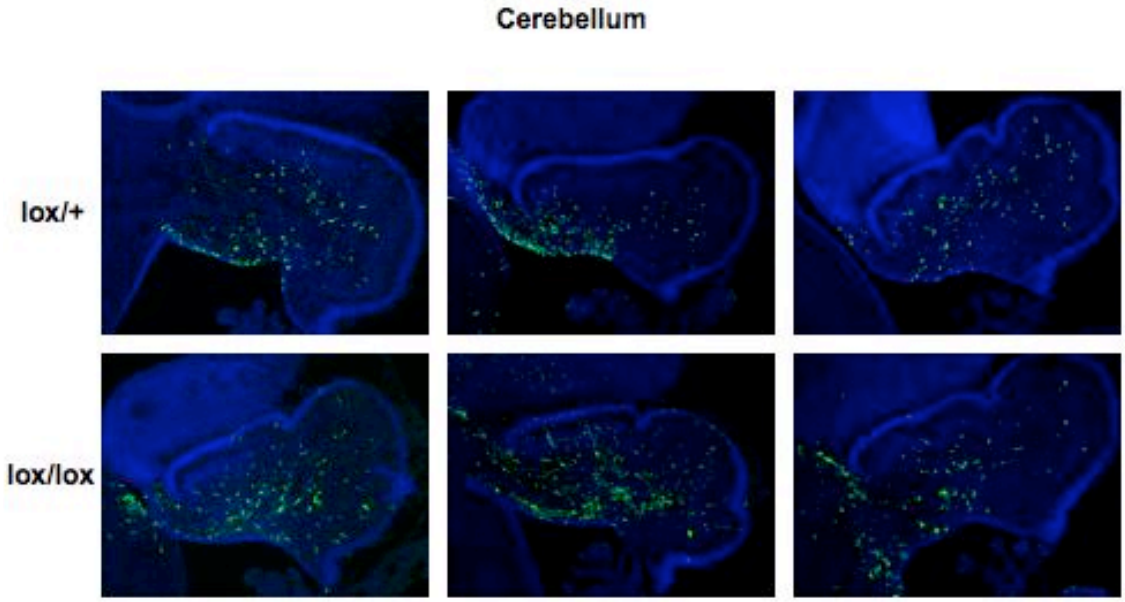

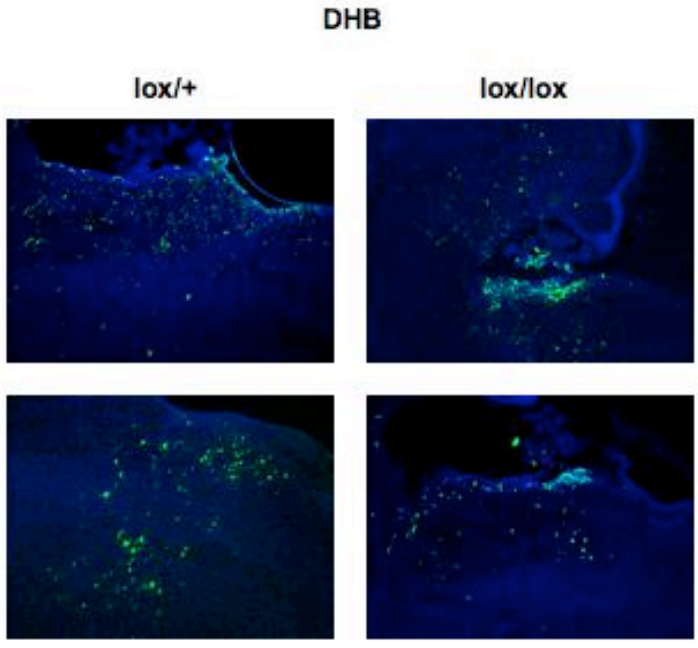

Appendix 6 – Comparison of GFP expression between genotypes

Total GFP+ cells/section compared between *Apc* genotype and *R26YFP* genotype

Animal ID	***Apc* genotype**	***R26YFP* genotype**	**Ave GFP+ cells/section**
APCFLX 20.1	*Lox/+*	*YFP-*	85.67
APCFLX 29.2	*Lox/+*	*YFP+*	171.33
APCFLX 29.3	*Lox/+*	*YFP+*	109.67
APCFLX 33.3	*Lox/+*	*YFP-*	96
APCFLX 23.1	*Lox/Lox*	*YFP+*	153.67
APCFLX 23.2	*Lox/Lox*	*YFP+*	168.67
APCFLX 29.1	*Lox/Lox*	*YFP+*	248.33
APCFLX 33.1	*Lox/Lox*	*YFP-*	73

Appendix 7 – Publications

Selvadurai, H. J. and Mason, J. O. (2011). Wnt/β-catenin Signalling is Active in a Highly Dynamic Pattern during Development of the Mouse Cerebellum. *PLoS ONE* **6**, e23012.

OPEN ACCESS Freely available online

PLoS one

Wnt/β-catenin Signalling Is Active in a Highly Dynamic Pattern during Development of the Mouse Cerebellum

Hayden J. Selvadurai, John O. Mason*

Centre for Integrative Physiology, School of Biomedical Sciences, University of Edinburgh, Edinburgh, United Kingdom

Abstract

The adult cerebellum is composed of several distinct cell types with well defined developmental origins. However, the molecular mechanisms that govern the generation of these cell types are only partially resolved. Wnt/β-catenin signalling has a wide variety of roles in generation of the central nervous system, though the specific activity of this pathway during cerebellum development is not well understood. Here, we present data that delineate the spatio-temporal specific pattern of Wnt/β-catenin signaling during mouse cerebellum development between E12.5 and P21. Using the BAT-gal Wnt/β-catenin reporter mouse, we found that Wnt/β-catenin activity is present transiently at the embryonic rhombic lip but not at later stages during the expansion of cell populations that arise from there. At late embryonic and early postnatal stages, Wnt/β-catenin activity shifts to the cerebellar ventricular zone and to cells arising from this germinal centre. Subsequently, the expression pattern becomes progressively restricted to Bergmann glial cells, which show expression of the reporter at P21. These results indicate a variety of potential functions for Wnt/β-catenin activity during cerebellum development.

Citation: Selvadurai HJ, Mason JO (2011) Wnt/β-catenin Signalling Is Active in a Highly Dynamic Pattern during Development of the Mouse Cerebellum. PLoS ONE 6(8): e23012. doi:10.1371/journal.pone.0023012

Editor: Cara Gottardi, Northwestern University Feinberg School of Medicine, United States of America

Received April 18, 2011; **Accepted** July 8, 2011; **Published** August 8, 2011

Funding: This work was funded by award number 083209/Z/07/A from the Wellcome Trust, www.wellcome.ac.uk. The funders had no role in study design, data collection and analysis, decision to publish, or preparation of the manuscript.

Competing Interests: The authors have declared that no competing interests exist.

* E-mail: john.mason@ed.ac.uk

Introduction

The cerebellum forms as a result of a highly regulated programme of cell specification, proliferation, differentiation and migration (reviewed in [1]). At the cellular level, the cerebellum is organised into distinct neuronal layers: the outermost molecular layer (ML), the Purkinje cell monolayer (PCL), the densely populated internal granule layer (IGL) and the innermost white matter (WM). The diverse cell types that make up these layers originate from two distinct germinal centres in the early cerebellum; the ventricular zone - a monolayer of cells lining the fourth ventricle on the ventral surface of the cerebellar anlage, and the rhombic lip - a transient structure in the most posterior part of the cerebellar anlage that forms the interface between the neural tube and non-neural roofplate ectoderm (reviewed in [2]).

The rhombic lip gives rise to the entire complement of glutamatergic neurons that populate the IGL. The first glutamatergic neurons born are the projection neurons of the deep cerebellar nuclei (DCN). In the mouse these arise between embryonic day (E) 10.5 and E12.5 [3], and migrate along the sub pial stream to the rostral end of the developing cerebellum. From E12.5 onwards, the rhombic lip generates granule progenitor cells (GPCs) and unipolar brush cells (UBCs) [4,5,6]. Exiting the rhombic lip, GPCs migrate rostrally across the pial surface of the cerebellum to form a secondary germinal zone, the external germinal layer (EGL), which covers the pial surface of the cerebellum. This cell layer proliferates extensively until the second postnatal week, producing a vast number of mature granule cells (GCs), which become post-mitotic within the EGL before migrating radially along Bergmann glial fibres into the IGL, a process that is complete by postnatal day (P) 21 [1,7,8].

Distinct from the rhombic lip, the ventricular zone gives rise to all cerebellar cells of the γ-aminobutyric acid (GABA)ergic, and glial lineages. The first of these, the Purkinje cells, are born from E10.5 then migrate radially towards the pial surface of the cerebellum and settle as a distinct monolayer of cells around the time of birth (E19.5-E20) [9]. Closely following this the Bergmann glia are generated and migrate radially behind the developing Purkinje cell population before undergoing morphological maturation postnatally [10,11]. Interneurons (including stellate, basket, Golgi and Lugaro interneurons) and the remaining glial population (velate and fibrous astrocytes) are then generated in a sequential manner. These cell types are derived from progenitors that delaminate from the ventricular zone and continue to divide in the WM [12,13,14,15,16,17].

These tightly coordinated developmental processes rely on the spatio-temporal specific activity of several key signalling pathways. The sonic hedgehog (Shh) signalling pathway, for example, is the main mitogenic factor driving GPC proliferation within the EGL [18,19]. The Wnt/β-catenin signalling pathway has been shown to play an important part in regulation of neural stem and progenitor populations within the central nervous system [20,21], but its role in cerebellum development is only partially defined. Wnt1 is an important regulator of early cerebellum development. It is expressed at the isthmus and rhombic lip [22,23,24,25], and in cells of the granule lineage [26] and *Wnt1*$^{-/-}$ mutant mice completely lack or exhibit a severely underdeveloped cerebellum [27,28,29]. No specific role for Wnt/β-catenin signalling in later stages of cerebellum development has yet been described. However, activating mutations in components of the Wnt/β-catenin signalling pathway have been identified in medulloblastomas, a paediatric tumour that arises in the posterior fossa

(cerebellum plus brainstem) [30,31]. Further, individuals carrying germline mutations in the tumour suppressor gene *APC* that constitutively activate Wnt/β-catenin signalling have a greatly elevated risk of developing medullobastoma [32]. This raises the possibility that Wnt/β-catenin signalling regulates developmental processes in the cerebellum, and that activation of this pathway may cause these processes to go awry, predisposing to the development of medulloblastoma (reviewed in [33]). Recent *in vivo* evidence supports this [34].

In order to investigate possible roles played by Wnt/β-catenin signalling during development of the cerebellum, we used the BAT-gal reporter transgenic mouse strain [35] to identify regions of the developing cerebellum where Wnt/β-catenin signalling is active. At mid-gestational stages, we found active Wnt/β-catenin signalling in the rhombic lip. At perinatal stages, activity was seen in the ventricular zone, but not in the EGL. Postnatally, signalling became progressively more restricted, and very few proliferating cells expressed the BAT-gal transgene. Surprisingly, we found that many of the Wnt/β-catenin responsive cells in the postnatal cerebellum were Bergmann glia.

Results

Wnt/β-catenin signalling is active at the isthmus and rhombic lip

The BAT-gal transgenic reporter strain expresses a *lacZ* gene under the control of β-catenin/T cell factor (TCF) responsive elements [35] and has been widely used as a general reporter of Wnt/β-catenin activity. We first examined the expression of β-galactosidase (the protein product of the *LacZ* transgene) from E12.5 to E14.5 in cerebellum sections from BAT-gal+ embryos. β-galactosidase expression was observed in a progressively restricted pattern (Fig. 1). Firstly, at E12.5 expression was observed at the isthmus in the anterior region of the cerebellum and at the rhombic lip forming the posterior region of the cerebellum (Fig. 1A). In addition β-galactosidase expressing (β-gal+) cells were observed spread diffusely through the anterior and posterior regions of the cerebellum, although were notably sparse within the ventricular zone.

In contrast, at E14.5 β-galactosidase expression was more restricted to the anterior and posterior ends of the cerebellum. While β-gal+ cells were absent from the ventricular zone, they were observed clearly at the rhombic lip (Fig. 1B). Staining for proliferating cell nuclear antigen (PCNA), which marks proliferating cells including those in the rhombic lip area, confirmed the presence of β-gal+ cells at the rhombic lip and within the population of early GPCs that have begun to migrate in an anterior direction along the pial surface of the cerebellum (arrowheads in Fig. 1B–C).

Since β-galactosidase protein is a stable protein and can persist in tissue after *lacZ* gene expression ceases [36], we also examined expression of *lacZ* mRNA by in situ hybridization (Fig. 1D–E). The expression pattern found was very similar to that observed by

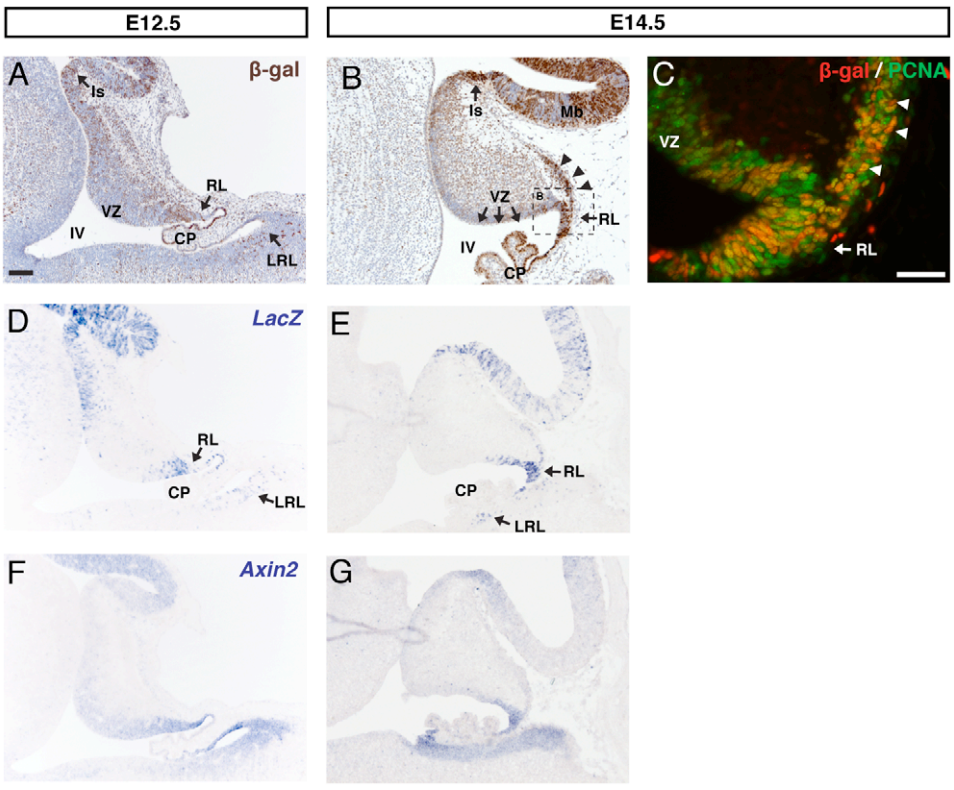

Figure 1. BAT-gal expression in the E12.5 and E14.5 cerebellum. (A) DAB Immunohistochemistry for β-galactosidase (β-gal) on sagittal sections of E12.5 cerebellum revealed two key expression domains: the isthmus (Is) and the cerebellar rhombic lip (RL). At E14.5 (B) expression was also found in the early external granule layer (EGL, black arrowheads) but was notably absent from the ventricular zone (VZ) lining the fourth ventricle (IV). (C) Double immunofluorescence for β-gal and PCNA confirms the expression of β-gal in the RL and EGL (white arrowheads). β-gal protein was validated as a Wnt/β-catenin reporter by *in situ* hybridisation for *LacZ* (D, E) and Wnt target *Axin2* (F, G)) mRNA. At both time points β-gal protein and *LacZ* mRNA were expressed in the same domains as *Axin2*, although the *LacZ* mRNA expression appeared less diffuse than that of *Axin2*. (A–B counterstained with hematoxylin. Scale bars: A, B, D–E = 100 μm, B = 50 μM).
doi:10.1371/journal.pone.0023012.g001

immunohistochemistry (compare Fig. 1A to 1D and 1B to 1E), although there are slight differences that would suggest the β-galactosidase protein expression may to some extent label cells that are no longer responding to a Wnt/β-catenin signal. For example, β-galactosidase protein expression was found in the dorsal aspect of the choroid plexus, whereas the expression of *LacZ* mRNA is restricted to the rhombic lip. Importantly however, the key β-gal protein expression domains identified (rhombic lip and isthmus) mirror those of the *LacZ* expression.

As an independent verification that BAT-gal reporter expression in the developing cerebellum truly indicates Wnt/β-catenin activity we also performed *in situ* hybridisation for *Axin2*. *Axin2* encodes a negative feedback inhibitor of the Wnt/β-catenin signalling pathway. It is a direct target of TCF/LEF-mediated transcription and is therefore widely used as a readout of Wnt/β-catenin signalling [37]. Within the isthmus and the rhombic lip, the expression of *Axin2* (Fig. 1F–G) closely mirrored both *LacZ* mRNA expression (Fig. 1D–E) and β-galactosidase protein expression (Fig. 1A–B). However, at E12.5, *Axin2* expression was not detected in the anterior portion of the cerebellum immediately below the isthmus (Fig. 1F). At E12.5 and E14.5, *Axin2* showed more diffuse expression in a gradient from both the upper and the lower rhombic lips (Fig. 1F–G), compared to both *LacZ* staining and β-galactosidase protein expression.

Wnt/β-catenin signalling is active in the ventricular zone but not in the EGL of the perinatal cerebellum

We next examined BAT-gal reporter expression at two perinatal stages, E18.5 and P1. In contrast to the highly restricted expression of β-galactosidase seen at E14.5, we found much more widespread expression at these time points (Fig. 2). β-gal+ cells were spread through several developing cell layers of the cerebellum, though were notably absent from the EGL (Fig. 2A–B). This pattern is also observed in the expression of *LacZ* (Fig. 2C–D), indicating that perdurance of β-galactosidase is not a significant issue at these ages.

While the rhombic lip and early migratory GPCs showed abundant expression of β-galactosidase at E14.5, the absence of detectable β-galactosidase expression within the EGL of the perinatal cerebellum suggests that Wnt/β-catenin signalling is not involved in the continued development of this cell population. PCNA staining clearly labels the EGL at E18.5 and P1 and co-staining for β-galactosidase clearly supported the lack of β-gal+ cells in the EGL at these stages (Fig. 2E–F).

An abundance of β-gal+ cells were identified in the cerebellar ventricular zone at E18.5 (Fig. 2A) and P1 (Fig. 2B), in contrast to E14.5. PCNA labelling clearly delineates the ventricular zone at these stages, visible as a thin layer of cells lining the fourth ventricle. Double staining for β-galactosidase and PCNA confirmed the presence of proliferative β-gal+ cells within the ventricular zone (arrowheads in Fig. 2G–H). Interestingly, by P1 there were a number of β-gal+ cells that did not express PCNA, indicative of a non-proliferative cell type. β-gal+ cells were also found within the developing cerebellar anlage, consistent with cells migrating from the progenitor monolayer (Fig. 2E–H). Some of these were PCNA-positive (arrowheads in Fig. 2E–F).

Wnt/β-catenin signalling becomes increasingly restricted and does not correlate with proliferation during postnatal development

We next examined patterns of BAT-gal reporter expression at later postnatal stages. By P5, all of the layers that make up the mature cerebellum (WM, IGL, PCL, ML) can be identified - along

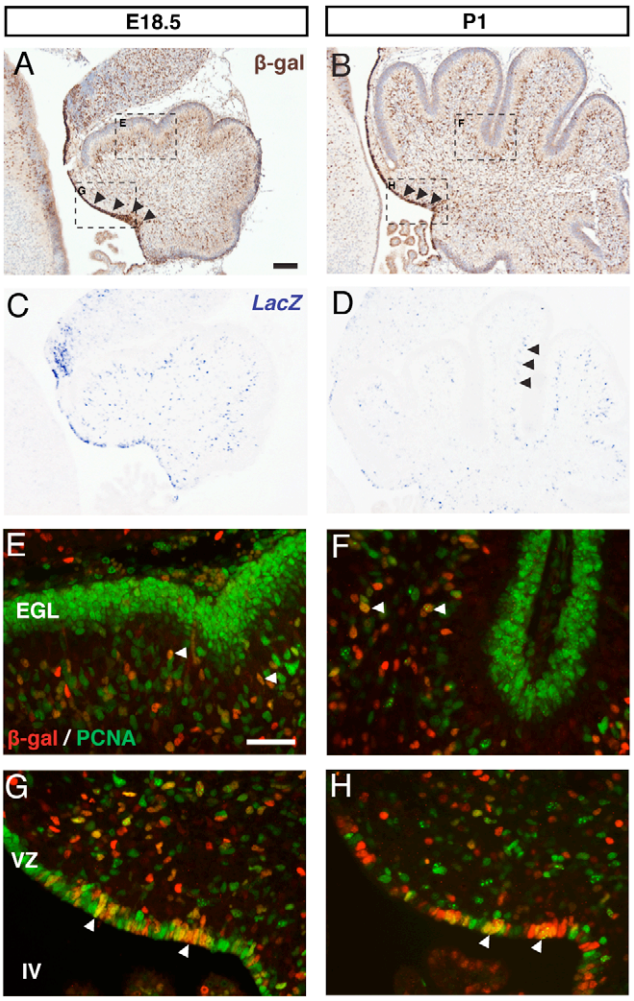

Figure 2. BAT-gal expression in the E18.5 and P1 cerebellum. DAB immunohistochemistry for β-gal in sagittal sections of the E18.5 cerebellum (A) reveals widespread expression, including predominant staining in the VZ (black arrowheads). A similar pattern is observed at P1 (B). These expression patterns are mirrored by those observed for *LacZ* mRNA visualised with in situ hybridisation (C–D). Double immunofluorescence for β-gal and PCNA reveals an almost complete lack of BAT-gal reporter expression in the EGL at both E18.5 (E) and P1 (F), though β-gal+ cells can be observed within the developing cerebellum at both time points, in some cases colocalised with PCNA (white arrows). At the VZ, BAT-gal expression can be observed colocalised with PCNA (white arrowheads) at both E18.5 (G) and P1 (H). (A–B counterstained with hematoxylin. Scale bars: A, B = 100 μm, E–H = 50 μm).
doi:10.1371/journal.pone.0023012.g002

with the transient EGL. We found β-gal+ cells in each of these layers, except for the EGL (Fig. 3A–B). A similar pattern was observed at P10 (Fig. 4A–B), although β-gal+ cells were most abundant within the PCL and WM at this stage. Increasingly restricted distribution was also seen at P21, by which time β-gal+ cells were largely restricted to the PCL (Fig. 5A–B). This pattern was also observed in the expression of *LacZ* mRNA (Fig. 3B, 4B), further illustrating that β-galactosidase immunohistochemistry accurately reflects expression of the BAT-gal transgene till P10. However, by P21 there was no identifiable expression of *LacZ* mRNA (data not shown) indicating that the β-gal+ cell types identified at that late stage may no longer be responding to a Wnt/β-catenin signal and could be maintaining detectable levels of the

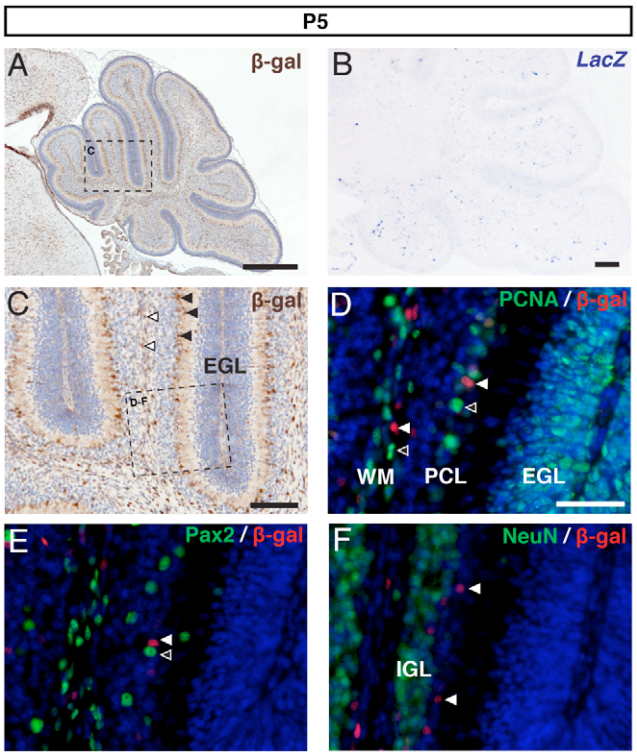

Figure 3. BAT-gal expression in the P5 cerebellum. (A) DAB immunohistochemistry for β-gal and (B) *LacZ* in situ hybridisation in the P5 cerebellum. (C) Higher magnification of the region boxed in (A) reveals expression spread through all layers except the EGL. The Purkinje cell layer (PCL) and the white matter (WM) in particular contained many β-gal+ cells (black and white arrowheads respectively). Double immunofluorescence for β-gal and PCNA (D) revealed the presence of β-gal+ cells within the PCL and white matter (white arrowheads). Although β-gal+ cells were observed in close proximity to proliferating cells (unfilled arrowheads) very few β-gal+/PCNA+ cells were observed. Double immunofluorescence for β-gal and Pax2 (E) showed the close proximity of β-gal+ cells (white arrowhead) to Pax2+ interneurons (unfilled arrowhead) but no double-labelled cells were observed. Double immunofluorescence for β-gal and NeuN showed β-gal+ cells (white arrows) located outwith the IGL. (A,C counterstained with hematoxylin and D–F with Topro3. Scale bars: A = 500 μm, B–C = 100 μm, D–E = 50 μm).
doi:10.1371/journal.pone.0023012.g003

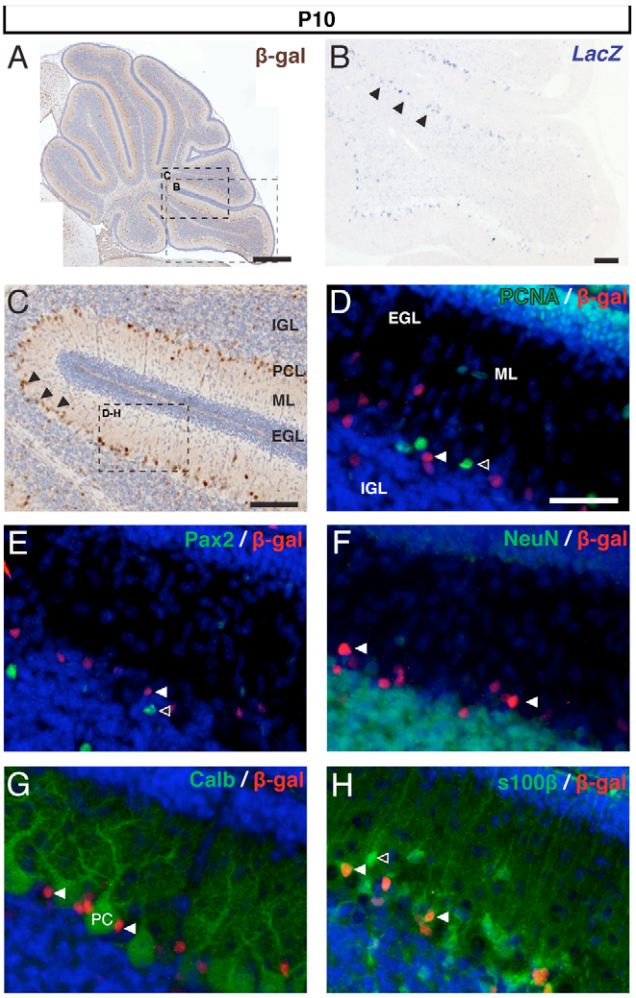

Figure 4. BAT-gal expression in the P10 cerebellum. (A) DAB β-gal immunohistochemistry and (B) *LacZ* in situ hybridisation in P10 cerebellum. (C) Higher magnification of the region boxed in (A) reveals a more restricted pattern than that seen at P5, with strongest staining observed within the PCL (black arrowheads – also in B). At higher magnification, β-gal+ cells within the PCL (white arrowheads) were observed in close proximity to both PCNA+ (D) and Pax2+ (E) cells (unfilled arrowheads), though no colocalisation was observed between β-gal and PCNA or Pax2. (F) Double immunofluorescence for β-gal and NeuN confirms the presence of β-gal+ cells at the PCL on the edge of the IGL, while double immunofluorescence for β-gal and calbindin (G) confirms the lack of BAT-gal reporter expression in Purkinje cells (PC). (H) Colocalisation with glial marker s100β confirms the identity of β-gal+ cells within the PCL as Bergmann glia (white arrowheads), though not all Bergmann glia express β-galactosidase (unfilled arrowhead). (A, C are counterstained with hematoxylin and D–H with Topro3 Scale bars: A = 500 μm, B–C = 100 μm, D–H = 50 μm).
doi:10.1371/journal.pone.0023012.g004

β-galactosidase protein from when they last transduced a Wnt/β-catenin signal.

As Wnt/β-catenin signalling is commonly associated with the control of cell proliferation, we wanted to determine whether the BAT-gal expression pattern correlated with proliferation between P5 and P10 (the most highly proliferative period of cerebellar development). We therefore performed double immunofluorescence staining for β-galactosidase and PCNA. A number of PCNA+ cells were seen in each layer at P5 (Fig. 3D), becoming restricted to the EGL, WM and PCL by P10 (Fig. 4D) reflecting the overall decrease in proliferation by this point. By P21 PCNA+ cells were largely restricted to the WM (data not shown), reflecting the proliferation of white matter progenitors. While β-gal+ cells were identified in all these key regions, very few β-gal+/PCNA+ cells were seen at P5 (Fig. 3D), and none were identified at P10 (Fig. 4D) or P21 (data not shown). Thus, we found little evidence for correlation between Wnt/β-catenin signalling and proliferation in the postnatal cerebellum, despite the identification of many β-gal+ cells in proliferative regions such as the WM and PCL.

Wnt/β-catenin signalling is seen in Bergmann glia in the postnatal cerebellum

We next sought to identify the specific cell type(s) within the postnatal cerebellum in which Wnt/β-catenin signalling is active. The locations of the β-gal+ cell population identified at each postnatal stage examined suggested a number of possible cell types, including interneuron and glial progenitors within the WM, granule cells, astrocytes, oligodendrocytes and interneurons within the IGL, Purkinje cells and Bergmann glia within the PCL and interneurons within the ML. To determine the identity of the β-

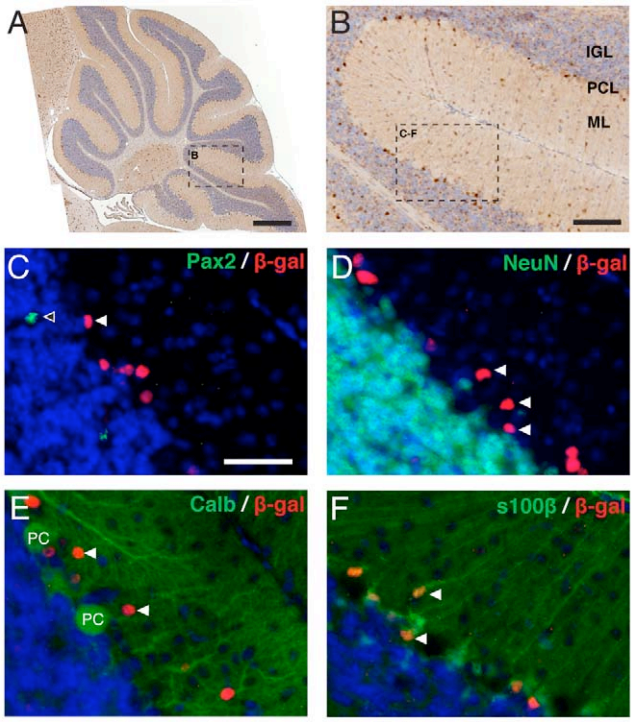

Figure 5. BAT-gal expression in the P21 cerebellum. (A) DAB immunohistochemistry for β-gal in the P21 cerebellum. (B) Higher magnification of the region boxed in (A) reveals that BAT-gal reporter expression is largely restricted to the PCL (black arrowheads), with few β-gal+ cells observed in other layers. Double immunofluorescence experiments confirmed this localisation of β-gal+ cells (C–F). Double immunofluorescence for Pax2 (C), NeuN (D) and Calbindin (E) show the β-gal+ cells (white arrows) located in the PCL do not express markers of interneurons, granule neurons or PCs respectively. (F) Colocalisation with glial marker s100β confirms the identity of these cells as Bergmann glia (white arrows). (A–B are counterstained with hematoxylin and C–F with Topro3. Scale bars: A = 500 μm, B = 100 μm, C–F = 50 μm).
doi:10.1371/journal.pone.0023012.g005

gal+ cells we performed double immunofluorescence experiments between β-galactosidase and a number of marker proteins known to label specific cerebellar cell types.

The transcription factor Pax2 is expressed in committed cerebellar interneurons after their exit from the ventricular zone and prior to their terminal differentiation [15]. Thus, colocalisation between Pax2 and β-galactosidase would indicate that committed interneuron progenitors were responding to a Wnt/β-catenin signal. The pattern of Pax2 expression identified at all three stages analysed was consistent with that expected for interneuron precursors. However, although many β-gal+ and Pax2+ cells were observed in the same cell layers, often in close proximity to each other, no colocalisation was observed in any sections analysed (Fig. 3E, 4E, 5C).

The β-gal+ cells in the IGL, PCL and ML could also be migratory post-mitotic granule cells, exiting the EGL towards their final destination in the IGL. However, double immunofluorescence between β-galactosidase and NeuN, a marker for post-mitotic granule cells [38], did not reveal any colocalisation of the two proteins in any sections analysed (Fig. 3F, 4F, 5D). Thus, Wnt/β-catenin signalling appears unlikely to be directly involved in the migration of post-mitotic granule cells.

Many β-gal+ cells were clearly localised to the PCL, suggesting the possibility that Purkinje cells may be responding to Wnt/β-catenin signalling. However, no colocalisation was observed between β-galactosidase and calbindin, a marker that clearly identifies Purkinje cells from P10, at either P10 (Fig. 4G) or P21 (Fig. 5E). Interestingly, many of the β-gal+ cells in the PCL were in close proximity to Purkinje cells, consistent with the location of Bergmann glia.

To determine whether Wnt/β-catenin signalling indeed marks a population of glial cells, we performed double immunofluorescence with s100β, a marker for Bergman glia and other astrocytes from P10 [39]. As expected, we identified β-gal+/s100β+ cells in the PCL at P10 (Fig. 4H) and P21 (Fig. 5F) consistent with the conclusion that a population of Bergman glia respond to a Wnt/β-catenin signal during development.

Discussion

In this study we have investigated the distribution of Wnt/β-catenin signalling during development of the cerebellum from E12.5 to P21 primarily using the BAT-gal Wnt reporter mouse strain [35]. The specific roles played by Wnt/β-catenin signalling during development of the cerebellum are not yet well characterised. Here, we provide evidence for a specific and dynamic spatio-temporal pattern of Wnt/β-catenin signalling through different stages of cerebellum development (summarised in Fig. 6).

Wnt/β-catenin signalling is active at the rhombic lip but not expansion or differentiation of GPCs

Our experiments revealed expression of the BAT-gal reporter at the rhombic lip at E12.5 and early EGL at E14.5. The rhombic lip gives birth to projection neurons of the deep cerebellar nuclei from E10.5 to E12.5 [3] followed by GPCs and unipolar brush cells from E12.5 onwards [4,5,6]. Because unipolar brush cells migrate along a different path than the dorsal stream that forms the EGL, we conclude that the BAT-gal reporter expression observed at E12.5 and E14.5 is potentially limited to GPCs and late born DCN neurons.

Consistent with this, a number of studies have identified expression of *Wnt1* at the rhombic lip and at the isthmus [22,23,24,25,26] and loss of *Wnt1* leads to a severe developmental phenotype of the cerebellum, most likely due to a failure to maintain the isthmus [27,28,29]. Due to the consistency between the known expression pattern of *Wnt1*, and its proven role as a key signalling molecule in this area, it is possible that Wnt1 activity is responsible for the active Wnt/β-catenin signalling at the embryonic isthmus and rhombic lip identified in our experiments. However, it remains to be established whether additional Wnt genes are expressed in this area.

While active Wnt/β-catenin signalling was observed in the early migrating GPCs at E14.5 (Fig. 1A–B), this was lost in the GPCs observed in the EGL during later stages of development. By E18.5, BAT-gal expression within the EGL was minimal and from P1 onwards, it was undetectable (Fig. 2A–D). These data are consistent with a potential role for Wnt/β-catenin signalling during early specification of GPCs but not in their further migration or proliferation. This is consistent with the fact that proliferation of this cell population during late embryogenesis and early postnatal development is driven by Sonic hedgehog secreted by neighbouring Purkinje cells [18,19].

Additionally, the absence of NeuN expression in any of the β-gal+ cells observed from P5-P21 demonstrates that Wnt/β-catenin signalling is also not active in the migration of terminally differentiated GCs from the EGL to the IGL. (Fig. 3E, 4E, 5D). NeuN is abundantly expressed in most classes of neurons [38] and has been identified in all stages of post-mitotic granule cell development [40]. Thus, the lack of NeuN expression in β-gal+

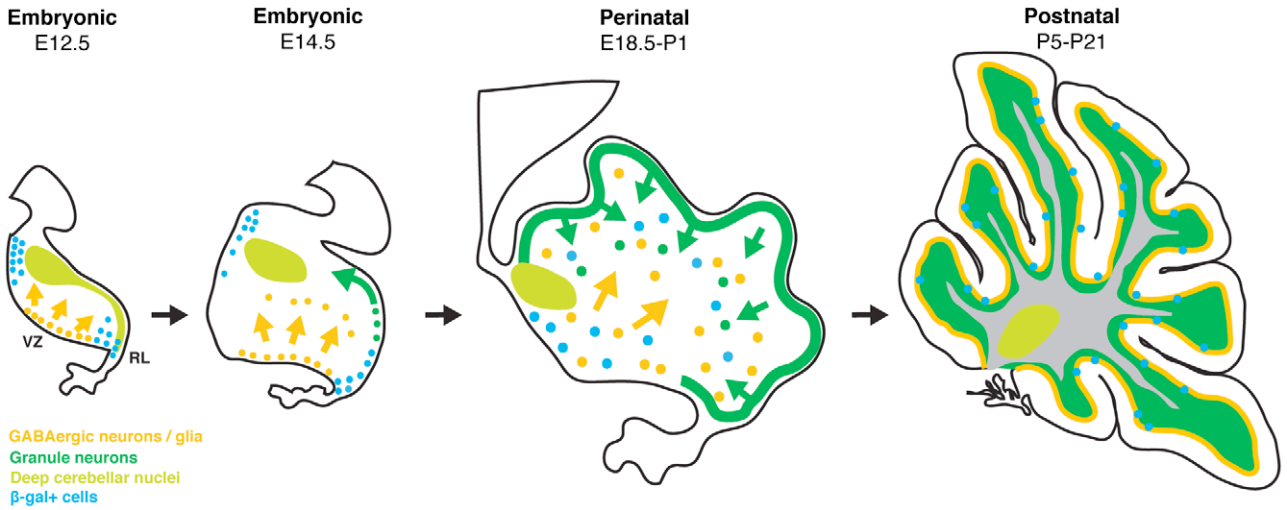

Figure 6. Summary of Wntβ-catenin signalling during cerebellum development. Wnt/β-catenin signalling is present in a dynamic spatio-temporal specific pattern in the developing cerebellum. Initially it is observed at the cerebellar rhombic lip but by E18.5 its expression expands into a more widespread pattern with particularly strong expression at the VZ during the birth of glia and interneurons. During postnatal development it is largely restricted to the PCL, consistent with a subpopulation of Bergmann glia.
doi:10.1371/journal.pone.0023012.g006

cells located in these regions indicates that they are not of the granule lineage.

A potential role for Wnt/β-catenin signalling in development of cell lineages from the cerebellar ventricular zone

At E18.5 and P1, many β-gal+ cells were seen in the ventricular zone (Fig. 2), although none were found there earlier (Fig. 1). This indicates that Wnt/β-catenin signalling is active in cell lineages originating at the ventricular zone at these time points. Purkinje cells arise at the onset of cerebellar neurogenesis between E10.5 and E12.5 [8,9]. The interneuron lineage can then be detected by the expression of Pax2 in scattered cells at the ventricular zone from E13.5 to E17.5 [15] from where they migrate radially as Pax2+ lineage restricted progenitors [14,15]. Concurrently, gliogenesis begins at the ventricular zone from E13.5, identified through the expression of S100β, BLBP and Sox9 [41]. The early Bergmann glial population exits the ventricular zone at E14.5 and follows a migratory path behind Purkinje cells [10]. Birth of the remaining cerebellar glial populations (astrocytes and oligodendrocytes) follows from this point. Our data suggest that the cell populations born at the ventricular zone between E18.5 and P1 could be doing so in response to a Wnt/β-catenin signal. Based upon the timing of known cell populations arising from the ventricular zone, this is most likely limited to glial and interneuron progenitors.

Wnt/β-catenin signalling may persist in the glial population throughout postnatal cerebellum development

Further to the identification of β-gal+ cells at the ventricular zone, we also observed a population of β-gal+ cells within all other layers of the cerebellum (excluding the EGL) from E18.5 through to P21. Lack of colocalisation between β-galactosidase and Pax2 (Fig. 3E, 4E, 5C), NeuN (Fig. 3F, 4F, 5D) and Calbindin (Fig. 4G, 5E) ruled out the possibility of the β-gal+ cell population being of the interneuron, granule or Purkinje cell types respectively.

The remaining alternative is that the β-gal+ cell population identified within the developing cerebellum are glia. Oligodendrocytes are thought to arise from extra-cerebellar tissue [42], while velate and fibrous astrocytes arise from ventricular zone derived WM progenitor cells. Bergmann glia are thought to follow a slightly different developmental path. Rather than arising during gliogenesis from WM progenitors like the rest of the astrocyte lineage, a population of early Bergmann glia arise from the ventricular zone and migrate in close proximity to - and remain developmentally intertwined with - Purkinje cells [10]. This wave of migration occurs from E14.5 onwards, and by E18.5 these glia come to lie in a pattern similar to that seen for some of the β-gal+ cell population we identified, outlining the developing folia inferior to the EGL. A β-gal+ cell population in this pattern was seen at all postnatal stages, though the number of labelled cells appears to decrease with age. While limitations of the antibody used mean we were unable to confirm the identity of this cell population prior to P5, colocalisation of β-galactosidase with s100β in cells present in close proximity to Purkinje cells at both P10 (Fig. 4G) and P21 (Fig. 5F) supports the hypothesis that some Bergmann glia respond to a Wnt/β-catenin signal during development. Expression of *LacZ* mRNA identified at all stages except for P21 supports a potential role for Wnt/β-catenin signalling during development, and would suggest that residual β-galactosidase protein has been identified at P21.

Interestingly, the lack of β-galactosidase expression at the ventricular zone at E14.5 indicates that Wnt/β-catenin signalling is not involved in the birth of the Bergmann glia but may be potentially involved in its further development and maturation. This is consistent with the postnatal dynamic transformation of Bergmann glia alongside dendritogenesis and synaptogenesis of Purkinje cells [11] and suggests a possible role for Wnt/β-catenin in this process.

Relevance to the developmental origins of medulloblastoma

We have shown that Wnt/β-catenin signalling is active in a highly dynamic and varied spatiotemporal pattern during key stages of cerebellum development. Surprisingly, Wnt/β-catenin is also active in a subset of Bergmann glia in the postnatal cerebellum. How these results relate to the development of medulloblastoma is confounded by recent findings by Gibson al

[34]. These authors provide evidence that constitutive activation of the Wnt/β-catenin pathway in BLBP expressing cerebellar precursors causes a defect in cell migration from the lower rhombic lip - which manifests eventually as medulloblastoma if tumour suppressor TP53 is also deactivated - while cell populations arising from the ventricular zone and rhombic lip do not show evidence for any developmental defect. Interestingly, we found BAT-gal and *Axin2* expression in the lower rhombic lip (Fig. 1) supporting their conclusion that the lower rhombic lip is a Wnt responsive area. However, our findings that Wnt/β-catenin signalling activity is in the upper rhombic lip and in cells arising from the ventricular zone now warrants more in depth functional investigation to determine the role of this pathway in development of these cell populations.

Methods

Mice

The licence authorising this work was approved by the University of Edinburgh's Ethical Review Committee on 22nd September 2008 (application number PL35-08) and by the Home Office on 6th November 2008. Animal husbandry was in accordance with the UK Animals (Scientific Procedures) Act 1986 regulations. To minimise animal suffering, pregnant dams were culled by cervical dislocation under terminal anaesthesia according to the Code of Practice for Humane Killing of Animals under Schedule 1 to the Animals (Scientific Procedures) Act 1986 issued by the Home Office. The day the vaginal plug was detected was designated E0.5 and the day of birth as P0. BAT-gal mice were maintained on a C57BL/6J genetic background and were genotyped as described previously [35]. Wild type mice on the same background were obtained by crossing mice hemizygous for the BAT-gal transgene and used as negative controls.

Histology

Embryos were collected at E12.5 and E18.5 and pups between P1 and P21. Whole E12.5 embryos, heads from E14.5 embryos and brains dissected from E18.5 embryos were immersion fixed in 4% paraformaldehyde (PFA) in phosphate buffered saline (PBS) overnight at 4°C. P1, 5, 10 and 21 pups were anaesthetised with Avertin and transcardially perfused with PFA, followed by tissue dissection and overnight immersion fixation in fresh PFA. Embryonic and postnatal tissue for immunohistochemistry and immunofluorescence were all processed following standard conditions [43], embedded in paraffin wax and cut in serial 10 µm sections on a sagittal plane. Tissue for *in situ* hybridisation was cryoprotected in 30% sucrose/PBS overnight before embedding in 30% sucrose/OCT (1:1) and snap freezing. Frozen sections were cut on a cryostat at 14 µm. At least two animals were analysed at each age.

Immunohistochemistry, immunofluorescence and *in situ* hybridisation

Immunohistochemistry and immunofluorescence were performed according to standard protocols. Antigen retrieval was achieved by microwaving sections at full power in 10 mM citrate buffer (pH6.0) for five minutes followed by 15 minutes at medium power. Primary antibodies were rabbit anti-β-galactosidase (Molecular Probes, 1:1000 for immunohistochemistry, 1:500 for immunofluorescence), mouse anti-β-galactosidase (DSHB, 1:500), mouse anti-PCNA (Abcam, 1:500), mouse anti-Pax2 (Covance, 1:200), mouse anti-NeuN (Millipore, 1:500), mouse anti-Calbindin (Swant, 1:500), mouse anti-s100β (Abcam, 1:500). Secondary non-fluorescent antibodies were biotinylated anti-rabbit IgG (Dako, 1:200).

For single immunohistochemistry experiments the dark brown signal was revealed after incubation with the ABC kit (Vector), followed by a diaminobenzidine (DAB) and hydrogen peroxide reaction using the DAB detection kit (Vector). For double immunofluorescence experiments, all primary antibodies were detected using goat anti-rabbit IgG or goat anti-mouse IgG secondary antibodies conjugated to Alexa fluor 568 or 488 dyes (Invitrogen, 1:200) respectively. Appropriate controls were used in all cases by incubating sections with all but the primary antibodies. No staining was observed under these conditions.

In situ hybridisation on frozen section was performed as described previously [44]. *LacZ* and *Axin2* antisense riboprobes [45] were labelled using the digoxigenin RNA labelling kit (Roche) according to the manufacturer's instructions.

Microscopy

A Leica brightfield microscope connected to a Leica DFC 480 digital camera was used to capture images of DAB labelled sections. A Leica brightfield microscope connected to a Leica DFC360Fx camera was used to capture images of fluorescently labelled sections.

Acknowledgments

We thank Dr Tom Pratt for useful comments on the manuscript. We are grateful to the staff of the University of Edinburgh Biological Research Resource facility for expert animal care. The mouse anti-β-galactosidase antibody was developed by J. Sanes, and obtained from the Developmental Studies Hybridoma Bank developed under the auspices of the National Institute of Child Health and Human Development and maintained by the University of Iowa (Department of Biological Sciences, Iowa City, IA).

Author Contributions

Conceived and designed the experiments: HS JOM. Performed the experiments: HS. Analyzed the data: HS JOM. Wrote the paper: HS JOM.

References

1. Sillitoe RV, Joyner AL (2007) Morphology, molecular codes, and circuitry produce the three-dimensional complexity of the cerebellum. Annu Rev Cell Dev Biol 23: 549–577.
2. Wingate RJ (2001) The rhombic lip and early cerebellar development. Curr Opin Neurobiol 11: 82–88.
3. Fink AJ, Englund C, Daza RA, Pham D, Lau C, et al. (2006) Development of the deep cerebellar nuclei: transcription factors and cell migration from the rhombic lip. J Neurosci 26: 3066–3076.
4. Wang VY, Rose MF, Zoghbi HY (2005) Math1 expression redefines the rhombic lip derivatives and reveals novel lineages within the brainstem and cerebellum. Neuron 48: 31–43.
5. Machold R, Fishell G (2005) Math1 Is Expressed in Temporally Discrete Pools of Cerebellar Rhombic-Lip Neural Progenitors. Neuron 48: 17–24.
6. Englund C, Kowalczyk T, Daza RA, Dagan A, Lau C, et al. (2006) Unipolar brush cells of the cerebellum are produced in the rhombic lip and migrate through developing white matter. J Neurosci 26: 9184–9195.
7. Wang VY, Zoghbi HY (2001) Genetic regulation of cerebellar development. Nat Rev Neurosci 2: 484–491.
8. Altman J, Bayer S (1997) Development of the cerebellar system in relation to its evolution, structures and function. New York CRC.
9. Hashimoto M, Mikoshiba K (2003) Mediolateral compartmentalization of the cerebellum is determined on the "birth date" of Purkinje cells. J Neurosci 23: 11342–11351.
10. Yamada K, Watanabe M (2002) Cytodifferentiation of Bergmann glia and its relationship with Purkinje cells. Anat Sci Int 77: 94–108.
11. Yamada K, Fukaya M, Shibata T, Kurihara H, Tanaka K, et al. (2000) Dynamic transformation of Bergmann glial fibers proceeds in correlation with dendritic outgrowth and synapse formation of cerebellar Purkinje cells. J Comp Neurol 418: 106–120.
12. Milosevic A, Goldman JE (2002) Progenitors in the postnatal cerebellar white matter are antigenically heterogeneous. J Comp Neurol 452: 192–203.

13. Milosevic A, Goldman JE (2004) Potential of progenitors from postnatal cerebellar neuroepithelium and white matter: lineage specified vs. multipotent fate. Mol Cell Neurosci 26: 342–353.
14. Weisheit G, Gliem M, Endl E, Pfeffer PL, Busslinger M, et al. (2006) Postnatal development of the murine cerebellar cortex: formation and early dispersal of basket, stellate and Golgi neurons. Eur J Neurosci 24: 466–478.
15. Maricich SM, Herrup K (1999) Pax-2 expression defines a subset of GABAergic interneurons and their precursors in the developing murine cerebellum. J Neurobiol 41: 281–294.
16. Leto K, Carletti B, Williams IM, Magrassi L, Rossi F (2006) Different types of cerebellar GABAergic interneurons originate from a common pool of multipotent progenitor cells. J Neurosci 26: 11682–11694.
17. Leto K, Bartolini A, Yanagawa Y, Obata K, Magrassi L, et al. (2009) Laminar fate and phenotype specification of cerebellar GABAergic interneurons. J Neurosci 29: 7079–7091.
18. Dahmane N, Ruiz i Altaba A (1999) Sonic hedgehog regulates the growth and patterning of the cerebellum. Development 126: 3089–3100.
19. Wechsler-Reya RJ, Scott MP (1999) Control of neuronal precursor proliferation in the cerebellum by Sonic Hedgehog. Neuron 22: 103–114.
20. Kalani MY, Cheshier SH, Cord BJ, Bababeygy SR, Vogel H, et al. (2008) Wnt-mediated self-renewal of neural stem/progenitor cells. Proc Natl Acad Sci USA 105: 16970–16975.
21. Wexler EM, Paucer A, Kornblum HI, Palmer TD, Plamer TD, et al. (2009) Endogenous Wnt signaling maintains neural progenitor cell potency. Stem Cells 27: 1130–1141.
22. Wilkinson DG, Bailes JA, McMahon AP (1987) Expression of the proto-oncogene int-1 is restricted to specific neural cells in the developing mouse embryo. Cell 50: 79–88.
23. Davis CA, Joyner AL (1988) Expression patterns of the homeo box-containing genes En-1 and En-2 and the proto-oncogene int-1 diverge during mouse development. Genes Dev 2: 1736–1744.
24. Dymecki SM, Tomasiewicz H (1998) Using Flp-recombinase to characterize expansion of Wnt1-expressing neural progenitors in the mouse. Dev Biol 201: 57–65.
25. Fischer T, Guimera J, Wurst W, Prakash N (2007) Distinct but redundant expression of the Frizzled Wnt receptor genes at signaling centers of the developing mouse brain. Neuroscience 147: 693–711.
26. Nichols DH, Bruce LL (2006) Migratory routes and fates of cells transcribing the Wnt-1 gene in the murine hindbrain. Dev Dyn 235: 285–300.
27. Thomas KR, Capecchi MR (1990) Targeted disruption of the murine int-1 proto-oncogene resulting in severe abnormalities in midbrain and cerebellar development. Nature 346: 847–850.
28. McMahon AP, Bradley A (1990) The Wnt-1 (int-1) proto-oncogene is required for development of a large region of the mouse brain. Cell 62: 1073–1085.
29. McMahon AP, Joyner AL, Bradley A, McMahon JA (1992) The midbrain-hindbrain phenotype of Wnt-1-/Wnt-1- mice results from stepwise deletion of engrailed-expressing cells by 9.5 days postcoitum. Cell 69: 581–595.
30. Zurawel RH, Chiappa SA, Allen C, Raffel C (1998) Sporadic medulloblastomas contain oncogenic beta-catenin mutations. Cancer Res 58: 896–899.
31. Eberhart CG, Tihan T, Burger PC (2000) Nuclear localization and mutation of beta-catenin in medulloblastomas. J Neuropathol Exp Neurol 59: 333–337.
32. Hamilton SR, Liu B, Parsons RE, Papadopoulos N, Jen J, et al. (1995) The molecular basis of Turcot's syndrome. N Engl J Med 332: 839–847.
33. Gilbertson RJ, Ellison DW (2008) The origins of medulloblastoma subtypes. Annual review of pathology 3: 341–365.
34. Gibson P, Tong Y, Robinson G, Thompson M, Currle DS, et al. (2010) Subtypes of medulloblastoma have distinct developmental origins. Nature 468: 1095–1099.
35. Maretto S, Cordenonsi M, Dupont S, Braghetta P, Broccoli V, et al. (2003) Mapping Wnt/beta-catenin signaling during mouse development and in colorectal tumors. Proc Natl Acad Sci USA 100: 3299–3304.
36. Machon O, Backman M, Machonova O, Kozmik Z, Vacik T, et al. (2007) A dynamic gradient of Wnt signaling controls initiation of neurogenesis in the mammalian cortex and cellular specification in the hippocampus. Dev Biol 311: 223–237.
37. Jho EH, Zhang T, Domon C, Joo CK, Freund JN, et al. (2002) Wnt/beta-catenin/Tcf signaling induces the transcription of Axin2, a negative regulator of the signaling pathway. Molecular and Cellular Biology 22: 1172–1183.
38. Mullen RJ, Buck CR, Smith AM (1992) NeuN, a neuronal specific nuclear protein in vertebrates. Development 116: 201–211.
39. Landry CF, Ivy GO, Dunn RJ, Marks A, Brown IR (1989) Expression of the gene encoding the beta-subunit of S-100 protein in the developing rat brain analyzed by in situ hybridization. Brain Res Mol Brain Res 6: 251–262.
40. Weyer A, Schilling K (2003) Developmental and cell type-specific expression of the neuronal marker NeuN in the murine cerebellum. J Neurosci Res 73: 400–409.
41. Hachem S, Laurenson AS, Hugnot JP, Legraverend C (2007) Expression of S100B during embryonic development of the mouse cerebellum. BMC Dev Biol 7: 17.
42. Grimaldi P, Parras C, Guillemot F, Rossi F, Wassef M (2009) Origins and control of the differentiation of inhibitory interneurons and glia in the cerebellum. Dev Biol 328: 422–433.
43. Fotaki V, Yu T, Zaki PA, Mason JO, Price DJ (2006) Abnormal positioning of diencephalic cell types in neocortical tissue in the dorsal telencephalon of mice lacking functional Gli3. J Neurosci 26: 9282–9292.
44. Wallace VA, Raff MC (1999) A role for Sonic hedgehog in axon-to-astrocyte signalling in the rodent optic nerve. Development 126: 2901–2909.
45. Fotaki V, Price DJ, Mason JO (2011) Wnt/β-catenin signaling is disrupted in the extra-toes (Gli3(Xt/Xt)) mutant from early stages of forebrain development, concomitant with anterior neural plate patterning defects. J Comp Neurol 519: 1640–1657.